UNIVERSIDADE ESTADUAL DE CAMPINAS
INSTITUTO DE BIOLOGIA

Catarina Rapôso Dias Carneiro

"VENENO E TOXINA DA ARANHA *Phoneutria nigriventer*: AÇÃO NO SISTEMA NERVOSO CENTRAL"

Tese apresentada ao Instituto de Biologia para obtenção do Título de Doutor em Biologia Celular e Estrutural, na área de Histologia.

Este exemplar corresponde à redação final da tese defendida pelo(a) candidato (a) Catarina Rapôso Dias Carneiro e aprovada pela Comissão Julgadora.

Orientadora: Profª Drª Maria Alice da Cruz-Höfling

Campinas, 2009

FICHA CATALOGRÁFICA ELABORADA PELA
BIBLIOTECA DO INSTITUTO DE BIOLOGIA – UNICAMP

C215v

Carneiro, Catarina Raposo Dias
Veneno e toxina da aranha *Phoneutria nigriventer*: ação no sistema nervoso central / Catarina Raposo Dias Carneiro. – Campinas, SP: [s.n.], 2009.

Orientadora: Maria Alice da Cruz-Höfling.
Tese (doutorado) – Universidade Estadual de Campinas, Instituto de Biologia.

1. Barreira hematoencefálica. 2. Astrócitos. 3. Inflamação. 4. Óxido nítrico. 5. Proteína FOS. I. Cruz-Höfling, Maria Alice. II. Universidade Estadual de Campinas. Instituto de Biologia. III. Título.

(rcdt/ib)

Título em inglês: Venom and toxin of *Phoneutria nigriventer* spider: action in the central nervous system.
Palavras-chave em inglês: Blood-brain barrier; Astrocytes; Inflammation; Nitric oxide; FOS protein.
Área de concentração: Biologia Celular.
Titulação: Doutora em Biologia Celular e Estrutural.
Banca examinadora: Maria Alice da Cruz-Höfling, Elenice Aparecida de Moraes Ferrari, Lanfranco Ranieri Paolo Troncone, Elaine Aparecida Del Bel Belluz Guimarães, Stephen Hyslop.
Data da defesa: 31/08/2009.
Programa de Pós-Graduação: Biologia Celular e Estrutural.

Campinas, 31 de agosto de 2009.

BANCA EXAMINADORA

Profa. Dra. Maria Alice da Cruz Höfling (Orientadora) _____
Assinatura

Profa. Dra. Elaine Aparecida Del Bel Belluz Guimarães _____
Assinatura

Profa. Dra. Elenice Aparecida de Moraes Ferrari _____
Assinatura

Prof. Dr. Lanfranco Ranieri Paolo Troncone _____
Assinatura

Prof. Dr. Stephen Hyslop _____
Assinatura

Profa. Dra. Ione Salgado _____
Assinatura

Prof. Dr. Ivo Lebrun _____
Assinatura

Profa. Dra. Luciana Le Sueur Maluf _____
Assinatura

O desenvolvimento de uma tese de doutorado é um exercício de raciocínio; é chegar ao limite (e aprender a ultrapassá-lo) da sua capacidade de pensar e inferir. Portanto, dedico este trabalho às duas pessoas que, durante esses três anos, me levaram a ter os mais complexos e profundos pensamentos:

À memória de C.S. Lewis, que (faço minhas as palavras de John Piper) me ensinou que sempre existe algo mais para ver naquilo que eu vejo;

Ao Pastor Leandro Borges Peixoto (Igreja Batista Central de Campinas), que me ensinou as coisas mais importantes que eu poderia aprender.

Agradecimentos _____

Agradeço primeiramente a Jesus Cristo, pois durante os últimos anos, mesmo diante da minha atitude arrogante de indiferença, conforme a sua promessa, Ele me deu abundantemente mais do que tudo o que pedi ou pensei. Além de proporcionar força e disciplina para alcançar objetivos, como a conclusão deste trabalho, Ele me deu a bênção de tremer diante dEle e de me humilhar sob Sua santidade arrebatadora. Além disso, Jesus Cristo criou o mundo, inclusive a mim, e mantém este mundo em funcionamento pela manifestação do seu poder. Cada expirar ou inspirar, cada batida do meu coração, cada momento em que vejo e ouço alguma coisa, cada pensamento e raciocínio, tudo devo à misericórdia constante e ao poder criativo de Jesus. Portanto, todos os outros agradecimentos são secundários e dependem exclusivamente dEle.

Agradeço à minha orientadora, Profa. Dra. Maria Alice da Cruz-Höfling, pelo seu apoio, confiança, amizade e dedicação. Por ter me dado a oportunidade de, nos últimos seis anos, assimilar um pouco do seu vasto conhecimento e de me espelhar na sua impecável conduta profissional. A profa. Maria Alice, ao mesmo tempo em que permitiu que eu tivesse liberdade no meu pensar e proceder durante o desenvolvimento deste trabalho, direcionou as minhas decisões, mostrando a maneira correta de agir.

Ao terminar a minha graduação em odontologia, na Universidade Federal de Pernambuco, não me senti totalmente realizada, sabia que eu seria muito mais útil em produzir e repassar conhecimento, do que exercendo a odontologia. Mas, por onde começar? Entrei em contato com a profa. Maria Alice, que me deu a oportunidade de estagiar em seu laboratório; em seguida ingressei no mestrado e, na sequência, entrei no doutorado sob a sua orientação. A oportunidade que ela me deu foi decisiva para a minha história profissional, pois aqui encontrei a pesquisa, que amo, me realizo e procuro fazer o melhor. Portanto, agradeço à profa. Maria Alice, por ter encontrado nela oportunidade, amizade, liberdade (vigiada) e conhecimento disponível.

Um agradecimento especial ao meu esposo, Marcos André Lins de Melo, que foi paciente, companheiro e presente. Sem o seu amor, eu não estaria completa. E às minhas filhas, Raphaela e Maria Gabriela, as quais tenho educado no temor a Deus e, como conseqüência, são meninas mais adoráveis do que eu jamais poderia desejar. Agradeço por que elas são parte da minha própria existência e por isso mesmo razão de tudo que faço.

Agradeço ao amor e carinho da minha família. À minha mãe, Maria do Socorro Brito Raposo, uma das pessoas em quem eu mais confio, pois sei que não mede esforços para me ajudar e orientar. Aos meus irmãos, Manuela Raposo e Thiago Raposo, por sua amizade incondicional. À minha sobrinha e afilhada, Marina Baptista, pela sua alegria e seu sorriso, que ajudaram a renovar minha coragem. Aos meus cunhados, Ruy Baptista e Mariana Leite por completarem essa família e tornarem a minha vida ainda mais repleta de motivos. À Inês Alves dos Santos, que escolheu fazer

parte da nossa família, sendo a nossa segunda mãe. Pela sua capacidade de se dedicar e amar sem cobranças e sem julgamentos. Por ela ser essa pessoa tão especial, que tenho o privilégio de amar.

À Marta Beatriz Leonardo, pelo excelente apoio técnico e amizade.

Aos alunos de iniciação científica, Paulo Alexandre Odorissi e Stefania Fioravante Savioli, por terem aceitado o desafio de participar da execução e interpretação de vários experimentos que hoje compõem esta tese e por tê-los feito com capricho e dedicação.

Aos colegas (amigos), Karina Fontana, Thalita Rocha, Carolina Carvalho, Junia Carolina dos Santos Silva, Gabriela Zago, Érika Freitas, Ângela Ito, e aos outros que, embora não tenha citado, levo na minha memória e no meu coração, pois todos foram solidários e companheiros, sempre.

Aos profissionais que colaboraram para o desenvolvimento deste trabalho: Prof. Dr. Lourival D. Possani e Freddy Coronas (Instituto de Biotecnologia, Universidad Nacional Autonoma de Mexico), por contribuírem para a purificação do veneno da aranha *P. nigriventer*, viabilizando os experimentos da ação de toxinas purificadas na permeabilização da barreira hematoencefálica; Prof. Dr. Stephen Hyslop e Profa. Dra. Alessandra Linardi, pelo apoio e disponibilização dos equipamentos para a dosagem de nitrito no meio de cultura; Prof. Dr. Hiroshi Aoyama, Profa. Dra. Carmem Veríssima Ferreira e Dra. Roberta Ruela Sousa (Departamento de Bioquímica, UNICAMP), pela contribuição na execução de experimentos de western blotting, bem como na interpretação dos resultados; Prof. Dr. Alexandre Leite Rodrigues de Oliveira e Dra. Renata Graciele Zanon (Departamento de Anatomia, Biologia Celular e Fisiologia, UNICAMP), pelo apoio na execução dos experimentos e na interpretação dos resultados dos trabalhos feitos com cultura de células.

À Líliam Panagio, pelo seu apoio, disponibilidade e excelente trabalho.

Aos membros da banca de análise prévia e da banca examinadora da tese, os (as) professores (as) Doutores (as): Elenice A. de Moraes Ferrari, Liana Lins Melo, Luciana Le Sueur Maluf, Lanfranco Ranieri Paolo Troncone, Stephen Hyslop, Elaine Aparecida Del Bel Belluz Guimarães, Ione Salgado e Ivo Lebrum, por, gentilmente, cederem seu tempo e conhecimento, analisando este trabalho com rico criticismo.

Ao Programa de Pós-Graduação em Biologia Celular e Estrutural.

Ao banco Santander, por conceder o Prêmio Cátedra Santander, que financiou a permanência da profa Maria Alice na Universidade Autônoma do México, para purificação das frações do veneno de *P. nigriventer*.

À FAPESP, CNPq, CAPES/PROEX, FAPEX/UNICAMP, pelo suporte financeiro.

Resumo

Venenos animais são fontes de substâncias neuroativas, algumas capazes de provocar paralisia e convulsão em mamíferos, com visível ação no sistema nervoso central (SNC). O veneno da aranha *Phoneutria nigriventer* (PNV) é composto por neurotoxinas que causam, experimentalmente, permeabilização da barreira hematoencefálica (BHE). A BHE é uma entidade tanto física, quanto molecular, composta pelos microvasos sanguíneos cerebrais, pelos pés astrocitários e pericitos adjacentes engajados no controle do tráfego de moléculas na interface sangue-cérebro. A BHE, embora imprescindível à manutenção da homeostase no SNC, pode representar um obstáculo ao acesso de drogas terapêuticas ao microambiente neural. Nossa proposta foi investigar a ação sistêmica do PNV após 15 min, 2 e 5 h da injeção i.v. em ratos Wistar adultos através de: (**1**) alterações na expressão das proteínas juncionais, de efluxo e transportador de glicose da BHE; (**2**) alterações na expressão da proteína conexina-43 (constituinte das junções comunicantes) e da proteína fosfatase pPP2A, uma vez que a fosforilação de resíduos de tirosina das proteínas juncionais tem papel no controle da integridade paracelular; (**3**) ativação de vias neuronais e sua modulação pelo óxido nítrico (NO). (**4**) Reação inflamatória e gliose reativa de astrócitos *in vivo e in vitro* e sua possível modulação pelo NO, (**5**) Purificação e identificação de toxinas do PNV com ação na BHE. A expressão das proteínas juncionais encontrava-se diminuída aos 15 min e 2 h, porém às 5 h pós-PNV a expressão das proteínas investigadas estava total ou parcialmente recuperada, sugerindo ser esse um dos mecanismos de abertura da BHE. Igualmente, a expressão da proteína de efluxo aumentou indicando mecanismo de *clearance* do agente tóxico. A expressão da conexina-43, e da pPP2A estavam aumentadas aos 15 min e diminuída às 5 h da injeção do PNV, mostrando não só que as comunicações célula-célula e o mecanismo de adesão célula-célula foram afetados, mas também que as alterações podem ser transitórias. Ademais, vias neuronais foram ativadas em áreas motoras e em núcleos do hipotálamo o que explicaria o comprometimento motor (convulsão, paralisia) e os sinais neurovegetativos (sialorréia, hipertensão, estresse respiratório, edema pulmonar, anúria) vistos em animais envenenados. Muitas dessas vias apontam modulação nitrérgica dos sinais tóxicos do envenenamento, uma vez que a inibição da síntese de NO pelo 7-nitroindazol (7-NI) diminuiu a ativação neuronal em algumas áreas e exacerbou em outras. Os astrócitos incubados com PNV, corroborando com estudos *in vivo,* expressaram citocinas pró-inflamatórias e apresentaram gliose reativa, porém a inibição da síntese do NO atenuou esses efeitos, confirmando que o NO tem um importante papel nos efeitos do PNV. Toxinas F8a-1 e F10a-1, purificadas do PNV, foram identificadas como responsáveis pela permeabilização da BHE, embora não esteja excluída a contribuição de outros componentes. O entendimento da ação do PNV e de suas toxinas no tecido neural e na BHE pode contribuir para o desenvolvimento de ferramentas úteis para uso clínico e em pesquisa.

Abstract

Animal venoms are source of neuroactive substances, some of them able to provoke paralysis and convulsion in mammals, indicating action on the central nervous system (CNS). The *Phoneutria nigriventer* spider venom (PNV) is composed of neurotoxins that cause, experimentally, blood-brain barrier (BBB) permeabilization. The BBB is both a physical and molecular entity, constituted by the cerebral microvessels and surrounding astrocytic end-feet and pericytes, all involved in the control of the traffic of molecules at the blood-brain interface. Even so the BBB presence is essential for the maintenance of CNS homeostasis; it also represents an obstacle for the therapeutical drugs access into the neural microenvironment. Our proposal was to investigate acute changes (15 min, 2 and 5 h) after PNV i.v. injection in adult Wistar rats through evaluation of the: (**1**) alterations in the expression of the BBB-junctional proteins, -efflux proteins, and -glucose transporter; (**2**) alterations in the expression of connexin-43 protein (gap junctions constituent) and protein phosphatase 2A (pPP2A, since phosphorylation of tyrosine residues from junctional proteins plays a role in controlling junctional integrity); (**3**) activation of neuronal pathways and its modulation by the nitric oxide (NO). (**4**) *In vivo* and *in vitro* astrocytes inflammatory reaction and reactive gliosis after incubation with PNV and its possible modulation by NO. (**5**) Purification and determination of BBB-acting from toxins PNV. The expression of the junctional proteins was diminished at 15 min and 2 h post-PNV exposure; however at 5 h the expression of most of the proteins investigated was total or partially recovered, suggesting that this might be one of the BBB opening mechanisms. Similarly, the venom increased the efflux protein expression, indicating ongoing clearance of toxic agents from the neural tissue. The expression of both connexin-43 and pPP2A increased after 15 min and diminished after 5 h of PNV injection, showing not only that cell-cell communication and cell-cell adhesion mechanism were affected, but that these alterations were transitory. Activated neuronal pathways have been observed in brain motor areas and hypothalamic nucleus, explaining the motor impairment (convulsion, paralysis) and neurovegetative signs (salivation, hypertension, respiratory stress, pulmonary edema, anuria) observed in the envenomed animals. Many of these neuronal pathways point to a nitrergic modulation of the envenomed toxic signs, since that NO synthesis inhibition by 7-nitroindazol (7-NI) decreased the neuronal activation in some areas and enhanced in others. The astrocytes incubated with PNV, in agreement with *in vivo* studies, expressed pro-inflammatory cytokines and presented reactive gliosis, however the pretreatment with 7-NI attenuated these effects, confirming that NO have an important role in the PNV effects. The F8a-1 and F10a-1 toxins, fractionated from the crude PNV, were identified as responsible by BBB permeabilization; despite, other venom components contribution can not be discarded. The understanding of the action of the venom of *Phoneutria nigriventer* and its toxins in the neural tissue and BBB can contribute for the development of useful tools for clinical and research purposes.

Sumário

Banca examinadora iii
Dedicatória iv
Agradecimentos v
Resumo vii
Abstract viii
Sumário ix
Índice de tabelas e figuras xi
Lista de abreviaturas xiii
Organização da tese xv

Capítulo I 1
INTRODUÇÃO 1
1. Barreira hematoencefálica: constituição e fisiologia 1
1.1. Estrutura e função 1
1.2. Astrócitos: papel na manutenção da BHE e na inflamação 5
2. Veneno da aranha *Phoneutria nigriventer* (PNV) 7
2.1. Composição e ação em sistemas biológicos 8
2.2. Ação na BHE e no SNC 9
2.3. Áreas do SNC ativadas pelo PNV 12
3. Óxido nítrico (NO) 15
OBJETIVOS 18

Capítulo II – Resultados 19
Phoneutria nigriventer venom impairs expression of junctional proteins in blood brain barrier through phosphatases deactivation pathway 20
Cx43, MRP1 and GLUT1 proteins involved in neuro-glial interaction are targets of the *Phoneutria nigriventer* spider venom 42
NO signaling mediates the neurotoxic effects of *Phoneutria nigriventer* spider venom in multiple brain regions of the rat 68
Cultured astrocyte activation by *Phoneutria nigriventer*. A conversation with nitric oxide 94
Purificação de toxinas do veneno de *P. nigriventer* e identificação de componentes responsáveis pela permeabilização da barreira hematoencefálica 117

Capítulo III 126
DISCUSSÃO GERAL 126
RESUMO DOS RESULTADOS E CONCLUSÕES 132
REFERÊNCIAS BIBLIOGRÁFICAS 134

Apêndice – Resultados obtidos em colaboração 143

Neuroinflammation and astrocytic reaction in the course of *Phoneutria nigriventer* (armed-spider) blood-brain barrier (bbb) opening. ……..……. 144

Anexo – Declaração comitê de ética em experimentação animal 155

Índice de tabelas e figuras

Capítulo I

Figura 1 – Microvaso cerebral (barreira hematoencefálica) 2

Figura 2 – Via paracelular da BHE 3

Figura 3 – Via transcelular da BHE 4

Figura 4 – *Phoneutria nigriventer* em posição de ataque 8

Capítulo II

Phoneutria nigriventer venom impairs expression of junctional proteins in blood brain barrier through phosphatases deactivation pathway

Figure 1 – Western blotting and immunofluorescency for laminin, in hippocampus and cerebellum…. 37

Figure 2 – Western blotting and immunofluorescency for Claudin-5, in hippocampus and cerebellum …….. 38

Figure 3 – Immunofluorescency for Pgp, in hippocampus ……..……...…….. 39

Figure 4 – Western blotting for ZO-1 and β-catenin, in hippocampus and cerebellum ……..…… 40

Figure 5 – Western blotting for occludin, and pPP2A, in hippocampus …..……..… 41

Cx43, MRP1 and GLUT1 proteins involved in neuro-glial interaction are targets of the *Phoneutria nigriventer* spider venom

Figure 1 – Immunofluorescence and western blotting for MRP1 in hippocampus ……..….. 62

Figure 2 – Immunofluorescence and western blotting for MRP1 in cerebellum ……...…..… 63

Figure 3 – Immunofluorescence and western blotting for GLUT1 in hippocampus ……...……..... 64

Figure 4 – Immunofluorescence and western blotting for GLUT1 in cerebellum ……..…… 65

Figure 5 – Immunofluorescence and western blotting for Cx43 in hippocampus ……...…..... 66

Figure 6 – Immunofluorescence and western blotting for Cx43 in cerebellum ……....……. 67

NO signaling mediates the neurotoxic effects of *Phoneutria nigriventer* spider venom in multiple brain regions of the rat

Figure 1 – Schematic representation of cross-sections of the brain showing the location of the regions in which FOS, NADPH-d and FOS/NADPH-d reactivity was quantified ……...……..…. 88

Figure 2 – Light micrograph showing the pattern of immunolabeling ……...……..… 88

Figure 3 – Schematic representation showing the time interval (in minutes) lasted from the treatment administration (0 min) until the onset of toxic signs by animals ……..……..… 89

Figure 4 – Representative light micrographs of the FOS protein immunolabeling and NADPH-d histochemistry in PMC, vPAG and dlPAG ……...……..…….. 90

Figure 5 – Representative light micrographs of the FOS protein immunolabeling and NADPH-d histochemistry in the in SON, PTN and PVN ……...……..… 91

Figure 6 – Histogram illustrating mean number of FOS, NADPH-d and double FOS/NADPH-reactive cells counted bilaterally ……...……...……. 92

Table 1 – Number of FOS, NADPH- d and double reactive neurons 93

Cultured astrocyte activation by *Phoneutria nigriventer*. A conversation with nitric oxide

Figure 1 – Photomicrographs of GFAP immunoreactivity in cortical astrocytes primary culture and analysis of the density of pixels ……...……. 112

Figure 2 – Micrographs from cortical astrocytes primary culture immunolabeled with TNFα …… 113

Figure 3 – Micrographs from primary culture of cortical astrocytes immunolabeled with INFγ ……. 114

Figure 4 – Micrographs from nNOS positive cortical astrocytes 115

Figure 5 – Histogram showing the Nitrite concentration in the culture medium of purified primary culture from cortical astrocytes …….....…… 116

Purificação de toxinas do veneno de P. nigriventer e identificação de componentes responsáveis pela permeabilização da barreira hematoencefálica

Figura 1 – Perfil cromatográfico da purificação do PNV 122

Figura 2 – Análise do extravasamento do corante Azul de Evans 123

Figura 3 – Secções semifinas de hipocampo de animais injetados com toxina do PNV, coradas com azul de toluidina 124

7NI – 7-nitroindazol

AE – azul de evans

AJ – adherens junction

BBB – blood brain barrier

BHE – barreira hematoencefálica

BM – basement membrane

BSA – bovine serum albumin

CER – cerebellum

CNS – central nervous system

Cx43 – connexin 43

dlPAG – dorsolateral periaqueductal gray matter

DMSO – dimethyl sulfoxide

GABA – gamma butyric acid

GFAP – glial fibrilar acidic protein

GJ – gap junction

GLUT1 – glucose transporter 1

HIP – hippocampus

HPLC – high performance liquid chromatography

IF – immunofluorescence

IH – immunohistochemistry

INFγ – Interferon-gamma

JA – junção aderente

JG – junção *gap*

JO – junção de oclusão

LPS – Lipopolysaccharide

MMP9 - matrix metalloproteinase-9

MRP1 – multidrug resistance protein 1

NADPH-d – reduced nicotinamide adenine dinucleotide phosphate diaphorase

NMDA – N-methyl-D-aspartic acid

nNOS – neuronal nitric oxide synthase

NO – nitric oxide

Pgp – P-glycoprotein

PMC – parietal motor cortex

PNV – *Phoneutria nigriventer* venom

PP2A – phosphatase proteín 2A

PTN – periventricular thalamic nucleus

PVN – paraventricular hypothalamic nucleus

RT – room temperature

SNC – sistema nervoso central

SNP – sistema nervoso periférico

SON – supraoptic nucleus

TJ – tight junction

TNFα – tumor necrosis factor-alpha

vPAG – ventral periaqueductal gray matter

WB – western blotting

Organização da tese

Este exemplar de tese está estruturado em quatro capítulos:

O ***Capítulo I*** apresenta uma introdução geral ao tema central da tese, "ação do veneno da aranha *Phoneutria nigriventer* (PNV) na barreira hematoencefálica (BHE) e no tecido neural (ativação neuronal, reação astrocitária e papel do óxido nítrico)". Além da Introdução, o *Capítulo I* contém os objetivos da tese. A Introdução foi organizada de forma a contemplar uma revisão sobre aspectos morfológicos, moleculares e funcionais dos componentes da BHE; a ação do PNV no tecido neural, periférico e central, e em particular na BHE (fruto de pesquisas do nosso laboratório). Por fim, foram abordados aspectos das funções biológicas do óxido nítrico, uma vez que esse gás parece ter um papel fundamental no mecanismo de ação do PNV no sistema nervoso central.

O ***Capítulo II*** contém resultados que deram origem a quatro trabalhos científicos, um deles envolvendo dois alunos de graduação, bolsistas de Iniciação Científica. Os artigos 1 e 2 estão mais diretamente relacionados a mecanismos que levam à permeabilização da BHE na vigência da presença sistêmica do PNV:

1- ***Phoneutria nigriventer*** **venom impairs expression of junctional proteins in blood-brain barrier through phosphatases deactivation pathway**; e

2- **Cx43, MRP1 and GLUT1 proteins involved in neuro-glial interaction are targets of the *Phoneutria nigriventer* spider venom**.

Os resultados abordando a ativação de vias neuronais, a neuroinflamação e o papel do óxido nítrico no mecanismo de ação do veneno compõem os artigos 3 e 4:

3- **NO signaling mediates the neurotoxic effects of *Phoneutria nigriventer* spider venom in multiple brain regions of the rat**; e

4 -**Cultured astrocyte activation by *Phoneutria nigriventer*. A conversation with nitric oxide**.

O *Capítulo II* é finalizado com a apresentação de dados parciais, sobre a ação de frações purificadas do PNV na BHE. Esse trabalho está em andamento, porém julgamos por bem incluí-lo na descrição das atividades de tese, uma vez que fazia parte de nosso projeto original. Esses resultados parciais estão apresentados em português, sob o título: Purificação de toxinas do veneno de *P. nigriventer* e identificação de componentes responsáveis pela permeabilização da BHE.

O ***Capítulo III*** traz uma discussão geral dos resultados obtidos no desenvolvimento desta tese, as conclusões e a lista das referências bibliográficas utilizadas na introdução e na discussão geral.

O ***Apêndice*** traz artigo recém publicado, contendo resultados que foram obtidos durante o mestrado da aluna Gabriela Mariotoni Zago, mas cujos experimentos, além de terem sido executados com a participação da aluna Catarina Rapôso, foram posteriormente ampliados com experimentos adicionais, realizados durante o período do presente trabalho de doutorado. O artigo foi intitulado:

5 -**Neuroinflammation and astrocytic reaction in the course of *Phoneutria nigriventer* (armed-spider) blood–brain barrier (BBB) opening, Neurotoxicology 30 (2009) 636-646**.

INTRODUÇÃO

1. Barreira hematoencefálica: constituição e fisiologia

1.1.Estrutura e função

A barreira hematoencefálica (BHE) é uma entidade tanto física, quanto molecular, responsável por controlar o tráfego de moléculas na interface sangue-cérebro. O principal componente da barreira física (via paracelular) é o endotélio dos microvasos cerebrais, o qual apresenta alta resistência elétrica e contato interendotelial fortemente vedado. Além disso, os prolongamentos dos astrócitos perivasculares, envolvendo a membrana basal endotelial e os pericitos vasculares contribuem para impedir o trânsito livre de macromoléculas (Rubin *et al*., 1991, Kacem *et al*., 1998). A barreira molecular (via transcelular) envolve receptores de membrana e um conjunto de carreadores específicos, presentes na bicamada lipídica e no citoplasma adluminal do endotélio.

Essa barreira física e molecular funciona como um regulador dinâmico do balanço de íons, um facilitador do transporte de nutrientes e uma barreira às moléculas potencialmente prejudiciais. Para alcançar essa função de barreira seletiva, a fenda interendotelial da microvasculatura cerebral é caracterizada pela presença do complexo juncional, que inclui junções aderentes (JAs) (Schulze & Firth, 1993), junções de oclusão (JOs) (Kniesel & Wolburg, 2000; Wolburg & Lippoldt, 2002) e possivelmente junções comunicantes (*gap*) (Tao-Cheng *et al*., 1987; Braet *et al*., 2001; Simard *et al*., 2003). Enquanto as junções *gap* medeiam a comunicação intercelular, as demais, JAs e JOs, agem restringindo essa passagem e, por consequência, apenas a via através do citoplasma endotelial é usada para as trocas na interface sangue-cérebro (Bazzoni & Dejana, 2004). Entretanto, essa rota transendotelial exerce um transporte altamente seletivo de substâncias, que é dependente, em grande medida, de receptores de membrana e carreadores altamente específicos (Lok *et al.,* 2007).

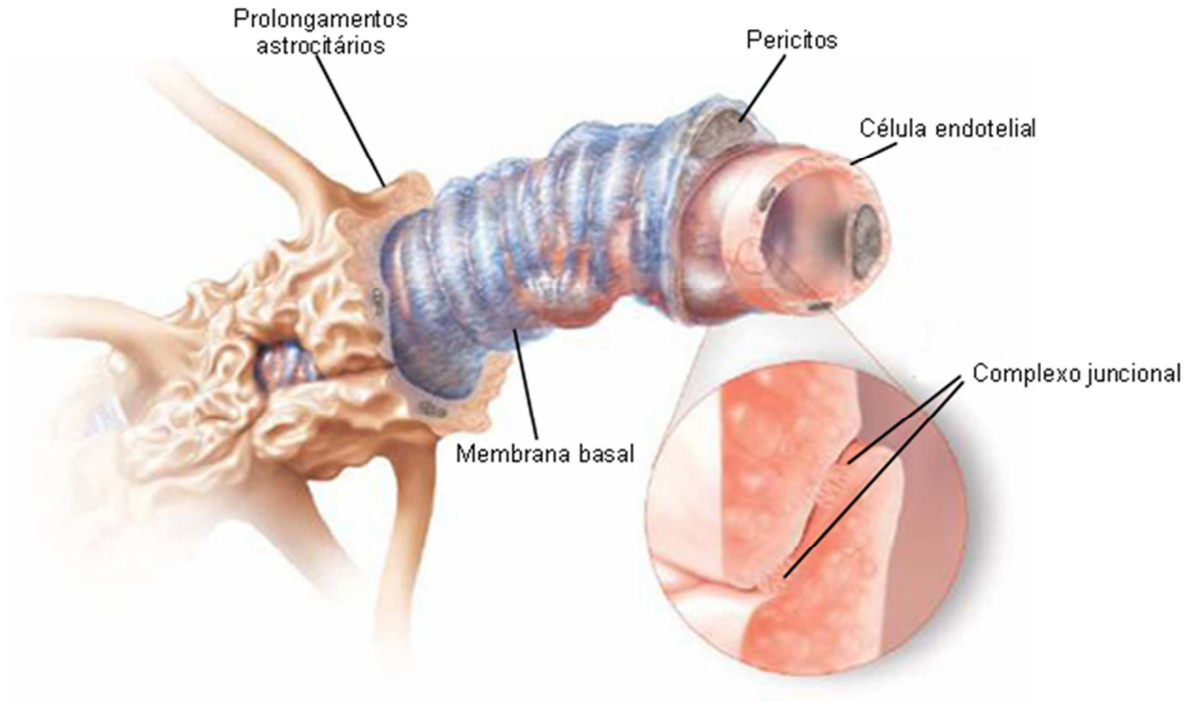

Figura 1: Microvaso cerebral (barreira hematoencefálica) – Os capilares cerebrais são envolvidos por diferentes tipos de células e pela membrana basal e apresentam complexo juncional bem desenvolvido entre as células endoteliais (Adaptado de Miller, 2002).

Portanto, pela sua estrutura peculiar, os vasos sanguíneos cerebrais são o componente principal da BHE (**Figura 1**). As JOs entre as células endoteliais são compostas pelas proteínas: ocludina, claudinas, ZO-1, ZO-2, ZO-3, cingulina, AF6, 7H6; as JAs são constituídas pelas caderinas, cateninas, vinculina e α-actinina; Há ainda as moléculas de adesão juncional (JAMs) (Ozaki *et al*., 1999; Wolburg & Lippoldt, 2002; Hawkins & Davis, 2005) (**Figura 2**). O citoplasma das células endoteliais tem espessura uniforme, com vesículas pinocíticas e sem fenestrações (Abbott, 2005). Portanto, as células endoteliais dos vasos sanguíneos cerebrais diferem das presentes em vasos periféricos por serem contínuas (livres de fenestrações) e possuírem JOs extensas e altamente resistentes, vedando, portanto, a via paracelular ao tráfego de moléculas.

A BHE é responsável pela manutenção do microambiente neuroparenquimal, protegendo o tecido neural contra toxinas e variações na composição do sangue, além de exercer um importante papel no transporte de nutrientes para o cérebro, através de um sistema altamente controlado mediado por transportadores e receptores, os quais selecionam moléculas que podem atravessar o citoplasma endotelial. As proteínas transportadoras de influxo asseguram a entrada de nutrientes, tais como

aminoácidos (por exemplo, LAT1 e sistema L de grandes aminoácidos neutros), nucleosídeos e nucleobases e glicose (Begley & Brightman, 2003; para revisão ver Persidsky *et al*., 2006). A glicose, por exemplo, o principal combustível para as células cerebrais, acessa o cérebro por difusão facilitada, via transportadores da família GLUT, localizados na membrana plasmática adluminal e adluminal das células endoteliais.

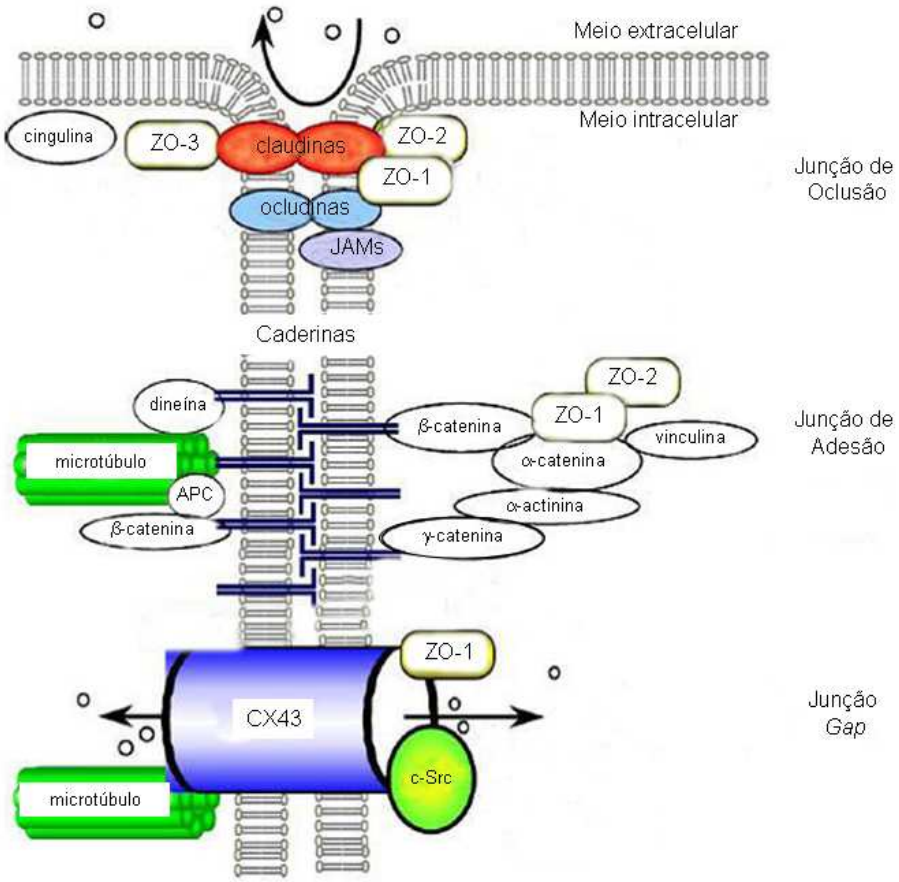

Figura 2: Via paracelular da BHE – Organização celular e molecular das junções entre células endoteliais (Adaptado de Giepmans, 2004).

Por outro lado, substâncias prejudiciais e até mesmo drogas terapêuticas não são capazes de atravessar os vasos sanguíneos cerebrais, devido à existência de um sistema de proteínas de efluxo. As proteínas transportadoras de efluxo removem eficazmente compostos através das células endoteliais, de volta ao sangue. A glicoproteína P (Pgp) é uma proteína transportadora de efluxo expressa pelas células endoteliais da BHE, pelos astrócitos e micróglia. As células endoteliais e a glia adjacente também expressam as proteínas de resistência a multidrogas (família de MRPs), entre outros transportadores de efluxo (**Figura 3**) (Para revisão, ver Liang & Aszalos, 2006).

A MRP1 foi primeiramente descrita por Cole *et al*. (1992). Essa proteína é um membro da superfamília dependente de ATP. Nos seres humanos, foi demonstrado que a MRP é uma família na qual sete homólogos foram identificados até agora (MRP1 – MRP7). Todos os membros da família MRP estão extensamente distribuídos na maioria dos tecidos humanos. Da família das MRPs, as isoformas MRP1 a MRP5 são expressos na BHE. As proteínas de efluxo podem significativamente afetar a farmacodinâmica e a farmacocinética das drogas. MRPs e Pgp têm um papel neuroprotetor em impedir a entrada e/ou o acúmulo de compostos tóxicos e drogas no tecido neural e contribuem para restringir a distribuição das drogas no organismo. Algumas drogas têm esses transportadores de efluxo como sítio alvo e podem ser usadas intencionalmente em propostas terapêuticas, para manipular a função das proteínas de efluxo, de modo que uma outra droga possa penetrar a BHE (que de outro modo seria removida pelos transportadores de efluxo antes que pudesse alcançar o seu alvo no tecido cerebral e exercer seu papel terapêutico) (Para revisão, ver: Liang & Aszalos, 2006).

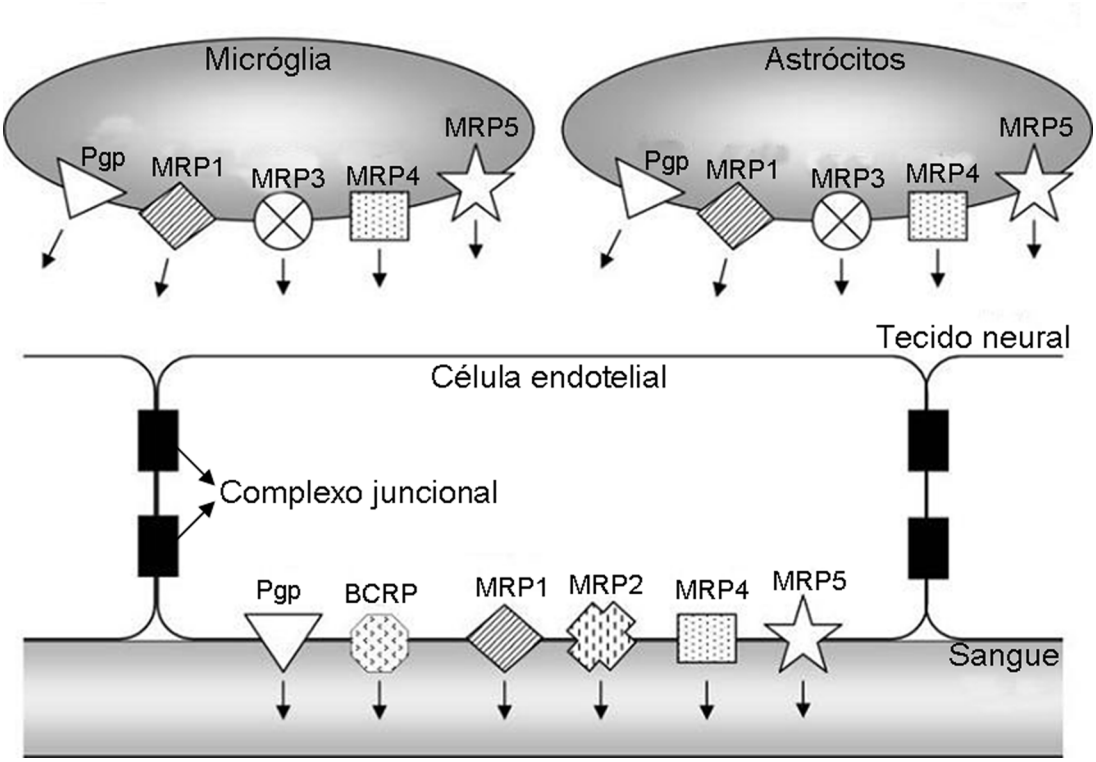

Figura 3: Via transcelular da BHE – As membranas luminal e adluminal das células endoteliais, bem como a membrana dos astrócitos e micróglia apresentam receptores transmembrana, que funcionam no efluxo e influxo de substâncias, restringindo o acesso das mesmas ao tecido neural (Adaptado de Dallas *et al*., 2006).

Portanto, a presença da BHE, embora seja imprescindível para a manutenção da homeostase (estado de equilíbrio) no sistema nervoso central (SNC), representa um imenso obstáculo para o efetivo acesso de drogas terapêuticas ao tecido neural. Muitas drogas potenciais, que são efetivas nos seus sítios

de ação, têm falhado e têm sido descartadas durante seu desenvolvimento para uso clínico devido à falha na sua biodistribuição e biodisponibilidade ao SNC. Portanto, o baixo número de drogas que alcançam o sucesso terapêutico é principalmente devido à complexidade do desenvolvimento de drogas que sejam capazes de atravessar a BHE em quantidades adequadas. Métodos que aumentem o acesso de drogas ao cérebro, portanto, são de grande interesse farmacêutico. Várias estratégias têm sido desenvolvidas, incluindo métodos invasivos e não-invasivos, como a manipulação de drogas visando transformá-las em análogos lipofílicos, pró-drogas, acesso de drogas mediadas por carreadores, abertura osmótica ou acesso intracranial de drogas por administração via intracerebroventricular, intracerebral ou intratecal (Para revisão, ver Pathan *et al*., 2009). Portanto, substâncias capazes de permeabilizar os microvasos cerebrais e aumentar o acesso de agentes terapêuticos ao tecido neural têm sido estudadas.

1.2. Astrócitos: papel na manutenção da BHE e na inflamação

Além da proeminente presença de células endoteliais altamente seladas pelas proteínas das JOs e JAs e das integrantes do sistemas de transportadores de efluxo e de influxo, a BHE é composta por outros componentes estruturais: prolongamentos astrocitários (pés-vasculares) e membrana basal, que formam uma camada limitante perivascular, além dos pericitos, envolvidos pela membrana basal endotelial (Rubin *et al*., 1991, Kacem *et al*., 1998; Ramsauer *et al*., 2002) (**Figura 1**). Todos esses elementos formam uma unidade neurogliovascular, engajados no controle do acesso de substâncias ao SNC, com vistas a um ambiente homeostático compatível com o funcionamento neuronal normal.

A íntima associação anatômica entre os pés-vasculares astrocitários e os microvasos cerebrais conduziu à sugestão de que essas células gliais poderiam mediar a indução e manutenção de características específicas do fenótipo de barreira no endotélio dos capilares cerebrais (Davson & Oldendorf, 1967). Estudos revelaram que astrócitos cultivados, implantados em áreas com vasos periféricos, normalmente com fenestras, podiam induzir a formação de capilares contínuos, típicos do SNC, indicando que os astrócitos são elementos chaves na formação e manutenção das características da BHE (Hayashi *et al*., 1997). Modelos de cultura de células forneceram muita informação acerca da indução do fenótipo da BHE no endotélio cerebral e confirmaram o papel chave dos astrócitos nessa indução (Bauer & Bauer, 2000). Os astrócitos podem regular as firmes junções de oclusão (Dehouck *et al*., 1990; Rubin *et al*., 1991), a expressão e localização polarizada de transportadores de efluxo, incluindo a Pgp (Schinkel, 1999), e de influxo, como a GLUT1 (McAllister *et al*., 2001). Portanto, os astrócitos, além de serem constituintes da BHE, induzem e mantêm o fenótipo característico das células endoteliais dos microvasos cerebrais. Nesse contexto, a presença das junções *gap* é essencial para estabelecer uma rede de conexões entre os componentes da BHE.

As junções *gap* são formadas por grupos de proteínas transmembrana, as conexinas (nos astrócitos, principalmente as conexinas 30 e 43) (Farahani *et al*., 2005), que formam sítios que conectam os citoplasmas de células contíguas e permitem trocas citosólicas de nutrientes, íons e segundos mensageiros, porém mantendo a individualidade gênica das células (Li *et al*., 2001). As junções *gap* são canais intercelulares que medeiam a difusão de íons e outras moléculas menores que 1 kDa, coordenando numerosos processos fisiológicos de sistemas multicelulares (Nicholson, 2003; Martin & Evans, 2004; Söhl & Willecke, 2004). As conexinas estão intimamente associadas com as proteínas das JOs das células endoteliais vasculares (Farquhar & Palade, 1963; Simionescu *et al*., 1975; Wagner & Kachar, 1995), interagindo diretamente com a ZO-1 (ligação da ZO1 com a sequência de aminoácidos 379-382 da conexina) (Giepmans & Moolenaar, 1998; Toyofuku *et al*., 1998; Giepmans, 2004; Herve´ *et al*., 2004).

Os astrócitos constituem as maiores e mais numerosas células gliais presentes no SNC dos mamíferos, excedendo em número a população de neurônios na proporção de 10:1 (Benveniste *et al*., 1992). Além de serem componentes da BHE e mediadores do fenótipo de barreira das células endoteliais, os astrócitos respondem rapidamente a injúrias do tecido neural. A proteína ácida fibrilar glial (GFAP) e a vimentina (VIM) são componentes dos filamentos intermediários presentes no citoesqueleto astrocitário (Bignami *et al*., 1994). Frente a agressões ao SNC, ocorre aumento na quantidade de GFAP no corpo e prolongamentos astrocitários (Bignami *et al*., 1994). O fenômeno, conhecido como astrocitose fibrilar reacional, está usualmente associado com o aumento do número (hiperplasia) e do tamanho (hipertrofia) dos astrócitos. Portanto, a GFAP tem sido usada para monitorar a resposta astrocitária em casos de insultos contra o SNC (Walz & Lang, 1998).

Os astrócitos contribuem também para o controle da imunidade no SNC (Farina *et al*., 2007). Agem como moduladores da resposta imune e inflamatória, e como coadjuvantes em vários distúrbios neurológicos (Aschner, 1998). Neuroinflamação no SNC compreende a ativação de células gliais, o recrutamento de células imunes periféricas e a produção de citocinas, tais como interferon-gama (IFN-γ) e fator de necrose tumoral – alfa (TNF-α) (Minghetti & Levi, 1998; Streit, 2000; Neumann, 2001). O TNF-α medeia as alterações citotóxicas dos neurônios e células gliais, enquanto o IFN-γ parece agir na indução de moléculas da superfície da célula para interações entre as células imunes e cerebrais (Imai *et al*., 2007). O conceito de que a disfunção dos astrócitos exerce um papel chave na patogênese do SNC é uma importante área em expansão.

2. Veneno da aranha *Phoneutria nigriventer* (PNV)

A principal função biológica do veneno das aranhas é paralisar a presa, portanto eles são compostos por uma variedade de toxinas que afetam o SNC (Rash & Hodgson, 2002). Por apresentarem diferentes sítios (moléculas) alvo, essas toxinas podem ser ferramentas úteis na compreensão de funções do organismo nos mecanismos fisiopatológicos, bem como no desenvolvimento de novos medicamentos.

No Brasil, os gêneros *Loxosceles* e *Phoneutria* são responsáveis pelos acidentes mais graves causados por aranhas venenosas. Os acidentes com aranhas do gênero *Phoneutria* são comuns na região de Campinas, embora os acidentes graves sejam raros, sendo observados em somente 0,5% do grupo estudado por Bucaretchi *et al.* (2000). Esses autores classificaram como leves 89,8% dos acidentes naquela população, como moderados, 8,5%, e como assintomáticos 1,2%. Foram considerados grupos de risco crianças com menos de 10 anos de idade e pacientes idosos (> 70 anos).

A aranha *Phoneutria nigriventer* (Ctenidae, Araneomorphae) (Figura 4), popularmente conhecida como "armadeira", é uma das aranhas mais agressivas e venenosas da América do Sul (Lucas, 1988), sendo responsável por cerca de 40% dos acidentes por picada de aranha em humanos no Estado de São Paulo (Ministério da Saúde, 1998; Bucaretchi *et al,* 2000). Seu veneno contém peptídeos neurotóxicos com efeitos nocivos em animais experimentais e em vítimas de acidentes (Antunes & Malaque, 2003). Os acidentes provocados por *P. nigriventer* constituem-se em problema de saúde pública, uma vez que apresentam incidência relativamente alta e, embora raramente sejam classificados como graves, podem causar diversos sinais e sintomas clínicos, eventualmente levando à morte. Alterações cardiovasculares e neurológicas, como hipertensão arterial, taquicardia, arritmia, distúrbios visuais e convulsões tônico-clônicas, têm sido descritas em casos graves de envenenamento. Os sintomas causados por envenenamento leve a moderado geralmente são dor e inchaço locais, eritema, sudorese, náusea, vômitos, salivação, diarréia, convulsões e priapismo (em criança), alguns dos quais indicam o envolvimento do sistema nervoso central e periférico (SNP). Em casos raros pode haver choque e edema pulmonar (Brazil & Vellard, 1925;1926; Bucaretchi *et al,* 2000, Antunes & Malaque, 2003).

Figura 4: *Phoneutria nigriventer* em posição de ataque, por isso conhecida como aranha "armadeira". Imagem disponível no web site da University of Washington (The Spider Myths Site; www.washington.edu).

2.1. Composição e ação do PNV em sistemas biológicos

Os venenos de aranha contêm moléculas com amplo espectro de massa (0,1-14 kDa), dentre elas, algumas alteram a função de canais iônicos e outros receptores celulares (Para revisão ver: Estrada *et al.,* 2007). Essas moléculas são potencialmente apropriadas para o estudo de mecanismos fisiológicos e fisiopatológicos em inúmeras células, tecidos e órgãos, principalmente os portadores de membranas excitáveis.

O veneno de *P. nigriventer* (PNV) é composto por uma complexa mistura de componentes neurofarmacologicamente ativos (Richardson *et al*., 2006; Rezende *et al*., 1991; Diniz *et al*., 1990; Cordeiro *et al*., 1992; Cordeiro *et al*., 1993). Há mais de 100 diferentes polipeptídeos na composição desse veneno (Richardson *et al*., 2006), os quais são ativos em canais iônicos neuronais (Ca^{2+}, Na^{+} e K^{+}) e em receptores de glutamato (NMDA) (Araujo *et al*., 1993; Troncone *et al*., 1995; Prado *et al*., 1996; Mafra *et al*., 1999; Figueiredo *et al*., 2001; dos Santos *et al*., 2002; Gomez *et al*., 2002; de Lima *et al*., 2002; Troncone *et al*., 2003; Vieira *et al*., 2005). Estudos de Fontana & Vital Brazil (1985) mostraram que o veneno ativa os canais de sódio voltagem dependentes. Em camundongos, a injeção de PNV intra-muscular ou no nervo ciático causa paralisia espástica dos membros posteriores, seguida por paralisia flácida. As alterações morfológicas incluem distorções no diâmetro das fibras nervosas periféricas com presença de vacúolos e aumento do volume dos nodos de Ranvier, locais de alta densidade de canais de Na^{+} envolvidos na transmissão saltatória. Essas alterações são compatíveis com aumento do influxo de Na^{+}, seguido passivamente por fluido (Cruz-Höfling *et al.,* 1985). Esses distúrbios fisiológicos e morfológicos são abolidos pelo pré-tratamento com TTX, um bloqueador de canais de Na^{+} (Love & Cruz-Höfling, 1986; Love *et al*., 1986).

Do ponto de vista bioquímico e farmacológico, esse veneno tem sido descrito como uma importante ferramenta para o desenvolvimento de novas moléculas biologicamente ativas com potencial de aplicação em medicina e agricultura (Escoubas *et al.,* 2000; Gomez *et al.,* 2002; Rash & Hodgson, 2002). Os primeiros estudos bioquímicos revelaram que o PNV possuía potentes neurotoxinas capazes de promover efeitos excitatórios, tais como salivação, lacrimação, priapismo, paralisia flácida e espástica dos membros anteriores e posteriores e morte em camundongos, após injeção intracerebral (Diniz, 1963; Entwistle *et al.,* 1982). Subsequentemente, três grupos de frações neurotóxicas (Phtx1, Phtx2 e Phtx3) e uma fração não tóxica, com atividade em músculo liso foram purificadas (Rezende *et al.,* 1991). Mais tarde, uma quarta fração (Phtx4) foi isolada, a qual foi extremamente tóxica em insetos da ordem Díptera e Dictióptera, mas com fracos efeitos tóxicos em camundongos (Figueiredo *et al.,* 1995). Os peptídeos denominados Tx2-5 e Tx2-6, provenientes do subfracionamento da Phtx2 do veneno de *P. nigriventer,* apresentaram efeito no tecido erétil de camundongo, após injeção direta nos corpos cavernosos. Esses peptídeos promovem relaxamento da musculatura lisa dos corpos cavernosos, causando ereção peniana (Andrade *et al*., 2008).

Portanto, a purificação de peptídeos tóxicos do PNV tem sido de grande interesse para o estudo da estrutura e papel fisiológico de canais iônicos e de receptores de membrana. A ação do veneno e de suas toxinas nas células, nos canais iônicos e em receptores alvo tem sido investigada no SNP, entretanto algumas das manifestações clínicas da intoxicação pelo PNV ou suas frações apontam o envolvimento do SNC. Essas questões levantaram a hipótese de, eventualmente, o veneno ser capaz de interagir com receptores/proteínas de membrana das células endoteliais, dos astrócitos ou da membrana basal dos microvasos cerebrais, alterando a permeabilidade da BHE. A investigação da ação central do PNV potencialmente aponta o veneno como importante ferramenta para estudar a barreira sangue-cérebro, com interesse do ponto de vista farmacêutico e biotecnológico.

2.2. *Ação do PNV na BHE e no SNC*

Vários venenos agem na integridade e funcionamento da BHE (Haspel *et al*., 2003; Le Sueur *et al*. 2003; Nunan *et al*., 2003; da Silva *et al*., 2004; Mortari *et al*., 2007; Rapôso *et al*., 2007) e têm sido úteis no entendimento da fisiopatologia dessa barreira. Estudos recentes demonstraram a ruptura da BHE pelo PNV (Le Sueur *et al*., 2003), através do aumento de transporte transcelular dependente de microtúbulos (Le Sueur *et al*. 2004) e de alterações nos níveis de laminina, proteína da membrana basal dos vasos da microcirculação cerebral (Rapôso *et al*., 2007). Foi demonstrado que essas alterações tinham diferentes modulações em função da área anatômica do SNC considerada e do tempo decorrido após a exposição ao veneno.

Foi observado que a quebra da BHE pelo PNV ocorreu no hipocampo, mas não ocorreu no córtex cerebral, cerebelo, tálamo e hipotálamo (Le Sueur *et al*., 2003). Esses estudos foram realizados utilizando o marcador extracelular nitrato de lantano ($LaNO_3$) injetado por via endovenosa que evidenciou aumento da população de vesículas de pinocitose contendo o traçador, sabidamente engajadas no transporte transcelular. O traçador também estava presente na fenda interendotelial, isto é, na via paracelular, que em condições normais é uma via interditada para o trânsito bidirecional de substâncias entre sangue-cérebro. O traçador foi ainda observado impregnando a membrana basal endotelial das células musculares das arteríolas e vênulas. Interessante notar que a permeabilização dos vasos foi diferencial dependendo do segmento vascular; as vênulas e arteríolas foram as primeiras a mostrar extravasamentos do traçador e só bem mais tarde é que os capilares o fizeram. Todas essas ocorrências eram uma clara indicação de que a BHE fora violada. Vários tempos de observação foram feitos no intervalo de 18 horas a 9 dias após o envenenamento.

Estudos posteriores investigaram o mecanismo de ação pelo qual o PNV alterava a permeabilidade da BHE 24 h e 9 dias após a injeção do veneno. Os autores constataram que a quebra da BHE ocorria pela via transcelular no endotélio dos microvasos hipocampais, através da alteração do transporte intravesicular dependente de microtúbulo (Le Sueur *et al.*, 2004). A análise da expressão imunohistoquímica e por *immunoblotting* de algumas proteínas juncionais (JO e JA - ocludina, ZO-1 e β-catenina) e do citoesqueleto endotelial, mostrou que a rota paracelular não estava envolvida nos tempos estudados (24 h e 9 dias) após o envenenamento. Entretanto, havia uma tendência de aumento (não significativo) na expressão da ocludina, sugerindo um mecanismo compensatório da via paracelular, em função da fragilização da via transcelular que fora violada nas suas propriedades de transporte restritivo e altamente seletivo (Le Sueur *et al*. 2004). Ademais, era necessário investigar se havia alteração de receptores transcelulares, tais como MRP, Pgp (proteínas de efluxo) ou GLUT (transportador de glicose), após a injeção do PNV, uma vez que esse veneno parece interferir na via transcelular.

Um ponto que precisava ser investigado era se em tempos mais precoces após o envenamento também ocorria quebra da BHE e se, nesses períodos, a via paracelular estava afetada. Os animais mostravam sinais clínicos de intoxicação (hiperemia, tremores, espasmos, sialorréia, paralisia flácida e espástica, convulsão, sofrimento respiratório e eventualmente morte) logo nos primeiros minutos após a injeção do veneno. Entretanto, o início da recuperação clínica nesses animais ocorria após 5 h aproximadamente e estendia-se até 12 horas, quando então se mostravam completamente normais. Hipotetizou-se que a permeabilidade da BHE poderia estar prejudicada desde tempos precoces após o envenenamento e, nesses tempos, as proteínas das JA e JO poderiam estar alteradas.

Dessa forma, o aumento da permeabilidade da BHE nos tempos de 15 minutos, 1, 2 e 5 horas após a injeção do veneno foi investigado em estudos prévios, pelo nosso grupo de pesquisa, através de

microscopia eletrônica de transmissão usando traçador eletro-opaco (nitrato de lantano) e imunohistoquímica para laminina (com a finalidade de avaliar a membrana basal), no hipocampo e cerebelo de ratos Wistar (Rapôso *et al*., 2007). Diferente do que fora observado por Le Sueur *et al*., (2003), nestes intervalos de tempo o extravasamento do traçador e o dano à membrana basal foi também observado no cerebelo. Os resultados mostraram a ocorrência de quebra da BHE após 1 e 2 horas, sendo que após 5 horas a permeabilidade dos capilares cerebrais diminuiu, sugerindo um início de recuperação da BHE, o que explica a melhora clínica do animal. Essas alterações caracterizavam-se pela presença de edema vasogênico e extravasamento do traçador e eram mais marcantes no hipocampo do que no cerebelo. Por outro lado, pés-astrocitários perivasculares edematosos, indicativo de gliose reativa, foram detectados somente no cerebelo. Também foi observada imediata (logo aos 15 min) e total diminuição no conteúdo da laminina, uma das principais proteínas da membrana basal e que influencia a expressão de proteínas das JOs (Tilling *et al*. 1998; Savettieri *et al*, 2000), resultando em total desaparecimento da visibilidade da membrana basal dos capilares cerebrais. Essas alterações foram transitórias, com gradual restabelecimento (a expressão da proteína foi se normalizando gradativamente, após 2 e 5 h da injeção do PNV) da imunomarcação da laminina, sendo esta recuperação mais rápida no cerebelo. Portanto, esses resultados sugeriam que a expressão das proteínas das JA e JO poderiam estar alteradas em momentos precoces do envenenamento pelo PNV (Rapôso *et al*., 2007).

Além da necessidade de investigar se as proteínas das JAs e JOs estariam alteradas pelo PNV, era também de interesse esclarecer o mecanismo (ou, ao menos, um dos mecanismos) pelo qual os componentes do veneno provocariam modificações nessas proteínas. A fosforilação das proteínas juncionais tem sido proposta como um mecanismo crítico na modulação da adesão e do contato célula-célula. Várias linhas de evidências sugerem que a fosforilação de resíduos de tirosina de complexos caderina-catenina regula a associação desses complexos com o citoesqueleto (Roura *et al*., 1999; Gaudry *et al*., 2001), influenciando a permeabilidade paracelular. A proteína fosfatase 2A (PP2A) tem sido apontada como responsável por cerca de 70 % de toda a atividade de defosforilação de resíduos de serina e treonina, em cérebro humano (Liu *et al*., 2005). Portanto, uma hipótese que precisava ser investigada era se ocorria diminuição da atividade da PP2A após a injeção do PNV, o que indicaria que as proteínas das JAs e JOs poderiam ter sido anormalmente hiperfosforiladas.

Temos demonstrado que as alterações induzidas pelo PNV na estrutura dos microvasos cerebrais são reversíveis e, como já mencionado, não atingem igualmente todas as regiões, mesmo em um quadro de intoxicação grave (dose sub-letal – 0,85 mg/Kg). Esse fato indica que a permeabilização da BHE pelo PNV é um evento transitório e, desde que afeta diferentemente diferentes regiões, tem caráter seletivo. Isso pode ser útil para o uso terapêutico dos componentes do veneno. Indica também que pode haver

diferenças regionais na permeabilidade da BHE. Isso é razoável uma vez que está bem estabelecida a existência de diferentes populações de astrócitos em diferentes áreas anatômicas do SNC.

A despeito da potencial aplicação terapêutica das toxinas do veneno, o mesmo causa efeitos tóxicos nos componentes do tecido. A toxicidade do PNV no SNC precisa ser investigada. Este ponto é de grande importância uma vez que os efeitos tóxicos são transitórios, a gravidade e letalidade dos acidentes são raras, características que podem ser extremamente favoráveis a aberturas temporárias da BHE para fins terapêuticos.

Os astrócitos são células que respondem prontamente ao veneno circulante, como visto pelos pés-vasculares astrocitários edemaciados observados ao microscópio eletrônico de transmissão (Le Sueur *et al*., 2003; Rapôso *et al*., 2007). É importante confirmar se marcadores típicos de ativação astrocitária, as proteínas GFAP (citoesqueleto) e S100 (metabolismo do cálcio) têm sua expressão alterada pelo PNV. Além disso, astrócitos reativos podem desencadear reação inflamatória, causando danos ao tecido. Estudos têm mostrado que mediadores inflamatórios, tais como as citocinas produzidas no sítio da inflamação, podem ser, pelo menos parcialmente, responsáveis pelas alterações na permeabilidade vascular. Injeções intra-craniais de TNF-α e interleucina-1beta (IL-1β) aumentam a permeabilidade da BHE em ratos, enquanto o lipopolissacarídeo (LPS) aumenta a permeabilidade de modelos *in vitro* de BHE (Abbott & Revest, 1991; Burke-Gaffney & Keenan, 1993; Yuan, 2000; Mayhan, 2001). Um outro ponto a ser inverstigado sobre a toxicidade do PNV é a integridade da comunicação astrócito-astrócito e astrócito-célula endotelial, por meio das junções tipo *gap*. A investigação da gliose reativa, da integridade das junções tipo *gap* e da expressão de citocinas inflamatórias no SNC, tanto *in vivo*, quanto em modelo *in vitro* de cultura primária de astrócitos, podem esclarecer a ação do veneno no tecido neural.

Embora a BHE seja claramente atingida pelo PNV, até o momento não conseguimos perceber alteração morfológica no corpo dos neurônios após o envenenamento. Entretanto, foram vistas alterações nos terminais sinápticos. Porém, estudos realizados com vistas a determinar a ação do veneno dessa aranha sobre a atividade neuronal, através do mapeamento da expressão da proteína FOS (fosfoproteína nuclear produzida nos neurônios em resposta a vários estímulos - Krukoff, 1993; Herrera & Robertson, 1996; Willoughby *et al,* 1997), revelaram que várias regiões do cérebro são ativadas (apresentam neurônios ativados) em decorrência da intoxicação.

2.3. Áreas do SNC ativadas pelo PNV

A marcação para FOS, proteína codificada por um gene de expressão primária, tem sido usada para determinar a ativação neuronal. A expressão dessa proteína é considerada uma ferramenta eficiente para identificar neurônios ativados sob diferentes condições experimentais (Dragunow & Robertson,

1987; Craner *et al.*, 1992; Hoffman *et al.*, 1993). Os neurônios estimulados por agentes tóxicos ativam genes de expressão primária como uma primeira onda de transcrição gênica. As proteínas desses genes são translocadas para o núcleo para ativar a transcrição de outros genes, resultando numa segunda onda de atividade gênica (Hughes & Dragunow, 1995). A proteína FOS pode influenciar a síntese de enzimas e a produção de neurotransmissores por meio de sua ligação a sequências específicas de DNA.

Estudos prévios, realizados em nosso laboratório, mostraram aumento significativo no número de neurônios FOS-positivos após injeção sistêmica do PNV em áreas relacionadas à motricidade/aversão/ansiedade/fuga, tais como o córtex motor parietal (PCM), a substância cinzenta periaquedutal ventral (vPAG) e dorsolateral (dlPAG) e o núcleo talâmico periventricular (PTN), e em áreas relacionadas a estresse agudo, tais como o córtex rinal (RC) e o núcleo septal lateral (LSN). O maior aumento relativo no número de neurônios FOS-positivos ocorreu nas áreas relacionadas com fuga/aversão/ansiedade/motricidade vPAG, PCM e PTN. A marcante ativação ocorrida nessas áreas e, em menor grau, nas áreas relacionadas ao estresse sugere o envolvimento de vias neuronais localizadas nessas regiões em resposta ao PNV. Com o objetivo de correlacionar essas possíveis vias neuronais ao envolvimento do óxido nítrico (NO), nessas mesmas áreas foi feita reação para imunodetectar neuônios positivos à sintase neuronal do óxido nítrico (nNOS). Os resultados mostraram que neurônios nNOS positivos predominaram no PTN, seguido por dlPAG e PCM, indicando que o NO é um mensageiro que pode estar envolvido no mecanismo da intoxicação pelo veneno (Cruz-Höfling *et al.,* 2007). Nossos resultados indicando que a proteína FOS está sendo expressa pelos neurônios de áreas cerebrais específicas sustentam a hipótese de que o veneno afeta a atividade neuronal, seja direta ou indiretamente (através de segundos mensageiros). A hipótese de que o NO pode estar envolvido nos efeitos do PNV no SNC precisava ser mais bem investigada.

Embora tenha sido observada, em estudos prévios, a ativação de vias neuronais em áreas do cérebro relacionadas com motricidade, os sinais clínicos do envenenamento pelo PNV envolvem tanto disfunções motoras (paralisia, convulsão), quanto neurovegetativas (estresse respiratório, edema pulmonar, salivação intensa, hipertensão, diminuição do volume urinário). O núcleo supraóptico (SON) é uma área reguladora do fluxo salivar, da excreção renal de sódio, do volume urinário e da pressão arterial e o NO influencia essa regulação (Saad *et al*., 2004). O núcleo hipotalâmico paraventricular (PVN) influencia a regulação de funções neuroendócrinas, cardiovasculares e respiratórias, em ratos (Yeh *et al*., 1997). Portanto, além das regiões cerebrais ligadas à motricidade/aversão/ansiedade/fuga (PCM, dlPAG, vPAG e PTN), seria provável que esses núcleos hipotalâmicos (SON e PVN) também estivessem envolvidos no mecanismo de intoxicação pelo PNV.

O corpo celular das células neurosecretórias magnocelulares do SON e do PVN representam a principal via neuroendócrina de síntese de vasopressina (AVP) e oxitocina (OT) (Brownstein *et al*.,1980;

Swanson & Sawchenko, 1983). A AVP é essencial para a homeostase, agindo via rim para regular a reabsorção de água, na vasculatura para regular o tônus do musculo liso e como um neurotransmissor central, na modulação da função autonômica do tronco cerebral (Barrett *et al*., 2007). OT está também envolvida na homeostase hidromineral e no relaxamento vascular e cardíaco (Conrad *et al*., 1986; Gutkowska *et al*., 2000; Jankowski *et al*., 2000). Como um componente genuíno do eixo neuroendócrino, as células neurosecretórias magnocelulares hipotalâmicas estão sob o controle de vários moduladores, dentre os quais o NO ganhou considerável atenção nos últimos anos (Kadowaki *et al*., 1994; Srisawat *et al*., 2000; Ventura *et al*., 2002, 2005; Stern *et al*., 2003). O NO é um radical livre gasoso, que age como um neuromodulador (Moncada *et al*., 1991). A idéia de que o NO poderia estar envolvido no controle da liberação de VPS e de OT foi reforçada pela identificação da enzima produtora desse gás (enzima sintase do óxido nítrico – NOS) no sistema hipotálamo-neurohipofisário (Bredt *et al*., 1990). Experimentos *in vivo* mostraram que o NO tem um efeito inibitório na liberação de OT (Kadekaro *et al*., 1998; Ventura *et al*., 2005), mas para AVP, a literatura é controversa (Yasin *et al*., 1993; Liu *et al*., 1998; Yamaguchi & Hama, 2003; Ventura *et al*., 2005). Interessantemente, estudos eletrofisiológicos demonstraram que o NO diminui a taxa de atividade das células neurosecretórias magnocelulares hipotalâmicas, sugerindo que o NO é um inibidor da liberação da AVP e da OT (Liu *et al*., 1997; Stern, 2004). Desde que a intoxicação pelo PNV altera o tônus vascular, causando hipertensão, e o volume urinário, é possível que as vias neuroendócrinas do SON e do PVN sejam afetadas.

Além de influenciar na liberação de AVP e OT, o NO presente no SON e na área septal medial exerce um papel inibitório na regulação da secreção salivar. Tanaka *et al*. (2008) demonstraram, usando coloração de Nissl e histoquímica para nicotinamida adenina dinucleotídeo fosfato diaforase (NADPH-d), que a produção de NO em neurônios do SON aumenta com a idade e que esse aumento pode ser um fator que contribui para a inibição da secreção salivar relacionada com a idade.

Saad *et al*. (2004) investigaram os efeitos da injeção direta no SON, de FK409 (um doador de NO) e do NW-nitro-L-arginina metil ester (L-NAME), um inibidor da NOS, na secreção salivar, na pressão arterial, na excreção de sódio e no volume urinário alterados pela pilocarpina. FK 409 atenuou o aumento da secreção salivar induzido pela pilocarpina. A pilocarpina aumentou a pressão arterial e o L-NAME potencializou esse aumento, enquanto o FK409 atenuou o efeito da pilocarpina na pressão arterial. Pilocarpina injetada no SON induziu aumento na excreção de sódio e no volume urinário. L-NAME potencializou o aumento na excreção de sódio e o volume urinário induzidos pela pilocarpina. FK409 diminuiu o volume urinário e a excreção de sódio induzidos pela pilocarpina. Uma vez que o PNV interfere na salivação, na pressão arterial e no volume urinário, é possível que o veneno atue no SON, alterando a liberação do NO.

O PNV também causa edema pulmonar e altera a função respiratória, podendo levar à morte. Neurônios do PVN e do SON participam na regulação da atividade respiratória e na coordenação das funções cardiovasculares (Yeh *et al*., 1997). Luo *et al*. (2000) examinaram os efeitos da hipóxia hipobárica (exposição a altitudes elevadas) nos neurônios do PVN e do SON do hipotálamo de ratos. A hipóxia hipobárica induziu a expressão de FOS e de nNOS no PVN e no SON. Portanto, tanto o PVN, quanto o SON de ratos adultos são ativados na hipóxia provocada pela exposição a altitudes elevadas e podem estar envolvidos na regulação de funções neuroendócrinas, cardiovasculares e respiratórias.

Portanto, os núcleos hipotalâmicos, SON e PTN, podem estar envolvidos na alteração de funções neurovegetativas induzidas pelo PNV (hipersalivação, hipertensão, alteração da frequência e função respiratória, diminuição do volume urinário e edema pulmonar). Além disso, uma vez que esses núcleos apresentam grande número de células expressando NOS, o NO pode ser um modulador da toxicidade do veneno, nessas vias.

3. Óxido nítrico (NO)

No final de 1980, foi demonstrado que alguns tipos celulares produzem NO e que essa molécula gasosa está envolvida na regulação dos sistemas cardiovascular, imune e nervoso. O NO é um radical livre, difusível através das membranas, capaz de modificar muitas condições fisiológicas e patológicas e de interagir com muitos alvos intracelulares para desencadear vias de transdução de sinais, resultando em saída de sinais estimulatórios ou inibitórios.

O NO é produzido a partir do aminoácido l-arginina por membros de uma família de enzimas sintases do NO (NOS), dependentes de calmodulina (Bredt & Snyder, 1990; Förstermann *et al*., 1991; Bredt, 1999). Essa enzima existe em três isoformas: NOS neuronal (nNOS), endotelial (eNOS) e induzível (iNOS) (Forstermann *et al*., 1991); A nNOS e a eNOS são enzimas expressas constitutivamente, citossólicas, Ca^{2+}/Calmodulina dependentes, cujas atividades são estimuladas pelo aumento de cálcio intracelular (Bredt & Snyder, 1990; Klatt *et al*., 1992; Bredt, 1999). A nNOS, no SNC, ocorre nos corpos celulares neuronais, dendritos e axônios (Bredt *et al*., 1990) e apresenta localização discreta em estruturas cerebrais (Barjavel & Bhargava, 1995). As funções imunes do NO são mediadas pela enzima independente de cálcio, iNOS. A expressão da enzima iNOS requer ativação transcricional, que é mediada por combinação específica de citocinas.

Uma vez que o NO é uma molécula gasosa, que se difunde rapidamente, esse modulador tem sido estudado indiretamente, através de imunohistoquímica para as NOS, detecção de nitrito (um metabólito estável do NO) e histoquímica para NADPH diaforase (NADPHd). A histoquímica para NADPH-d marca seletivamente populações de neurônios que expressam as NOS, pois essas enzimas são competitivamente

inibidas pelo substrato da NADPH-d, *nitroblue tetrazolium*. Tem sido demonstrado que essa técnica proporciona um marcador histoquímico específico para neurônios que produzem NO (Bruce *et al*., 1991).

No SNC, o NO tem algumas funções, tais como regulação da plasticidade sináptica, do ciclo do sono, regulação do tônus dos vasos sanguíneos, secreção de hormônios, neurotransmissão e resposta imune e inflamatória. A primeira evidência do papel do NO como um neurotransmissor foi descrita por Garthwaite *et al*. (1988), que demonstrou que a estimulação dos receptores de glutamato do tipo NMDA (N-metil d-aspartato) cerebelares causava a liberação de uma molécula difusível com grande similaridade com o fator de relaxamento derivado do endotélio (FRDE) (Garthwaite *et al*., 1988; Marletta, 1993; Feelisch *et al*., 1994; Hobbs & Ignarro, 1996). Pouco antes de esse estudo ser publicado, o NO foi identificado como sendo o próprio FRDE (Ignarro *et al*., 1987; Palmer *et al*., 1987). Subsequentemente, foi demonstrado que o NO age como um neurotransmissor, tanto no SNC quanto no SNP por mecanismos que são dependentes de GMP (Sanders & Ward, 1992; Garthwaite & Boulton, 1995). O NO tem também um papel neuromodulador, regulando a liberação de neurotransmissores em muitas áreas do cérebro (Bredt *et al*., 1991; Brenma & Bredt, 1996). Seu papel na resposta imune e inflamatória no cérebro envolve as células gliais, principalmente astrócitos e micróglia, que são os principais componentes que medeiam a resposta imune e a inflamação no SNC (Allan & Rothwell, 2001). As células gliais podem produzir citocinas, radicais reativos de oxigênio e NO em resposta a vários insultos, levando à exacerbação do processo de doença. A resposta inflamatória das células gliais exerce papel em muitas condições patológicas, incluindo doenças neurodegenerativas, acidentes vasculares cerebrais, injúria traumática e doenças infecciosas (Barone & Feuerstein, 1999; González-Scarano & Baltuch, 1999). O NO pode ter, portanto, dentre outros, o papel de um neurotransmissor ou neuromodulador, alterando a atividade neuronal, bem como de um mediador da resposta imune, modulando a reação de gliose (Choi & Koh, 2008).

Particularmente interessante é que o NO, em quantidades fisiológicas, tem papel neuroprotetor, enquanto altas concentrações são claramente neurotóxicas (para revisão, ver Calabrese *et al*., 2007). Além disso, se uma célula está em estado pró-oxidante, o NO pode ser submetido a reações de óxido-redução, dando forma a compostos tóxicos (estes pertencem a uma família conhecida como espécies reativas de nitrogênio – por exemplo, o peroxinitrito), os quais causam dano celular. O NO e as espécies reativas de nitrogênio têm sido implicados na patogênese de desordens neurodegenerativas (Castegna *et al*., 2003; Sultana *et al*., 2006).

A influência do NO na toxicidade induzida pelo PNV tem sido estudada. Yonamine *et al*. (2004) reportaram que o pré-tratamento com 7-nitroindazole (inibidor seletivo da nNOS) aboliu sinais da intoxicação causados pela injeção intraperitoneal da toxina isolada do PNV, Tx2-5, tais como priapismo, salivação e edema pulmonar, em ratos. Os autores concluíram que o NO é o principal mediador envolvido

nessa resposta. Concorrentemente, como já mencionado, ativação neuronal (vista através do aumento da marcação de FOS) foi demonstrada em neurônios de áreas relacionadas com motricidade/aversão/ansiedade/fuga e stress agudo, a maioria delas também ricas em neurônios positivos para nNOS, após administração sistêmica do PNV, em ratos (Cruz-Höfling *et al*., 2007). É necessário investigar melhor, em modelos *in vivo* e *in vitro*, o papel do NO no envenenamento, tanto como um neurotransmissor e neuromodulador (influenciando na ativação de vias neuronais), quanto como um mediador da inflamação (influenciando a resposta astrocitária ao PNV). A injeção de PNV pode ser um modelo útil de estudo do NO e, além disso, a partir do entendimento do mecanismo de ação do veneno, novos tratamentos para os casos de acidentes por *Phoneutria nigriventer* podem surgir.

OBJETIVOS

O presente trabalho se propôs a investigar:

***I.* A toxicidade e ação do veneno de *P. nigriventer* na BHE, em períodos precoces (15 min, 2 e 5 h) após injeção sistêmica (i.v.):**

a) Alterações na expressão de proteínas da via paracelular da BHE (ocludina, ZO1, β-catenina, claudina-5) e da membrana basal (laminina), através de imunofluorescência e/ou western blotting;

b) Alterações na expressão da proteína fosfatase 2A (PP2A) em seu estado inativado (fosforilado – pPP2A), através de western blotting. Aumento na expressão da pPP2A indica alterações nos mecanismos de defosforilação das proteínas de junção da BHE e aumento da permeabilidade;

c) O envolvimento da via transcelular da BHE, através da análise, por imunofluorescência e/ou western blotting, da expressão das proteínas de efluxo, P-glicoproteína (Pgp) e MRP1, e de influxo, transportador de glicose GLUT1;

d) A participação das junções *gap* na sinalização célula-célula durante o envenenamento pelo PNV, avaliando a expressão da conexina 43, através de imunofluorescência e western blotting.

***II.* A toxicidade e ação do veneno de *P. nigriventer* no tecido neural e o envolvimento do óxido nítrico:**

a) O envolvimento do óxido nítrico na ativação de circuitos neuronais específicos após a injeção sistêmica do PNV, através de marcação histoquímica para NADPH-d e imunohistoquímica para proteína FOS (dupla-marcação FOS/NADPH-d). O papel do óxido nítrico também foi investigado pelo tratamento (injeção i.p) com inibidor seletivo da nNOS (7- Nitroindazol), antes da injeção do PNV, seguido de dupla-marcação do tecido para proteína FOS e NADPH-d;

b) Análise da expressão de GFAP, nNOS e das citocinas inflamatórias INFγ e TNFα, em cultura primária de astrócitos corticais de ratos recém nascidos incubada com PNV, associado ou não ao 7-Nitroindazol. Medida da liberação de nitrito no meio de cultura, indicador indireto da produção de óxido nítrico pelos astrócitos, após incubação com PNV, associado ou não ao 7NI.

***III.* A permeabilização da BHE por frações purificadas do veneno de *P. nigriventer*:**

a) Identificar neurotoxinas purificadas do veneno de *P. nigriventer* por HPLC (*high performance liquid chromatography*), responsáveis por provocar a permeabilização da BHE. A ação das toxinas purificadas na BHE foi avaliada através da injeção i.v. de cada uma separadamente, seguida pela injeção i.v. do corante vital Azul de Evans.

Estudos ao microscópio de luz e eletrônico de transmissão estão em andamento com o objetivo de quantificar e qualificar a ação dessas frações na permeabilidade da BHE.

CAPÍTULO II - RESULTADOS

*****Maria Alice da Cruz-Höfling
Departamento de Histologia e Embriologia
Instituto de Biologia, C.P. 6109
Universidade Estadual de Campinas (UNICAMP)
13 087-130, Campinas – SP – BRASIL
E-mail: hofling@unicamp.br
Tel. (55)(19) 3521 6224; Fax. (55)(19) 3289 3124

Phoneutria nigriventer venom impairs expression of junctional proteins in blood brain barrier through phosphatases deactivation pathway

Catarina Rapôs [1], Paulo Alexandre Miranda Odorissi[1], Roberta R Sousa[2], Hiroshi Aoyama[2], Carmen Verissima Ferreira[2], Liana Verinaud[3], Karina Fontana[4], Maria Alice da Cruz-Höfling[1*]

[1]Departamento de Histologia e Embriologia, [2]Departamento de Bioquímica and [3]Departamento de Microbiologia e Imunologia, Instituto de Biologia; [4]Departamento de Farmacologia, Faculdade de Ciências Médicas, Universidade Estadual de Campinas – UNICAMP, Campinas, SP, Brazil

Abbreviated title: Venom impairs paracellular BBB by phosphatase pathway

Abstract

The regulation of BBB permeability is complex and involves intracellular signaling and rearrangement of tight (TJ) and adherens (AJ) junction proteins. Protein phosphatase 2A (PP2A), a serine/threonine phosphatase, has key role in signal transduction pathways and regulates the phosphorylation/integrity of TJ/AJ proteins. Systemic *P. nigriventer* spider venom (PNV) induces transient BBB opening, seen through extracellular tracer vascular leakage, perivascular edema, reactive astrogliosis, neuroinflammation and FOS and nNOS expression in multiple brain regions of rats. Here, the investigation, by western blotting and immunofluorescence, of mechanisms by which PNV increased microvascular permeability in hippocampus and cerebellum at acute stages showed immediate decrease in the expression level of ZO1, occludin, claudin-5 and betacatenin, laminin and the efflux protein P-gp, concomitant with increased phosphorylated PP2A. The expression of all studied proteins was resolved between 2-5 h, simultaneous to clinical evolution of envenoming signals. In general, the impairment of the proteins expression was more prominent in cerebellum, even though the recovery of cerebellum was faster than hippocampus. The fast recovery of protein expression suggests that PNV could be useful as tool for temporary opening of BBB. Further investigation might be addressed towards its therapeutic use as a mean to drug delivery to the CNS.

Keywords: endothelial cells, adhesion molecules, efflux protein, basement membrane spider venom.

Introduction

The wandering Brazilian armed-spider *Phoneutria nigriventer* (Ctenidae, Araneomorpha) is responsible for most cases of envenomation in Brazil (Bücherl and Buckley, 1976). The *P. nigriventer* venom (PNV) contains various Ca^{2+}, K^+ and Na^+ channels-acting basic peptides (Gomez *et al*, 2002) that are capable of inducing neurotoxic and excitatory actions in mammals and insects (Brazil and Vellard, 1925; Cruz-Höfling *et al*, 1985; Love and Cruz-Höfling, 1986), increase vascular permeability (Antunes et al. 1992), arterial blood pressure (Costa *et al*, 1996), activate capsaicin sensory nerves, induce paw oedema (Costa *et al* 1997, 2001), cause penile erection (Nunes *et al*, 2008), activate specific brain areas (Cruz-Höfling *et al*, 2007), cause neuroinflammation (Cruz-Höfling *et al*, 2009) and induce blood-brain barrier (BBB) breakdown (Le Sueur *et al*, 2003, Rapôso *et al*, 2007).

The PNV-induced BBB breakdown resulted from increased microtubulemediated vesicular transport, apparently with no compromise of TJ/AJ proteins in the periods investigated (1 and 9 days) (Le Sueur *et al*, 2004). The BBB breakdown was variable in magnitude and chronology in different CNS regions (Le Sueur *et al*, 2003, Rapôso *et al*, 2007) leading us to infer that paracellular disruption could occur temporarily. Some evidences support this hypothesis: the clinical evolution of the neurotoxic signs changed from intense soon after envenoming to moderate 5 h later (Rapôso *et al*, 2007), and was absent at 12 h (Le Sueur *et al*, 2003; 2004), suggesting that the neurological outcome has been resolved; biodistribution studies of PnTx2-6, a Na^+ channel-acting neurotoxin of PNV, showed that the maximum toxin concentration into the brain was achieved between 5-15 min after i.p. injection, thereafter it was drastically reduced, despite growing toxin uptake by the thyroid gland from circulation continued for hours (Yonamine *et al*, 2005). These findings suggest that BBB opening might likely have occurred very early after envenoming, and that a mechanism of repair was straight away activated. Such hypothesis are consistent with reduction of tracer leakage and laminin loss from cerebellar and hippocampal microvessels subsequent to the initial acute periods (Rapôso *et al*, 2007).

Phosphorylation of junctional proteins is a critical step in cell-cell adhesion and contact modulation. Several lines of evidences suggest that tyrosine phosphorylation of the cadherin-catenin complex regulates the association of the complex with the cytoskeleton (Roura *et al*, 1999; Gaudry *et al*, 2001), and influence paracellular permeability. Protein phosphatase PP2A has been pointed as responsible for over 70% of all phosphoseryl/phosphothreonyl activity in human brain (Liu *et al*, 2005). We hypothesized that at early period post-PNV injection TJ and AJ proteins could be abnormally hyperphosphorylated by downregulation of PP2A activity.

Here, the hypothesis that BBB permeability could take place through the interendothelial cleft was investigated. The expression of the junctional proteins, occludin, claudin-5, ZO1 (TJ), β-catenin (AJ) and the phosphorylation changes were investigated through phosphoPP2A (pPP2A) activation. In addition, the expression of P-glycoprotein (P-gp), a transcytosis-acting protein efflux, and laminin, both the major protein of the basement membrane and a common ligand for cell-to-matrix proteins were investigated.

Experimental procedures

Animals and venom

Male Wistar rats (250–300 g) were obtained from an established colony maintained by the Central Animal House Service at UNICAMP. One batch of lyophilized *P. nigriventer* crude venom (PNV) was supplied by Instituto Butantan (São Paulo, SP, Brazil). The venom was stored at -20ºC and dissolved in 0.9% sterile saline solution immediately before use. The experiments were done according to the guidelines of the Brazilian College for Animal Experimentation (COBEA) and approved by the University's Ethics Committee in Experimental Animal Use (CEEA/IB/UNICAMP, protocol n. 1700-1).

Envenoming procedure

Male rats were given a single i.v. injection of PNV (0.85 mg/kg in 0.5 ml saline) in the tail vein. The PNV concentration was selected based on previous studies in our laboratory (Le Sueur et al., 2003, 2004). To control group was given the same volume of 0.9% sterile saline solution (sham group). 15 min, 2 and 5 h after PNV or saline injection (n = 5/time interval), the animals were anesthetized with an i.p. injection (2 mg/mg body mass) of 3:1 mixture of ketamine chloride (Dopalen®, 100 mg kg^{-1} body weight) and xylazine chloride (Anasedan®, 10mgkg^{-1} body weight) (Vertbrands, Jacarei, SP, Brazil).

Western Blotting (WB)

Control and PNV-treated rats were anaesthetized and killed by decapitation 15 min, 2 and 5 h after saline or venom injection. The brains and cerebella were quickly dissected; the hippocampus was isolated from brain and both regions were homogenized in an extraction cocktail (10 mM EDTA, Amresco, Solon, Ohio, USA; 2 mM PMSF, 100 mM NaF, 10 mM sodium pyrophosphate, 10 mM NaVO4, 10 μg of aprotinin/ml and 100 mM Tris, pH 7.4, all by Sigma, Saint Louis, Missouri, USA). Hippocampi or cerebella from animals killed 15 min, 2 h or 5 h after saline-injection were mixed and homogenized to form a control pool from each region (n = 15 total each

region). This single control was used for evaluating WB of protein contents in hippocampus or cerebellum and comparison with the PNV-treated (15 min, 2 h or 5 h). The homogenate was centrifuged at 3000xg for 10 min and the supernatants collected and stored at -70ºC until used for immunoblotting. The proteins (50 μg) were separated on 6.5 % (for ZO1), 8 % (for occludin, β-catenin, laminin and pPP2A) and 12% (for claudin-5) sodium dodecyl sulfate-polyacrylamide (Amresco, Solon, Ohio, USA) by gel electrophoresis under reducing conditions and were electrophoretically transferred onto nitrocellulose membrane (BioRad Laboratories, ref. 162-0115, Hercules, CA, USA). After blocking overnight at 4ºC with 5 % or 2.5 % non-fat milk in TBS-T (Tris-buffered saline 0.1 % with 0.05 % Tween 20, pH 7.4), the membranes were incubated at room temperature (RT) for 4 h, with rabbit polyclonal antibody against claudin-5 (1:250), occludin (1:500), β-catenin (1:1000), ZO1 (1:500) (Zymed, San Francisco, CA, Refs. 1393424, 352500, 711500 and 138400, respectively), laminin (1:500) (Sigma, Ref. L9393), pPP2A (1:500, Santa Cruz Biotechnology, Santa Cruz, CA, USA), diluted in buffer solution TBS-T containing 3 % non-fat milk. After washing (five times, 8 min each) in TBS-T, the membranes were further reacted with horseradish peroxidaseconjugated anti-rabbit or anti-mouse IgG (1:1000, Sigma, Refs. A6154 and A9309, respectively), diluted in TBS-T with 1 % non-fat milk, for 1 h, at RT. A chemiluminescence reagent (Super Signal, Pierce, Rockford, IL, USA) was used to make the labeled protein bands visible and the blots were developed on X-ray film (Fuji Medical, Kodak, Ref Z358487-50EA, Rochester, N.Y., USA). For quantification, the density of each band was determined by the NIH Image 1.41 program (available at ftp from *zippy.nimh.nih.gov/* or from *http://rsb.info.nih.gov/nih-image*; developed by Wayne Rasband, NIH, Bethesda, MD). For each protein investigated the results were confirmed in three sets of experiments. Immunoblot for β-actin was done as a control for the above protein blots. After protein blots visualization with enhanced chemiluminescence, the protein antibodies were stripped from the membranes, which were reprobed with monoclonal anti-β-actin antibody (1:250, Sigma, USA) and subsequently protein densitometry was done. The ratio of each investigated protein/β- actin was calculated and compared to saline-pooled (sham) control.

Immunofluorescence (IF)

In order to determine displacement or expression changes in the proteins studied, the IF was assessed in hippocampus and cerebellum of saline and PNVinjected rats. Animals were anesthetized and perfused transcardiacally with 4 % paraformaldehyde (Synth, Diadema, São Paulo, Brazil) in ice-cold PBS (0.1 M, pH 7.4, Synth). The brains were dissected and immersed in 15 % sucrose overnight, after which were included in OCT-Tissue Tek (Sakura Finetek, Torrance, CA, USA) and frozen in *n*-hexane (Dinâmica, São Paulo, SP, Brazil) with liquid nitrogen. Cryosections, 10 μm

thick, were collected on glass slides and air dried. After washing in TBS, the sections were permeabilized with 0.3% Triton X-100 for 10 min at RT and treated with 5 % nonfat milk for 1 h added with 0.1% Tween 20, to block nonspecific binding of antibodies. Subsequently, the sections were reacted with same antibody described in "Western blotting" sub-section for laminin, occludin, claudin-5 and P-glycoprotein (dilution for all was 1:50) (Sigma, Ref. P7965). The primary antibodies were incubated overnight at 4ºC, afterward were washed with TBS, then incubated with FITC- or TRITCconjugated polyclonal secondary antibody against rabbit or mouse immunoglobulins (SIGMA, Ref. F6257 and B7151 respectively, 1:200) for 1 h at RT. The slides were then washed with TBS and mounted in fluorescent mounting medium (DakoCytomation) for observation under a fluorescence microscope (Olympus).

Statistical analysis

The results were expressed as means ± S.E.M, where appropriate. The densitometric values of the immunoreactive bands (immunoblotting) were analyzed using the Graphpad Prism software package. Student t test, or One-way analysis of variance (ANOVA) followed by the *Tukey-Kramer post-test* was used to compare the treated and control groups. A value of $P < 0.05$ indicated statistical significance.

Results

PNV induces clinical signs of neurotoxicity

After venom administration the animals showed signals of intoxication which included variably hyperemia, piloerection, tremors, hypersalivation, reduced locomotor's and diuresis activity and some difficulty in breathing. Practically all animals presented flaccidity followed by spastic paralysis of posterior legs and tonic convulsion. At least 0.5% of the animals died soon after venom i.v. injection. After 3 h animals showed clear signal that recovery was underway; salivation, tremors and paralysis of members had vanished, but prostration and/or low locomotor activity persisted. At 5 h post-PNV injection the clinical condition had improved, but it was only at 12 h that the complete recovery was achieved, corroborating earlier findings (Le Sueur et al., 2003). Rats injected with sterile saline (sham controls) appeared normal and showed none of the clinical signs described above whatever the survival period. Since clinically sham controls from different time-points were indistinguishable from each other, hippocampus or cerebellum from all time-points were homogenized together to form a single control for WB assays (n= 15).

Western blotting and immunofluorescence

The effect of PNV on the paracellular barrier of the hippocampal and cerebellar endothelia was assessed, by WB and/or IF, based on the content of some proteins associated with cell-cell adhesion (TJ- and AJ-associated proteins) and cell-matrix adhesion (laminin). Despite efforts we were unsuccessful to detect Pgp by WB. Then, this protein was investigated just by IF. On the other hand, occludin, β-catenin, ZO1 and pPP2A were evaluated only through WB. Laminin and claudin-5 were assessed by both WB and IF.

PNV caused immediate decrease in the expression level of tight- and adherens junctions-associated proteins, laminin and P-gp-efflux proteins in hippocampus and cerebellum. The expression of all studied proteins was recovered between 2-5 h. In general, the proteins reduction was more prominent in cerebellum, even though the recovery was faster in cerebellum than in hippocampus.

Laminin: Laminin appeared as continuous fluorescent labeling outlining the endothelial wall of the brain microvessels in controls (**Figure** 1A,B,C). PNV injection promoted an immediate (15 min) decrease in laminin immunolabeling (IF) and content (WB) both in hippocampus and cerebellum; WB bands density indicated equal content of the protein in both regions. There was significant reduction of the protein content in all time-points ($P < 0.001$) in hippocampus, whereas just at 15min in cerebellum ($P < 0.001$), followed by a subsequent significant increase at 2 h ($P < 0.05$). The immunofluorescence intensity at the time intervals examined practically paralleled the laminin immunoblots content represented by the histogram. Subtle differences between IF and WB were ought to specificities of the techniques. While IF is obtained from cryo-histological sections, immunoblots result from homogenate of the whole cerebral region examined. An overview of the IF intensity in the time-points studied was displayed in Figure 1D,F,H,J (hippocampus) and Figure 1E,G,I,K (cerebellum).

Claudin-5: The histogram representative of claudin-5 immunoblots from controls showed higher content of the protein in hippocampus compared to cerebellum. The tendencies to increase or decrease the density of pixels of claudin-5 immunoblots did not achieve statistic significance both in hippocampus and cerebellum of PNVexposed rats and this was attributed to individual differences (n = 5) (Figure 2A,B,C). Claudin-5 immunofluorescence appeared as discrete, frequently uneven fluorescent labeling outlining the endothelial wall of brain microvessels (Figure 2, D-K).; this “patch-like” pattern can be explained by the protein location just at junctional sites of endothelial cells, differently from laminin which is part of the basement membrane surrounding the

entire endothelium Both in hippocampus and cerebellum, the changes in immunofluorescence observed in the different time-points were dim, consistent with the WB findings. Nevertheless, both in hippocampus (Figure 2E,F) and cerebellum (Figure 2I,J) the protein immunofluorescence decreased until 2 h post-envenoming indicating a progressive disorganization and probably internalization of claudin-5. After that, claudin-5 gained stronger immunolabeling in hippocampus (Figure 2G) and principally in cerebellum (Figure 2K) of PNV-5 h animals, indicating that recovery was underway. Vessels limits became visible again. Moreover, in the cerebellum the vessels labeling indicates claudin-5 upregulation (panel K).

P-glycoprotein: This protein was seen delineating the vessels, but in some points the IF was brighter, probably where P-gp was more concentrated (Figure 3). Qualitative IF analysis showed P-gp poorly expressed in hippocampus (Figure 3A) whereas strongly in cerebellum; tangential sections of the vessels showed that the protein was spread all over the vessels' surface in controls (Figure 3B). The protein expression level was stable at PNV-15 min, decreased in PNV-2 h and was overexpressed at PNV-5 h in hippocampus (Figure 3C,E,G). In cerebellum, after an immediate and abrupt reduction, P-gp expression gradually recovered and in the PNV-5 h group this efflux transporter protein was consistently and strongly upregulated in microvessels of variable caliber (compare Fig 3H with 3B,D,F).

ZO-1: The ZO-1 protein content, assessed by WB, showed an immediate significant decrease in hippocampus (* $p < 0.05$) and cerebellum (*** $p < 0.001$) at 15 min. This reduction was sustained at the same level by 2 h post-PNV (* $p < 0.05$) in hippocampus, but tended to recuperate in cerebellum, although still significantly below the control level (* $p < 0.05$). The findings showed that the content of this TJ protein involved in cell-cell adhesion is higher in cerebellum than in hippocampus, and that in cerebellum the downregulation provoked by venom is more accentuated than in hippocampus despite a faster recovery in the former (Figure 4A,B,C).

β-catenin: The β-catenin content was similar in hippocampus and cerebellum of sham animals. Endovenous administration of PNV induced immediate (15 min) and significant reduction (** $p < 0.01$) of this AJ protein. In the hippocampus, the reduction of the protein level was sustained (* $p < 0.05$) whereas in the cerebellum this was transient since β-catenin content showed gradual significant recuperation close to control level. Differences were seen between the lowest (15 min) and highest level (5 h) of β-catenin in cerebellum (# $p < 0.05$), indicating a significant reactive synthesis of the protein to re-establish cell adhesion (Figure 4D,E,F). As for laminin, claudin-5 and ZO-1, β-catenin reduction in response to systemic PNV was more prominent in cerebellum, nevertheless the recovery of all proteins was faster in cerebellum than in hippocampus.

Occludin: In control group, the occludin content was higher in hippocampus than in cerebellum (Figure 5A,B,C). The i.v. administration of PNV produced a drastic immediate (15 min) reduction (~50%) of the protein content in the hippocampus (** $p < 0.01$) while it induced a trend for increase in cerebellum. Moreover, the tendency for occludin increase persisted in cerebellum in the subsequent time points postenvenoming in such a way that at 5 h the level of the protein was ~25% higher than the basal content of controls. In contrast, despite a gradual recuperation of the protein, in hippocampus the occludin content remained below the control level at 2 h (* $p < 0.05$) and 5 h (not significant given the deviation size). Significant differences were seen between PNV-15 min and PNV-2 h (# $p < 0.05$), (Figure 5, A-C).

PNV increased pPP2A content soon after PNV injection (15 min), both in cerebellum and hippocampus, indicating deactivation of this phosphatase. The cerebellum showed faster recovery than hippocampus.

Phosphorylated-PP2A content increased significantly as early as 15 min post- PNV injection both in hippocampus (** $p < 0.01$) and cerebellum (* $p < 0.05$). Afterward, a reducing tendency towards the reestablishment of the controls levels was seen in hippocampus (Figure 5D,E). In the cerebellum, the reduction down the control content seen in PNV-2h produced a significant difference in relation to PNV-2 h (## $p < 0.01$) (Figure 5 D and F).The return to levels close to basal's indicates a normal phosphorylation state of PP2A, and explains the recuperation of junctional proteins.

Discussion

A bulk of information has been accumulated on the interaction of *P. nigriventer* venom and CNS, and particularly in regard to its action on BBB (Le Sueur *et al*, 2003, 2004; Cruz-Höfling *et al*, 2007, 2009, Rapôso *et al*, 2007). These studies have shown that chronologically and regionally the venom actions seem to exhibit different time- course and degrees of intensity, or even be absent. Since the venom is a rich mixture of polypeptides acting on ion channels of excitable membranes and neurotransmitter release (Cruz-Höfling *et al*, 1985; Love and Cruz-Höfling, 1986; Gomez *et al*, 2002) the investigation of its action in molecules involved in blood-brain barrier function is highly useful, particularly considering that experimentally the effect are short-lived and only 0.5% of the accidents with Phoneutria were graded as grave (Bucaretchi *et al*, 2000). The venom was shown to affect microtubule-mediated transcytotic traffic through vessels endothelium after 24 h and 9 days of exposure (Le Sueur *et al*, 2004), but evidences suggest that the paracellular normally forbidden

traffic could also be affected in other periods after of time. TJ and AJ proteins would be likely targets of the venom and hence the paracellular route could be affected. The expression and phosphorylation state of these are known to contribute for maintenance of the BBB integrity (Fiala *et al*, 2002; Plumb *et al*, 2002; Staddon *et al*, 1995a,b). The phosphorylation is a very fast, dynamic process (Rubin and Staddon, 1999) and junctional opening can be a transient episode during BBB permeabilization, hence supporting intermittent opening and closure of paracellular route. Other proteins having critical role in BBB function are P-glycoprotein (P-gp) and laminin from vessels basement membrane. P-glycoprotein is a representative efflux transporter protein of brain vessels preventing drug accumulation into the cerebral milieu (Roberts and Goralski, 2008). Laminin is the main protein of basement membrane (BM) and BM is a true physical barrier against the free transit of macromolecules through the BBB. Collectively, the proteins constitutes the operational and physical center of the BBB and are assisted by the components of endothelial basement membrane, pericytes and a surrounding astrocytic end-feet sheath.

In this study, immunofluorescence and/or immunoblotting were used to locate and follow the expression at structure level (IF) of some TJ and AJ proteins, P-gp, laminin as well as to evaluate their content in hippocampus or cerebellum homogenates (WB). The degree of AT and AJ proteins were indirectly evaluated through the level of phosphorylation of the protein phosphatase 2A (PP2A). The investigation allows differentiating in each region the dynamics of the molecular mechanisms underlying the transient BBB disruption caused by the systemic *P. nigriventer* venom (PNV). The study is useful for therapeutic management in cases of envenoming and/or to add new information about the venom action viewing the discovery of novel pharmacological tools.

There was significant decrease of occludin, ZO-1, β-catenin and laminin 15 min and/or 2 h and simultaneous pPP2A increase (15 min) after PNV injection, in hippocampus and cerebellum, compared with controls. The IF results showed decrease of claudin-5 labeling in hippocampus and cerebellum vessels besides an uneven spatial distribution. In general, the changes were more accentuated and/or precocious in the cerebellum; however the recover of the proteins expression/content was faster than in hippocampus. As a rule, the most of the proteins were overexpressed at 5 h time-point. This time interval matches with the onset of clinical recuperation of envenomed animals suggesting that the signs of animal intoxication were likely due to the BBB paracellular pathway impairment.

In regard to P-gp, there was a fast decline in its immunoreactivity in the cerebellum (15 min) suggesting protein degradation. The immunolabeling of P-gp was very discrete in control. At PNV-2 h it was practically negative but at PNV-5 h the fluorescence was bright and intense above the seen in control. A number of physiologic properties make the endothelium of the CNS unique.

Among them, xenobiotic transporters, such as P-gp and MRPs (multidrug resistance proteins) family proteins play special role in the physiology of central vasculature (Abbott, 2002). These transporters extrude drugs and toxins if they gain access into the cytoplasm of brain endothelial cells before they enter the brain. The present results suggest P-gp as a target of PNV, as well as indicate the existence of an efficient intrinsic mechanism which promotes synthesis of efflux transporter proteins likely destined to drive out the toxic agent from the CNS. Recent results (unpublished), using the same experimental design, showed increase of the MRP1 efflux transporter protein expression and level from 15 min to 5 h after the systemic PNV exposure; this may suggest that venom degrades specifically P-gp, but not MRP1. However, the two proteins have in common to be upregulated at 5 h of the PNV injection, implying that organism strengthen the mechanisms of detoxification in the CNS. Pharmacological tools aiming triggering such mechanisms can be useful in some neurological disorders.

The partial or total collapse of the molecular barrier present in the endothelium of brain microvessels are evidences of BBB impairment. The BBB functioning works through physical and molecular interdependent mechanims, whose sequence is unclear and can be likely variable. Typical TJ proteins include, among others, claudins and occludin (Stevenson *et al*, 1986; Willot *et al*, 1992; Furuse *et al*, 1993; Furuse *et al*, 1998). Claudins constitute the backbone of TJ strands, by forming dimmers and binding homotypically to claudins on adjacent cells to produce the primary seal of the TJ. Occludin functions as a dynamic regulatory protein, whose presence in the membrane is correlated with increased electrical resistance across the membrane and decreased paracellular permeability (Simon *et al*, 1999; Furuse *et al*, 2001). The immediate decrease of the levels of the proteins occludin and laminin, besides spatial rearrangement of claudin-5, showed in this work, indicates that systemic PNV is able to induce paracellular permeability in very early stages. Besides, a complex organization of proteins (Geiger *et al*, 1987; Jockusch and Rüdiger, 1996), links the transmembrane proteins of TJs to actin microfilaments and provides the structural basis for cell-cell adhesion and signaling. ZO-1 is one of the several cytoplasmic accessory proteins of TJs involved in transmembrane proteins-cytoskeleton coupling. Chemical or physical agents can determine redistribution of TJ molecules (Huber and Egleton, 2001; Wachtel *et al*, 1999) and BBB permeabilization. These include exogenous or endogenous molecules, such as cytokines and matrix metalloproteases released very early after insult (Gasche *et al*, 1999; Gloor *et al*, 2001). For instance, loss of ZO-1 and occludin and rearrangement of vinculin have been demonstrated 1 h after interleukin administration (Bolton *et al*, 1998). Here, the reduction of ZO1 in the groups PNV-15 min and/or PNV-2 h suggest them targets of the PNV and likely involvement in BBB disruption. Recent unpublished data with the same experimental model show increase of matrix

metalloproteinase-9 (MMP9) at 15 min and 2 h after PVN injection. This can explain the early (15 min) ZO-1 and P-gp degradation.

The phosphorylation of some junctional proteins (implicated in the regulatory mechanisms of BBB permeability), such as occludin and β-catenin, occurs especially at tyrosine residues, through regulatory kinases and phosphatases located at the junctional site (Rubin and Staddon, 1999). Tyrosine phosphatase inhibitors or the overexpression of tyrosine kinases leads to a state of continuous phosphorylation that decreases the transcellular electrical resistance and rapidly increases the ionic permeability of the TJs in epithelium and endothelium *in vivo* and *in vitro* (Staddon et al., 1995 a,b; Le Sueur *et al*, 2004). In the current study, PP2A had its activity decreased after PNV i.v. administration, concomitant to decreasing TJ protein levels. Phosphorylated PP2A (pPP2A) occurs when the protein function is downregulated and, consequently, junction proteins are overphosphorylated and downregulated. Therefore, the present results suggest that PP2A inactivation was probably the mechanism of junctional opening and BBB permeabilization by PNV.

In conclusion, the initial hypothesis that *P. nigriventer* venom changes tight and adherens junctions proteins expression in early periods after systemic injection was confirmed, and this reflects BBB permeabilization, explaining the clinical signs of intoxication. Such alterations were probably elicited by a very fast and dynamic phosphorylation process of junctional proteins, which was transient and self-limiting. Identification of substances that allows manipulating brain-blood barrier is relevant for the development of successful therapeutic strategies for overcoming restricted drug delivery into the brain.

Disclosure/Conflict of Interest: I have no duality of interest to declare

References

Abbott N (2002) Astrocyte-endothelial interactions and blood-brain barrier permeability. J Anat 200:527.

Antunes E, Marangoni RA, Brain SD, Nucci G (1992) *Phoneutria nigriventer* (armed spider) venom induces increased vascular permeability in rat and rabbit skin in vivo. Toxicon 30:1011-6.

Bolton SJ, Anthony DC, Perry VH (1998) Loss of tight junction proteins occludin and zonula occludens-1 from cerebral vascular endothelium during neutrophil-induced blood – brain barrier breakdown in vivo. Neuroscience 86:1245-57.

Brazil V, Vellard J (1925) Contribuição ao estudo do veneno das aranhas. Mem Inst Butantan 2:5– 77.

Bucaretchi F, Deus Reinaldo CR, Hyslop S, Madureira PR, De Captani EM, Vieira RJ (2000) A clinico epidemiological study of bites by spiders of the genus *Phoneutria.* Rev Inst Med Trop Sao Paulo 42: 17-21.

Bücherl W, Buckley E (eds) (1971) Venomous Animals and their Venoms. Vol. III, New York, NY: Academic Press.

Costa SK, Moreno H Jr, Brain SD, De Nucci G, Antunes E (1996) The effect of *Phoneutria nigriventer* (armed spider) venom on arterial blood pressure of anaesthetized rats. Eur J Pharmacol 298:113-20.

Costa SKP, Esquisatto LCM, Camargo E, Gambero A, Brain SD, De Nucci G, Antunes E (2001) Comparative effect of *Phoneutria nigriventer* spider venom and capsaicin on the rat paw oedema. Life Sciences 69:1573-85.

Costa SKP**,** Nucci G**,** Antunes E**,** Brain SD (1997) *Phoneutria nigriventer* spider venom induces oedema in rat skin by activation of capsaicin sensory nerves. Eur J Pharmacol 339: 223-6.

Cruz-Höfling MA, Love S, Brook G, Duchen LW (1985) Effects of *Phoneutria nigriventer* spider venom on mouse peripheral nerve. Q J Exp Physiol 70:623-40.

Cruz-Höfling MA, Rapôso C, Verinaud L, Zago GM 2009 Neuroinflammation and astrocytic reaction in the course of *Phoneutria nigriventer* (armed-spider) blood-brain barrier (BBB) opening. NeuroToxicology 30:636-46.

Cruz-Höfling MA, Zago GM, Melo LL, Rapôso C 2007 c-FOS and n-NOS reactive neurons in response to circulating *Phoneutria nigriventer* spider venom. Brain Res Bull 73:114-26.

Fiala M, Liu QN, Sayre J, Pop V, Brahmandam V, Graves MC, Vinters HV. (2002) Cyclooxygenase-2-positive macrophages infiltrate the Alzheimer's disease brain and damage the blood–brain barrier. Eur J Clin Investig 32:360–71.

Furuse M, Furuse K, Sasaki H, Tsukita S (2001) Conversion of Zonulae occludentes from tight to leaky strand type by introducing claudin-2 into Madin-Darby canine kidney I cells. J Cell Biol 153: 263-72.

Furuse M, Hirase T, Itoh M, Nagafuchi A, Yonemura S, Tsukita S (1993) Occludin: a novel integral membrane protein localizing at tight junctions. J Cell Biol 123: 1777-88.

Furuse M, Fujita K, Hiiragi T, Fujimoto K, Tsukita S (1998) Claudin-1 and -2: novel integral membrane proteins localizing at tight junctions with no sequence similarity to occludin. J Cell Biol 141:1539-50.

Gasche Y, Fujimura M, Morita-Fujimura Y, Copin JC, Kawase M, Massengale J, Chan PH (1999) Early appearance of activated Matrix Metalloproteinase-9 after focal cerebral ischemia in mice: a possible role in blood–brain barrier dysfunction. J Cereb Blood Flow Metab 19:1020-8.

Gaudry CA, Palka HL, Dusek RL, Huen AC, Handekar MJ, Hudson LG, Green KJ (2001) Tyrosine-phosphorylated plakoglibin is associated with desmogleins but not desmoplakin after epidermal growth factor receptor activation. J Biol Chem 276:24871- 80.

Geiger B, Volk T, Volberg T, Bendor R (1987) Molecular interactions in adherens type contacts. J Cell Sci 8:251-72.

Gloor SM, Wachtel M, Bolliger MF, Ishihara H, Landmann R, Frei K (2001) Molecular and cellular permeability control at the blood– brain barrier. Brain Res Rev 36:258-64.

Gomez MV, Kalapothakis E, Guatimosim C, Prado MA (2002) *Phoneutria nigriventer* venom: a cocktail of toxins that affect ion channels. Cell Mol Neurobiol 22:579-88.

Huber JD, Egleton RD, Davis TP (2001) Molecular physiology and pathophysiology of tight junctions in the blood – brain barrier. Trends Neurosci 24:719-25

Jockusch BM, Rüdiger M (1996) Crosstalk between cell adhesion molecules: vinculin as a paradigm for regulation by conformation, Trends Cell Biol 6:311-5.

Le Sueur LP, Collares-Buzato CB, Cruz-Höfling MA (2004) Mechanisms involved in the blood-brain barrier increased permeability induced by *Phoneutria nigriventer* spider venom in rats. Brain Res 1027:38-47.

Le Sueur LP, Kalapothakis E, Cruz-Höfling MA (2003) Breakdown of the blood–brain barrier and neuropathological changes induced by *Phoneutria nigriventer* spider venom, Acta Neuropathol 105:125-34

Liu F, Grundke-Iqbal I, Iqbal K, Gong CX (2005) Contributions of protein phosphatases PP1, PP2A, PP2B and PP5 to the regulation of tau phosphorylation. Eur J Neurosci 22:1942-50.

Love S, Cruz-Höfling MA (1986) Acute swelling of nodes of Ranvier caused by venoms which slow inactivation of sodium channels. Acta Neuropathol 70:1-9. Nunes KP, Costa-Gonçalves A, Lanza LF, Cortes SF, Cordeiro MN, Richardson M,

Pimenta AM, Webb Rc, Leite R, De Lima ME (2008) Tx2-6 toxin of the *Phoneutria nigriventer* spider potentiates rat erectile function. Toxicon 51:1197-206.

Plumb J, McQuaid S, Mirakhur M, Kirk J (2002) Abnormal endothelial tight junctions in active lesions and normal-appearing white matter in multiple sclerosis. Brain Pathol 12:154-69.

Rapôso C, Zago GM, da Silva GH, da Cruz Höfling MA (2007) Acute blood-brain barrier permeabilization in rats after systemic *Phoneutria nigriventer* venom. Brain Res 1149:18-29.

Roberts DJ, Goralski KB (2008) A critical overview of the influence of inflammation and infection on P-glycoprotein expression and activity in the brain. *Expert Opin Drug Metab Toxicol* 4: 1245-64

Roura S, Miravet S, Piedra J, García de Herreros A, Duñach M (1999) Regulation of Ecadherin/Catenin association by tyrosine phosphorylation. J Biol Chem 1999 274:36734-40.

Rubin LL, Staddon JM (1999) The cell biology of the blood–brain barrier. Annu Rev Neurosci 22:11-28.

Simon DB, Lu Y, Choate KA, Velazquez H, Al-Sabban E, Praga M, Casari G, Bettinelli A, Colussi G, Rodriguez-Soriano J, McCredie D, Milford D, Sanjad S, Lifton RP (1999) Paracellin-1, a renal tight junction protein required for paracellular Mg2 resorption. Science 285:103-6.

Staddon JM, Herrenknecht K, Schulze C, Smales C, Rubin LL (1995a) Signal transduction at the blood-brain barrier. Biochem Soc Trans 23:475-9.

Staddon JM, Herrenknecht K, Smales C, Rubin LL (1995b) Evidence that tyrosine phosphorylation may increase tight junction permeability. J Cell Sci 108:609-19.

Stevenson BR, Siliciano JD, Mooseker MS, Goodenough DA (1986) Identification of ZO-1: a high molecular weight polypeptide associated with the tight junction (zonula occludens) in a variety of epithelia. J Cell Biol 103:755-66.

Wachtel M, Frei K, Ehler E, Fontana A, Winterhalter K, Gloor SM (1999) Occludin proteolysis and increased permeability in endothelial cells through tyrosine phosphatase inhibition. J Cell Sci 112:4347-56.

Yonamine CM, Costa H, Silva JAA, Muramoto E, Rogero JR, Troncone LRP, Camillo MAP (2005) Biodistribution studies of bee venom and spider toxin using radiotracers. J venom Anim Toxins Incl Trop Dis 11:39-50.

Titles and Legend to Figures

Figure 1: *Laminin:* **A** – Immunoblots of laminin in hippocampus (HIP) and cerebellum (CER) of rats injected with saline (Cont, n=15 as described in Western blotting procedures section) or with PNV and sacrificed at 15 min, 2 and 5 h (n=5 each). The membranes were stripped and reprobed to

β-actin, confirming equal protein loading in the gel. Panels B and C show ratios of the laminin band intensity over corresponding β- actin intensity. A value of $P < 0.05$ indicated statistical significance (**$p < 0.01$, ***$p < 0.001$, comparing to control; #$p < 0.05$, comparing to PNV-15 min). The intensity of the IF in the three time-points (panels D to K) greatly matches with the protein blots. There was marked and immediate (F,G) decrease in the intensity of laminin staining in envenomed animals. The recovery of the laminin expression was faster in the cerebellum (I) than in hippocampus (J); 5 h post-PNV the intensity of the immunolabeling has not reached the control level. Bars: D, F, H = 70 μm; J, E, G, I, K = 35 μm. Each value represents the mean ± S.E.M. Student-t test and one-way analysis of variance (ANOVA) followed by the Tukey-Kramer post-test were used to compare the treated and control groups.

Figure 2: *Claudin*-5. Immunoblots analysis and representative histogram of the densitometric protein values in hippocampus (HIP) and cerebellum (CER) of rats injected with saline (Cont, n=15, see description in Western blotting procedures section) or PNV in different time-points (n=5 each) (A,B,C). β-actin served as reference of the loading control of protein for each sample and panels B and C show ratios of the claudin-5 band intensity over corresponding β-actin intensity. The data showed that the ratios of claudin-5 band intensity over corresponding β-actin intensity were higher in hippocampus of controls; in contrast at 5 h post-PNV the higher intensity was in cerebellum. IF confirmed these data. In hippocampus, the immunoreactivity was higher than in cerebellum, both in controls and in PNV-15 min and PNV-2 h (compare D,E,F with H,I,J). However, 5 h after PNV exposure the reactivity was much stronger in cerebellum (K) than in hippocampus (G); the endothelial cell limits which were poorly visible at 15 min/2 h became visible again.Immunofluorescence of claudin-5 tipically showed a dotted pattern due to its tight-junction location; the venom promoted losses and progressive disorganization of the protein since the labelling was absent or very discontinuous. Each value represents the mean ± S.E.M. Student-t test and one-way analysis of variance (ANOVA) followed by the Tukey-Kramer post-test were used to compare the treated and control groups.Bars: D-G = 70 μm; H-K = 35 μm.

Figure 3: *P-glycoprotein.* Immunofluorescence (FITC-conjugated) showed much lower expression of the P-glycoprotein in the hippocampus of control and envenomed animals (A,C,E,G) than in cerebellum (B,D,F,H). In both regions, the expression level decreased after envenoming; the decrease was much prolonged in hippocampus (until 2 h). In PNV-5 h group (G,H), the efflux transporter protein, Pgp, was overexpressed. Bars: A, C, E, G = 35 μm; B, D, F, H = 70 μm.

Figure 4: *ZO-1* and β-*catenin.* Immunoblots of both proteins in hippocampus (HIP) and cerebellum (CER) with β-actin blots which served as reference of the loading control of protein for each sample and the representative content (panels A and D). The ratios of the ZO-1 (B,C) and β-catenin (E,F) bands intensity over corresponding β-actin intensity are represented. The venom induced decrease of all proteins both in hippocampus and cerebellum followed by recovery to levels near to the control (Cont) levels; (* $p < 0.05$; ** $p < 0.01$; *** $p < 0.001$ differences in relation to control; #$p < 0.05$ difference in relation to PNV-15 min). Each value represents the mean ± S.E.M. Student-t test and one-way analysis of variance (ANOVA) followed by the Tukey-Kramer post-test were used to compare the treated and control groups.

Figure 5: *Occludin* and *phosphorylated Phosphatase Protein 2A (pPP2A).* Immunoblots of ocluddin in hippocampus (HIP) and cerebellum (CER) of control (Cont, n=15, see description in Western blotting procedures section). The venom induced decrease of occluding in hippocampus (B, * $p < 0.05$; ** $p < 0.01$) compared to control, followed by increase (#$p < 0.05$, compared to PNV-15 min). In the cerebellum (C), the venom induced a growing increase. with β-actin blots which served as reference of the loading control of protein for each sample and the representative content (panels A and D). Immunoblots of pPP2A showed significant increase of the protein content both in hippocampus (** $p < 0.01$) and cerebellum (* $p < 0.05$); after the pPP2A decreased gradually next to control level after 5 h of PNV injection hippocampus, whereas in the cerebellum the protein content increased again reaching level superior to control's at the end of 5 h; ##$p < 0.01$ indicated content reduction in relation to PNV-15 min. β-Actin served as reference of the loading control of protein for each sample, and panels B, C shows ratios of the occludin or pPP2A bands intensity over corresponding β-actin intensity. Each value represents the mean ± S.E.M. Student-t test and one-way analysis of variance (ANOVA) followed by the Tukey-Kramer post-test were used to compare the treated and control groups.

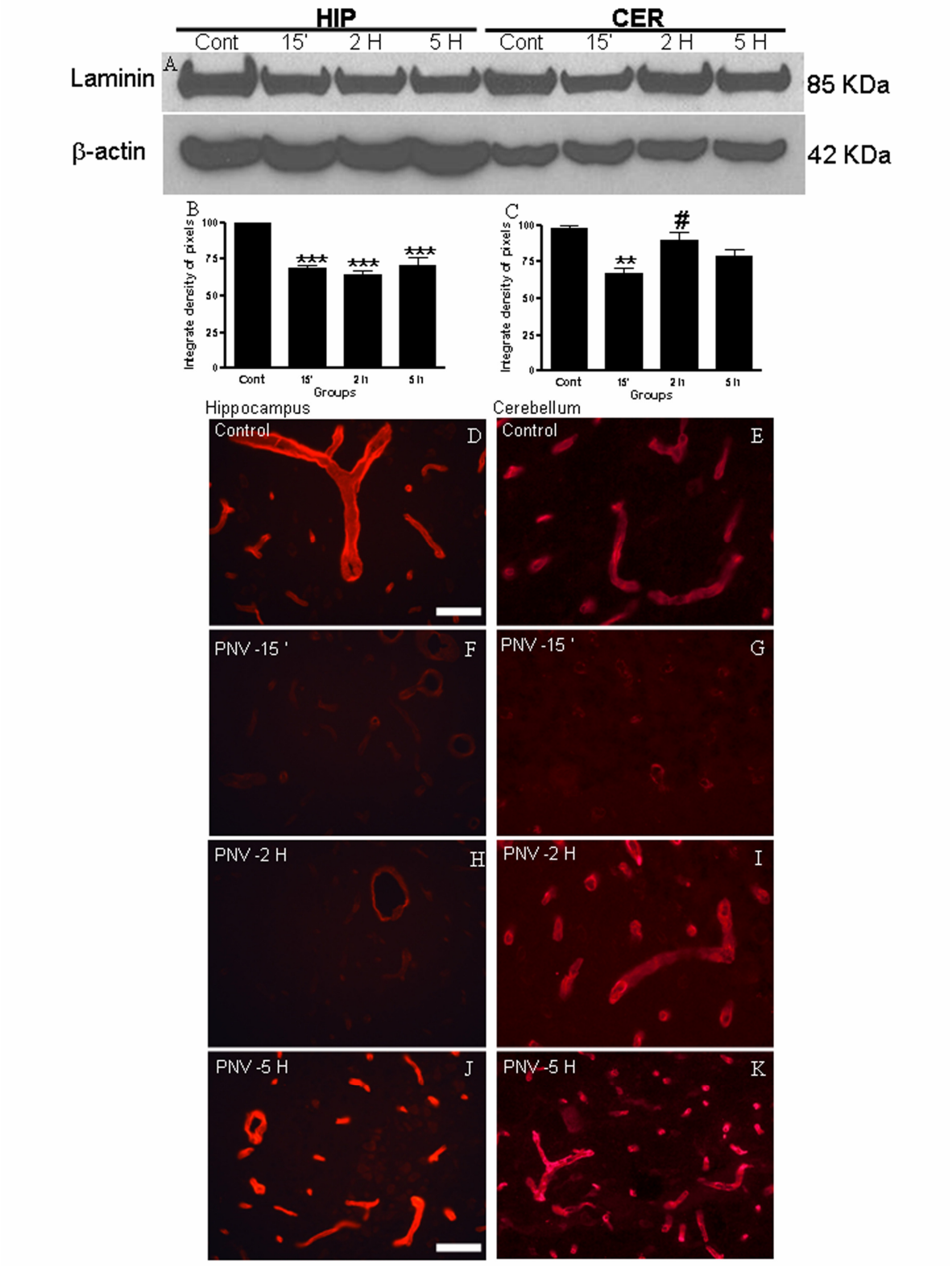
HIP
CER
Cont
15'
2 H
5 H
Cont
15'
2 H
5 H
A
Laminin
85 KDa
β-actin
42 KDa
B
Integrate density of pixels
Cont
15'
2 h
5 h
Groups
C
Integrate density of pixels
Cont
15'
2 h
5 h
Groups
Hippocampus
Cerebellum
Control
D
Control
E
PNV -15 '
F
PNV -15 '
G
PNV -2 H
H
PNV -2 H
I
PNV -5 H
J
PNV -5 H
K

Figure 1

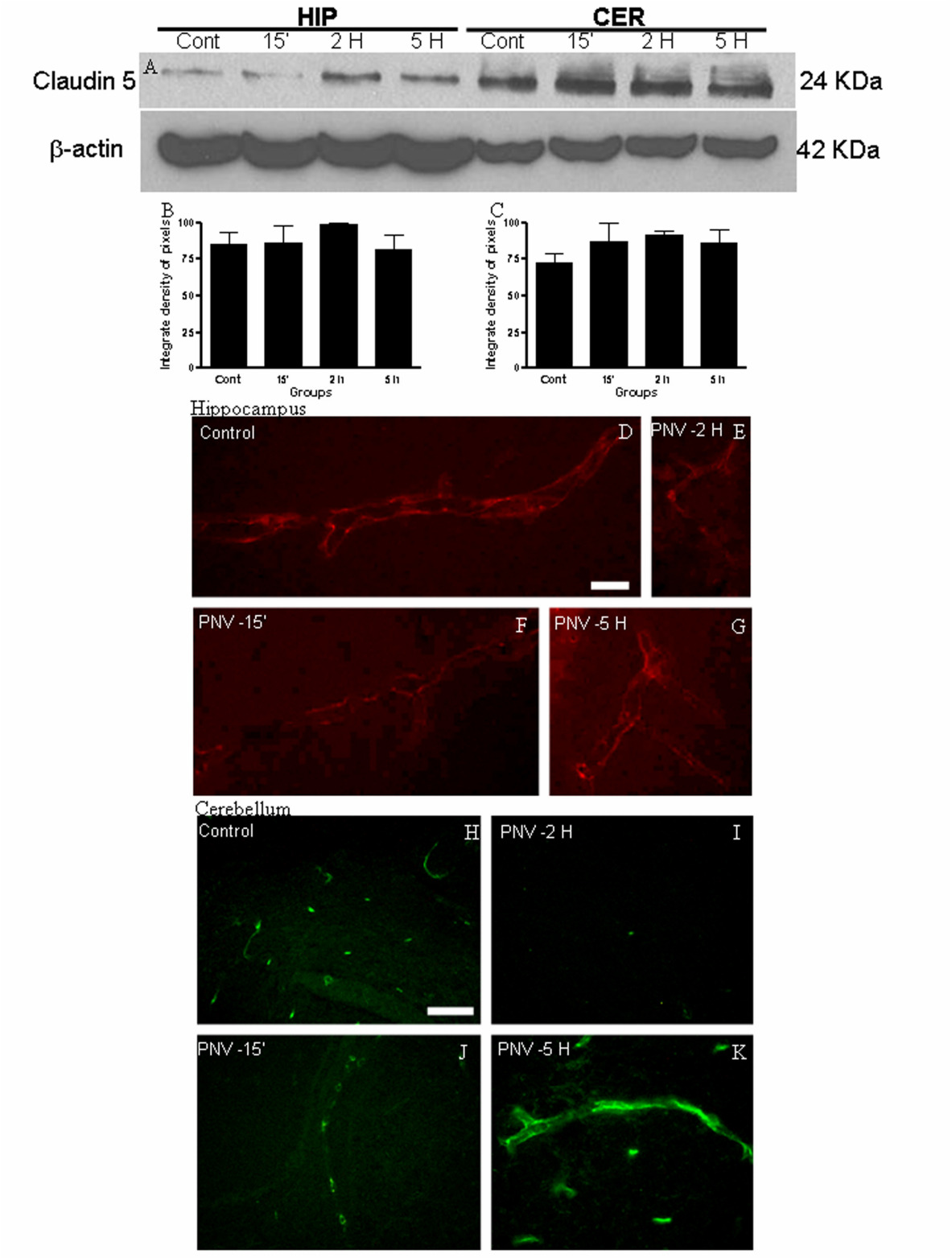
HIP
CER
Cont
15'
2 H
5 H
Cont
15'
2 H
5 H
A
Claudin 5
24 KDa
β-actin
42 KDa
B
Integrate density of pixels
Cont
15'
2 h
5 h
Groups
C
Integrate density of pixels
Cont
15'
2 h
5 h
Groups
Hippocampus
Control
D
PNV -2 H
E
PNV -15'
F
PNV -5 H
G
Cerebellum
Control
H
PNV -2 H
I
PNV -15'
J
PNV -5 H
K

Figure 2

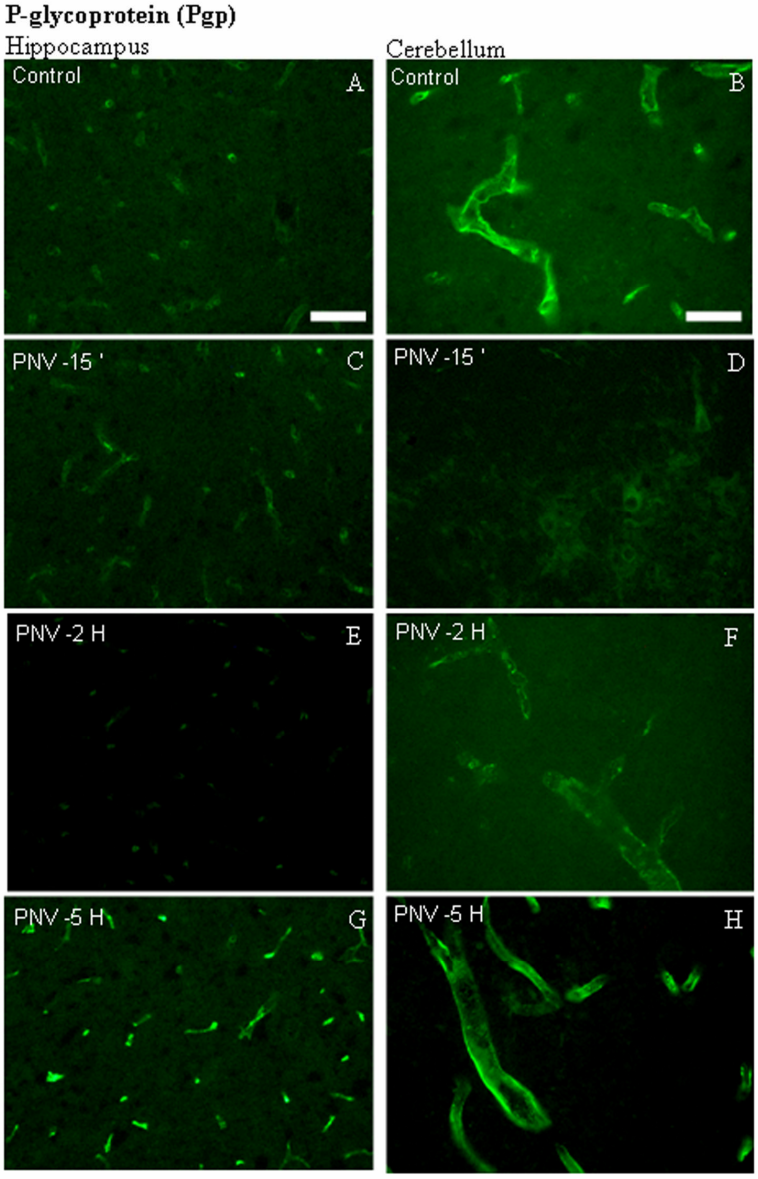
P-glycoprotein (Pgp)
Hippocampus
Cerebellum
Control
A
Control
B
PNV -15 '
C
PNV -15 '
D
PNV -2 H
E
PNV -2 H
F
PNV -5 H
G
PNV -5 H
H

Figure 3

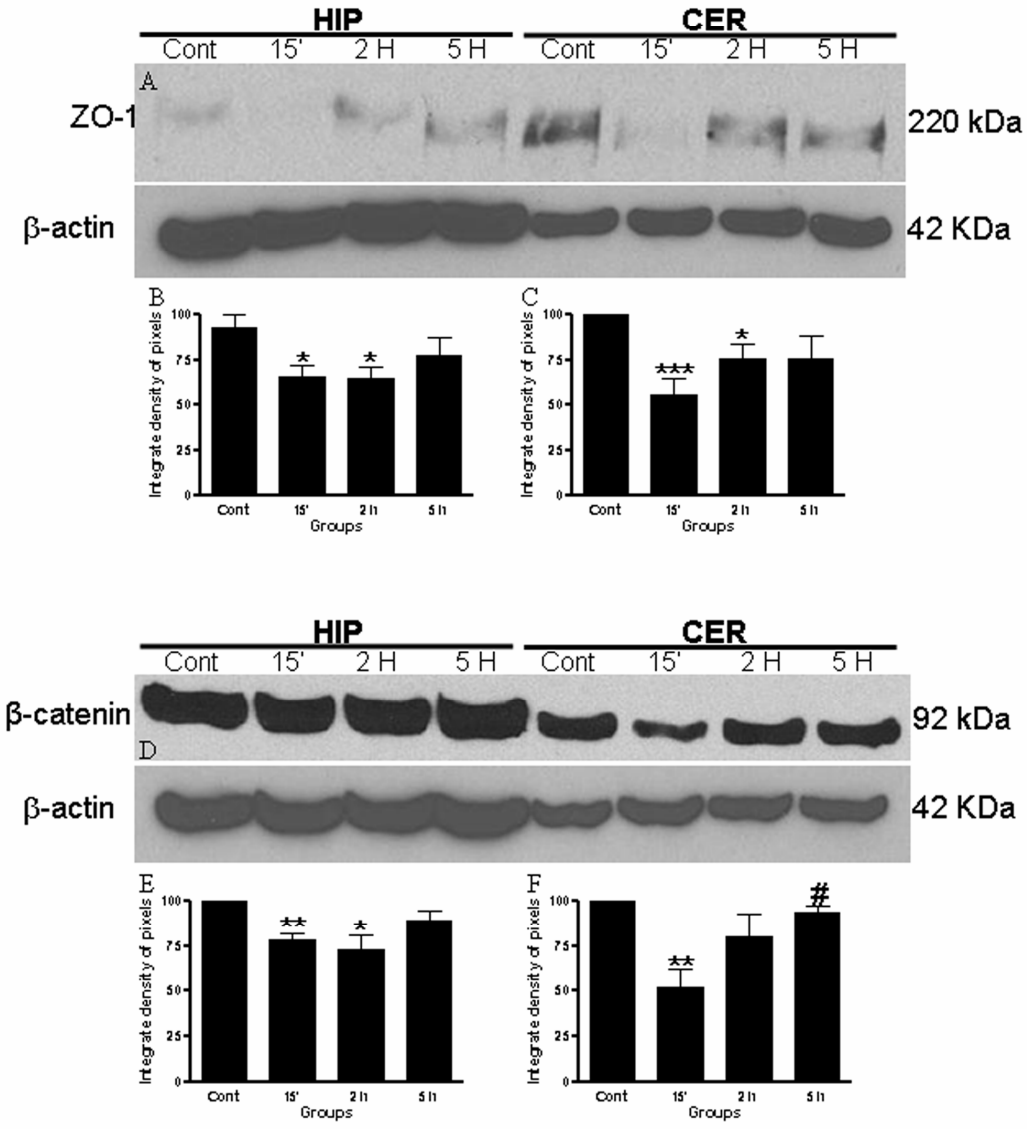
HIP
CER
Cont
15'
2 H
5 H
A
ZO-1
220 kDa
β-actin
42 KDa
B
C
Integrate density of pixels
Groups
β-catenin
92 kDa
D
E
F

Figure 4

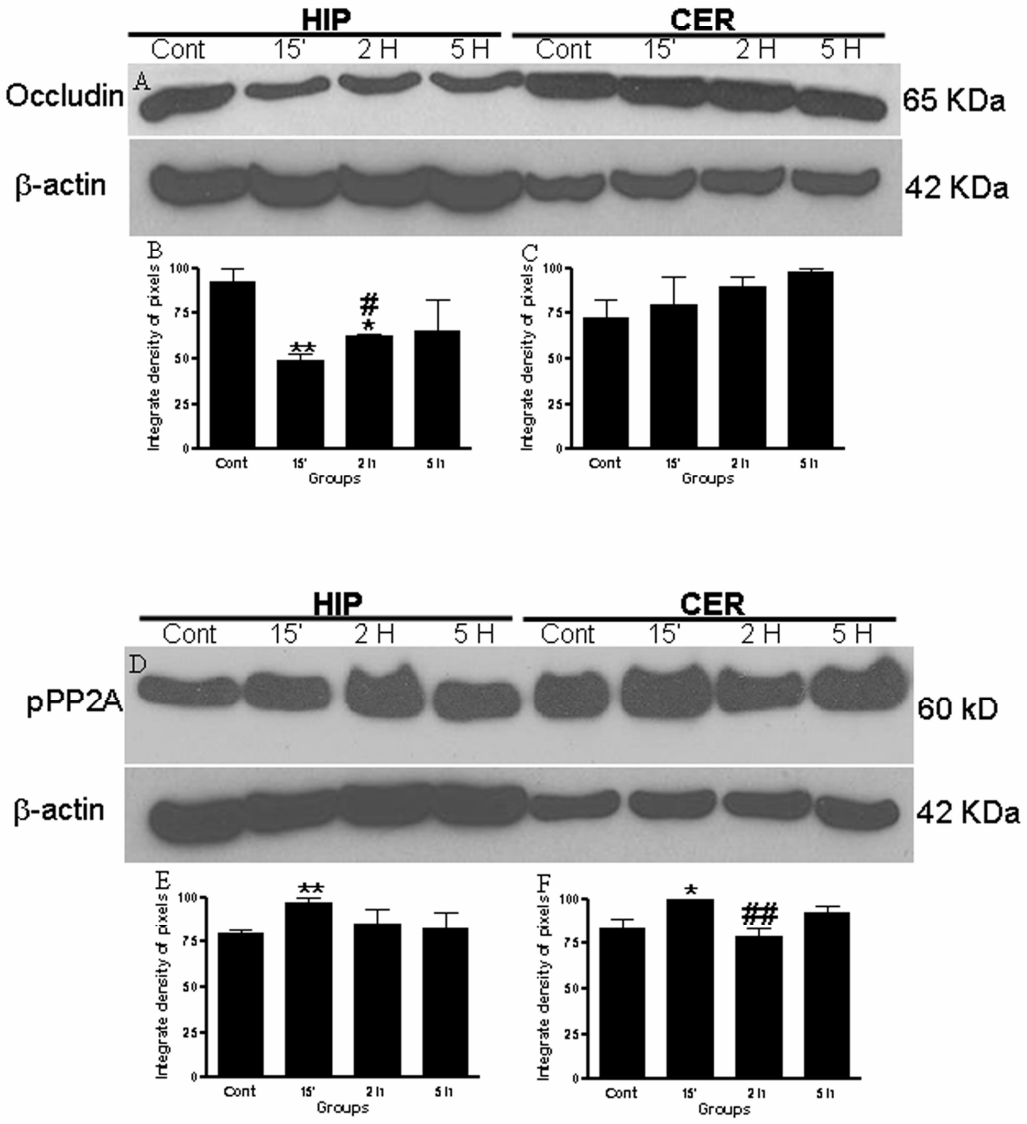
HIP
CER
Cont
15'
2 H
5 H
Occludin
A
65 KDa
β-actin
42 KDa
B
C
Integrate density of pixels
Groups
pPP2A
D
60 kD
E
F

Figure 5

*****Maria Alice da **Cruz-Höfling**
Departamento de Histologia e Embriologia
Instituto de Biologia, C.P. 6109
Universidade Estadual de Campinas
(UNICAMP) 13 087-130, Campinas – SP –BRASIL
E-mail: hofling@unicamp.br
Tel. (55)(19) 3521 6224; Fax. (55)(19) 3521 3124

Cx43, MRP1 and GLUT1 proteins involved in neuro-glial interaction are targets of the *Phoneutria nigriventer* spider venom

Paulo Alexandre Miranda Odorissi1, Stefania Fioravanti Savioli1, Catarina Rapôso, Maria Alice da Cruz-Höfling*

Department of Histology and Embryology, Institute of Biology, P.O. Box 6109, University of Campinas- UNICAMP, Zip Code 13 083-970 Campinas, SP, Brazil
1Contributed equally to the development of this work

Running title: Neuro-glia interaction as target for venom

Abstract

BBB permeability caused by *Phoneutria nigriventer* spider venom has been described. Immunofluorescence-(IF) and western blotting-(WB) were used to investigate the temporal dynamics of venom-induced changes on the multi-resistance drug protein-MRP1, glucose transporter protein 1-GLUT1, and connexin-43 in hippocampus and cerebellum. MRP-1 takes part in the efflux of some therapeutic drugs out the CNS; GLUT-1 is a typical endothelial cell marker and an indicator of the BBB functionality; Cx43 is the most representative protein of gap junction involved in cell-cell communication. The IF-labeled sections and WB bands densitometric values were quantified. Rats endovenously-injected with venom and euthanized 15 min, 2 and 5 h after, showed significant growing levels of MRP1 and GLUT1 in hippocampus. In the cerebellum, despite the expression/content of the MRP1 and GLUT1 were higher, their variability was lower than in hippocampus. Besides, the recovery of MRP1 to values closer to controls' was earlier. Cx43 content (=WB-values), in contrast, was higher in hippocampus, despite showing lower expression (=IF-values) than in cerebellum. After an immediate and significant increase (at 15 min), the Cx43 reactivity gradually decreased, achieving in hippocampus values lower than in control. The highest (MRP1-GLUT1) and the lowest (Cx43) values coincided with the intoxication signs remission (2-5 h post-PNV), suggesting ongoing clearance of venom in parallel with higher local glucose utilization, whereas cell-cell communication was impaired. Given the Cx43, GLUT1 and MRP1 has been described as having roles in astrocytes, pericytes, endothelial cells and neurons interactions we suggest their mechanistic involvement in BBB impairment by *P. nigriventer* venom.

Key words: Astrocytes, blood-brain barrier, efflux protein, gap junction, glucose transporter

Introduction

The blood–brain barrier (BBB) is both a physical and molecular entity responsible for controlling the traffic of molecules at the blood-brain interface. The principal component of the physical barrier is the endothelium of the cerebral microvessels, which is unique because has high electric resistance and tightly-attached interendothelial contacts which hampers transit through it. Besides, extended processes from perivascular astrocytes embracing the endothelial basement membrane and vascular pericytes contribute for preventing a free transit of macromolecules (Kacem et al., 1998; Rubin et al., 1991). The molecular barrier involves junctional proteins, membrane receptors and a set of selected carriers besides the proper lipid bi-layer of endothelial membrane. Small lipophilic molecules such as oxygen, CO2 and ethanol can freely diffuse across the lipid bi-layer. Small polar solutes, such as glucose, require specific transporter, among which the glucose transporter protein isoform 1, or GLUT1 (Duelli and Kuschinsky, 2001). Others mediate the efflux of potentially toxic metabolites out the CNS (e.g. multidrug resistance proteins (MRPs) and P-glycoprotein (Pgp)) (Abbott, 2002). The physical and molecular barriers restrict the paracellular traffic, hence compelling substances through the strictly regulated transcellular route. Both play a key role in the homeostatic regulation of the brain microenvironment (Yang & Aschner, 2003), providing important mechanism for protecting neural function from accidental fluctuations in plasma composition generated by circulating xenobiotics (Abbott and Romero, 1996). Several pathological conditions may disrupt BBB mechanism (Rubin and Staddon, 1999; Sawada et al., 2003; Wolburg and Lippoldt, 2002). Neurotoxins-containing venoms can also insult CNS and cause BBB breakdown. Our previous studies have shown that the venom of *Phoneutria nigriventer* provokes neurointoxication and BBB opening by disturbing both microtubule-mediated transcytosis (Le Sueur et al., 2003; 2004), and endothelial cell-cell contact (unpublishe), induces inflammation and reactive gliosis (Cruz-Höfling et al., 2009; Rapôso et al., 2007), causes neuron activation in CNS (Cruz-Höfling et al., 2007) having nitric oxide as mediator in several brain regions (unpublished). These effects are transitory. The venom is rich in voltage-gated sodium, calcium, and potassium channels-acting neurotoxins which affect peripheral and central neurotransmitter release (Cruz-Höfling et al., 1985; Fontana and Vital-Brazil, 1985; Gomez et al., 2002). The application of pharmacological tools for studying the modulation of the BBB transcellular and paracellular pathways is relevant clinically (Banks, 2008).

The close anatomical apposition between astrocytic end-feets and endothelial cells predicts a role for astrocytes in BBB functionality. In support, development and preservation of BBB phenotype in brain endothelium has been conditioned to the presence of astrocytes (Abbott, 2000; Davson and Oldendorf, 1967). In conformity, the presence of gap junctions is essential for

establishing a network among the BBB components viewing integrated actions in favor of CNS homeostasis. Gap junctions are intercellular protein channels in charge of coordinating the bi-directional exchange of cellular messengers (ions and small molecules) for integration of the physiological processes (Martin and Evans, 2004; Nicholson, 2003; Sáez et al., 2003; Söhl and Willecke, 2004).

Herein, the hypothesis that gap junctions proteins are modulated in *P. nigriventer* envenoming was investigated. Additionally, the expression of the endothelial transporters, MRP1 and GLUT1, was evaluated. A better understanding of the venom mechanisms in the BBB disturbance has important implications in development of therapeutic approaches in case of spider bite accidents.

Materials and Methods

Animals and venom

Male Wistar rats (250–300 g) were obtained from an established colony maintained by the Central Animal House Service at UNICAMP, and kept in a cycle of 12/12 hours light/dark period with food and water supplied *ad libitum*. One batch of lyophilized *P. nigriventer* crude venom (PNV) was supplied by Instituto Butantan (São Paulo, SP, Brazil). The venom was stored at - 20ºC and dissolved in 0.9% sterile saline solution immediately before use (0.5 mg of veneno/1ml saline).

PNV treatment

Male Wistar rats were divided into two groups. One group received a single intravenous (i.v.) injection of *Phoneutria nigriventer* venom (PNV, 850 μg/kg in 0.5 ml) (Le Sueur et al., 2003) in the tail vein, while the other (control sham group) was given the same volume of 0.9% sterile saline solution. Fifteen minutes, 2 and 5 hours post-injection, the venom and saline-injected rats were anesthetized (via i.p.) with ketamine chloride (Dopalen®) and xylazine chloride (Anasedan®), 100 and 10 mg/kg respectively (both from Vertbrands, Jacarei, SP, Brazil), before euthanasia. These time intervals have been shown to be adequate for evaluating acute PNV-induced BBB breakdown (Rapôso et al., 2007). The experiments were approved by the Universiy's Ethic in Animal Experimentation Committee (CEEA, (protocol number: 1429-1)) whose procedures are in line with the guidelines of the Brazilian College for Animal Experimentation (COBEA)

Immunofluorescence (IF)

Animal protocols for western blotting and immunohistochemistry study were done in separate (n = 5/time interval/technical assay/saline or venom, total of animals for IF=30) In order to determine displacement or alterations in the expression of proteins studied, the immunofluorescence was assessed in hippocampus and cerebellum of saline (sham controls) and PNV-injected rats. Animals were anesthetized and transcardiac perfusion with physiologic solution (150 ml) followed by fixative (250 ml of 4 % paraformaldehyde in ice-cold 0.1 M phosphate-buffered saline - PBS, pH 7.4) was done. After, the brains were dissected and immersed in 15% sucrose, overnight, then embedded in OCT-Tissue Tek and frozen in *n*-hexane with liquid N2. Cryostat sections, 12 μm thick, were collected on glass slides and air dried. After washing in TBS, the sections were permeabilized with 0.1% Triton X-100 for 10 min at room temperature (RT) (just for GLUT1, before Triton X-100, the slices were incubated with ethanol, followed by methanol, for 10 min each, at -20º C), followed by 0.1% Tween 20 in TBS containing 5% non-fat milk for 1 h at RT to block nonspecific binding of antibodies. Subsequently, sections were reacted with one of the following monoclonal primary antibodies diluted in TBS/3% nonfat milk: anti-MRP1 (Zymed, 187246 - 1:100), anti-GLUT1 (Alpha Diagnostic, GT11-S - 1:100), both raised in mouse, and anti-connexin-43 (Sigma, C6219 – 1:500), produced in rabbit. The primary antibodies were incubated overnight at 4ºC (just for GLUT1, the incubation was for 2 h in RT), afterward were washed with TBS, then incubated with FITC- or TRITC-conjugated polyclonal secondary antibody against rabbit or mouse immunoglobulins (Anti-rabbit IgG TRITC conjugate – T5268 – 1:1500; Anti-mouse IgG FITC conjugate – F6257 – 1:1500, Sigma), diluted in TBS/1% non-fat milk for 1 h at RT, in the dark. All incubations were carried out in a humidified chamber; IF was performed in batches, each batch containing the three time-points of control and PNV equally represented within each batch in order to diminish non-specific inter-group staining variability. The slices were then washed with TBS and mounted in glycerinated gelatin. Quantification of the protein expression was performed with enhanced contrast and density slicing feature of IMAGEJ software (version 1.33u, NIH, USA). Four sections per animal in each of the time-points (n=5 animals), control and envenomed, were immunolabeled. Six images/animal (=30 images/group) were captured using a fluorescence microscope (Olympus, Tokyo, Japan) equipped with Image-Pro Plus image analyzer software (USA). The integrated density of pixels was systematically measured in six areas per animal.

Western Blot (WB)

Fifteen min, 2 and 5 h after PNV or saline injection (n = 5 animals/time interval; Ntotal= 30 animals), the animals were anesthetized as described above, and killed by decapitation. Hippocampus and cerebellum from each time-point of PNV-injected animals were quickly dissected and each group homogenized in lysis buffer (10 mM EDTA, 2 mMPMSF, 100 mM NaF, 10 mM sodium pyrophosphate, 10 mM NaVO4, 10 mg of aprotinin/ml and 100 mMTris, pH 7.4). Hippocampus or cerebellum from animals killed at 15 min, 2 h or 5 h after saline-injection was mixed and homogenized to form a control pool from each region (n = 15 control hippocampus or cerebellum). This single control was used for evaluating WB of protein contents in hippocampus or cerebellum and comparison with the PNV-15 min, PNV-2 h or PNV-5 h). This was done because there was no visible clinical sign indicating any alteration in the animal aspect caused by saline injection, allowing the use of a "pooled-control". In contrast, for the clinical and immunohistochemical observations, the sham control was time-to-time paired with PNV-exposed animals for comparison purposes. Homogenates were centrifuged at 3000 g for 10 min and the supernatant collected and stored at -70ºC until use for immunoblotting. The proteins (50 μg) were separated on 10% (MRP1), 15% (GLUT1 or Cx43) sodium dodecyl sulfate-polyacrylamide by gel electrophoresis (SDSPAGE) under reducing conditions were electrophoretically transferred onto nitrocellulose membrane (BioRad Laboratories, ref. 162-0115). After overnight blocking at 4ºC with 5 % non-fat milk in TBS-T (Tris-buffered saline 0.1 % with 0.05 % Tween 20, pH 7.4), the membranes were again incubated at RT for 4 h, with primary antibodies described in *Imunofluorescence* sub-section (dilutions: MRP1 – 1:200; GLUT1 – 1:400; Cx43 – 1:600), diluted in buffer solution TBS-T containing 3% nonfat milk. After washing (five times, 8 min each) in TBS-T, the membranes were further reacted with secondary horseradish peroxidase-conjugated anti-rabbit or anti-mouse IgG antibodies (1:1000, Sigma, Refs. A6154 and A9309, respectively), diluted in TBS-T with 1% non-fat milk, for 1 h, at RT. A chemiluminescence reagent (Super Signal, Pierce) was used to make the labeled protein bands visible and the blots were then developed on X-ray film (Fuji Medical, Kodak, Ref Z358487-50EA). Each band was quantified by densitometry using the IMAGEJ software (version 1.33u, NIH, USA). For each protein investigated the results were confirmed in three sets of experiments. In all, immunoblot of β-actin was analyzed as a loading control for the other protein blots. After visualization, the protein antibodies were stripped from the membranes, which were reprobed with monoclonal anti-β-actin antibody (1:250, Sigma, USA); subsequently the protein densitometry was done. The ratio MRP1/β-actin, GLUT1/β-actin and Cx43/β-actin was calculated and compared to saline-pooled (sham) control. Negative control was provided by omitting the primary antibody.

Statistical analysis

The results were expressed as means ± S.E.M.. The densitometric values of the immunoreactive bands (WB) and fluorescence labeling of proteins (IF) were analyzed using the Graphpad Prism software package. Student t test, or one-way analysis of variance (ANOVA) followed by the Tukey-Kramer post-test, was used to compare the treated with the time-to-time paired control (for IF data) or the treated with the pooled control (for WB data). A value of $P < 0.05$ indicated statistical significance.

Results

Clinical observations

The rats injected with venom showed variably intense neurotoxic signs, indicating peripheral (flaccid and spastic paralysis of hindlimbs), autonomic (hyperemia, tremors, salivation, lachrymation and piloerection) and central nervous commitment (prostration, tonic-clonic convulsion and respiratory stress). At least 0.5% of the animals died soon after venom i.v. injection. After 5 h of PNV injection, the neurotoxic signs were partially resolved, with animals recovering gradually the locomotor and respiratory normal capacity. In the saline control group, none intoxication sign was observed regardless the survival time interval.

MRP1

MRP1 immunolabeling appeared as fluorescent dots outlining the endothelial wall of brain microvessels (Figure 1). There was a correspondence in the expression and level of the MRP1 efflux protein in hippocampus as seen by IF and WB data. There was a gradual increase of the protein IF labeling which was significantly different from control only at 5 h post-PNV injection ($p<0.05$). WB values showed significantly higher levels of MRP1 at 5 h compared to either control ($p<0.05$) or PNV-15 min ($p<0.001$) or PNV-2 h ($p<0.01$). The immunolabeling of the MRP1 efflux protein in hippocampus was less intense than in cerebellum, as was so the content of the protein seen by immunoblotting. Besides, instead of the dot-like staining seen in hippocampus, in cerebellum the majority of vessels showed a continuous ribbon of staining around vessels lumen (Figure 2). Quantification of pixels showed a significant increase of MRP1 expression in PNV-2 h group compared to control ($p<0.05$) (Figure 2A-E). The curve profile of the blots densitometric values rigorously matched with the curve profile of the IF immunolabeling quantification (compare Figure 2E and 2G), but there was not statistic difference in MRP1 content among groups. Despite, a tendency to decrease both the expression and content of the efflux transporter protein at PNV-5 h (see a dot-like pattern of MRP1 staining in this time interval), its level remained moderately higher

than in control. The data indicates hippocampus as more sensitive to the venom than cerebellum; however, cerebellum seemed more efficient in clearing up the intoxicant, probably for presenting higher levels of MRP1 than hippocampus.

GLUT1

The GLUT1 immunostaining appears as small dots delineating blood vessels profiles. When the expression of the protein was higher the dots coalesced to form a more continuous lining around vessels lumen; in envenomed animals immunoreactivity seen outside the vessels was likely the protein presence in astrocytes (see (*) in panels of Figures 3 and 4). The IF and WB assays showed that the cerebellum contains higher expression and content of the glucose transporter protein, GLUT1, than hippocampus. The major expression/content of GLUT1 in both regions was seen at 5 h post-PNV. Hippocampus was more sensitive than cerebellum to the toxicant since the increase in the protein content in this region was double the observed in the cerebellum (44% *vs.* 22% at PNV-5 h compared to control. A similar proportion between the two regions was observed in relation to the IF labeling quantification, ~39% *vs.* 20%, respectively). In hippocampus, the difference in the expression of GLUT1 was significant between control *vs.* PNV-2 h ($p < 0.01$), control *vs.* PNV-5 h ($p < 0.05$), PNV-15 min *vs.* PNV-2 h ($p < 0.01$) and PNV-15 min *vs.* PNV-5 h ($p <0.05$) (Figure 3A,B,C,D,E). The WB bands densitometric analysis showed similar increase tendency, but the differences were significant only between the PNV groups, 15 min *vs.* 5 h ($p < 0.001$). In cerebellum, IF labeling remained quite constant in PNV-15 min, PNV-2 h, and their paired controls. A significant enhanced expression of GLUT1 occurred thereafter ((PNV-5 h *vs.* PNV-15 min ($p < 0.05$), and PNV-5 h *vs* PNV-2 h ($p < 0.05$)) (Figure 4A,B,C,D,E). The GLUT1 content, measured by WB density values, showed similarity with the obtained by IF evaluation: differences were significant between PNV-5 h x pooled-control ($p < 0.05$), or x PNV-15 min groups ($p < 0.001$) (Figure 4G).

Connexin-43

Cx43 reactivity appeared in the microvessels'walls and in hippocampal and cerebellar parenchyma. In microvessels of hippocampus and cerebellum, the protein is likely being expressed in endothelium-astrocytic-end-feet-pericytes contacts. In hippocampus, the Cx43 labeling was increased in the PNV-15 min group ($p < 0.05$), compared to sham-15 min followed by a gradual decrease. Differently from controls, where reactivity is barely seen in the hippocampal parenchyma, in PNV-15 min a marked labeling was found, probably due to staining of astrocyte-astrocyte-neuronneuron contacts. After, the immunolabeling density of Cx43 became significantly reduced.

Differences were significant between control-5 h and PNV-5 h ($p < 0.01$), PNV-15 min and PNV-5 h ($p < 0.001$) and PNV-2 h x PNV-5 h ($p < 0.01$) (Figure 5E). The WB bands densitometric values paralleled with IF data (compare Figures 5E,F,G), but variation in the levels of Cx43 did not reach statistic significance. In cerebellum, the reactivity is stronger in granule cell layer of the cerebellar cortex (Figure 6A). PNV caused immediate (15 min) increase of the reactivity ($p < 0.05$), particularly on the Purkinje layer, but also in the granular cell layer (Figure 6B); thereby there was a trend for reduction (Figure 6C). In the molecular layer, fluorescent labeling was seen. The densitometric analysis of WB bands labeling density showed a tendency to maintain increased the levels of Cx43 in envenomed groups compared to pooled-control.

Discussion

The spider *Phoneutria nigriventer* (Ctenidae, Araneomorpha) is responsible for the majority of accidents involving venomous spider in the Southeast Brazil; the victims of Phoneutriism present intoxication signs indicative of central, peripheral and autonomic nervous system involvement which, in severe cases, can be manifested by seizures (Bucaretchi et al., 2000). This fact has motivated the investigation of the venom toxic action in the CNS and specifically in the blood brain barrier.

In this study, with immunofluorescence (IF) and immunoblotting (WB) we analyzed the expression and content of some proteins associated with the BBB function to advance in the knowledge of molecular mechanisms of BBB breakdown caused by *P. nigriventer* venom (PNV). This knowledge also gives basis for therapeutic management in cases of envenoming with this armed-spider. Whereas WB is able to detect the proteins in the whole homogenate of hippocampus or cerebellum, but allows no cell type or layer specific distribution, IF is able to track expression of them at the cellular or structure level. In both, quantitative evaluation is feasible. The expression over the basal levels of each of the proteins along the trial period showed a practically equal curve pattern regardless the technique assessed.

The putative proteins targeted by the PNV were chosen based on the critical roles they exerts in the BBB functionality. MRP1 belongs to a family of proteins which are ATP-driven pumps which mediates translocation of cytotoxic substances and some drugs out the CNS (Kubota et al., 2006). Glucose is the primary energy fuel for brain metabolism. The brain taking up of glucose is promoted by the facilitative GLUT1 transporter protein through the capillary endothelial cells; an increased expression/content of GLUT1 reflects elevated levels of circulating glucose. Also, the augment of the local cerebral glucose utilization is correlated positively with elevated expression of GLUT1 (Choeiri et al., 2005). Gap junctions (GJ) are specialized structures formed

by integral membrane proteins termed connexins which form intercellular channels providing diffusion of chemical and electrical information between adjacent cells. The most conspicuous connexin forming the GJ is Cx43; it is also the predominant isoform in astrocytes (Rouach et al., 2004). Cx43 has been also described in the porcine blood-brain barrier endothelial cells (Nagasawa et al., 2006).

The data showed that the presence of PNV in the circulation was able to affect the proteins studied. However, the expression/content of each one showed particular dynamics along the trial period and depending on being expressed, either in hippocampus or cerebellum. Studies have shown that MRP1 is located in the luminal aspect of the BBB (Nies et al., 2004), is expressed by cultured astrocytes of rodents and humans and by reactive astrocytes of human brain, but was not detected in non-reactive ones (see Hirrlinger et al., 2005). Our results showed MRP1 labeling located at the BBB; but the light microscopy resolution did not permit to affirm if the labeling corresponds to the protein localization in endothelium, astrocytic end-feet or pericytes (Shimizu et al., 2008), or in all or some of them. GLUT1 labeling appeared outlining the vessels lumen; in envenomed animals also appeared in the parenchyma ground suggesting astrocytes reactivity. In the brain, GLUT1 derived of the same gene appears in two isoforms, one vascular and the other astrocytic (Kacem et al., 1998), depending on the molecular weight; GLUT1 density is particularly high in cortical structures, such as the frontal cortex and the motor cortex as well as in the hippocampus and the cerebellum (Choeiri et al., 2002). Here, the cerebellum showed greater basal contents of MRP1 and GLUT1 than the hippocampus; cerebellum also showed lesser variability in the proteins level in PNV-groups during the trial period. These data corroborate with previous studies showing hippocampus more susceptible to the systemic PNV, with BBB breakdown effects more evident, whereas cerebellum was unchanged (Le Sueur et al., 2004), or its recovery was faster, (Rapôso et al., 2007). A possible explanation would be that the cerebellum greater content, including basally, of GLUT1 would supply in part the extra-needs for fuel. Whether the cerebellar basal content of these proteins is reflex of a more efficient system for drug exclusion (and tightness of BBB), and transport of glucose, allowing non-significant extra-requirements of these proteins in PNV-groups is undetermined so far. The fact is that hippocampus showed higher sensitivity to PNV, as shown by the growing significant increases in both proteins levels/expression. It might reflect that the hippocampus consumption for glucose in PNV-exposed animals is higher than that by cerebellum, since high levels of GLUT1 expression have been associated with augment of the local cerebral glucose utilization (Choeiri et al., 2005). In agreement, MRP1 in cerebellum showed a tendency to return to basal levels between 2 and 5 h, whereas in hippocampus a continued significant increase was seen until 5 h post-venom exposure. At this time interval (2-5 h) the

attenuation of the intoxication signs (salivation, piloerection, lachrymation, tremors, respiratory stress) and progress of exploratory and locomotor's behavior were in frank course (Rapôso et al., 2007). It also coincides with increased S100, TNF-α and IFN-γ reactivity and regression of GFAP content (5 h) subsequent to a previous gliosis by perivascular astrocytes in hippocampus and by the specialized astrocytes from cerebellum, the Bergmann glia, using the same experimental model (Cruz-Höfling et al., 2009). The high levels/expression of MRP1 and GLUT1 between 2-5 h after envenoming might represent an adaptive reaction of the animals' organism to prevent the minor molecular weight PNV toxins from entering the brain (MRP1), and to facilitate the glucose entrance for supplying increased brain metabolism induced by the stress of animal and/or by venom pharmacological action (GLUT1). Little has been reported about interactions between multidrug resistance protein and glucose transporter protein. However, it is conceivable that cytotoxic xenobiotics insulting the CNS demands greater resources of glucose and mechanism for eliminating the toxic agent. An increased rate of facilitative glucose transport and level of GLUT1 expression paralleled with increased vincristine resistance, active vincristine efflux and decreased vincristine steady-state accumulation in *in vitro* cell lines; moreover, glucose transport inhibitors (cytochalasin B and Phloretin) blocked the active efflux and increased steady-state accumulation of vincristine (Martell et al., 1997). Various factors, such as drug metabolism, alteration of target proteins, increased CNS elimination, and decreased cellular drug accumulation have been ascribed to the development of cellular drug resistance (MDR) phenotype (Dallas et al., 2006; Dean et al., 2001). The use of inhibitors against efflux proteins, such as the members of ABC transporters family, including the MRPs, have been investigated in order to decrease the resistance to the entry of therapeutic drugs (Kubota et al., 2006). The present results showing that the PNV induced increase in MRP1 expression, at same time that maintain active the transport/consumption of glucose (higher GLUT1 expression/content) elects the venom as a useful tool for future researches about MDR phenotype development and drug efflux.

Taken together, the present results support previous studies indicating that changes in the BBB function caused by the venom of *P. nigriventer* result mainly in alterations of the transcellular transport (Le Sueur et al., 2004) since, as seen here both the transcellular influx (glucose) and efflux (venom neurotoxins) were affected at the blood-brain interface.

Recent study, using the present experimental design, showed that 2 h post-PNV administration, neurons from several motor-related and stress-related cerebral areas exhibited activation, as shown by upregulated FOS reactivity (Cruz-Höfling et al., 2007). The brain capillary phenotype, typical of the BBB, is critically dependent on interactions with cells found closely associated with brain capillaries, such as pericytes (Shimizu et al., 2008) and astrocytes (Abbott,

2002). Like the brain endothelial cells, the pericytes express some barrier-related transporter proteins, the drug-efflux MRP1 and the substrate-influx GLUT1, as well as the tight junction molecules, occludin and ZO-1, indicating functional cooperation with endothelial cells (Shimizu et al., 2008).

Astrocytes are eclectic glial cells, whose variety of functions aims primarily to maintain CNS homeostasis for normal neuronal activity. Being the most abundant cell type in the CNS, the different populations of astrocytes, establish interactions to each other (homotypic interaction), with capillary endothelium, other glial cells and to neurons (heterotypic interaction) (Abbott, 2002; Giaume et al., 1997). The homotypic coupling among the astrocytes is extensively established through gap junctions (GJ) composed mostly by Cx43, being both the expression of the protein as well the permeability of the GJ closely regulated (Giaume and McCarthy, 1996).

Herein, it was found a two-step Cx43 reactivity characterized by significant increase soon at 15 min post-PNV exposure, both in hippocampus and cerebellum, followed by significant decrease in hippocampus thereafter, and a trend for decrease in cerebellum. The findings indicate that the systemic PNV affects GJs' stability, and hence homotypic and heterotypic cell interactions, probably one of the mechanistic causes of BBB permeability induced by PNV. Tabernero and co-workers (2006) identified steps and molecular pathways that reinforce the hypothesis of a potential link between GJs and energy metabolism in astrocytes. Interestingly, the inhibition of Cx43 and decrease of GJs specialized membrane regions causes increase of glucose transport by astrocytes through GJs (Giaume et al., 1997) which is associated with upregulation of Na+/K+-ATPase activity. Also, the treatment of GJs with inhibitors, such as endothelin-1 or carbenoxolone, decreases the expression of Cx43. Moreover, when Cx43 was silenced in astrocytes by siRNA, the knock down of Cx43 increased the rate of glucose uptake, characterized by the upregulation of GLUT1 (Herrero-González et al., 2009). In conformity, comparing the present results for GLUT1 and Cx43, one can see an inverse relationship between these proteins expression, that is, when the Cx43 expression decreased, gradually increased the expression of GLUT1. The basis of this relationship is still unknown, but it is plausible to think that situations that insult the CNS may lead to negative interference in cell-to-cell communication, homeostasis loss and hence higher needs for energy resources.

It is also elusive why PNV affects the exchange of information by GJs differently in the hippocampus and cerebellum. Likely, the type and/or number of the colonized astrocytes, neurons, membrane receptors, the extent of the microcirculation, among others, might be behind the differences in the response to venom exhibited by both brain regions. In line, neurons from

hippocampus and cerebellum have distinct properties, and studies indicate that GP communication and Cxs expression in astrocytes are controlled by neurons (Rouach et al., 2004).

Increasing body of evidences indicates a mutual influence between the astrocytes and neurons, with astrocyte function extrapolating the widespread notion of simply brain support. In fact, *in vitro*, *in situ* and *in vivo* studies have given strong evidences on the existence of glutamatergic, GABAergic, adrenergic, peptidergic, serotoninergic, purinergic and muscarinic receptors in several astrocytic cells populations, including the protoplasmatic and fibrous astrocytes, and the specialized Bergmann glia, Müller glia and pituicytes. The expression of these neurotransmitter receptors by astrocytes were shown to vary regionally and intra-regionally and in response to injury (Porter and McCarthy, 1997).

P. nigriventer venom consists of serotonin, histamine (Schenberg and Pereira- Lima, 1978), and several pharmacologically-active neurotoxins, some excitotoxic (Brazil and Veillard, 1925) targeting the voltage-gated Ca^{2+}, K^+ and Na^+ channels conductance (Gomez et al., 2002; Rezende et al., 1991). Some neurotoxins block Ca^{2+} channels, inhibit glutamate release (Romano-Silva et al., 1993), induce vascular permeability in rat and rabbit which is associated with activation of histamine and serotonin receptors (Antunes et al., 1992), and activates type 5-HT4 receptors in vagus nerve preparations, probably a mechanism involved in pain and inflammation caused by venom (Costa et al., 2003).

As seen, the PNV has a number of pharmacological attributes which potentially may affect the BBB-associated cells and molecules, for instance, the glutamatergic and serotoninergic receptors and the ionic channels (principally the Ca^{2+} channels) from astrocytes and neurons. In response to pre-synaptic neurons evoked inward currents of Ca^{2+} into the astrocytes, these cells in turn release neurotransmitters, such as, glutamate and ATP; which, in sequence either feed-back pre-synaptic terminals to activate or depress activity, or directly acts onto post-synaptic neurons producing then excitatory or inhibitory responses (Newman, 2003; Santello and Volterra, 2009).

In summary, since the presence of molecular expression of Cx43, GLUT1 and MRP1 was detected in astrocytes, pericytes, endothelial cells and neurons, and given these proteins underwent changes by the PNV, it is likely that modulation of neuro-glial interactions, and even heterotypic interactions might have occurred eventually explaining the BBB permeabilization and clinical neurological signs of victims of Phoneutriism. The increases in MRP1 and GLUT1 and the decrease of Cx43 contents seen mainly between 2-5 h after envenoming suggests continuing toxin clearance, accelerated glucose uptake and utilization and deficit in the communication network among astrocytes, astrocytes-endothelial cells, and likely astrocytes-neuronal cells. We suggest that the deficit in cell-cell communication is protective against excitotoxic toxins present in the venom. At

this time interval, the recovery of the intoxication signs is underway. Hence, the venom of the spider *P. nigriventer* promotes transient changes in BBB (Cruz-Höfling et al., 2009; Le Sueur et al., 2003; Rapôso et al., 2007); the use of inhibitors of protein efflux, for instances spider venom toxins, associated with the maintenance of the transport of glucose can provide good prospects for transient openings of the barrier to the entry of drugs of interest.

Acknowledgements: The authors thank Instituto Butantan (São Paulo, SP, BR) for venom donation. The authors also thank Mrs. Marta Beatriz Leonardo (BSc) for excellent technical assistance, and Mr. Miguel Silva and Mr. Marcos Silva for animal care. This work hás been funded by grants from Fundação de Amparo à Pesquisa do Estado de São Paulo (FAPESP # 07/50242-6) and Conselho Nacional de Desenvolvimento Científico e Tecnológico (CNPq, grant #. 481316/2008-6). P.A.M.O. and C.R are recipients of scholarship from FAPESP (grant # 07/56715-7 and 07/50272-6, respectively); S.F.S. is recipient from scholarship from CNPq (grant # 504732/2007-2). M.A.C.H. is 1A research fellow from CNPq (# 302206/2008-6).

References

Abbott NJ, Romero IA. 1996. Transporting therapeutics across the blood–brain barrier. Mol Med Today 2:106-113.

Abbott N. 2002. Astrocyte-endothelial interactions and blood-brain barrier permeability. J Anat 200:527.

Antunes E, Marangoni RA, Brain SD, De Nucci G. 1992. *Phoneutria nigriventer* (armed spider) venom induces increased vascular permeability in rat and rabbit skin *in vivo*. Toxicon 30:1011-1016.

Banks WA. 2008. Developing drugs that can cross the blood-brain barrier: applications to Alzheimer's disease. BMC Neurosci 10:1-4.

Bucaretchi F, Deus Reinaldo CR, Hyslop S, Madureira PR, De Capitani EM, Vieira RJ. 2000. A clinico-epidemiological study of bites by spiders of the genus *Phoneutria*. Ver Inst Méd Trop São Paulo 42:17-21.

Brazil V, Veillard J. 1925. Contribuição ao estudo do veneno das aranhas. Mem Inst Butantan 2:5-77.

Choeiri C, Staines W, Messier C. 2002. Immunohistochemical localization and quantification of glucose transporters in the mouse brain. Neuroscience 111:19-34.

Choeiri C, Staines W, Miki T, Seino T, Messier C. 2005. Glucose transporter plasticity during memory processing. Neuroscience 130:591-600.

Costa SK, Brain SD, Antunes E, De Nucci G, Docherty RJ. 2003. *Phoneutria nigriventer* spider venom activates 5-HT4 receptors in rat-isolated vagus nerve. Br J Pharmacol 139:59-64.

Cruz-Höfling MA, Love S, Brook G, Duchen LW. 1985. Effects of *Phoneutria nigriventer* spider venom on mouse peripheral nerve. Q J Exp Physiol 70:623-640.

Cruz-Höfling MA, Zago GM, Melo LL, Rapôso C. 2007. c-FOS and n-NOS reactive neurons in response to circulating *Phoneutria nigriventer* spider venom. Brain Res Bull 73:114-126.

Cruz-Höfling MA, Rapôso C, Verinaud L, Zago GM. 2009. Neuroinflammation and astrocytic reaction in the course of *Phoneutria nigriventer* (armed-spider) blood-brain barrier (BBB) opening. NeuroToxicology 30:636-46.

Dallas S, Miller DS, Bendayan R. 2006. Multidrug resistance-associated proteins: expression and function in the central nervous system. Pharmacol Rev 58:140-161.

Davson H, Oldendorf WH. 1967. Transport in the central nervous system. Proc Royal Soc Med 60:326-328.

Dean M, Hamon Y, Chimini G. 2001. The human ATP-binding cassette (ABC) transporter superfamily. J Lipid Res 42:1007-1017.

Duelli R, Kuschinsky W. 2001. Brain glucose transporters: relationship to local energy demand. News Physiol Sci 16:71-76.

Estrada G, Villegas E, Corzo G. 2007. Spider venoms: a rich source of acylpolyamines and peptides as new leads for CNS drugs. Nat Prod Rep 24:145-161.

Farquhar MG, Palade GE. 1963. Junctional complexes in various epithelia. J Cell Biol 17:375–412.

Fontana MD, Vital-Brazil O. 1985. Mode of action of *Phoneutria nigriventer* spider venom at the isolated phrenic nerve-diaphragm of the rat. Braz J Med Biol Res 18:557-565.

Giaume C, Tabernero A, Medina JM. 1997. Metabolic trafficking through astrocytic gap junctions. Glia 21:114-123.

Giaume C, McCarthy KD. 1996. Control of gap-junctional communication in astrocytic networks. Trends Neurosci. 19:319-325.

Gomez MV, Kalapothakis E, Guatimosim C, Prado MA. 2002. *Phoneutria nigriventer* venom: a cocktail of toxins that affect ion channels. Cell Mol Neurobiol 22:579-588.

Herrero–González S, Valle–Casuso JC, Sánchez–Alvarez R, Giaume C, Medina JM, Tabernero A. 2009. Connexin43 is involved in the effect of endothelin–1 on astrocyte proliferation and glucose uptake. Glia 57:222-233.

Hirrlinger J, Moeller H, Kirchhoff F, Dringen R. 2005. Expression of multidrug resistance proteins (Mrps) in astrocytes of the mouse brain: a single cell RT-PCR study. Neurosci Res 30:1237-1244.

Kacem K, Lacombe P, Seylaz J, Bonvento G. 1998. Structural organization of the perivascular astrocyte endfeet and their relationship with the endothelial glucose transporter: a confocal microscopy study. Glia 23:1–10.

Kubota H, Ishihara H, Langmann T, Schmitz G, Stieger B, Wieser HG, Yonekawa Y, Frei K. 2006. Distribution and functional activity of P-glycoprotein and multidrug resistance-associated proteins in human brain microvascular endothelial cells in hippocampal sclerosis. Epilepsy Res, 68:213-228.

Le Sueur LP, Collares-Buzato CB, Cruz-Höfling MA. 2004. Mechanisms involved in the blood-brain barrier increased permeability induced by *Phoneutria nigriventer* spider venom in rats. Brain Res 1027:38-47.

Le Sueur LP, Kalapothakis E, Cruz-Höfling MA. 2003. Breakdown of the blood–brain barrier and neuropathological changes induced by *Phoneutria nigriventer* spider venom. Acta Neuropathol 105:125-134.

Martell RL, Slapak CA, Levy SB. 1997. Effect of glucose transport inhibitors on vincristine efflux in multidrug-resistant murine erythroleukaemia cells overexpressing the multidrug resistance-associated protein (MRP) and two glucose transport proteins, GLUT1 and GLUT3. Br J Cancer 75:161-168.

Martin PEM, Evans WH. 2004. Incorporation of connexins into plasma membranes and gap junctions. Cardiovasc Res 62:378-387.

Nagasawa K, Chiba H, Fujita H, Kojima T, Saito T, Endo T, Sawada N. 2006. Possible involvement of gap junctions in the barrier function of tight junctions of brain and lung endothelial cells. J Cell Physiol 208:123-132.

Newman EA. 2003. New roles for astrocytes: regulation of synaptic transmission. Trends Neurosci 26:536-542.

Nicholson BJ. 2003. Gap junctions—From cell to molecule. J Cell Sci 116:4479–4481.

Nies AT, Jedlitschky G, König J, Herold-Mende C, Steiner HH, Schmitt HP, Kepler D. 2004. Expression and immunolocalization of the multidrug resistance proteins, MRP1- MRP6 (ABCC1-ABCC6), in human brain. Neuroscience 129:349-360.

Porter JT, McCarthy KD. 1997. Astrocytic neurotransmitter receptors in situ and in vivo. Prog Neurobiol 51:439-455.

Rapôso C, Zago GM, da Silva GH, da Cruz-Höfling MA. 2007. Acute blood-brain barrier permeabilization in rats after systemic *Phoneutria nigriventer* venom. Brain Res 1149:18-29.

Rezende JL, Cordeiro MN, Oliveira EB, Diniz CR. 1991. Isolation of neurotoxic peptides from the venom of the "armed" spider *Phoneutria nigriventer*. Toxicon 29:1225-1233.

Romano-Silva MA, Ribeiro-Santos MA, Ribeiro AM, Gomez MV, Diniz CR, Cordeiro MN, Brammer MJ. 1993. Rat cortical synaptosomes have more than one mechanism for Ca2+ entry linked to rapid glutamate release: studies using the *Phoneutria nigriventer* toxin PhTX2 and potassium depolarization. Biochem J 296:313-319.

Rouach N, Koulakoff A, Giaume C. 2004. Neurons set the tone of gap junctional communication in astrocytic networks. Neurochem Int 45:265-272.

Rubin LL, Hall DE, Porter S, Barbu K, Cannon C, Horner HC, Janatpour M, Liaw CW, Manning K, Morales J, Tanner L, Tbmaselli KJ, Bard F. 1991. A cell culture model of the blood-brain barrier. J Cell Biol 115:1725-1735.

Rubin LL, Staddon JM. 1999. The cell biology of the blood–brain barrier. Annu Rev Neurosci 22:11-28.

Schenberg S, Pereira-Lima FA. 1978. Handbook of Experimental Pharmacology, vol. 48. New York, Berlin, Heilderberg: Springer, p. 217-44.

Sáez JC, Berhoud VM, Branes MC, Martı´nez AG, Beyer EC. 2003. Plasma membrane channels formed by connexins: Their regulation and functions. Physiol Rev 85:1359-1400.

Santello M, Volterra A. 2009. Synaptic modulation by astrocytes via Ca2+-dependent glutamate release. Neuroscience 158:253-259.

Sawada N, Murata M, Kikuchi K, Osanai M, Tobioka H, Kojima T, Chiba H. 2003. Tight junctions and human diseases. Med Electron Microsc 36:147–156.

Shimizu F, Sano Y, Maeda T, Abe MA, Nakayama H, Takahashi R, Ueda M, Ohtsuki S, Terasaki T, Obinata M, Kanda T. 2008. Peripheral nerve pericytes originating from the blood-nerve barrier expresses tight junctional molecules and transporters as barrierforming cells. J Cell Physiol 217:388-399.

Söhl G, Willecke K. 2004. Gap junctions and the connexin protein family. Cardiovasc Res 62:228-232.

Tabernero A, Medina JM, Giaume C. 2006. Glucose metabolism and proliferation in glia: role of astrocytic gap junctions. J Neurochem 99:1049-1061.

Wolburg H, Lippoldt A. 2002. Tight junctions of the blood-brain barrier: Development, composition and regulation. Vascul Pharmacol 38:323-337.

Yang J, Aschner M. 2003. Developmental aspects of blood–brain barrier (BBB) and rat brain endothelial (RBE4) cells as in vitro model for studies on chlorpyrifos transport. NeuroToxicolology 24:741-745.

Legend for figures

Figure 1: *Immunofluorescence (IF) and western blotting for MRP1 in hippocampus:* There was gradual increase in the reactivity of the protein in relation to control (**A-D**; Bar= 35 μm). **E:** IF densitometric values showed a significant increase in PNV-5 h compared to control (* $p<0.05$) (n=5 each). **G**: The level of MRP1 increased in PNV-5 h group (n=5) which was significant in relation to control pool (n=15, * $p<0.05$), PNV- 15 min (n=5, † † † $p < 0.001$) and PNV-2 h (n=5, # # $p < 0.01$). β-Actin served as reference of the loading control of protein for each sample, and panel G shows ratios of the MRP1 band intensity over corresponding β-actin intensity. Each value represents the mean ± S.E.M. IF and WB data were analyzed by one-way ANOVA followed by the Tukey-Kramer post-test. Unpaired t-test was used if necessary. The results were confirmed in three sets of experiments; v = blood vessel.

Figure 2: *Immunofluorescence and western blotting for MRP1 in cerebellum:* The immunolabeling of the drug resistance protein, MRP1, showed significant increase until 2 h post-PNV injection

(panels **A,B,C,E**, * p<0.05, Scale bar = 35 μm, n=5/experimental group), after which there was a tendency for a decreased expression (**D**). A similar behavior was shown by the level of the protein along the time-course (**G**); differences in the protein level between venom-treated groups (n=5/group) and pooled-control (n=15 rats) have no statistic significance. β-Actin served as reference of the loading control of protein for each sample, and panel G shows ratios of the MRP1 band intensity over corresponding β-actin intensity. Each value represents the mean ± S.E.M. IF and WB data were analyzed by one-way analysis of variance (ANOVA) followed by the Tukey-Kramer post-test. Unpaired t-test was used if necessary. The results were confirmed in three sets of experiments; v = blood vessel.

Figure 3: *Immunofluorescence and western blotting for GLUT1 in hippocampus:* The reactivity of the glucose transporter protein isoform 1, GLUT1, increased significantly at 2 h and 5 h, compared to paired control (panels **A – D**, Bar = 35 μm). Panel **E** shows that the differences were significant when compared control with both PNV-2 h (* * p < 0.01) and PNV-5 h (* p < 0.05), or comparing PNV-15 minutes with PNV-2 h († † p < 0.01) or PNV-5 h († p <0.05). In panel **G**, the ratios of the GLUT1 band intensity over corresponding β-actin intensity content seen through the WB bands densitometry showed that the differences were significant between the envenomed groups, PNV-15 min *vs.* PNV-5 h groups († † † p < 0.001). β-Actin served as reference of the loading control of protein for each sample.Each value represents the mean ± S.E.M. IF and WB data were analyzed by one-way analysis of variance (ANOVA) followed by the Tukey-Kramer post-test. Unpaired t-test was used if necessary. The results were confirmed in three sets of experiments; v = blood vessel; * = astrocytic labeling.

Figure 4: *Immunofluorescence and western blotting for GLUT1 in cerebellum:* IF showed that there was an enhanced immunolabeling of GLUT1 in cerebellum vessels of PNV-5 h group (panels **A – D**, Bar=35 μm). Labeling quantification (**E**) showed that the increase in the GLUT1 content in PNV-5h was significant in relation to PNV-15 min († p <0.05) and PNV-2 h (# p <0.05). Panel **G** showed practically unchanged the protein content until 2 h post-venom injection; thereafter, occurred an increase in the PNV-5 h group, which was significant when compared with control (* p < 0.05), and with 15 min group († † † p < 0.001). β-Actin served as reference of the loading control of protein for each sample, and panel **G** shows ratios of the GLUT1 band intensity over corresponding β-actin intensity. Each value represents the mean ± S.E.M. IF and WB data were analyzed by one-way analysis of variance (ANOVA) followed by the Tukey-Kramer post-test.

Unpaired t-test was used if necessary. The results were confirmed in three sets of experiments; v = blood vessel; * = astrocytic labeling.

Figure 5: *Immunofluorescence and western blotting for Cx43 in hippocampus:* Reactivity of Cx43 delineates the blood vessels (v) profiles (**A,B,C,D**); at 15 min of envenoming the astrocytes are also labeled (see asterisks), Bar = 35 μm (C). Panel **E** shows a significant increase of Cx43 reactivity at PNV-15 min (* $p < 0.05$) followed by marked decrease at PNV-5 h (** $p < 0.01$), compared with time-matched control group. Differences were also seen between PNV-15 min and PNV-5 h (# # $p < 0.001$), and PNV-2 h and -5 h († † † $p < 0.01$). **G:** WB blots and quantification shows similar pattern of Cx43 content as for IF assay, although differences were not significant. β-Actin served as reference of the loading control of protein for each sample, and panel G shows ratios of the Cx43 band intensity over corresponding β-act in intensity. Each value represents the mean ± S.E.M. IF and WB data were analyzed by one-way analysis of variance (ANOVA) followed by the Tukey-Kramer post-test. Unpaired t-test was used if necessary. The results were confirmed in three sets of experiments; v = blood vessel; * = astrocytic labeling = comparing with PNV-2 h.

Figure 6: *Immunofluorescence and western blotting for Cx43 in cerebellum:* There was increase in the labeling of the protein in PNV-15 min (* $p < 0.05$), compared to corresponding control; thereafter a trend for decreasing was seen (**A,B,C,D,E**). The labeling was mainly in the granule and Purkinje layers of the cerebellar cortex. The densitometric values of the WB bands showed a tendency of increase. β-Actin served as reference of the loading control of protein for each sample, and panel G shows ratios of the Cx43 band intensity over corresponding β-actin intensity. Each value represents the mean ± S.E.M. IF and WB data were analyzed by one-way analysis of variance (ANOVA) followed by the Tukey-Kramer post-test. Unpaired t-test was used if necessary. The results were confirmed in three sets of experiments. Bars = 70 μm (A,B,D); 35 μm (C).

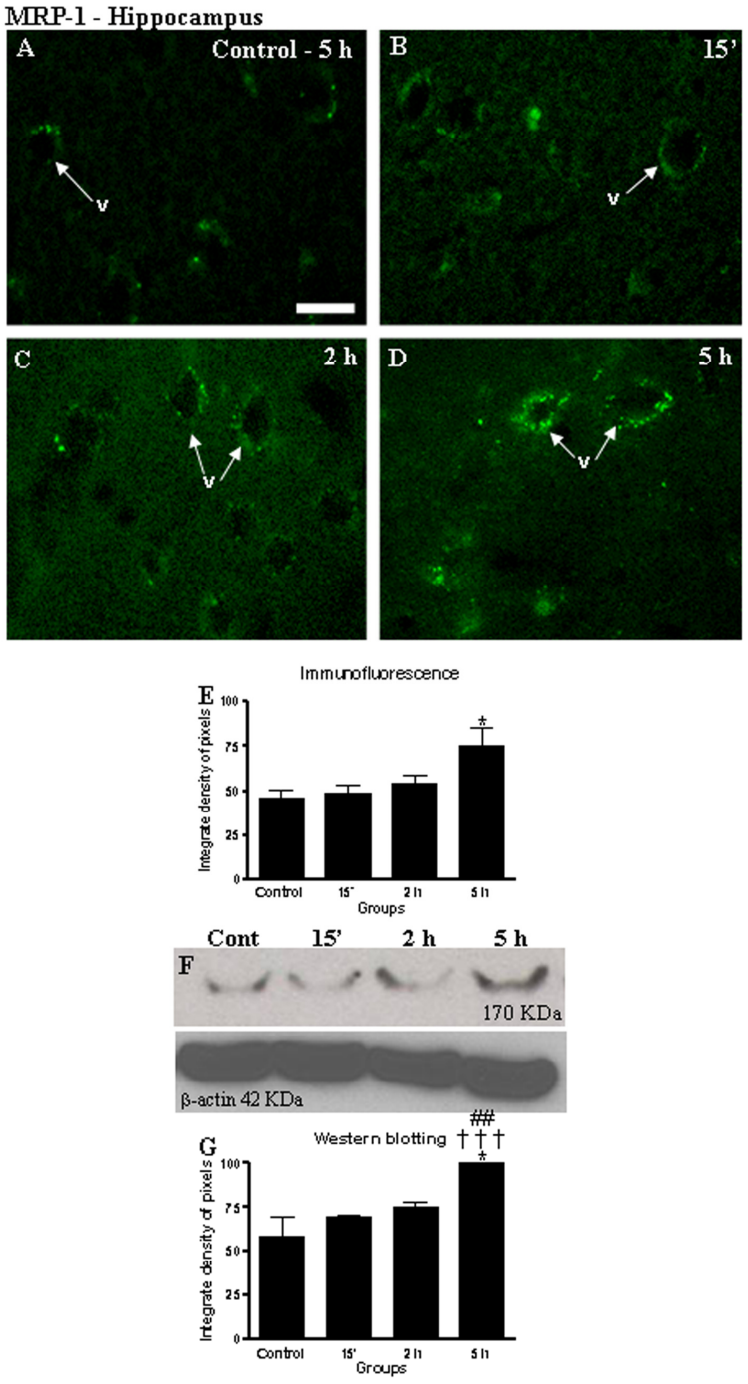
MRP-1 - Hippocampus
A
Control - 5 h
B
15'
C
2 h
D
5 h
v
Immunofluorescence
E
Integrate density of pixels
Control
15'
2 h
5 h
Groups
Cont
15'
2 h
5 h
F
170 KDa
β-actin 42 KDa
Western blotting
G
Integrate density of pixels
Control
15'
2 h
5 h
Groups

Figure 1

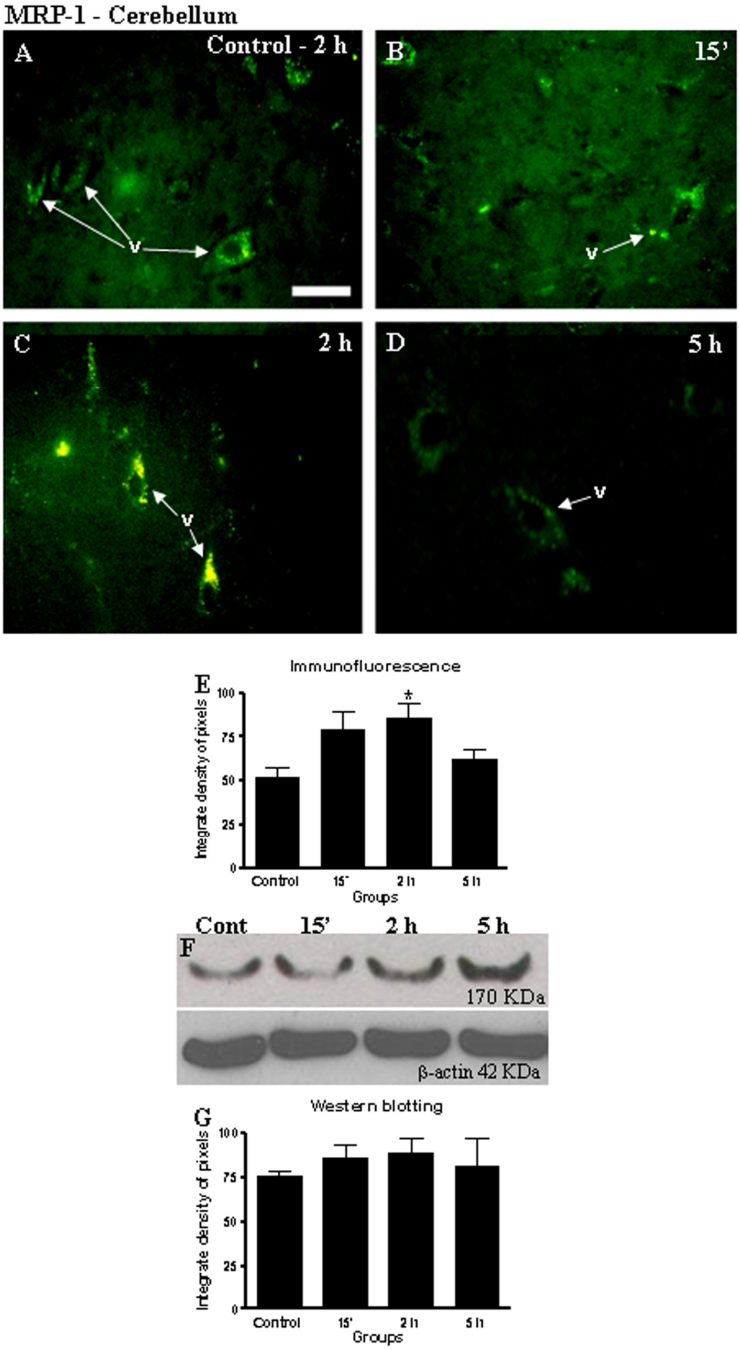
MRP-1 - Cerebellum
A
Control - 2 h
B
15'
C
2 h
D
5 h
v
Immunofluorescence
E
Integrate density of pixels
100
75
50
25
0
*
Control
15'
2 h
5 h
Groups
Cont
15'
2 h
5 h
F
170 KDa
β-actin 42 KDa
Western blotting
G
Integrate density of pixels
100
75
50
25
0
Control
15'
2 h
5 h
Groups

Figure 2

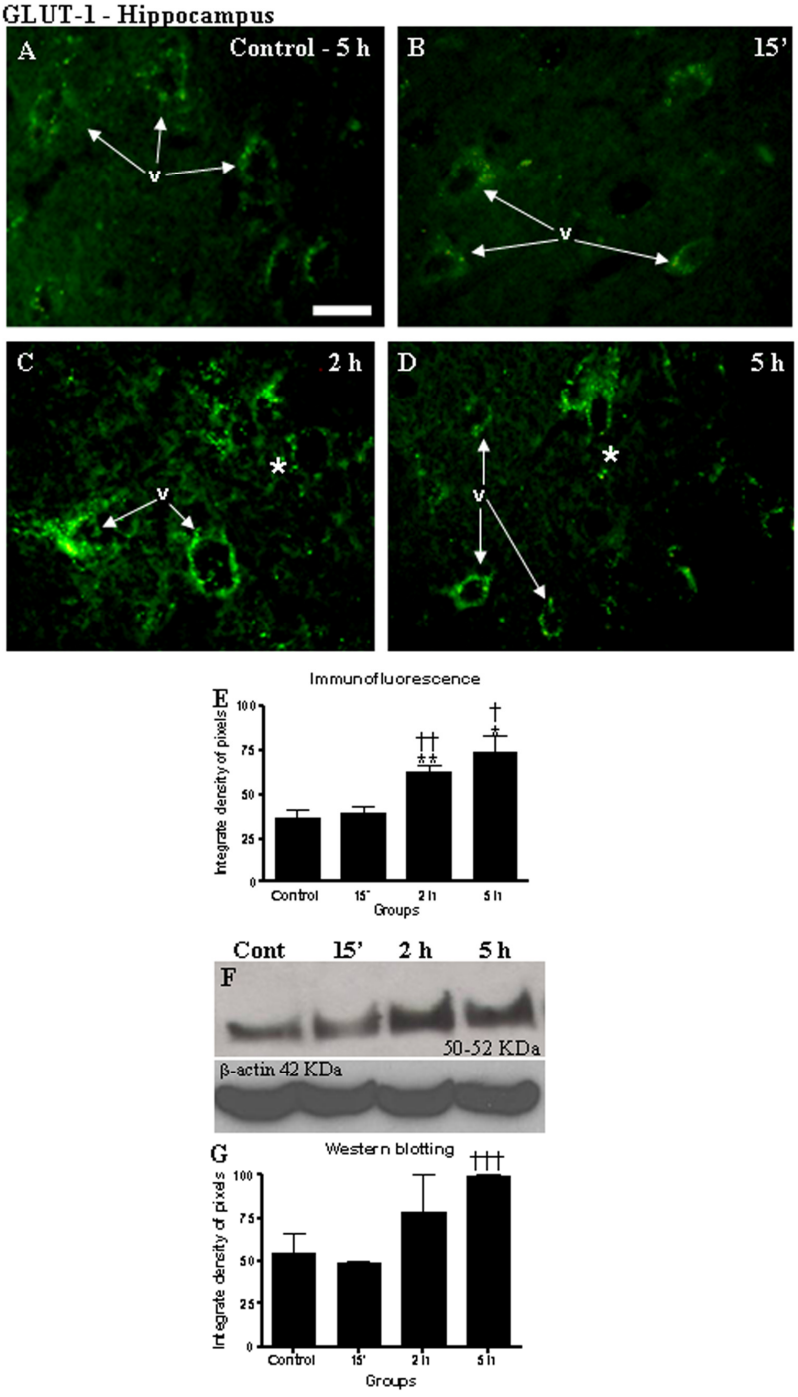
GLUT-1 - Hippocampus
A
Control - 5 h
B
15'
C
2 h
D
5 h
v
*
Immunofluorescence
E
Integrate density of pixels
Control
15'
2 h
5 h
Groups
Cont
15'
2 h
5 h
F
50-52 KDa
β-actin 42 KDa
Western blotting
G
Integrate density of pixels
Control
15'
2 h
5 h
Groups

Figure 3

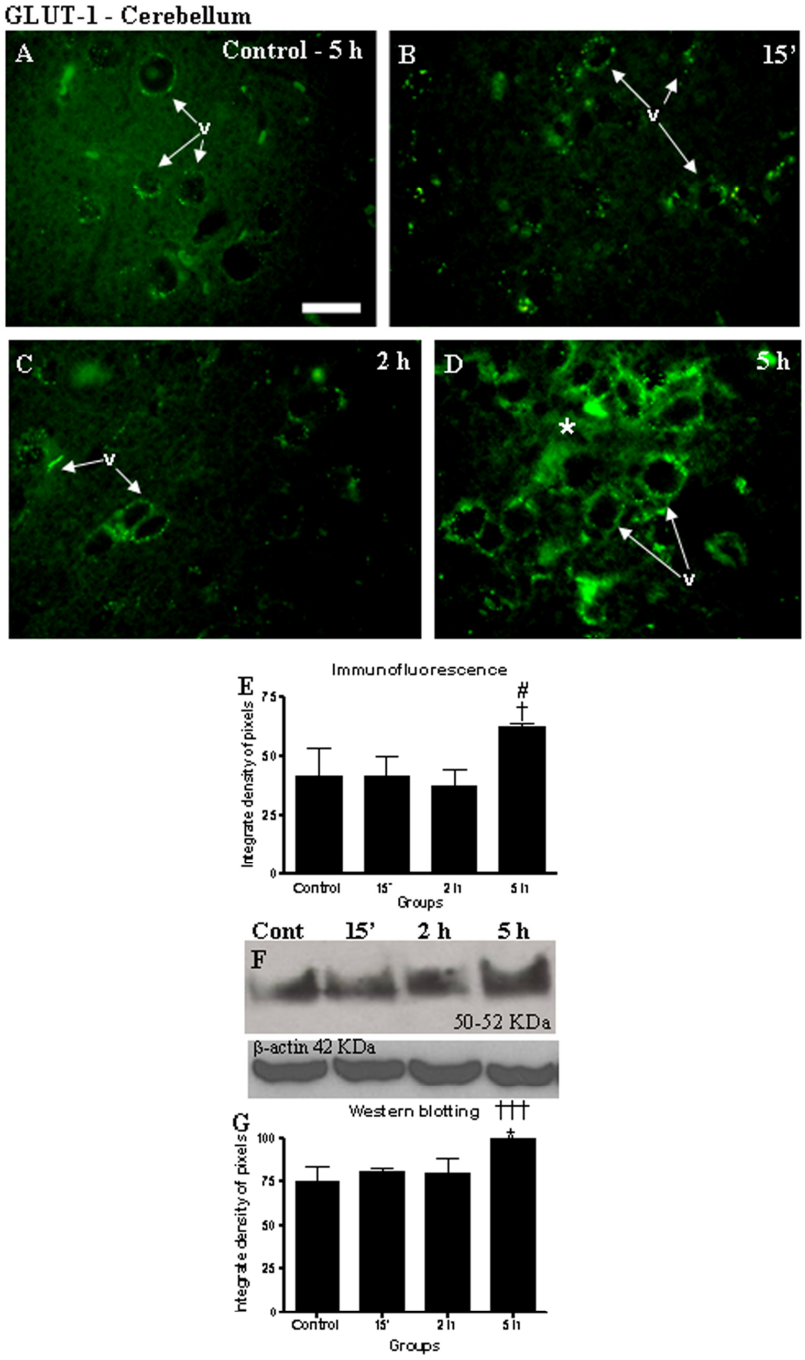
GLUT-1 - Cerebellum
A
Control - 5 h
B
15'
C
2 h
D
5 h
Immunofluorescence
E
Integrate density of pixels
Control
15'
2 h
5 h
Groups
Cont
15'
2 h
5 h
F
50-52 KDa
β-actin 42 KDa
Western blotting
G
Integrate density of pixels
Control
15'
2 h
5 h
Groups

Figure 4

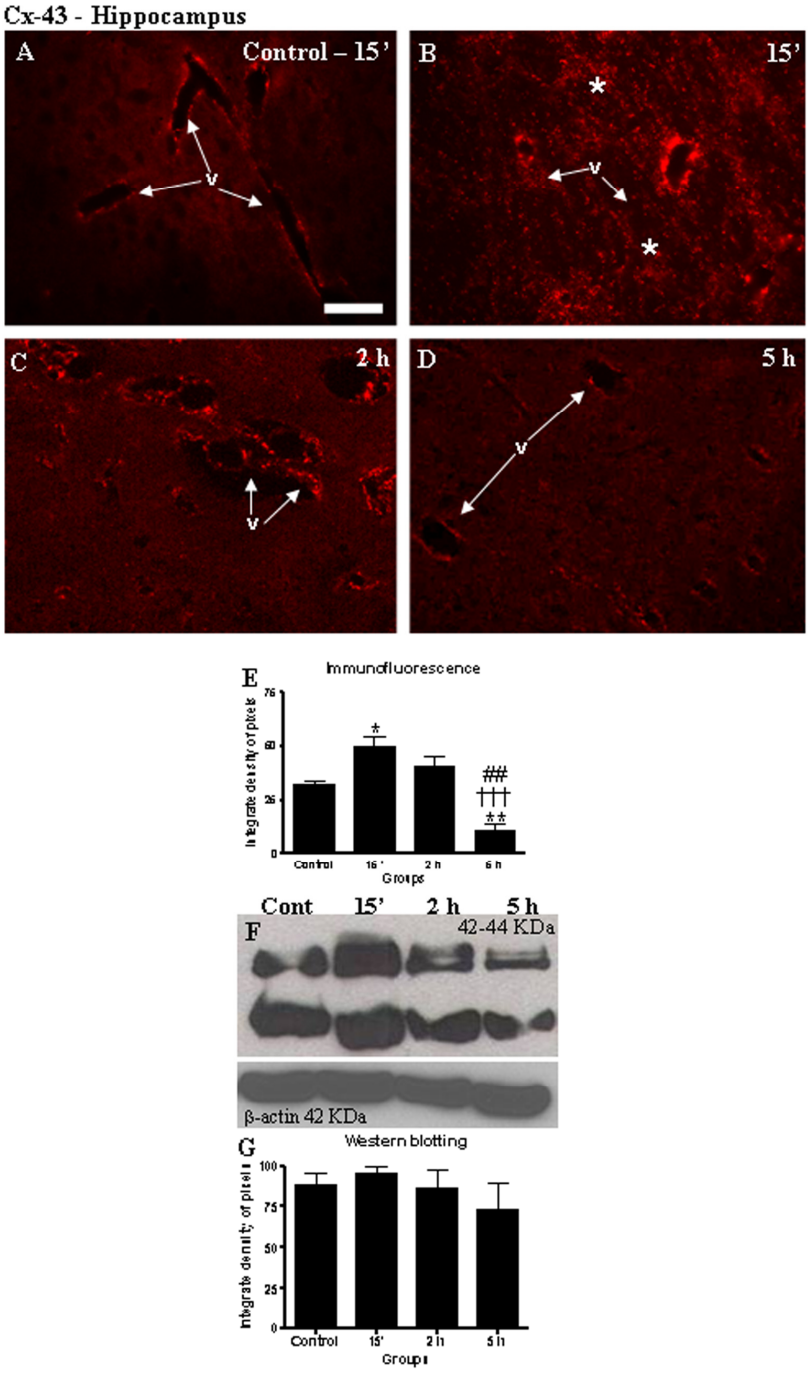
Cx-43 - Hippocampus
A
Control – 15'
B
15'
C
2 h
D
5 h
E
Immunofluorescence
Integrate density of pixels
Control
15'
2 h
5 h
Groups
Cont
15'
2 h
5 h
F
42-44 KDa
β-actin 42 KDa
G
Western blotting
Integrate density of pixels
Control
15'
2 h
5 h
Groups

Figure 5

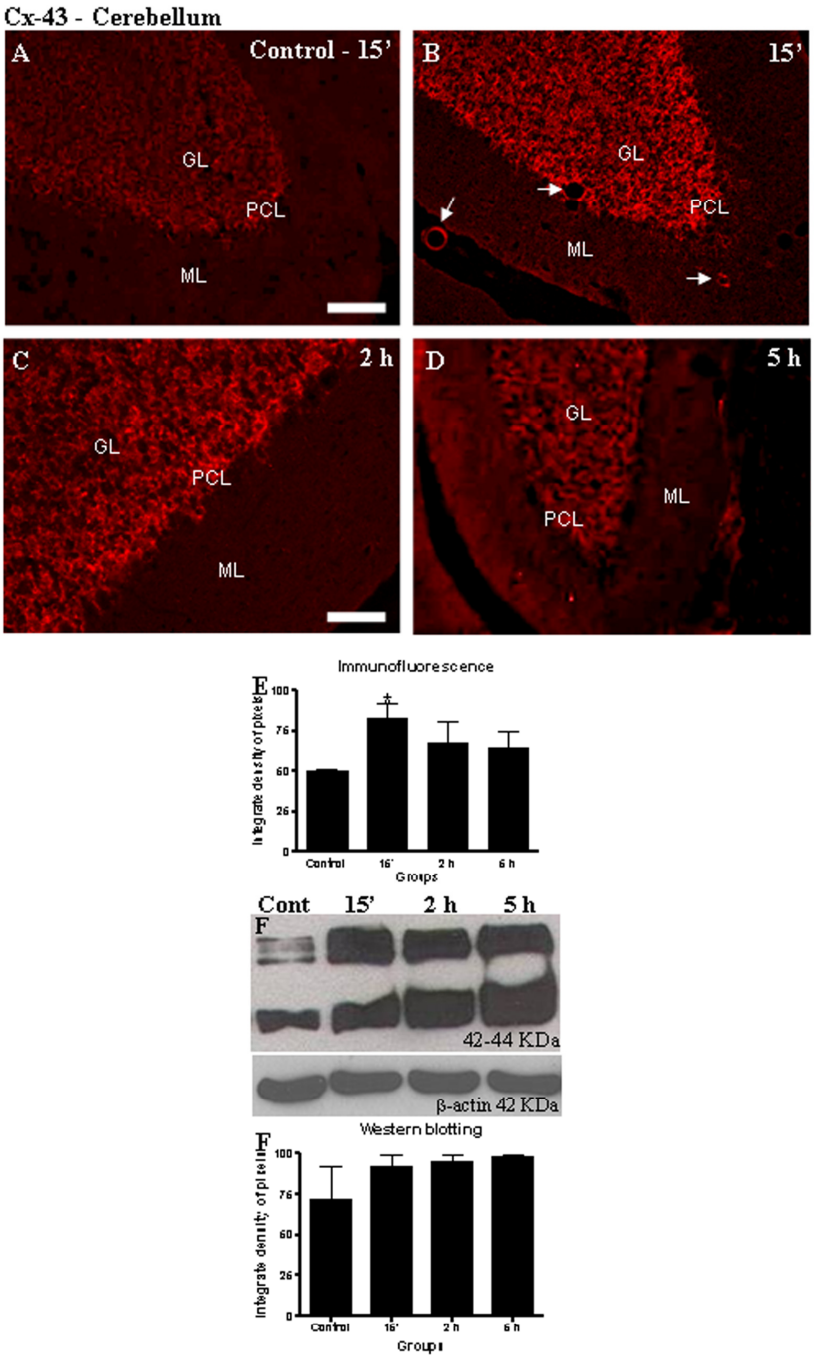
Cx-43 - Cerebellum
A
Control - 15'
GL
PCL
ML
B
15'
GL
PCL
ML
C
2 h
GL
PCL
ML
D
5 h
GL
ML
PCL
Immunofluorescence
E
Integrate density of pixels
Control
15'
2 h
6 h
Groups
Cont
15'
2 h
5 h
F
42-44 KDa
β-actin 42 KDa
Western blotting
F
Integrate density of pixels
Control
15'
2 h
6 h
Groups

Figure 6

*Maria Alice da **Cruz-Höfling**
Departamento de Histologia e Embriologia
Instituto de Biologia, C.P. 6109
Universidade Esta dual de Campinas -UNICAMP
CEP13 087-930, Campinas – SP – BRASIL
E-mail: hofling@unicamp.br
Tel/Fax (55)(19) 3521 6224; Fax. (55)(19) 3289 3124

NO signaling mediates the neurotoxic effects of *Phoneutria nigriventer* spider venom in multiple brain regions of the rat*

[1] Catarina Rapôso, [1, 2]Karina Fontana, [1 *]Maria Alice da Cruz-Höfling*

[1]Departamento de Histologia e Embriologia, Instituto de Biologia; [2] Departamento de Farmacologia, Faculdade de Ciências Médicas, Universidade Estadual de Campinas - UNICAMP, Campinas, SP, Brazil.

Running Title: **Dual role of NO in *P. nigriventer* envenoming**

(*) Supported by grants from Fundação de Amparo à Pesquisa do Estado de São Paulo (FAPESP # 07/50242-6) and Conselho Nacional de Desenvolvimento Científico e Tecnológico (CNPq # 302206/2008-6/481316/2008-6). C.R is recipient of scholarship from FAPESP. M.A.C.H. is a IA research fellow from CNPq.

Abstract

Phoneutria nigriventer spider venom (PNV) causes neurotoxic signs, blood-brain barrier breakdown and neuronal activation in CNS regions, some of which rich in nNOS-immunoreactive neurons. We examined the role of NO signaling in mediating the neurotoxic effect of the spider venom in multiple brain regions of the rat. The neuronal NOS inhibitor 7-nitroindazole was administered systemically prior to PNV exposure to determine if activation of NO signaling was responsible for observed neurotoxic signs including behavioral changes and measures of neuronal activation. Animals injected with: 1)-saline, 2)-PNV, 3)-7NI/PNV, 4)-DMSO/PNV (7NI vehicle pretreatment) and 5)-7NI were used and FOS-, NADPH-d- and double-stained neurons were counted. The onset/intensity of neurotoxic signs was registered. In 7NI/PNV, the signs were markedly precocious and intense, compared to PNV alone, suggesting downregulation of PNV toxicity by NO. PNV increased the number of FOS-positive neurons in almost all examined brain regions. NADPH-d-positive cells were found to be elevated in the ventral periaqueductal gray (vPAG) and paraventricular hypothalamic nucleus (PVN). Double-labeled cells were elevated in the PVN and supraoptic nucleus (SON). These effects were attenuated by 7-NI pretreatment in some regions and augmented in others, indicating a complex regionally specific role for NO in these effects.

Keywords: NADPH-d, FOS, nNOS, arthropod venom

Introduction

Phoneutria nigriventer venom (PNV) is a rich mixture of neuropeptides, several of which act on voltage-gated sodium-, calcium-, and potassium channels and interfere in mechanism of neurotransmitter release (1). PNV intraneural injection in mouse causes swelling of the nodes of Ranvier secondary to influx of Na^+, and iterative depolarization of nerve fibers resulting in discharge of cholinergic synaptic vesicles, and flaccid and spastic paralysis of hindlimbs (2). PNV intravenous injection in rats causes clinical signs, such as convulsions, prostration, flaccid/spastic paralysis, tremors, decrease of urinary volume, and intense salivation; simultaneous to blood-brain barrier breakdown (3-5). PNV also activates neurons, as shown by FOS immunolabeling, and increases neuronal nitric oxide synthase (nNOS) immunolabeling (6). The FOS-like positive neurons predominated in motor-related areas, such as dorsolateral and ventral periaqueductal gray matter, frontal and parietal motor cortex, and periventricular thalamic nucleus. In acute stress-related areas, the rhinal cortex and lateral septal nuclei were the most activated. Interestingly, several of these activated neurons-containing areas, also showed increase of nNOS immunoreactive neurons. Taken together, these data suggest that systemic *P. nigriventer* venom triggers neuronal pathways involved in the symptoms elicited likely through a nitric oxide-mediated mechanism (6).

The main purpose of this work is to confirm or not the participation of NO as well the nature of it in multiple brain regions of the rat. The neuronal NOS inhibitor 7-nitroindazole (7NI) was administered intraperitoneally prior the PNV to determine if the clinical signs and neural activation caused by envenoming were affected. Regions associated with the clinical signs of neurotoxicity such as the related to motility, stress/fear, and neurovegetative control were screened. The number of FOS-immunoreactive neurons and NADPH-d (reduced nicotinamide adenine dinucleotide phosphate diaphorase)-positive neurons were determined by counting stained cells in six areas of the CNS. In addition, double-staining (FOS plus NADPH-d) was employed to identify co-localization of neuronal activation and nitrergic neurons.

Materials and methods

Animals and venom

Male Wistar rats (250–300 g) were obtained from an established colony maintained by the Central Animal House Service at UNICAMP. One batch of lyophilized *P. nigriventer* crude venom (PNV) was supplied by Instituto Butantan (São Paulo, SP, Brazil). The venom was stored at -20ºC and dissolved in 0.9% sterile saline solution immediately before use.

Clinical signs

Animals belonging to each of the experimental and control groups (see below) were observed after procedures and the clinical signs were registered. Each animal was placed on the top of a bench in order to better allow observation of behavior and signs of intoxication. Three observers registered independently the time interval lasted from the treatment and the onset of signs: hyperaemia; salivation; flaccid paralysis; spastic paralysis; respiratory distress, and death. The mean of the time interval registered was calculated and statistically analyzed.

Experimental groups

The animals were divided into five groups (n = 4/group). The group PNV received a single intravenous (i.v.) injection of venom (850 µg/kg in 0.5 ml saline) in the tail vein (3); to group 7NI/PNV was given an i.p injection of 7-NI (selective nNOS inhibitor; Sigma; 50 mg/Kg), 30 min before intravenous injection of PNV. The group DMSO received the vehicle for 7NI, 30 min before intravenous injection of PNV. These groups were compared to two control groups: saline (0.9 %) i.v.-injected or 7NI (50 mg/Kg)-i.p.-injected groups. Two hours after treatment the animals were anesthetized, for the ensuing technical procedures. The experiments were done according to the guidelines of the Brazilian College for Animal Experimentation (COBEA) (Protocol n. 1700-1).

FOS/NADPH-d labeling

Two hours after PNV administration animals were anesthetized with (2 µg/mg body mass) of a 3:1 mixture of ketamine chloride (Dopalen, 100 mg/kg of animal) and xylazine chloride (Anasedan, 10 mg/kg,) (Vetbrands, Jacarei, SP, Brazil), and perfused transcardially with 0.9% saline followed by 4% paraformaldehyde in 0.1 M phosphate buffer (PBS, pH 7.4). Brains were removed and post fixed over 2 h in paraformaldehyde and stored for at least 30 h in 30% sucrose for cryoprotection. Coronal sections (40 µm) were obtained in a cryostat and collected in 16 wells containing cold PBS, 0.01 M. Consecutive wells received sections cut 600 µm apart. The sections were first processed for FOS immunohistochemistry, as previously described (7). Briefly, tissue sections were washed and endogenous peroxidase were blocked with 0.3 % H_2O_2 in 50% ethanol for 10 min, and with 1% bovine serum albumin (BSA) in 0.01 M PBS, containing 0.5 % TritonX-100, for 1 h. In sequence, the tissue was incubated for three nights at 4ºC with rabbit anti-FOS IgG (1/1500 into PBS 0.01 M/BSA 1%, sc-253, Santa Cruz Biotechnology, CA, USA). After incubation with the primary antiserum, the tissue sections were washed in 1% PBS/BSA and sequentially incubated with a biotinilated goat anti-rabbit IgG (1:500). The immunohistochemical reaction was visualized using an avidin-biotin kit (ABC – Staining System; Santa Cruz Biotechnology, CA,

USA, ref. sc-2018). Protein FOS immunoreactivity was revealed by adding the diaminobenzidine chromogen and visualized as a brown reaction product inside the neuronal nuclei. The specificity of the immunoreaction was assessed by omitting the primary antibody. For NADPH-d histochemistry, sections were incubated for 1 h in a solution containing 1 mg β-NADPH (Sigma Aldrich, ref. N1630), 0.1 mg/ml nitroblue tetrazolium (Sigma Aldrich, ref. N6876) and 0.6% Triton X-100 in PBS 0.1 M (pH 7.4). NADPH-d-stained cells were visualized as a blue reaction product inside the neuronal cytoplasm. For double staining, tissue sections processed for FOS immunohistochemistry assay were further processed for NADPH-d. The number of FOS, NADPH-d and doubled-stained cells was separately counted with a computer-aided image analysis system (Image Pro-Plus 4.0, Media Cybernetics) connected to a light microscope (Olympus) adapted with a digital camera to capture images. The stained cells contained in an area probe measuring 0.35 mm^2 in each region were counted bilaterally in four sections from each animal group. The mean value obtained from each region per treatment (n = 4) was calculated and expressed as the number of positive cells/0.35 mm^2 of tissue. The coordinates of the transversal planes and limits of each of the regions studied, supraoptic nucleus (SON), periventricular thalamic nucleus (PTN,), parietal motor cortex (PMC), paraventricular hypothalamic nucleus (PVN)**,** ventral periaqueductal gray (vPAG) and dorsolateral periaqueductal gray matter (dlPAG) were identified in 40 μm thick coronal sections with the help of a stereotaxic atlas (8) for rat brain (Figure 1). Figure 2 illustrates neurons labeled for FOS alone, NADPH-d alone and double-labeled (FOS/NADPH-d).

Data analysis

FOS reactivity was immunodetected in brain neurons nuclei as brownish round-like dots whereas NADPH-d stained cell bodies and processes were in blue. Both FOS-like and NADPH-d-positive neurons were counted using 20 X objective (Olympus, Nikon, Japan). The total number of rats used for counting FOS, NADPH-d and double-labeled neurons and for clinical observations was 20 (n = 4/group). For each rat, six sections (40 μm thick) from different stereotaxic coordinates were collected to ensure that all areas of interest were included. For each anatomical region, the number of n-NOS and NADPH-d or double-positive cells was counted within a 0.35 mm^2 sized area in the selected brain region.

Statistic analysis

The data were analyzed using the Student unpaired t test, or one-way analysis of variance (*ANOVA)* followed by the *Tukey Kramer post-hoc test* was used to compare the treated and control

groups. The data are presented as mean ± SE (Figure 5) or mean ± SD (Table 1). P values < 0.05 were considered significant.

Results

Inhibition of nNOS by 7-nitroindazole accelerates and aggravates clinical signs of intoxication by P. nigriventer venom

The time interval elapsed between the administration of saline solution, PNV, 7NI + PNV or DMSO + PNV and the onset of envenoming signs, such as hyperemia, salivation, flaccid and spastic paralysis of hindlimbs, respiratory stress, tonic-clonic convulsion, spasm or death, if any, were registered by three observers. In 7NI/PNV group neurotoxic signs, such as prostration, hyper-salivation and hindlimbs spastic paralysis were markedly more precocious, intense and longer-lasting compared to PNV alone or DMSO/PNV group. Salivation was observed after 17 min in DMSO/PNV group, 10 min in PNV group, and 1 min in 7NI/PNV group ($p < 0.01$). Spastic paralysis was seen after 35 min in DMSO/PNV, 20 min in PNV, and 9 min in 7NI/PNV after i.v. injection of PNV ($p < 0.05$). Flaccid paralysis was seen at 30 min in DMSO/PNV, 20 min in PNV and 5 min in 7NI/PNV post-envenoming ($p < 0.01$). Moreover, no death was registered in any of the animals of the PNV group, whereas there was one in DMSO/PNV and three in 7NI/PNV (15-45 min after injection) In the control saline (sham group), none intoxication sign was observed. 7NI-injected animal showed locomotors and exploration activity decreased, but they did not show the toxic signs exhibited by the other groups. The data are summarized in Figure 3.

FOS positive neurons were increased in animals treated with P. nigriventer venom except in PTN. The prior administration of 7-NI antagonized the PNV effect in vPAG, dlPAG, PVN and PMC, but accentuated it in SON, evidenciang a dual mediation role for NO depending on the brain region.

Saline x PNV- The number of FOS-positive neurons increased significantly in PVN, PMC, SON, vPAG and dlPAG regions in animals of PNV-group compared to saline-group ($P<0.05$).

Saline x 7NI/PNV- When nNOS was inhibited (7NI/PNV group), the number of FOS-positive neurons was potentiated in SON whereas in PMC although significantly increased in relation to control group ($P<0.05$), there was not potentiation, meaning that the mediation of NO was not stronger enough to abolish PNV effect. The other regions (vPAG, dlPAG, PVN and PTN) showed no significant alteration in the number of FOS-positive neurons.

Saline x 7NI comparison showed significant increase in the number of FOS-immunolabeled neurons in SON, PTN, dlPAG and vPAG. In SON, the increase was smaller than the observed in saline x 7NI/PNV (suggesting that diminishion of NO availability had a role in neurons activation, and that the 7NI effect was summed to the venom effect). It is worth noting, that only 7NI alone was able to increase the number of neurons immunolabeled for FOS in PTN. All the other treatments (PNV and the association 7NI/PNV or DMSO/PNV) were innocuous to activate neurons in PTN. In the other brain regions (PVN and PMC) the 7NI alone showed no effect in relation to saline.

Saline x DMSO/PNV- Pre-treatment with 7NI's vehicle showed no effect in all regions.

PNV x 7NI/PNV- There were significant decrease in the number of FOS-positive neurons in vPAG, dlPAG, PMC and PVN and increase in SON of animals pretreated with the nNOS inhibitor.

PNV x DMSO/PNV- No significant effect was observed in any of the regions screened.

7NI X 7NI/PNV- There was significant decrease in the number of activated neurons in vPAG and dlPAG of 7NI/PNV-treatedanimals compared to 7NI-treated ones.

The labeling pattern of each region is illustrated in Figures 3A-O and 5A-O. The data obtained from counting cells labeled for FOS were summarized in Figure 6A-F.

NADPH-d positive neurons were increased in in vPAG and PVN of animals administered P. nigriventer venom. Previous inhibition of nNOS by 7NI antagonized significantly the venom tendency to decrease NADPH-d positive neurons in dlPAG.

Saline x PNV and ***Saline x 7NI/PNV -*** In vPAG and PVN regions, the NADPH-d-labeled neurons of PNV and 7NI/PNV groups outnumbered the ones of saline group.

Saline x 7NI- I.p. administration of 7NI increased NADPH-d+ neurons in PVN and SON regions and decreased in PTN compared to saline.

Saline x DMSO/PNV- The 7NI vehicle plus PNV increased the NADPH-d positive neurons in PVN region. All other treatments (PNV, 7NI/PNV, 7NI and DMSO/PNV) also promoted increase in the labeled neurons number in this region compared to saline group.

PNV x 7NI/PNV- The nNOS blocker rouse the number of NADPH-d neurons in dlPAG.

PNV x DMSO/PNV- No effect was produced in any of the regions screened.

7NI X 7NI/PNV- The number of NADPH-d stained neurons increased significantly in 7NI/PNV when compared to 7N1 group in dlPAG; in contrast it decreased in PVN.

The labeling pattern of each area is illustrated in Figures 4A-O and 5A-O. The data obtained from counting neurons positive for NADPH-d were summarized in Figure 6A-F.

Two brain areas showed differences in the double-labeling for FOS and NADH-d-positive neurons: SON and PVN

Co-FOS/NADPH-d-labeled neurons significantly increased in number in PVN and SON regions in all groups (PNV, 7NI/PNV, DMSO/PNV and 7NI) compared to saline sham. The prior 7NI treatment,(7NI/PNV) reduced significantly the double-labeled neurons in PVN compared to PNV alone suggesting an antagonistic effect between venom and NO; in contrast, 7NI alone increased NADPH-d positive neurons compared to PNV group. Double-labeled neurons are illustrated Figure 2; data were summarized in Figure 6A-F.

Discussion

The hypothesis that NO could mediate PNV effects in some CNS regions was recently raised by us (6). To prove if NO signaling has a role in the *P. nigriventer* neurotoxic effects, the neuronal NOS was inhibited by 7nitroindazole and activated neurons and NO-synthesizing neurons were counted in multiple brain regions. FOS-positive, NADPH-d-positive and double-stained neurons were counted in motor, escape and fear related regions (PMC, PTN, dlPAG and vPAG), and regions related to neurovegetative functions (blood pressure, urinary volume, salivation, respiratory function/frequency) (SON, PVN) of animals administered venom (PNV group), the neuronal NOS inhibitor 7-nitroindazole (7NI) alone, or prior venom (7NI/PNV group), the vehicle of 7NI+venom (DMSO/PNV group) or saline injection only. The findings were correlated with the onset/intensity of clinical neurotoxic signs of animals.

Clinical signs

The present results are consistent with activation of neuronal pathways related with motor function such as paralysis and convulsion and neurovegetative dysfunction; besides give strong evidence that such effects are NO-mediated. The inhibition of nNOS by 7NI prior the venom administration accelerated the signals of intoxication compared to animals administered PNV only (20 min *vs*. 9 min for spastic paralysis and 20 min *vs*. 7 min for flaccid paralysis appearance). The venom also caused respiratory anguish, lung edema (seen in necropsy of animals), intense salivation and decrease of urinary volume. In 7NI/PNV-treated animals the onset of such signs were abbreviated suggesting that neuronal pathways related to neurovegetative dysfunctions elicited by PNV was also NO-mediated. Pharmacological controls for vehicle (DMSO/PNV group) retarded the onset of clinical signs of intoxication, indicating that the aggravation of clinical signs in 7NI/PNV animals was not caused by vehicle.

Animals injected with saline solution (sham group) did not show any clinical sign indicating discomfort, pain or difficulty in movements. However, the manipulation and tail saline injection induced stress and certain degree of neuronal activation. The regions vPAG, SON, PMC and dlPAG showed very low activation (3 ± 2.8 to 8 ± 0.0); these regions are related with motor/scape/fear (vPAG, dlPAG, PMC) and neurovegetative functions linked with water balance, such as salivary flux, renal excretion, urinary volume, blood pressure (SON) (9). PVN and PTN of controls shwed moderate number of FOS-positive neurons (54 ± 24 and 36 ± 1); these regions integrate endocrine and autonomic-stress-evoked response, including respiratory and cardiovascular (PVN) (10) and are related with motor/fear/scape (PMC). The findings are consistent with the feelings experienced by animals during manipulation.

Activated Neurons FOS-positive

PNV increased the number of FOS positive neurons in almost all examined brain regions, except in PTN, compared to sham controls. PMC was the area most affected by PNV; in contrast, dlPAG was the least affected. These effects were attenuated by 7-NI pretreatment in the majority of regions, except for SON where it was augmented indicating a complex regionally specific role for NO in these effects. Whether these results reflect differences in the tightness of the BBB was not clear. If this is true, the region less vulnerable to the systemic PNV was PTN since only 7NI alone affected the number of FOS-positive cells. It is interesting mention that PNV or 7NI, in separate, increased FOS-positive neurons in vPAG and dlPAG, but when together (7NI/PNV) their number fell down the level seen in PNV group indicating that in these fear/motor/escape-related regions the interaction PNV-7NI produced opposed action.. In contrast, in SON the interaction PNV-7NI showed synergic effect, leading to significant increase of the FOS-labeled neurons. Taken together such results indicate different pathways for activation of neurons, probably depending on the interaction of drugs and brain area considered.

NADPH-d-stained neurons and NADPH-d/FOS-double stained neurons

The nitrergic neurons shared the same anatomical regions with FOS-positive neurons. dlPAG region showed the highest number of NADPH-d whereas PMC showed the least. PNV injection did not change this proportion; however the inhibition of nNOS (7NI/PNV group) did, suggesting region-stimulus specificity. In 7NI/PNV animals, the highest number of NADPH-d-positive neurons passed to be the SON followed by dlPAG, whereas PMC maintained the least number. Interestingly, PVN, the area where the suppression of nNOS activity promoted minor increase of FOS-positive neurons, exhibited the highest increase of NADPH-d-positive neurons in

response to all the treatments (PNV, 7NI/PNV, 7NI and DMSO/PNV). These treatments also increased the number of FOS/NADPH-d-double-stained neurons in PVN. Taken together the finding reinforces the idea that NO could have a damaging role enhancing the neurovegetative unbalance (respiratory distress, blood pressure increase) of animals.

An interesting finding was that the increase of FOS-immunoreactive neurons was accompanied by increase in NADPH-d-stained neurons in PVN, PTN, PMC and vPAG after 7NI/PNV treatment compared to PNV-treated animals. This finding suggests likely a harmful gas mediation role in the sense that it paralleled with toxic signs. In contrast, SON was the only area where the nNOS blockade before PNV injection caused elevation in the number of NADPH-d and double-stained neurons. The finding suggests a benefic role exerted by NO in this region, what was corroborated by the clinical signs findings.

It is noteworthy that PTN was affected solely by 7NI alone; the treatment increased FOS-positive neurons whereas reduced the NO-synthesizing ones. Such interesting result may mean absence of NO mediation for this aversive/escape/fear/motor-related region, what is consistent with the lack of double staining in PTN.

Both, PNV and 7NI/PNV treatment increased significantly the number of NADPH-d-stained neurons compared to saline control in the motor/fear/escape- (vPAG) and respiratory and cardiovascular function/frequency-related region (PVN). 7NI per se was the agent which affected more the number of nitrergic neurons, elevating significantly, or as a tendency, the number in SON, PVN dlPAG and vPAG.

Available literature indicates that NO behaves as an atypical neurotransmitter, since is capable of producing dual/biphasic effects even within a specified system depending on the basal level of activity, type of stimulus or both; NO also modulates the release of various neurotransmitters (11). Since PNV is a cocktail of neurotoxins acting both in excitatory and inhibitory neuronal pathways, it is possible that NO mediates neurotransmitters release evoked by venom on a region dependent manner, being this synergistic or antagonistic in relation to venom.

The venom of the spider *P. nigriventer* contains several toxic fractions (such as PhTx2, PhTx4(5-5), PhTx3, PhTx3-4) with different targets in mammals and/or insects. PhTx2 is able to evoke acetylcholine release from rat cortical synaptosomes and this effect is dependent on extracellular calcium availability; PhTx2 is inhibited by tetrodotoxin, a blocking Na^+ channel (12). PhTx4(5-5) inhibits the NMDA-subtype of the ionotropic glutamate receptor, while having little or no effect on the AMPA- or kainate-receptor subtypes or on the GABA-gated chloride channel (13). PhTx3 is a broad-spectrum Ca^{2+} channel blocker toxin that in synaptosomes inhibits Ca^{2+}-dependent calcium uptake and glutamate release and uptake, and provokes flaccid paralysis when

injected intracerebroventricularly (14). The toxin PhTx3-4 decreases the evoked glutamate release from synaptosomes by inhibiting Ca^{2+} entry via voltage-dependent Ca^{2+} channels; it is also able to inhibit time-dependently glutamate uptake by synaptosomes, which in turn leads to decrease in the Ca^{2+}-independent release of glutamate (15). In the nervous system, NO is synthesized from L-arginine by the Ca^{2+}/calmodulin-dependent enzyme nNOS. This enzyme is activated by the calcium influx induced by the activation of glutamate receptors (16, 17). Since PhTx3 blocks voltage-gated Ca^{2+} channels, this toxin could also inhibit n-NOS-Ca^{2+}/calmodulin-dependent activity. Our results suggest that PNV and 7NI may have synergistic action in promoting inhibition of glutamate release and NO synthesis, depending on the intrinsic signaling pathway regulating the region.

Studies have shown that NO and the nuclear protein FOS (a component of the c-Fos family of immediate early genes) share roles in CNS neurointoxication (18). The pretreatment with the non-selective NOS inhibitor L-NAME reduced the penile erection and was partially protective from the lethal effects of the PNV toxin PhTx2-5, whereas the pretreatment with 7-NI completely abolished all the PhTx2-5 toxic effects, including penile erection and death (19). The authors suggest that NO is the major player in this intoxication. In the present study, the data with the whole venom showed opposite effects elicited by the selective nNOS blocker 7NI, given the neurotoxic signs were severely more intense in 7NI/PNV-treated animals than in animals with venom in blood circulation (PNV group). Studies indicate that physiological amounts of NO are neuroprotective, whereas higher concentrations could be clearly neurotoxic (18).

NO is associated with a range of different behavior, including learning and memory formation, feeding, sleeping and male and female reproductive behavior, as well with sensory and motor function. Within the SON, the endogenous NO system may act as a physiological inhibitory factor that modulates NMDA-induced responses. In fact, in hypothalamic slices, NMDA-induced depolarization of SON neurons was inhibited by NO-releasing drugs and is enhanced by NOS inhibitors (20). Age-related inhibition of salivary secretion has been demonstrated in rats, and the NO present in the SON has been reported to play an inhibitory role in the regulation of salivary secretion (21). PNV injection induced intense salivation, which was more voluminous in animals receiving the nNOS inhibitor before the PNV. In other words, nNOS inhibition by 7NI induced hyper salivation in animals, suggesting a synergistic effect of both in promoting syalorrhea. Therefore, the downregulation of NO synthesis by venom (and likely the inhibition of glutamate release and/or glutamate receptors by some venom toxins) could be likely one of the mechanism by which *P. nigriventer* venom promotes enhanced secretion of salivary glands. *Mutatis mutandis*, this same mechanism may be acting at the dlPAG and vPAG, i.e., the reduction of synthesis/release of NO by venom (or both by 7NI alone or 7NI plus PNV, synergism of actions) caused the reduction

of motor activity and led to animal prostration, what would explain a lower number of FOS-labeled neurons (or lower neuronal activation). In summary, we suggest that PNV and 7NI share a similar mechanism in SON and PAGs, in spite of having each distinct function as seen by clinical signs.

Magnocellular neuron populations distributed between the supraoptic (SON) and paraventricular nucleus (PVN) of the hypothalamus synthetize vasopressin (AVP) and oxitocin (OT) (22, 23). Both hormones are essential for homeostasis, AVP acts as antidiuretic in response to rise in extracellular solute concentration and a vasoconstrictor in response to hypovolemia and hypotension; AVP also modulates the autonomic function of the cerebral trunk (24). OT promotes smooth muscle contraction acting in parturition, lactation and in rats cause natriuresis in response to plasma hyperosmolality (hydromineral homeostasis); OT has also a cardiovascular relaxing action (25-27). As genuine integrants of the neuroendocrine axis, the magnocellular neurons from hypothalamus are under control of a variety of modulators, among which the nitric oxide has lately gained particular attention (28-32). The hypothesis that NO could be involved in AVP and OT releasing regulation was reinforced by the detection of NO synthetase in the hypothalamic-neuropituitary system (33). *In vivo* studies demonstrate an inhibitor OT releasing effect by NO (31, 34, 35), whereas is disputed a NO role in relation to AVP (31, 36-38). Despite, interestingly, electrophysiological findings has demonstrated a reduction in the activity of the hypothalamic magnocellular secretory neurons induced by NO, suggestive of an inhibitory releasing role against AVP and OT (39, 40). Since the envenoming by *P. nigriventer* venom causes a bi-phasic effect in blood pressure (41), it is likely that change in the muscular tonus, causing both hypotension (short-lasting) or hypertension (sustained) has the participation of NO. Such changes were expected to have a reflex in urinary volume and natriuresis levels. It is likely, that neuroendocrine pathways associated with hypothalamic SON and PVN, had been affected by Phoneutria venom, since clinically animals showed urinary retention.

Tanaka et al. (21) demonstrated by NADPH-d histochemistry and Nissl staining a direct correlation between the NO production by SON neurons and decreased salivary glands activity. The administration of NO donator directly in SON counteracts the hypertensive action, increased sodium excretion and urinary volume promoted by pilocarpine, while L-NAME potentiated these effects (9). Given the PNV administration produces syalorrhea, is hypertensive, alters vessels permeability, affects smooth muscle contractility and produces anuria in rats, it is highly viable that the changes produced in the FOS- and NADPH-d positive neurons were NO-mediated.

The venom also produced lung edema and respiratory anguish. PVN and SON neurons integrate endocrine and autonomic-stress-evoked responses including respiratory function and coordination of cardiovascular functions (10). Luo et al. (42) verified that the exposure to hypobaric

hypoxia (high altitudes exposure) provoked high level of FOS and nNOS expression in PVN and SON hypothalamic neurons of rats. The findings give evidence of their role in the regulation of neuroendocrine, cardiovascular and respiratory functions. We suggest that the increase of FOS-positive neurons by PNV and antagonized by 7NI/PNV in PVN region, and the increase in double-labeled FOS/NADPH-d-positive neurons induced by all the treatments (PNV, 7NI/PNV, DMSO/PNV and 7NI) in SON region are strong evidence of these neuronal pathways involvement in envenoming and likely the NO mediation in the clinical neurovegetative signs.

The injection of NO donors into the dlPAG induces motor reaction (43) and the inhibition by 7NI of NO-dependent pathways provokes anxiolytic effect (44). As shown here, there was a significantly higher expression of FOS reactivity in dlPAG neurons of PNV-treated rats. But, when 7NI was injected before the PNV, dlPAG activation was less intense. Even so, PNV caused tonic-clonic convulsion (excitatory sign), and also induced flaccid and spastic paralysis of hind members besides serious prostration (inhibitory signs). Glutamate agonists injected into the dlPAG induce flight behavior characterized by running and jumps (45). In contrast, PNV injection led animals to be immobilized for a period without any capacity to run or jump. Intra-dlPAG injections of nNOS inhibitor completely blocked the glutamate agonist effects (46). These findings suggest that 7NI may be antagonistic to excitatory activated pathways (indicated by decrease of FOS-labeling), but agonistic to inhibitory-activated pathway caused by venom. NO inhibition also may be a mechanism responsible for inhibiting motility caused by PNV-intoxication, resulting in aggravation of animal prostration.

Venoms from spiders are important source of toxins that can help understanding the mechanism involved in neurotransmission. Particularly, PNV neurotoxins act both in excitatory and inhibitory neuronal pathways. Our findings explain the down activation of motor-related regions and the hyper activation of salivation-related ones of 7NI/PNV-treated animals compared to PNV-treated ones. Since the synthesis of NO derived from nNOS, and the enzyme expression was impaired by 7NI, and that this aggravated the clinical signs of envenoming, we conclude that NO has role in envenoming effects whose mediation is protective for some regions and potentiates the venom effects in others. Nitrergic cells likely exerted here an essential regulatory function (47). Although we showed that the NO can have a beneficial action in some areas and be harmful for others, clinically its overall effect appears as beneficial, attenuating PNV effects. In conclusion, we suggest that some of the PNV toxins can inhibit NO release whilst others can activate it. We conclude that NO is likely directly involved in the quality of the neurotoxic signs elicited in victims of *P. nigriventer* accidents, although mechanism other than nitrergic ones can be involved. Study of

the NO role can contribute for the understanding of the *Phoneutria* envenoming mechanisms, as well as can be useful for therapeutic purposes.

Acknowledgements: The authors thank Instituto Butantan (São Paulo, SP, BR) for venom donation. The authors also thank Ms. Marta Beatriz Leonardo (BSc) for excellent technical assistance, and Mr. Miguel Silva and Mr. Marcos Silva for animal care. This work has been funded by grants from Fundação de Amparo à Pesquisa do Estado de São Paulo (FAPESP # 07/50242-6) and Conselho Nacional de Desenvolvimento Científico e Tecnológico (CNPq # 302206/2008-6/481316/2008-6). C.R is recipient of scholarship from FAPESP. M.A.C.H. is a IA research fellow from CNPq.

Abbreviations

dlPAG- *dorsolateral periaqueductal gray;* DMSO- *dimethyl sulfoxide;* GABA- *gamma butyric acid;* PVN- *Paraventricular hypothalamic nucleus;* NADPH-d- *reduced nicotinamide adenine dinucleotide phosphate diaphorase;* NMDA- *N-methyl-D-aspartic acid;* nNOS- *neuronal nitric oxide synthase;* NO- *nitric oxide;* PMC- *árietal motor cortex;* PNV- *Phoneutria nigriventer venom;* PTN- *periventricular thalamic nucleus;* SON- *supraoptic nucleus;* 7NI- *7-nitroindazole;* vPAG- *ventral periaqueductal gray.*

References

1. Gomez MV, Kalapothakis E, Guatimosim C, et al. *Phoneutria nigriventer* venom: a cocktail of toxins that affect ion channels. Cell Mol Neurobiol 2002; 22: 579--88

2. Cruz-Höfling MA, Love S, Brook G, et al. Effects of *Phoneutria nigriventer* spider venom on mouse peripheral nerve. Q J Exp Physiol 1985; 70:623--40

3. Le Sueur LP, Kalapothakis E, Cruz-Höfling MA. Breakdown of the blood-brain barrier and neuropathological changes induced by Phoneutria nigriventer spider venom. Acta Neuropathol 2003; 105:125--34

4. Le Sueur LP, Collares-Buzato CB, Cruz-Höfling MA, Mechanisms involved in the blood-brain barrier increased permeability induced by Phoneutria nigriventer sipder venom in rats. Brain Res 2004 1027:38-47

5. Rapôso C, Zago GM, Silva GH, et al. Acute blood-brain barrier permeabilization in rats after systemic *Phoneutria nigriventer* venom. Brain Res 2007; 1149:18-29

6. Cruz-Höfling MA, Zago GM, Melo LL, et al. cFOS and n-NOS reactive neurons in response to circulating Phoneutria nigriventer spider vneom. Brain Res Bull 2007; 73: 114--26.

7. Pardutz I, Krizbai S, Multon L, et al. Systemic nitroglycerin increases n-NOS levels in rat trigeminal nucleus caudalis. NeuroReport 2000; 11:3071--75

8. Palkovits M, Brownstein M. *Maps and Guide to Microdissection of the Rat Brain.* New York, USA: Elsevier 1988

9. Saad WA, Gutierrez LI, Guarda IF, et al. Nitric oxide of the supraoptic nucleus influences the salivary secretion, sodium renal excretion, urinary volume and arterial blood pressure induced by pilocarpine. Life Sci 2004; 74:1593--603

10. Yeh ER, Erokwu B, LaManna JC, et al. The paraventricular nucleus of the hypothalamus influences respiratory timing and activity in the rat. Nurosci Lett 1997; 232:63--6

11. Garthwaite J, et al. Concepts of neural nitric oxide-mediated transmission. Eur J Neurosci 2008; 27:2783--802

12. Moura JR, Prado MA, Gómez MV, et al. Investigation of the effect of PhTx2, from the venom of the spider *Phoneutria nigriventer*, on the release of [3H]-acetylcholine from rat cerebrocortical synaptosomes. Toxicon 1998; 36:1189--92

13. Figueiredo SG, Lima ME, Nascimento Cordeiro M, et al. Purificationand amino acid sequence of a highly insecticidal toxin from the venom of the Brazilian spider *Phoneutria nigriventer* which inhibits NMDA-evoked currents in rat hippocampal neurones. Toxicon 2001; 39:309--17.

14. Prado MAM, Guatimosim C, Gómez MV, et al. A novel tool for the investigation of glutamate release from rat cerebrocortical synaptosomes: the toxin Tx3-3 from the venom of the spider *Phoneutria nigriventer*. Biochem J 1996; 314:145--50

15. Reis HJ, Prado MA, Kalapothakis E, et al. Inhibition of glutamate uptake by a polypeptide toxin (phoneutriatoxin 3-4) from the spider *Phoneutria nigriventer*. Biochem J 1999; 2:413--8

16. Garthwaite J, Charles SL, Chess-Williams R. Endothelium-derived relaxing factor release on activation of NMDA receptors suggests role as intercellular messenger in the brain. Nature 1988; 336:385--8

17. Garthwaite J, Garthwaite G, Palmer RM, et al. NMDA receptor activation induces nitric oxide synthesis from arginine in rat brain slices. Eur J Pharmacol 1989; 172:413--6

18. Calabrese V, Mancuso C, Calvani M, et al. Nitric oxide in the central nervous system: neuroprotection versus neurotoxicity. Nat Rev Neurosci 2007; 10:766--75

19. Yonamine CM, Troncone LR, Camillo MA. Blockade of neuronal nitric oxide synthase abolishes the toxic effects of Tx2-5, a lethal Phoneutria nigriventer spider toxin. Toxicon 2004; 44:169--72

20. Cui LN, Inenaga K, Nagatomo T, et al. Sodium nitroprusside modulates NMDA response in the rat supraoptica neurons in vitro. Brain Res Bull 2007; 35:253--60

21. Tanaka T, Tamada Y, Suwa F. Influence of age-related changes in nitric oxide synthase-expressing neurons in the rat supraoptic nucleus on inhibition of salivary secretion. Okajimas Folia Anat Jpn 2008; 84:125--31

22. Brownstein MJ, Russell JT, Gainer H. Synthesis, transport, and release of posterior pituitary hormones. Science 1980; 207:373-8

23. Swanson LW, Sawchenko PE. Hypothalamic integration: organization of the paraventricular and supraoptic nuclei. Annu Rev Neurosci 1983; 6:269-324

24. Barrett LK, Singer M, Clapp LH. Vasopressin: mechanisms of action on the vasculature in health and in septic shock. Crit Care Med 2007; 35:33-40

25. Conrad KP, Gellai M, North WG, et al. Influence of oxytocin on renal hemodynamics and electrolyte and water excretion. American J Physiol 1986; 251:290-96

26. Jankowski M, Wang D, Haijar F, et al. Oxytocin and its receptors are synthesized in the rat vasculature. Proc Natl Acad Sci USA 2000; 97:6207--11

27. Gutkowska J, Jankowski M, Mukaddam-Daher S, et al. Oxytocin is a cardiovascular hormone. Braz J Med Biol Res 2000; 33:625-33.

28. Kadowaki K, Kishimoto J, Leng G, et al. Up-regulation of nitric oxide synthase (NOS) gene expression together with NOS activity in the rat hypothalamo-hypophysial system after chronic salt loading: evidence of a neuromodulatory role of nitric oxide in arginine vasopressin and oxytocin secretion. Endocrinology 1994; 134:1011--17

29. Srisawat R, Ludwig M, Bull PM, et al. Nitric oxide and the oxytocin system in pregnancy. J Neurosci 2000; 20:6721--27

30. Ventura RR, Giusti-Paiva A, Gomes DA, et al. Antunes-Rodrigues J. Neuronal nitric oxide synthase inhibition differentially affects oxytocin and vasopressin secretion in salt loaded rats. Neurosci Lett 2005; 379:75-80

31. Ventura RR, Gomes DA, Reis WL, et al. Nitrergic modulation of vasopressin, oxytocin and atrial natriuretic peptide secretion in response to sodium intake and hypertonic blood volume expansion. Braz J Med Biol Res 2002; 35:1101--09

32. Stern JE, Li Y, Zhang W, et al. Nitric oxide: a local signalling molecule controlling the activity of pre-autonomic neurones in the paraventricular nucleus of the hypothalamus. Acta Physiol Scand 2003; 177:37-42

33. Bredt DS. Endogenous nitric oxide synthesis: biological functions and pathophysiology. Free Radic Res 1999; 31:577--96

34. Koehler EM, McLemore GL, Tang W, et al. Osmoregulation of the magnocellular system during pregnancy and lactation. Am J Physiol 1993; 264:555--60

35. Kadekaro M, Terrell ML, Liu H, Gestl S, et al. Effects of L-NAME on cerebral metabolic, vasopressin, oxytocin, and blood pressure responses in hemorrhaged rats. Am J Physiol 1998; 274:1070--77

36. Yasin S, Costa A, Trainer P, et al. Nitric oxide modulates the release of vasopressin from rat hypothalamic explants. Endocrinology 1993; 133:1466--69

37. Liu H, Terrell ML, Bui V, et al. Nitric oxide control of drinking, vasopressin and oxytocin release and blood-pressure in dehydrated rats. Physiol Behav 1998; 63:763--69

38. Yamaguchi K, Hama H. A study on the mechanism by which sodium nitroprusside, a nitric oxide donor, applied to the anteroventral third ventricular region provokes facilitation of vasopressin secretion in conscious rats. Brain Res 2003; 968:35-43

39. Liu QS, Jia YS, Ju G. Nitric oxide inhibits neuronal activity in the supraoptic nucleus of the rat hypothalamic slices. Brain Res Bull 1997; 43:121--25

40. Stern JE. Nitric oxide and homeostatic control: an intercellular signaling molecule contributing to autonomic and neuroendocrine integration? Prog Biophys Mol Biol 2004; 84:197-215

41. Costa SKP, Moreno Jr. H, Brain SD, et al. The effect of *Phoneutria nigriventer* (armed spider) venom on arterial blood pressure of anaesthetised rats. Eur J Pharmacol 1996; 298:113--20

42. Luo Y, Kaur C, Ling EA. Hypobaric hypoxia induces fos and neuronal nitric oxide synthase expression in the paraventricular and supraoptic nucleus in rats. Neurosci Lett 2000; 296:145--8

43. Oliveira RW, Del Bel EA, Guimarães FS. Behavioral and c-Fos expression changes induced by nitric oxide donors microinjected into the dorsal periaqueductal gray, Brain Res Bull 2000; 52:457--64

44. Morato GS, Ortiga RM, Ferreira VM. Involvement of nitric oxide-dependent pathways of dorsolateral periaqueductal gray in the effects of ethanol in rats submitted to the elevated plus-maze test. Behav Brain Res 2004; 153:341--9

45. Moreira, F.A., Molchanov, M.L. & Guimarães, F.S. (2004) Ionotropic glutamate-receptor antagonists inhibit the aversive effects of nitric oxide donor injected into the dorsolateral periaqueductal gray of rats. *Psychophamacology*, **171**, 199-203.

46. Miguel TT, Nunes-de-Souza RL. Defesnsive-like behaviors and antinociception induced by NMDA injection into the periaqueductal gray of mice depend on nitric oxide synthesis. Brain Res 2006; 1076:42--8

47. Huynh P, Boyd SK. Nitric oxide synthase and NADPH diaphorase distribution in the bullfrog (Rana catesbeiana) CNS: pathways and functional implications. Brain Behav Evol 2007; 70:145--63

Legend for Figures

Figure 1: Schematic representation of cross-sections of the brain showing the location of the regions in which FOS, NADPH-d and FOS/NADPH-d reactivity was quantified. Brain areas were selected according to Palkovits and Bronstein, 1988. Abbreviations are defined in Table 1.

Figure 2: Light micrograph showing the pattern of immunolabeling of the immediate early gene FOS protein (neuron nucleus appears stained in brown, see arrowhead), NADPH-d-stained neurons

(for detection of nNOS synthesising neuron; body and processes of neuron appear stained in blue, see double-legged arrow) and neurons double-labeled for FOS plus NADPH-d (arrow). Supraoptic nucleus (SON) of a rat injected with 7-nitroindazole prior systemic administration of *Phoneutria nigriventer* spider venom. Bar = 35 µm.

Figure 3: Schematic representation showing the time interval (in minutes) lasted from the treatment administration (0 min) until the onset of toxic signs by animals after intra-venous injection of PNV alone (PNV); 7-nitroindazole (i.p.) before PNV injection (7NI/PNV) and the vehicle for 7NI prior PNV injection (DMSO/PNV). In 7NI/PNV group, all neurotoxic signs were markedly more precocious, when compared to PNV alone and/or DMSO/PNV groups. Intense salivation started at 17 min in DMSO/PNV-group, 10 min in PNV-group, and 1 min in 7NI/PNV-group. Spastic paralysis was seen after 35 min in DMSO/PNV, 20 min in PNV, and 9 min in 7NI/PNV. Moreover, none animal died in PNV group, whereas one died in DMSO/PNV and 3 in 7NI/PNV. 7NI-i.p.-injected animals decreased locomotors activity but did not exhibit the typical signs of intoxication. Saline-injected animals (sham control) appeared normal. The data (registered by three independent observers) were presented as means ± SD, $P < 0.05$ was considered significant (Student unpaired t test, or one-way ANOVA followed by the Tukey *Kramer* multiple comparison post test); * $P < 0.05$; ** $P < 0.01$. (HYP = Hyperaemia; Sal = Salivation; FP = Flaccid paralysis; SP = Spastic paralysis; RD = Respiratory distress.

Figure 4: Representative light micrographs of the immediate early gene FOS protein immunolabeling (neurons nuclei appear stained in brown, see arrows) and NADPH-d histochemistry for detection of nNOS synthesising neurons (body and processes of neurons appear stained in blue, see arrowheads) in the motor/fear/escape-related regions (PMC - parietal motor cortex, vPAG - ventral periaqueductal gray matter and dlPAG - dorsolateral periaqueductal gray matter) after injection in rats of saline solution (sham group), *Phoneutria nigriventer* venom (PNV group), dimetylsulfoxide plus PNV (DMSO/PNV group), 7-nitroindazole plus PNV (7NI/PNV group) or 7NI alone (7NI group). PMC (Panels: A – E), vPAG (Panels: F – J), and dlPAG (Panels: K – O). In all regions FOS positive neuronal nuclei were more numerous after PNV injection (B, G and L); their number decrease in DMSO/PNV (C, H and M); are sparse in 7NI/PNV (D, I and N), and absent in the saline control (A, F and K). In 7NI group, FOS-labeling is low in PMC (panel E), vPAG and dlPAG (panels J, O) regions. Very low number of NADPH-d-labeled neurons was seen in PMC of all groups; in contrast they are numerous in, vPAG and dlPAG (including in the control group of the latter). In vPAG, the number of NADPH-d-positive-neurons increased after PNV, but

showed a trend to decrease in 7NI/PNV group (compare F, G and I). In dlPAG, NADPH-d-positive neurons of 7NI/PNV-treated animals outnumbered the other groups. bv - blood vessel. Bar = 35 µm for panels A-E and 70 µm for panels F-O.

Figure 5: Representative light micrographs of the immediate early gene FOS protein immunolabeling (neurons nuclei appear stained in brown, see arrows) and NADPH-d histochemistry for detection of nNOS-synthesising neurons (body and processes of neurons appear in blue, see arrowheads) in the water balance regulatory region (SON - supraoptical nucleus), motor/escape/fear/aversive-related region (PTN - paraventricular thalamic nucleus), and respiratory-cardiovascular-related region (PVN – paraventricular hypothalamic nucleus) after injection in rats of saline solution (sham group), *Phoneutria nigriventer* venom (PNV group), dimetylsulfoxide plus PNV (DMSO/PNV group), 7-nitroindazole plus PNV (7NI/PNV group) or 7NI alone (7NI group). SON (Panels: A – E), PTN (Panels: F – J), and PVN (Panels: K – O). In all areas, the FOS labeling increased in PNV group, except in PTN; the treatment with 7NI before PNV (7NI/PNV group) decreased the expression of the early immediate gene FOS protein in PVN, increased in SON and maintained unaltered in PTN (compare panels D, I and N to B, G, L). NADPH-d-stained neurons (or nNOS synthesising neurons) were seen in SON, PTN and PVN of control group. In PVN, all treatments increased the number of stained cells, whereas for SON only 7NI alone increased them. Bar = 35 µm for panel A and 70 µm for panels B – O.

Figure 6: Histogram illustrating mean number of FOS, NADPH-d and double FOS/NADPH-reactive cells counted bilaterally in a 0.35 mm^2 area of representative sections of each brain region displayed in A to F panels and analysed in sham control (Sal), venom- (PNV), vehicle/venom-(DMSO/PNV), 7-nitroindazole nNOS inhibitor plus venom- (7NI/PNV), and 7-nitroindazole-(7NI)-treated rats. The results are expressed as the mean ± S.E.M; Student unpaired t test, or one-way analysis of variance (ANOVA) followed by the Tukey Kramer post-hoc test was used $^{*}P < 0.05$, $^{**}P < 0.01$, $^{***}P < 0.001$ – compared treated groups to control group. $^{\#}P < 0.05$, $^{\#\#}P < 0.01$, $^{\#\#\#}P < 0.001$ – compared treated groups to PNV or DMSO/PNV groups and $^{\Delta}P<0.05$ – compared 7NI/PNV with 7NI group.

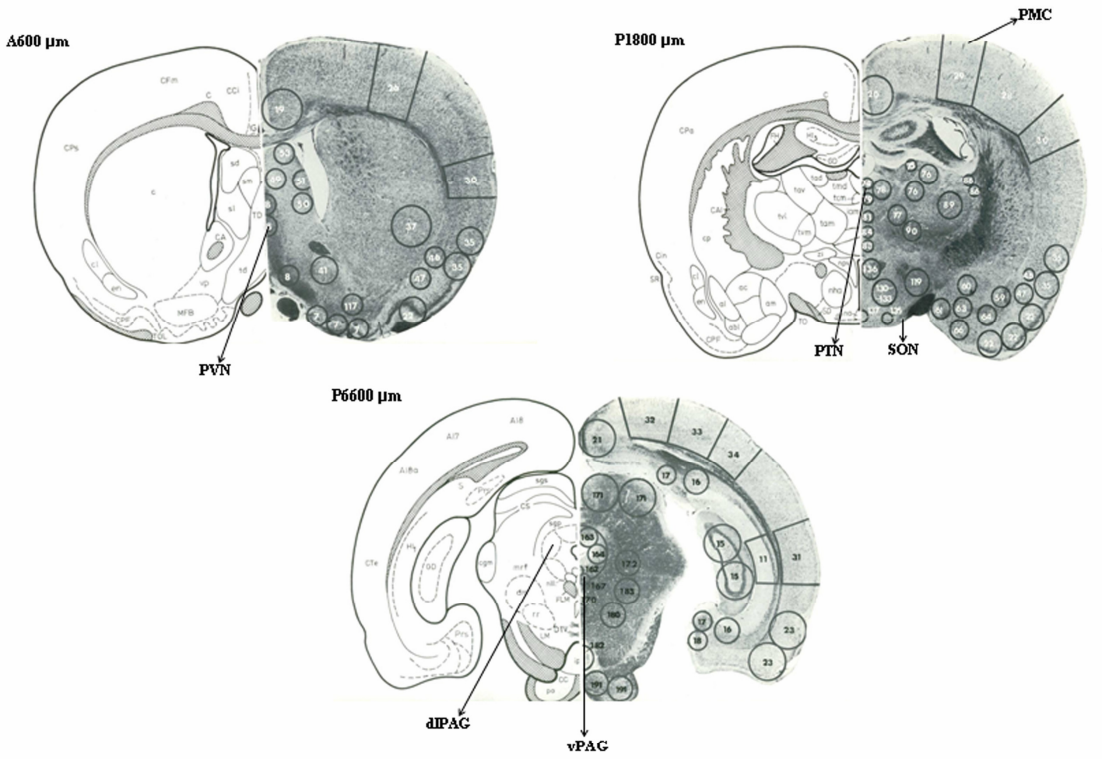

Figure 1

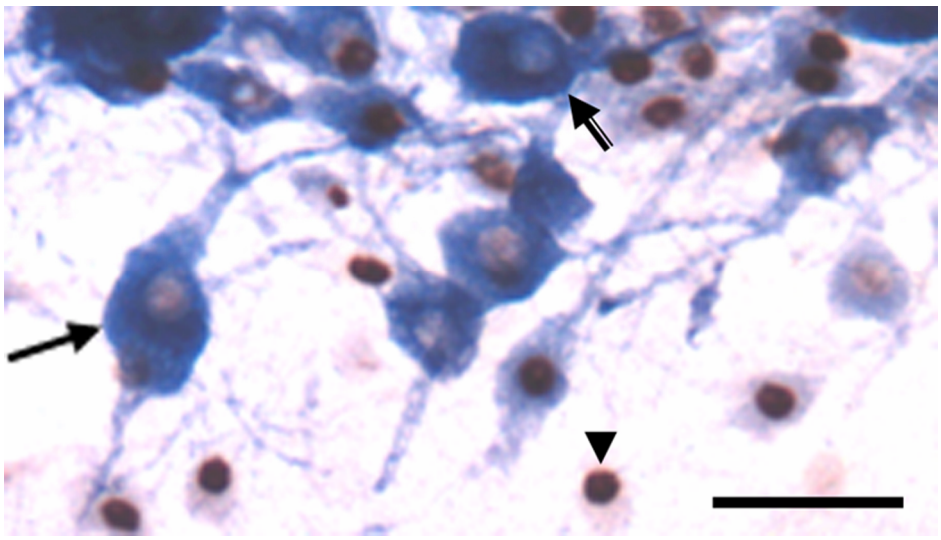

Figure 2

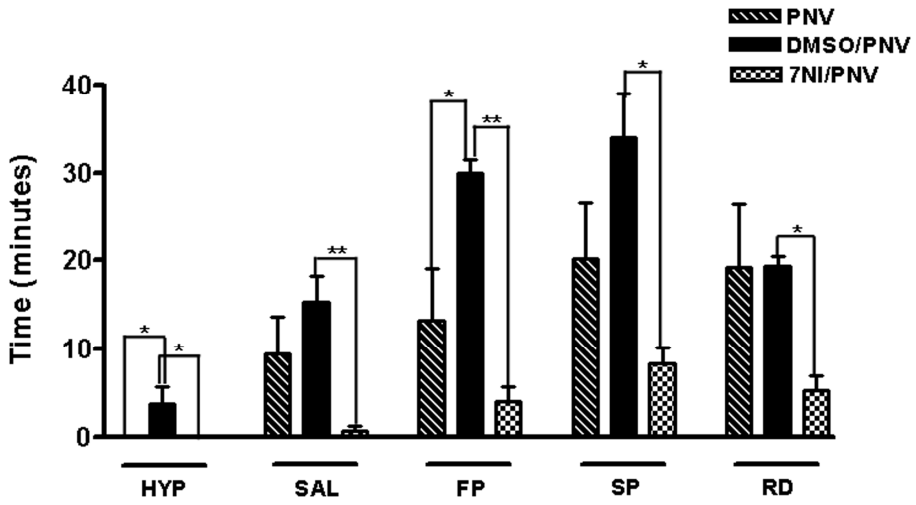

Figure 3

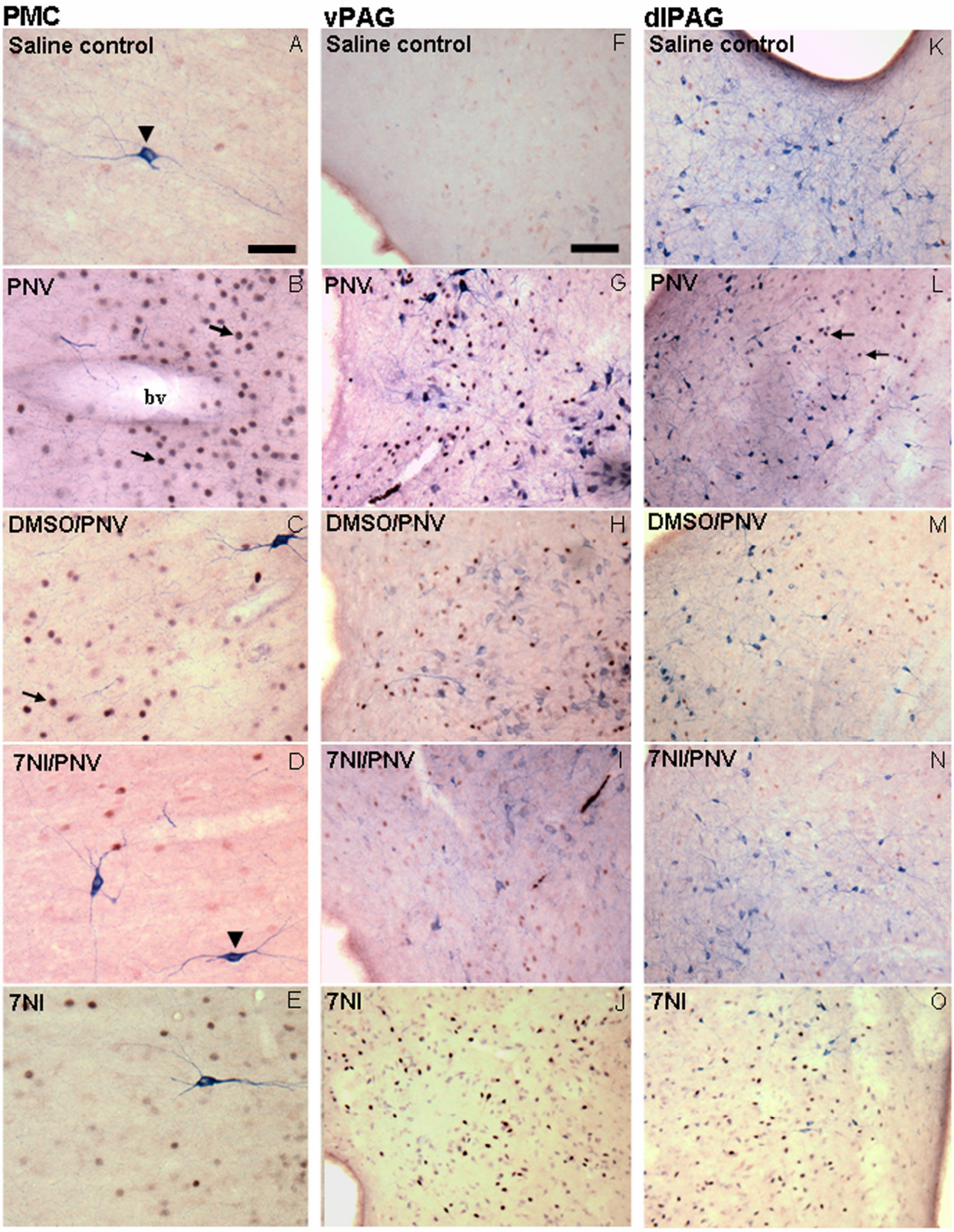
PMC
vPAG
dlPAG
Saline control
A
Saline control
F
Saline control
K
PNV
B
bv
PNV
G
PNV
L
DMSO/PNV
C
DMSO/PNV
H
DMSO/PNV
M
7NI/PNV
D
7NI/PNV
I
7NI/PNV
N
7NI
E
7NI
J
7NI
O

Figure 4

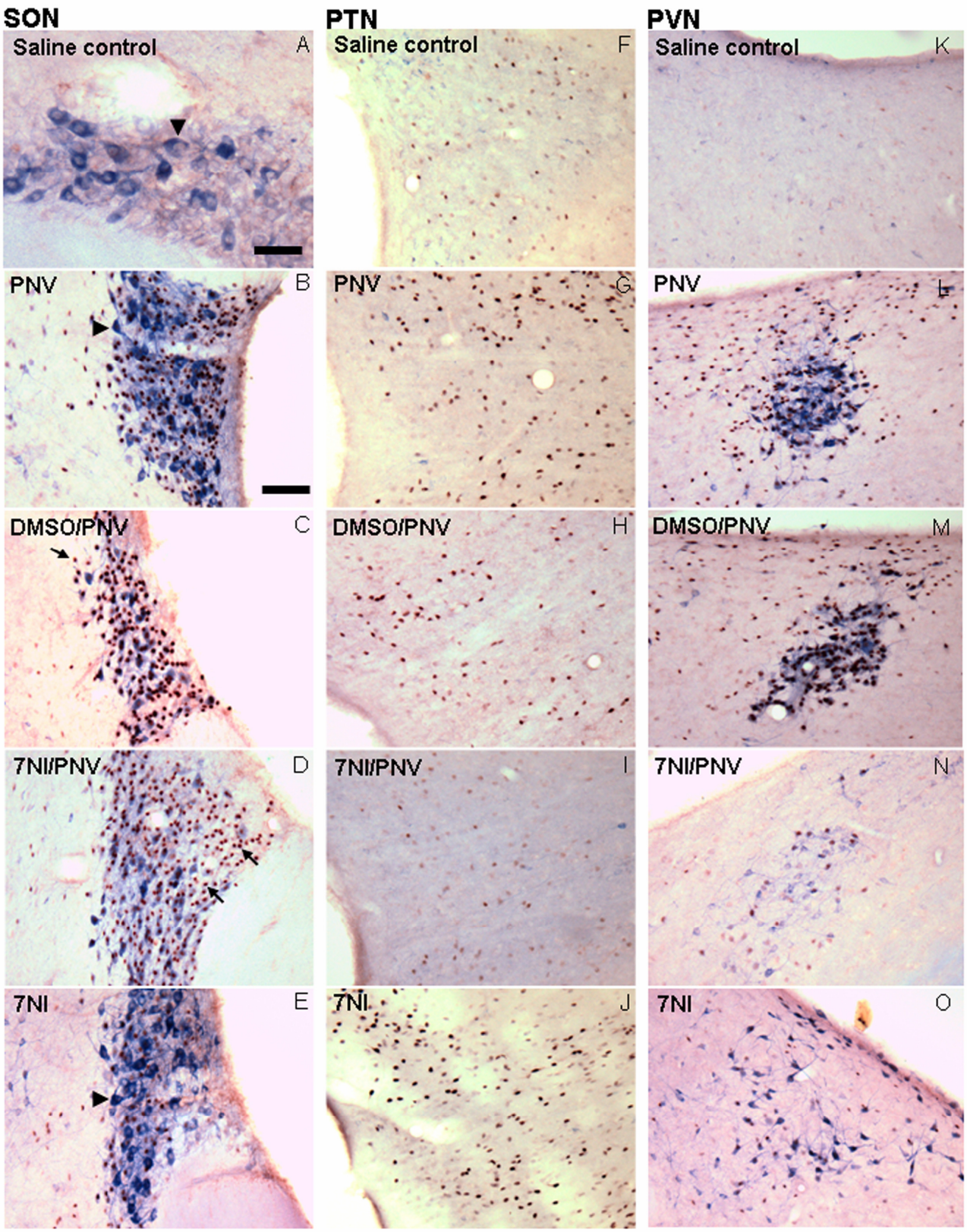
SON
PTN
PVN
Saline control
A
Saline control
F
Saline control
K
PNV
B
PNV
G
PNV
L
DMSO/PNV
C
DMSO/PNV
H
DMSO/PNV
M
7NI/PNV
D
7NI/PNV
I
7NI/PNV
N
7NI
E
7NI
J
7NI
O

Figure 5

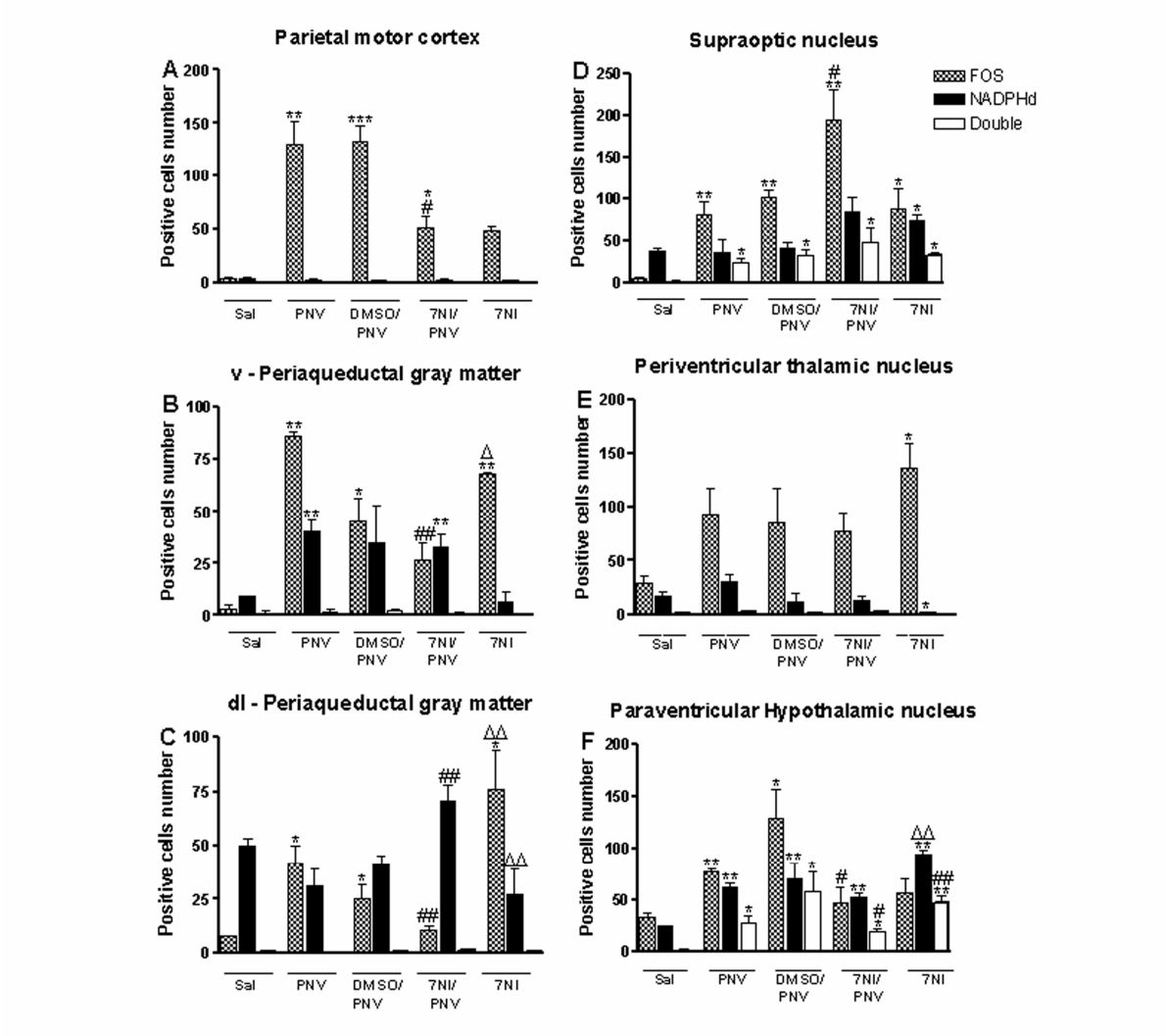
Parietal motor cortex
A
Positive cells number
Sal
PNV
DMSO/ PNV
7NI/ PNV
7NI
Supraoptic nucleus
D
FOS
NADPHd
Double
v - Periaqueductal gray matter
B
Periventricular thalamic nucleus
E
dl - Periaqueductal gray matter
C
Paraventricular Hypothalamic nucleus
F

Figure 6

Table 1

Number of FOS, NADPH- d and double reactive neurons in anatomical regions of the brain

	Saline			PNV			DMSO/PNV			7NI/PNV			7NI		
	FOS	NADPHd	Double	FOS	NADPHd	Double	FOS	NADPHd	Double	FOS	NADPHd	Double	FOS	NADPH	Double
Parietal motor cortex (PMC)	5.5±0.7	5.0±2.8	0.0	149±24	2.5±1.7	0.0	133±23	2.6±0.5	0.0	51±25	2.5±1.2	0.0	48.5±6.3	2.5±0.7	0.0
Supraoptic nucleus (SON)	4.6±4.7	38±6	2.3±1.1	80.5±21.9	37±9	24±7	101±14	40±13	38±5	246±52	110±20	38±7	106±38	73±12	38±8
Periventricular thalamic nucleus (PTN)	36±1	20±4	2±1	116±15	30±11	1.2±1.9	110±53	2.5±0.7	1.3±2.3	50±19	8.8±5	1.6±2.7	136±31	1.7±0.7	0.0
Paraventricular Hypothalamic nucleus (PVN)	54±24	24±0.0	1.6±1.5	65±14	62±4.9	27 ±11	129±39	76±19	55±20	32±6	52±10	19±5	56±19	94±5.6	47±9
dl – Periaqueductal gray matte (dlPAG)	8±0.0	50±5	0.6±1	42±13	39±18	0.2±0.5	25±9	41±5	0.5±0.7	10±4	65±17	1±0.8	76±25	27±16	0.5±0.7
v – Periaqueductal gray matter (vPAG)	3±2.8	9±0.0	1±1.7	86±2.8	40±7.7	4.6±5.6	45±15	34±26	2±1.4	26±16	32±12	1±1	68±1.4	6.5±6.3	0.0

Corresponding author: ***Maria Alice da **Cruz-Höfling
Departamento de Histologia e Embriologia
Instituto de Biologia, C.P. 6109
Universidade Estadual de Campinas (UNICAMP)
13 087-130, Campinas – SP – BRASIL
E-mail: hofling@unicamp.br
Tel. (55)(19) 3521 6224; Fax. (55)(19) 3289 3124

Cultured astrocyte activation by *Phoneutria nigriventer*. A conversation with nitric oxide

Catarina Rapôso[1], Renata Graciele Zanon[2], Alexandre Leite Rodrigues de Oliveira[2], Maria Alice da Cruz-Höfling[1*]

[1]Departamento de Histologia e Embriologia, [2]Departamento de Anatomia, Biologia Celular e Fisiologia e Biofísica, Instituto de Biologia, Universidade Estadual de Campinas- UNICAMP, Campinas, SP, Brazil

ABSTRACT

In vivo studies in rats have demonstrated the neurotoxic involvement of *Phoneutria nigriventer* venom (PNV) in particular brain areas by increased Fos-like positive neurons. In much of these areas, nNOS immunoreactive neurons were found. Moreover, increased GFAP, S100, IFN-γ and TNF-α expression indicated astrocytes and neuron activation in hippocampus and cerebellum. In order to verify whether the astrocytes interact directly with PNV components, and if nitric oxide (NO) contribute to PNV intoxication and inflammation, purified rat cortical astrocytes were cultured with 14.6 μg/ml PNV; 7-nitroindazol (7NI, an inhibitor of nNOS, 1 mg/ml) alone or plus PNV (7NI/PNV), and the cells survived for 15 min, 2 and 5 h. LPS incubation was used as positive control (1 μg/ml). GFAP, IFN-γ , TNF-α, and n-NOS were immunolabeled and the density of pixels was systematically measured. The amount of NO released from astrocytes was determined by assaying nitrite in incubation medium. Comparing with control, GFAP expression significantly increased 15 min, 2 and 5 h after PNV; TNF-α and IFN-γ increased after 2 h; and nNOS showed a trend for increase. 7NI/PNVincubated astrocytes reduced significantly GFAP, TNF-α and IFN-γ expression, as well as increased the release of nitrite. Changes in astrocytes morphology accompanied the alterations. This study using primary culture from cortical astrocytes showed that PNV was able to change astrocyte metabolism of some proteins. One point to stress would be the action of PNV in NO regulation by this astrocytic population and vice-versa that is the NO mediation of PNV toxic effects.

***Keywords*:** GFAP, astrocyte, TNFα, IFNγ , nNOS, nitric oxide, 7-nitroindazol

Introduction

Astrocytes, the most abundant cell type in the CNS, are central for neuronal survival and function (for review, see [1]). These cells are active players in the formation and maintenance of a safe blood-brain barrier (BBB), restrict the free traffic of substances between the blood and brain [2,3], respond to stress and insults by transiently upregulating inflammatory processes [4], and contribute to the control of immune responses [5] by acting as modulators of immune and inflammatory responses in several neurological disturbances [6], among others.

Neuroinflammation in the CNS comprises the activation of glial cells, recruitment of peripheral immune cells and production of cytokines, such as Interferon-gamma (IFN-γ) and Tumor Necrosis Factor-alpha (TNF-α) [7-9]. TNF-α mediates cytotoxic damage to glial cells and neurons, while IFN-γ induces cell surface molecules required for interactions between immune and brain cells [10]. Inflammatory processes are accompanied by proliferation of astrocytes and upregulation of constitutive cytoskeletal and metabolic proteins, such GFAP and S100, respectively, considered as markers of insult against CNS [11-13].

Recent study has shown the occurrence of astrogliosis and upregulation of GFAP, S100, IFN-γ and TNF-α in neurons and astrocytes of hippocampus and cerebellum after systemic injection of *Phoneutria nigriventer* venom in rats (PNV) [14]. PNV induced early and transitory perivascular astrocytic edema accompanied by BBB breakdown in these regions [15-17]. The venom is rich in small basic polypeptides, 3,500 and 9,000 Da, with numerous pharmacological properties which include action on voltage-gated ion channels and neurotransmitter release [18,19]. Impairment of the BBB permeability can induce pro-inflammatory-mediated reaction creating a chain of interactions between blood-derived cells, neuronal and glial cells [20].

In a number of situations nitric oxide (NO) acts as a neuromodulator of the inflammatory process, altering neural activity and gliosis reaction in brain [21]. We showed that the PNV causes *in vivo* increase in nNOS-positive neurons of several brain motor- and stress-related areas, in most of which paralleled increased number of cFOS immunoreactive neurons (indicative of neuronal activation) [22]. The influence of NO in the toxicity induced by the i.p. injection of the Tx2-5 toxin isolated from PNV in rats has been studied [23]. The authors showed that the pretreatment with 7-nitroindazol (7-NI), a selective inhibitor of the constitutive neuronal nitric oxide synthase (nNOS) [24] abolished the signs of intoxication caused, such as priapism, salivation and lung edema, indicating a potentiating effect of the gas in intoxication mechanism. In contrast, the same treatment with 7NI but using the crude venom markedly induced more precocious and intense signs of intoxication, such prostration, higher salivation and hindlimbs spastic paralysis, suggesting a neuroprotector role for NO in the PNV toxicity (unpublished). Besides, the number of cFOS

positive neurons decreased in the majority of the regions examined, but augmented in others showing a complex regionally specific role for NO in the venom effects.

In order to check if the *in vitro* studies reinforce the data of the studies *in vivo*, astrocytes purified primary cultures were incubated with venom or with venom plus 7NI and quantification of GFAP, TNF-α, IFN-γ, and nNOS was evaluated. The approach will allow inferring if the inflammatory reaction is intrinsic or acquired from PNV systemic circulation. *P. nigriventer* is an aggressive spider species responsible for many accidents with venomous spiders in Brazil; however fatal cases are rare [25]. This study can contribute for the understanding of the *Phoneutria* envenoming mechanisms as well as can be useful for therapeutic purposes.

Materials and methods

Astrocyte purified primary cell cultures

Newborn Wistar rats (postnatal day 0-2) were obtained from CEMIB/UNICAMP. Primary cell culture of astrocytes derived from cerebral cortices was prepared [26]. Briefly, the cortices from four rats were separated and dissected free from the meninges. Thereafter, they were dissociated and trypsinized. The resulting cell suspension was centrifuged (1300 rpm, 8 min) in 4% bovine serum albumin (BSA) in DMEM. Precipitated cells were resuspended in DMEM and seeded onto 25cm^2 bottle and were kept in an incubator at 37°C, under 5% CO_2 atmosphere until achieving semiconfluence (~ 90% of the total area of culture). Following analysis of the morphology and GFAP positivity for confirmation of the culture purity, the cells were trypsinized and centrifuged again. Precipitated cells were resuspended in DMEM and seeded onto 24-well cell culture plates (104 cells per well). The plates were kept in an incubator until the beginning of the experimental procedures when the cultures reached around 90% confluence.

Phoneutria nigriventer venom and astrocytes treatment

Lyophilized *P. nigriventer* enom (PNV) from batches of crude venom milked from spiders was yielded by Instituto Butantan (São Paulo – Brasil). The venom was stored at -20ºC and diluted in culture medium immediately before use. After cell confluence, the culture medium was carefully removed by aspiration and replaced by fresh medium. After 24 h, the medium was added with *P. nigriventer* crude venom at concentrations of 14.6 µg of PNV/ml or 292 µg of PNV/ml. The control group received the same volume of culture media without venom. After PNV-treatment, the cells were maintained in a 5% CO_2 humidified atmosphere at 37 ºC up to 15 min, 2 and 5 h. These time-points were chosen based on previous evidence showing variable degree of BBB breakdown by PNV in rats [17]. The *in vitro* venom concentration (14.6 µg of PNV/ml) was selected as a function

of the concentration already adopted for *in vivo* experiments (0.85 mg of PNV/kg rat) [15,27]. This *in vivo* dose mimics in rats some clinical signs caused by accidents scored as severe in humans, such as arterial hypertension, tachycardia, arrhythmia, visual disturbances and tonic convulsions [28,29]. For the calculation of the *in vitro* PNV concentration, we considered: (i) rats with a weight average of 250 g, and (ii) that rats with this weight have a plasma volume average of 14.5 ml [30,31]. Thus, the 14.6 μg of PNV/ml dose is obtained by applying the *in vivo* concentration (0.85 mg/kg - 0.21 mg/0.25 kg) to the plasma volume (14.5 ml) of a 250 g rat. To test whether the PNV effect was concentration-dependent we used the dose of 292 μg of PNV/ml (a 20-fold higher concentration). To confirm if NO contributed to PNV intoxication, astrocyte primary cell cultures were also treated with the nNOS inhibitor, 7-nitroindazol (7NI - 1mg/ml) alone or followed by PNV (14.6 μg PNV/ml). Lipopolysaccharide (LPS) was used as positive control of reactive astrocytes (1 μg/ml). The cells were maintained in a 5% CO_2 humidified atmosphere at 37 ºC only up to 2 h for 7NI, 7NI/PNV or PNV at highest concentration (292 μg /ml) since this was considered the time interval with more intense venom effects [14,17], and up to 5 h for LPS (positive control). All experiments were performed in triplicate.

Immunohistochemistry

The cultures were fixed with 4% paraformaldehyde in DMEM and rinsed three times with 0.1 M PBS. Non-specific binding sites was blocked with 10% BSA for 1 h at room temperature; then the cultures were incubated for 2 h with rabbit polyclonal primary antibodies: anti-GFAP (1:100, DakoCytomation, CA.,USA; Catalog numbers: ZO 334), anti-IFN-γ, anti-TNF-α (1:100, 1:200; Peprotech-Rocky Hills, NJ, USA; Catalog numbers: 500-P64 and 500-P119, respectively), and anti-nNOS (1:200; Transduction Laboratories, ref. N53130) diluted in phosphate buffer solution, 0.05 M containing 1 % BSA. After the primary anti-sera, the cultures were washed and incubated for 45 min with Cy3-conjugated secondary anti-sera (1:250, Jackson Immunoresearch). Cells were then mounted in a mixture of glycerol/PBS (3:1) and observed with a fluorescence microscope (TS100, Nikon). The images were captured in a microscope coupled camera (DXM 1200, Nikon). For quantification, the density of immunofluorescence was determined by the IMAGEJ software (version 1.33u, NIH, USA).

Measurement of released nitrite

Since NO is unstable and is rapidly oxidized to nitrite and nitrate, extracellular nitrite concentration is a useful indirect indicator of increased NO production. Therefore, the amount of NO released from astrocytes was determined by assaying nitrite concentrations in the supernatants

[32]. Briefly, Griess reagent contains two chemicals, sulfanilic acid and N-l-(naphthalenediamine). Under acidic conditions, sulfanilic acid is converted by nitrite to a diazonium salt, which readily couples with Nl-(naphthalenediamine) to form a highly colored azo dye that can be detected by UV plate reader. The optical density of the assay samples was measured in plate reader ELISA at 540 nm. Nitrite concentration was determined from a standard curve constructed using the known concentrations of sodium nitrite (0 – 35 Mol), through a nitrite/nitrate assay kit (Nitrate/Nitrite Colorimetric Assay Kit – Cayman Chemical – catalog nº 780001).

Statistical analysis

The data were analyzed using the *Graphpad Prism* software package. Student t test, or one-way analysis of variance (*ANOVA)* followed by the *Tukey Kramer post-test* was used to compare the treated and control groups. A value of $P < 0.05$ indicated statistical significance.

Results

The crude venom of Phoneutria nigriventer incubated with cultured cortical astrocytes from rats caused a dose dependent, but transient effect in the expression level of GFAP. Astrogliosis was prevented by prior treatment with 7NI.

A basal GFAP expression was seen in the astrocytes of any of the time-points of control group (incubated in DMEM) (Fig. 1A). The exposure to venom resulted in hypertrophied somata and thickened and longer processes revealed by immediate GFAP immunoreactivity in astrocytes of the PNV-15 min group (Fig. 1B) and PNV-2 h group (Fig. 1C). The reactivity of astrocytes was transient and at 5 h following PNV exposure, cell processes were thinner and fewer than in the previous time-points but still more hype throphic than corresponding control (Fig. 1D). The pre-treatment with 7NI followed by PNV (7NI/PNV group), or by 7NI alone resulted in drastic decrease of astrocytes somata and cytoplasmic processes (Fig. 1E,F). The exposure to a 20-fold higher concentration of PNV resulted in extensive reactivity from cortical astrocytes (Fig. 1G), indicating a dose dependent effects. A positive control attested the validity of the GFAP immunofluorescence in cells incubated with LPS (Fig. 1H).The optical density estimated in pixels percentual from GFAP immunofluorescence corroborated the morphological analysis of the immunohistochemical assays. Compared to the control basal level, an immediate significant growing increase of the cytoskeletal protein GFAP was seen at 15 min (** $p < 0.01$) and 2 h (* $p < 0.05$), followed by a significant decrease at 5 h PNV exposure compared with PNV 15 min and 2 h (# $p < 0.05$). However, the expression of GFAP remained significantly higher than the control- 5 h (* $p < 0.05$). The blockade

of astrocytic nNOS by 7NI preincubation followed by PNV (7NI/PNV group) substantially reduced the GFAP density of pixels percentual in comparison to PNV-15 min ($p < 0.001$), PNV-2 h ($p < 0.01$) or PNV-5 h ($p < 0.01$). The venom concentration 20-fold higher than the used in the three time-points produced the highest increase in the GFAP expression level in comparison to control (*** $p < 0.001$), becoming practically alike the LPS positive control. The quantitative data were displayed in Figure 1I.

*The crude venom of Phoneutria nigriventer incubated with cultured cortical astrocytes from rats caused a dose dependent but transient effect in the expression level of TNF-α by the glial cells. 7NI pretreatment reduced this effect***.**

There was a very tenuous expression of TNF-α in control culture (Fig. 2A), which increased markedly in PNV-15 min and PNV-2 h, returning to the control labeling pattern at 5 h (compare Figs. 2B,C,D, respectively). Both cultures, either incubated with 7NI/PNV or PNV alone (Fig. 2E,F, respectively) showed GFAP immunoreactivity very much alike that of control culture. Astrocytes labeling was also seen in cells cultured with the 20x higher PNV concentration (5 h) which parallel in the labeling pattern of LPS-incubated astrocytes (Fig. 2G,H, respectively). Data of pixels quantification (Fig. 2I) showed significant increase of the TNF-α expression at PNV-2 h compared to control (** $p < 0.01$). Further, there was a significant reduction (close to the control level) of the pro-inflammatory cytokine expression in the astrocytes of the PNV-5 h compared to those of PNV-2 h (# $p < 0.05$). The 7NI incubation (30 min) followed by PNV (2 h) did not show any statistical difference in relation to the percentual of pixels density of TNF- labeling of the control group, but it was effective in reducing it when compared to PNV-2 h ($p < 0.05$). The nNOS inhibitor by itself did not influence this cytokine expression in relation to control. The PNV-20-fold higher concentration increased TNF-α immunolabeling (** $p < 0.01$) in relation to control. The exposure of the glial cells to LPS validated the data by confirming the induction of the inflammatory reaction (TNF- α positivity).

*The crude venom of Phoneutria nigriventer incubated with cultured cortical astrocytes from rats caused a dose dependent but transient effect in the expression level of IFN-γ by the glial cells. 7NI pretreatment reduced this effect***.**

There was a faint immunolabeling of the pro-inflammatory cytokine IFN-γ in cortical astrocytes cultured in DMEM (control) (Fig. 3A). The incubation with PNV at any time-course

increased the IFN-γ immunoreactivity, which is mostly expressed in perikarya (Figs. 3B,C,D, respectively at 15 min, 2 h and 5 h). The incubation with the blocker of nNOS, 7 nitroindazole, reduced markedly the cytokine labeling (Figs. 3E,F). The higher concentration of PNV (292 μ/ml) used to check a dose response by the glial cells showed the highest increment of the labeling (Fig. 3G). The positive control (LPS incubation) validated the reactivity for the cytokine (Fig. 3H). The computer quantification of the density of pixels of the immunoassay showed significant increase in the IFN-γ expression level at 2 h following the PNV exposure (** $p < 0.01$). After, a trend for expression decrease was seen at 5 h. The treatment with 7NI (30 min) before the ensuing PNV exposure markedly reduced the astrocytic IFN-γ expression in comparison to PNV-15 min ($p < 0.01$) and PNV-2 h ($p < 0.001$). 7NI itself decreased IFN-γ expression, comparing with control ($p < 0.001$). Similarly to the other proteins here investigated, the PNV 20 x concentrated dose provoked the highest elevation in this inflammatory cytokine in relation to control (** $p < 0.01$). LPS treatment confirmed the astrocytic reactivity to IFN-γ. The representative histogram of the data is displayed in Figure 3I.

The crude venom of Phoneutria nigriventer incubated with cultured cortical astrocytes from rats caused an immediate but transient trend for increasing the nNOS expression level by the glial cells, since at 2 and 5 h incubation the expression returned to basal level. 7NI pretreatment did not alter significantly the expression of the enzyme, but 7NI alone did.

Control astrocytes showed a subtle immunolabeling, which became stronger and concentrated in the perikaryon as soon as 15 min of PNV incubation (Fig. 4A,B, respectively). Thereafter, the reactivity became more diffuse and weaker (Figs. 4C,D, respectively after 2 and 5 h of PNV). Such pattern was also exhibited by astrocytes incubated with 7NI/PNV (Fig. 4E). Interestingly, astrocytes incubated with 7NI alone exhibited stronger immunolabeling both at the perikaryon and astrocytic processes (Fig. 4F). With the highest PNV dose (292 μg/ml) astrocytes nNOS immunoreactivity was tenuous (Fig. 4G), whereas those incubated with LPS was strong (Fig. 4H). The density of pixels quantified from the nNOS immunostaining showed that the trend for increase after 15 min did not achieve statistic significance compared to control. Interestingly, astrocytes incubated with 7NI alone showed marked increment in the density of pixels compared with 7NI plus PNV ($p < 0.01$), suggesting a venom inhibitory effect against the 7NI-mediated upregulation of nNOS. The PNV 20x dose induced a remarkable decrease in this enzyme immunolabeling expression compared to controls (** $p<0.01$).

Measurement of released nitrite

The control group showed a basal nitrite level, which was maintained stable in 15 min and 5 h venom incubation media. Astrocytes culture incubated with PNV for 2 h. showed a significant increase in the extracellular nitrite level in comparison to PNV-15 min (# $p < 0.05$). Significant reduction of nitrite in the incubation medium was seen in 7NI/PNV in comparison to PNV-2 h ($p < 0.05$), suggesting that the selective blockade of the constitutive nNOS enzyme by 7-nitroindazole reduces the formation of nitrite from NO. 7NI itself induced a significant decrease in the nitrite formation compared to control (* $p < 0.05$), as was so the incubation with 292 μg/ml PNV (** $p< 0.01$). The highest nitrite release was shown by cultured cortical astrocytes in response to LPS exposure.

Discussion

The microenvironment of the CNS is considered as immunoprivileged due to the BBB surveillance against the entrance of undesirable substances. Despite, the lack of lymphatic drainage and the relatively low levels of resident immune cells suggest that putative local immune and inflammatory reactions do occur by either an intrinsic mechanism and/or are imported systemically through a damaged BBB [21].

P. nigriventer is an aggressive spider species responsible for many accidents with venomous spiders in Brazil; however fatal cases are very rare [25]. Human systemic envenomation is associated with a number of adverse effects, the nature and severity of which depends on the ratio amount of venom administered/victim body mass and physical health condition and the time between accident and appropriate medical treatment. Variably, the *Phoneutria* biting causes irradiating pain, and toxic symptoms, such as cramps, tremors, tonic convulsions, spastic paralysis, priapism, sialorrhea, arrhythmias, visual disturbance, and cold sudoresis ([28,33], reviewed by [34]). In general, the major targets of animal venoms are the somatic nervous system because they do not cross the blood-brain barrier. Because accidents graded as grave may cause convulsion, the Phoneutria venom action on the CNS have been investigated by us.

The *P. nigriventer* venom (PNV) is composed by basic polypeptides with molecular weight between 3,500 – 9,000 Da, the majority Na^+, K^+ and Ca^{2+} acting neurotoxins interfering in histamine, serotonin, acetylcholine, and glutamate neurotransmitter release [18,19, 35-37]. The venom effect on several regions of the CNS [14,22], and in particular at the BBB level, have been shown in our laboratory [15-17]. Strong evidences indicate that the venom disrupts the BBB, induces CNS inflammation and neuron and astrocyte activation, at least in part with the participation of the nitric oxide, either with a neuroprotector or a neurotoxic role. Astrocytes are key

actors in the insults inflicted to CNS, and NO has been shown to be participants in many neuropathologies.

Here, a pure cortical astrocyte primary culture was incubated with the crude PNV alone or in combination with a pretreatment with 7-nitroindazol (7NI), a selective blocker of nNOS, and the expression of nNOS, GFAP, and the pro-inflammatory cytokines, TNF-α and IFN-γ, was investigated. A controlled system, such as *in vitro* cultured cell, permits direct evaluation of cell events without the highly interdependent mechanisms normally affecting neurological processes.

The studies here have revealed that the earlier reactive changes (15 min) in astrocytes in response to PNV exposure were characterized by cytoplasmic hypertrophy and intense GFAP expression. Only later on (2 h) the astrocytes reacted by significantly express TNF-α and IFN-γ, a time interval where the release of nitrite was raised significantly. The astrogliosis after brain injuries and diseases is a well known and vastly documented event; however the exact mechanism eliciting this reaction is poorly understood. What seems clear is that reactive astrocytes altered the expression of many genes, some related with the synthesis of the cytoskeletal proteins from the intermediate filaments, mainly GFAP and also nestin and vimentin [38].

The findings also revealed that the changes and tendencies for changes were transient and after the peak at 2 h, a downregulation in the expression level of the proteins investigated occurred at 5 h of PNV exposure. These data corroborate our previous studies showing that the PNV effects were self-limited, both clinically and molecularly [16,17,22].

The present results give strong evidence that the NO may be directly involved in astrocytic reaction and inflammation response against PNV toxicity. We showed that the nNOS inhibition by the pretreatment of cultures with 7NI reduced markedly the GFAP and IFN-γ expression to levels lower and much lower, respectively, than the exhibited by controls. In addition, 7NI treatment before the addition of PNV promoted a trend for reducing TNF-α. On the other hand, astrocytes incubated with 7NI, alone showed increased expression of nNOS, what likely suggests, a compensatory mechanism. Interestingly, the combination 7NI plus venom kept the nNOS in physiological levels evidencing a venom inhibitory effect against the upregulation promoted by 7NI alone. The alteration in the expression of the proteins studied was accompanied by morphological alterations of the astrocytes, which is seen as soon as 15 min of PNV exposure. The data substantiate previous *in vivo* studies suggesting the existence of a mechanism of defense in the CNS which in response to circulating *P. nigriventer* venom promptly trigger machinery for synthesis of proteins, such as GFAP and S100, and to induce the expression of proinflammatory cytokines [14].

NO is a highly reactive radical product of the amino acid arginine, generated by the action of nitric oxide synthase. NO mediates the function of a variety of physiological systems [39,40],

such as vascular tonus and permeability, platelet function, macrophages cytotoxic action, inflammation and immunoregulation and neurotransmission [40-44]. While playing a central role in physiological homeostasis, overproduction of NO can aggravate inflammation.

Recent *in vivo* data (unpublished) has demonstrated that the blockade of nNOS by 7NI i.p. injection before crude PNV administration protected the activation of some brain regions, such as parietal motor cortex, hypothalamic nucleus, periaqueductal gray matter pars ventral and lateral, but increased the activation of the supraoptical nucleus, seen through the significant increase in number of Fos-like positive neurons. The results indicated that in this model, the NO showed a dual role, protective or noxious, depending on the cerebral regions. In parallel, the clinical signs of envenoming, such as, hyperemia, salivation, flaccid and spastic paralysis, anuria and respiratory distress were aggravated and anticipated, indicating a benefic role in the overall clinical condition of the animals. Yonamine et al. [23], reported that the pretreatment with 7-NI, abolished signs of intoxication caused by intraperitoneal injection of the toxin Tx2-5, such as priapism, salivation and lung edema in rats, indicating that NO aggravates the toxicity of the toxin in contrast to our results. The venom of *P. nigriventer* consists of a multitude of pharmacologically active components (toxins, acylpolyamines and the like), and alike in other venomous animals, the venom components have evolved to assist in the paralysis or death of prey, as well as for use in defence against predators. Each toxin has a particular target or targets to achieve an efficient capture of prey. In this sense, the venom components may have synergic or antagonistic action in different targets, what could explain the conflicting data in relation to NO role seen with the crude venom and the Tx2-5 toxin [23].

A point to discussion is that the brain inflammation occurs inside the brain which is walled by the blood-brain barrier, and thus differs from inflammation in the periphery by the relative absence of leucocytes and circulating antibodies. However, it is now recognized that there is a limited traffic of inflammatory factors across the barrier in physiological basis, and this traffic can be increased by inflammation [45]. Recent *in vivo* results [14] showed that GFAP, S100, TNF-α and INF-γ expression in astrocytes and neurons were increased after PNV systemic injection, suggesting that the expression of pro-inflammatory cytokines is part of the immune response against the neurotoxic injury caused by PNV. But, until now, we did not know if the cytokines were locally released by resident brain cells or secreted from cells invading the CNS tissue from blood stream. Since TNF-α increases vascular-brain permeability, systemic TNF-α would gain access to brain through a specific transport system [46]. This question was partially solved in this work, since it was confirmed the resident inflammatory response by astrocytes in culture. However, this not excludes an additional response by immune cells infiltrated or through microglial response in living

systems. Since IFN-γ is required for interactions between immune and brain cells, increases microglia neuroprotective effect and induces neurotrophic factor receptors [10], it is likely that the significant increase here seen may predict for both endogenous and exogenous resources of IFN-γ in adverse brain conditions. Future experiments with markers for resident or infiltrated immune cells and for activated microglia will be done in our experimental model.

Another open question is whether the bulk of inflammatory and gliosis effects hitherto known be provoked by systemic PNV results from a direct action of the contact between venom and brain cells (so components of the venom could gain access to brain), and/or from peripheral- or endogenous-generated secondary messengers elicited during contact of venom/toxins with endothelial cells and after BBB permeabilization. In this work, the results showed that the direct contact with PNV induces gliosis and inflammatory reaction in cultured astrocytes. However, pro-inflammatory cytokines traversing the BBB also did; similarly, NO generated by astrocytes in response to insult may also induce gliosis and/or inflammation. Astrocytes react to oscillations of Ca^{2+} and glutamate, and PNV interferes with both [19], what suggest another pathway involving BBB disruption caused by Phoneutria venom directly or by mediators such as cytokines, free radicals, excitatory neurotransmitters released from activated astrocytes, or others.

The nitric oxide showed to be an efficient inflammatory and gliosis modulator of astrocytes after PNV exposure, but for a better understanding of the NO role in the armed-spider envenoming, future experiments need to be performed with NO-donors before PNV exposure in culture astrocytes or before PNV-envenoming *in vivo*. The richness of neurotoxins in the *P. nigriventer* spider venom elects it as a powerful tool for using in physiopathological, pharmacological and cell biology events in the CNS and other systems. The model is useful for the study the regulation of inflammatory reaction and gliosis associated with BBB.

Acknowledgements: The authors thank Instituto Butantan (São Paulo, SP, BR) for venom donation, Mss. Marta Beatriz Leonardo (BSc) for excellent technical assistance, and Mr. Miguel Silva and Mr. Marcos Silva for animal care. This work has been funded by grants from Fundação de Amparo à Pesquisa do Estado de São Paulo (FAPESP # 07/50242-6) and Conselho Nacional de Desenvolvimento Científico e Tecnológico (CNPq #). C.R is recipient of scholarship from FAPESP. M.A.C.H. is a 1A research fellow from CNPq.

References

[1] J. De Keyser, J.P. Mostert, M.W. Koch, Dysfunctional astrocytes as key players in the pathogenesis of central nervous system disorders, J. Neurol. Sci. 267 (2008) 3-16.

[2] L.F. Eng, R.S. Ghirnikar, GFAP and astrogliosis, Brain Pathol. 4 (1994) 229-237.

[3] B. Ransom, T. Behar, M. Nedergaard, New roles for astrocytes (stars at last), Trends Neurosci. 26 (2003) 520-522.

[4] S.D. Skaper, The brain as a target for inflammatory processes and neuroprotective strategies, Ann. N. Y. Acad. Sci. 1122 (2007) 23-34.

[5] C. Farina, F. Aloisi, E. Meinl, Astrocytes are active players in cerebral innate immunity, Trends Immunol. 28 (2007) 138-145.

[6] M. Aschner, Immune and inflammatory responses in the CNS: modulation by astrocytes, Toxicol. Lett. 102-103 (1998) 283-287.

[7] L. Minghetti, G. Levi, Microglia as effector cells in brain damage and repair: focus on prostanoids and nitric oxide, Prog. Neurobiol. 54 (1998) 99-125.

[8] W.J. Streit, Microglial response to brain injury: a brief synopsis, Toxicol. Pathol. 28 (2000) 28-30.

[9] H. Neumann, Control of glial immune function by neurons, Glia 36 (2001) 191-199.

[10] F. Imai, H. Suzuki, J. Oda, T. Ninomiya, K. Ono, H. Sano, M. Sawada, Neuroprotective effect of exogenous microglia in global brain ischemia, J. Cereb. Blood Flow Metab. 27 (2007) 488-500.

[11] W. Walz, M.K. Lang, Immunocytochemical evidence for a distinct GFAP-negative subpopulation of astrocytes in the adult rat hippocampus, Neurosci. Lett. 257 (1998) 127-130.

[12] V.L. Savchenko, J.A. McKanna, I.R. Nikomenko, G.G. Skibo, Microglia and astrocytes in the adult rat brain: comparative immunocytochemical analysis demonstrates the efficacy of lipocortin 1 immunoreactivity, Neuroscience 96 (2000) 195-203.

[13] L.F. Eng, R.S. Ghirnikar, Y.L. Lee, Glial fibrillary acidic protein: GFAP-thirty-one years (1969-2000), Neurochem. Res. 25 (2000) 1439-1451.

[14] M.A. Cruz-Höfling, C. Rapôso, L. Verinaud, G.M. Zago, Neuroinflammation and astrocytic reaction in the course of phoneutria nigriventer (armed-spider) blood-brain barrier (bbb) opening, Neurotoxicology 30 (2009) 636-646.

[15] P.L. Le Sueur, E. Kalapothakis, M.A. Cruz-Höfling, Breakdown of the blood-brain barrier and neuropathological changes induced by *Phoneutria nigriventer* spider venom, Acta Neuropathol. 105 (2003) 125-134.

[16] L.P. Le Sueur, C.B. Collares-Buzato, M.A. Cruz-Höfling, Mechanisms involved in the blood-brain barrier increased permeability induced by *Phoneutria nigriventer* spider venom in rats, Brain Res. 1027 (2004) 38-47.

[17] C. Rapôso, G.M. Zago, da G.H. Silva, M.A. Cruz-Höfling, Acute blood-brain barrier permeabiliation in rats after systemic *Phoneutria nigriventer* venom, Brain Res. 1149 (2007) 18-29.

[18] E. Antunes, C.M.S. Malaque, Mecanismo de ação do veneno de *Phoneutria* e aspectos clínicos do foneutrismo, In: J. L. C. Cardoso, F.O.S. França, F.W. Wen, C.M.S. Málaque, V. Haddad-Jr. (Ed.), Animais Peçonhentos no Brasil: Biologia, Clínica e Terapêutica, Sarvier, São Paulo (2003) pp. 150-159.

[19] M.V. Gomez, E. Kalapothakis, C. Guatimosim, M.A. Prado, *Phoneutria nigriventer* venom: a cocktail of toxins that affect ion channels, Cell Mol. Neurobiol. 22 (2002) 579-588.

[20] D. Wong, K. Dorovini-Zis, S.R. Vincent, Cytokines, nitric oxide, and cGMP modulate the permeability of an in vitro model of the human blood-brain barrier, Exp. Neurol. 190 (2004) 446-455.

[21] J. Choi, S. Koh, Role of brain inflammation in epileptogenesis, Yonsei Med. J. 49 (2008) 1-18.

[22] M.A. Cruz-Höfling, G.M. Zago, L.L. Melo, C. Rapôso, c-FOS and n-NOS reactive neurons in response to circulating *Phoneutria nigriventer* spider venom, Brain Res. Bull. 73 (2007) 114-126.

[23] C.M. Yonamine, L.R.P. Troncone, M.A.P. Camilloa, Blockade of neuronal nitric oxide synthase abolishes the toxic effects of Tx2-5, a lethal *Phoneutria nigriventer* spider toxin, Toxicon 44 (2004) 169-172.

[24] P.K. Moore, P. Wallace, Z. Gaffen, S.L. Hart, R.C. Babbedge, Characterization of the novel nitric oxide synthase inhibitor 7-nitro indazole and related indazoles: antinociceptive and cardiovascular effects, Br. J. Pharmacol. 110 (1993) 219-24.

[25] F. Bucaretchi, C.R. Deus Reinaldo, S. Hyslop, P.R. Madureira, E.M. De Captani, R.J. Vieira, A clinico-epidemiological study of bites by spiders of the genus *Phoneutria,* Rev. Inst. Med. Trop. Sao Paulo 42 (2000) 17-21.

[26] K.D. McCarthy, J. de Vellis, Preparation of separate astroglial and oligodendroglial cell cultures from rat cerebral tissue. J. Cell Biol. 85 (1980) 890-902.

[27] L.P. Le Sueur, C.B. Collares-Buzato, E. Kalapothakis, M.A. Cruz-Höfling, *In vitro* effect of the *Phoneutria nigriventer* spider venom on cell viability, paracellular barrier function and transcellular transport in cultured cell lines, Toxicon 46 (2005) 130-141.

[28] V. Brazil, J. Vellard, Contribuição ao estudo do veneno das aranhas, Mem. Inst. Butantan 2, (1925) 5–77.

[29] V. Brazil, J. Vellard, Contribuição ao estudo do veneno das aranhas II. Mem. Inst. Butantan, 3 (1926) 3–77.

[30] J.G. Filep, A. Delalandre, M. Beauchamp, Dual role for nitric oxide in the regulation of plasma volume and albumin escape during endotoxin shock in conscious rats, Circ. Res. 81 (1997) 840-847.

[31] F. Lo, S. Kaufman, Effect of 5 alpha-pregnan-3 alpha-ol-20-one on nitric oxide biosynthesis and plasma volume in rats, Am. J. Physiol. Regul. Integr. Comp. Physiol. 280 (2001) 1902-1905.

[32] Green L.C., Wagner D.A., Glogowski J., Skipper P.L., Wishnok J.S. Tannenbaum S.R. Analysis of nitrate, nitrite, and [15N]nitrate in biological fluids. Anal. Biochem. (1982) 126:131-138.

[33] S. Schenberg, F.A. Lima, Pharmacology of the polypeptides from venom of the spider *Phoneutria fera*, Mem. Inst. Butantan 33 (1966) 627-638.

[34] S. Lucas Spiders in Brazil, Toxicon 26 (1988) 759-772.

[35] M.A. Cruz-Höfling, S. Love, G. Brook, L.W. Duchen, Effects of *Phoneutria nigriventer* venom on mouse peripheral nerve, Q. J. Exp. Physiol. 70 (1985) 623-640.

[36] E. Antunes, R.A. Marangoni, S.D. Brain, G. De Nucci, *Phoneutria nigriventer* (armed spider) venom induces increased vascular permeability in rat and rabbit skin *in vivo*, Toxicon 30 (1992) 1011-1016.

[37] S.K. Costa, S.D. Brain, E. Antunes, G. De Nucci, R.J. Docherty, *Phoneutria nigriventer* spider venom activates 5-HT4 receptors in rat-isolated vagus nerve, Br. J. Pharmacol. 139 (2003) 59-64.

[38] M. Pekny, U. Wilhelmsson, Y.R. Bogestål, M. Pekna, The role of astrocytes and complement system in neural plasticity, Int. Rev. Neurobiol. 82 (2007) 95-111.

[39] F.Y. Liew, Interactions between cytokines and nitric oxide, Adv. Neuroimmunol. 5 (1995) 201-209.

[40] C. Nathan, Natural resistance and nitric oxide, Cell 82 (1995) 873-876.

[41] F.Y. Liew, Role of cytokines in killing of intracellular pathogens, Immunol. Lett. 30 (1991) 193-197.

[42] A.W. Taylor-Robinson, F.Y. Liew, A. Severn, D. Xu, S.J. McSorley, P. Garside, J. Padron, R.S. Phillips, Regulation of the immune response by nitric oxide differentially produced by T helper type 1 and T helper type 2 cells, Eur. J. Immunol. 24 (1994) 980-984.

[43] H.Y. Yun, V.L. Dawson, T.M. Dawson, Neurobiology of nitric oxide, Crit. Rev. Neurobiol. 10 (1996) 291-316.

[44] H. Bauer, T. Jung, D. Tsikas, D.O. Stichtenoth, J.C. Frölich, C. Neumann, Nitric oxide inhibits the secretion of T-helper 1- and T-helper 2-associated cytokines in activated human T cells, Immunology 90 (1997) 205-211.

[45] B. Engelhardt, R.M. Ransohoff, The ins and outs of T-lymphocyte trafficking to the CNS: anatomical sites and molecular mechanisms, Trends Immunol. 26 (2005) 485-495.

[46] E.G. Gutiérrez, W.A. Banks, A.J. Kastin, Murine tumor necrosis factor alpha is transported from blood to brain in the mouse, J. Neuroimmunol. 47 (1993) 169-176.

Legends for figures

Figure 1: Representative photomicrographs of GFAP immunoreactivity in cortical astrocytes primary culture and comparative analysis of the density of pixels evaluated from the intensity and extensity of GFAP labeling. Comparison with time-paired controls, the PNV-incubated culture (14.6 μg PNV/ml) showed reactive astrocytes with both hypertrophied somata and processes and increased expression of GFAP (panels A,B,C,D). LPS-exposed astrocytes represent positive controls of the immunoreaction (E). The treatment with the selective inhibitor of nNOS (F), or with 7NI plus PNV (7NI/PNV group, panel G) remarkably downregulated the expression of GFAP and

the astrocytic reactivity. A dose-dependent reactive astrocytes/GFAP expression was demonstrated with a 20-fold higher concentration of PNV (H). Scale bar for all panels = 50 m. Quantification of the density of pixels (panel I) showed significant increases over the paired controls in PNV-15 min (* * $p < 0.01$), PNV-2 h (* $p < 0.05$) and PNV- 5 h (* $p < 0.05$). Although high than the control, PNV-5 h GFAP pixels density was decreased significantly compared to PNV-15 min and PNV-2 h (* $p < 0.05$). Astrocytes of the 7NI/PNV and 7NI groups showed remarkable reduction in pixels density compared to all PNV-groups (PNV-15 min, $p < 0.001$), PNV-2 h, $p < 0.01$) or PNV-5 h, $p < 0.01$).. The highest density of pixels was achieved by the PNV-20- fold higher concentration (292 μg PNV/ml) group;compared to control-5 h (*** $p < 0.001$). LPS group, used as positive control, showed intense GFAP density of pixels compared to control Data were expressed as mean S.E.M. Student t test or one-way ANOVA followed by the Tukey–Kramer multiple comparison test were used to compare the treated and paired controls.

Figure 2: Micrographs from cortical astrocytes primary culture immunolabeled with TNF-α show light fluorescence in control (A), increased staining in 15 min (B) followed by gradual decrease at 2 and 5 h (C,D), and in 7NI and 7NI/PNV cultured astrocytes (E,F). The highest immunoreaction was with PNV-20x and LPS (G,H). Scale bar: 50 m. In panel I, the density of pixels showed a trend to TNF-α increase in PNV-15 min (non significant) and PNV-2 h (** $p < 0.01$) compared to control. In atrocytes treated with 7NI before PNV, the TNF-α expression decreased, comparing to PNV-2h group ($p < 0.05$). PNV 20 x showed a dose-dependent increase in TNF-α expression (** $p < 0.01$), comparing to control. Data were expressed as mean S.E.M. Student t test or one-way ANOVA followed by the Tukey–Kramer multiple comparison test were used to compare the treated and paired controls.

Figure 3: Representative micrographs from primary culture of cortical astrocytes immunolabeled with INF-γ. Astrocytes incubated with DMEM (control) showed IFN-γ reactivity mainly in nucleus and diffuse in cytoplasm (A). In PNV-incubated astrocytes morphology changed both in nucleus and cytoplasm; besides the cytokine labeling was stronger in the three time intervals (B,C,D). In atrocytes treated with 7NI alone (E) or with 7NI plus PNV (F) the reactivity decreased, and so glia morphology. The highest expression of IFN-γ was displayed by PNV-20x indicating a dose-dependency of cytokine expression; the staining is strong both in nucleus and cytoplasm (G). LPSincubated glia exhibits morphology similar to control, but the staining is stronger (H). Scale bar: 50 m. The pixels density of the protein expression (panel I) was increased in PNV-15 min (non significant) and PNV-2 h (** $p < 0.01$), after what occurred a tendency for decrease in PNV-5 h. In

atrocytes incubated with 7NI alone or with 7NI plus PNV, the density of pixels decreased markedly in relation to control (*** $p < 0.001$ and p** < 0.01, respectively), and in relation to PNV-15 min ($p < 0.01$) and PNV-2 h ($p < 0.001$). Data were expressed as mean S.E.M. Student t test or one-way ANOVA followed by the Tukey–Kramer multiple comparison test were used to compare the treated and paired controls.

Figure 4: Micrographs from nNOS positive cortical astrocytes incubated with DMEM (A) and with Phoneutria venom for 15 min (B), 2 h (C) and 5 h (D). Both the morphology as well the intensity of labeling was changed with venom. The highest expression was achieved at 15 min. The nNOS expression decreased in astrocytes pretreated with 7NI followed by PNV (E), but increased strongly in those incubated with the 7NI alone (F). In PNV-20x (panel G) the astrocytes showed a subtle nNOS labeling, hence not exhibiting a dose-dependency. LPS, used as positive control, showed the highest nNOS expression; scale bar: 50 m. Panel I shows that there was statistic significance in the density of pixels for nNOS only for PNV-20x compared with control (** $p < 0.01$) and between 7NI- and 7NI/PNV-incubated astrocytes ($p < 0.05$). Data were expressed as mean S.E.M. Student t test or one-way ANOVA followed by the Tukey–Kramer multiple comparison test were used to compare the treated and paired controls.

Figure 5: Histogram showing the Nitrite concentration in the culture medium of purified primary culture from cortical astrocytes. The glial cells incubated for 2 h with PNV showed augment of nitrite concentration in the incubation medium in comparison to PNV-15 min (# $p < 0.05$) whereas cells incubated with the nNOS inhibitor 7NI followed by PNV showed reduction of nitrite compared to PNV-2 h ($p < 0.05$); *$P < 0.05$ and **$P < 0.01$ indicate significant difference between 7NI alone and control and PNV-20x and control, respectively. LPS showed the highest nitrite release to the incubation medium. The results are expressed as the mean ± S.E.M. (Student t test or one-way ANOVA followed by the Tukey–Kramer multiple comparison test, for compare the treated with controls).

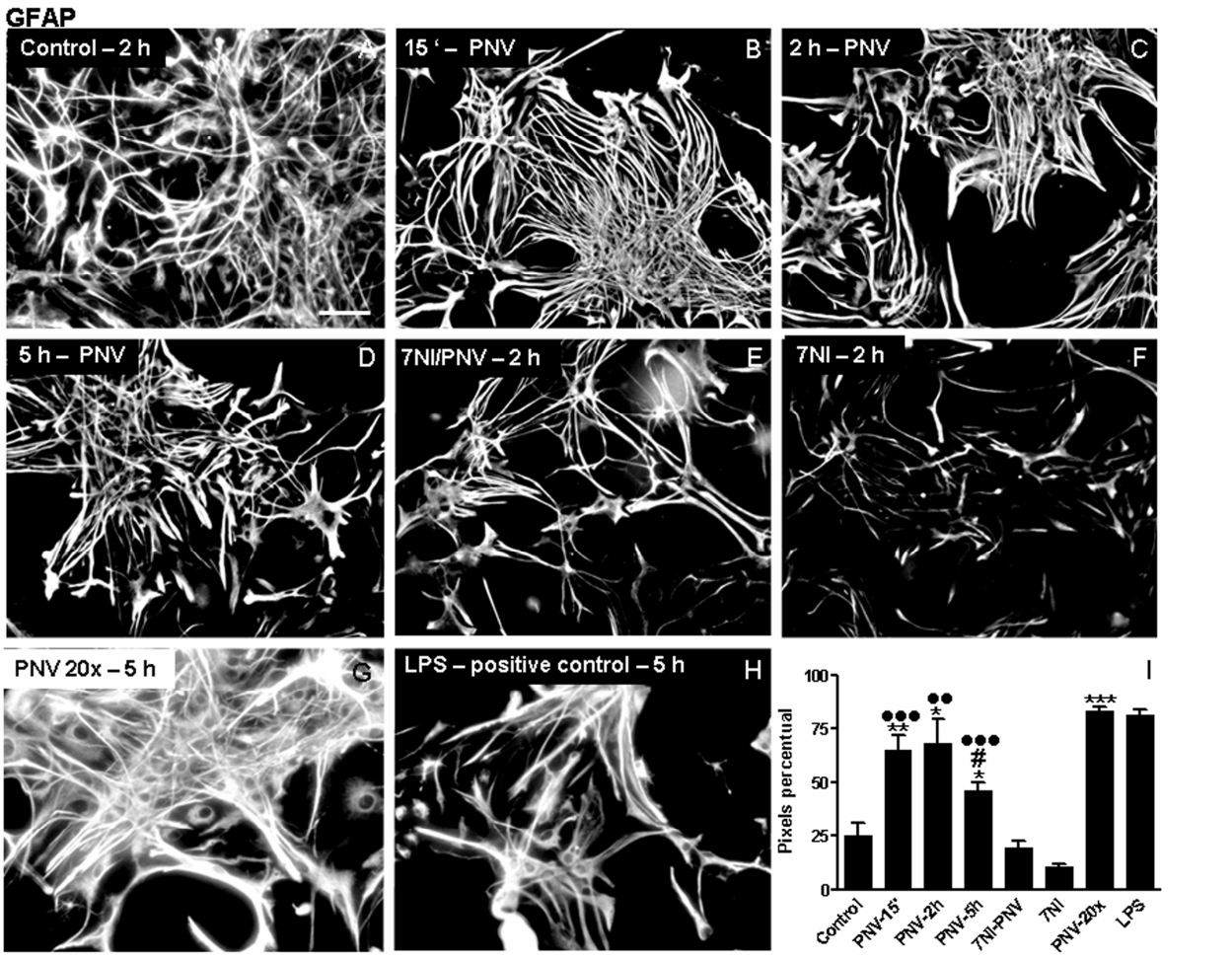
GFAP
Control – 2 h
A
15 ' – PNV
B
2 h – PNV
C
5 h – PNV
D
7NI/PNV – 2 h
E
7NI – 2 h
F
PNV 20x – 5 h
G
LPS – positive control – 5 h
H
I
Pixels per centual
100
75
50
25
0
Control
PNV-15'
PNV-2h
PNV-5h
7NI-PNV
7NI
PNV-20x
LPS

Figure 1

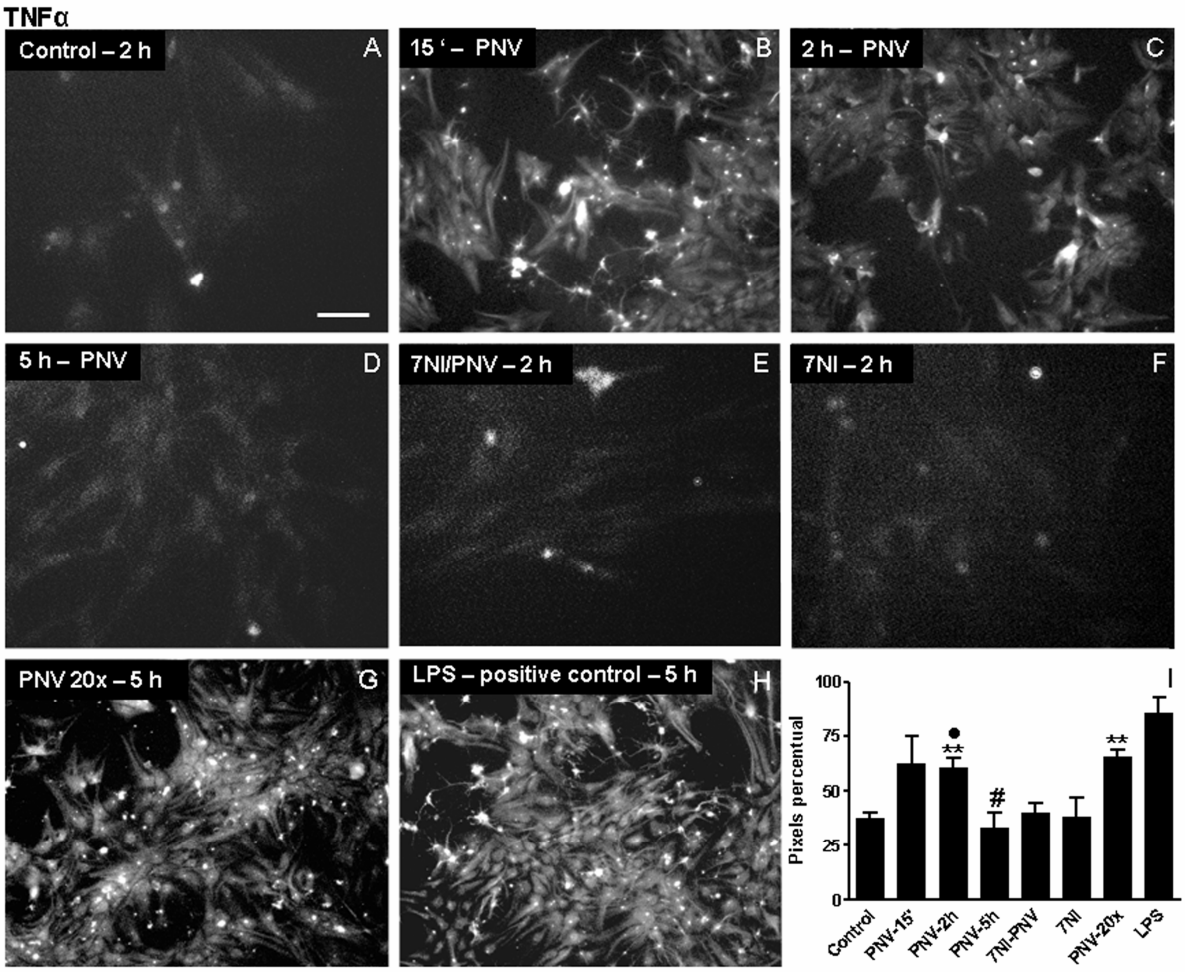
TNFα
Control – 2 h
A
15 ' – PNV
B
2 h – PNV
C
5 h – PNV
D
7NI/PNV – 2 h
E
7NI – 2 h
F
PNV 20x – 5 h
G
LPS – positive control – 5 h
H
I
Pixels percentual
100
75
50
25
0
Control
PNV-15'
PNV-2h
PNV-5h
7NI-PNV
7NI
PNV-20x
LPS

Figure 2

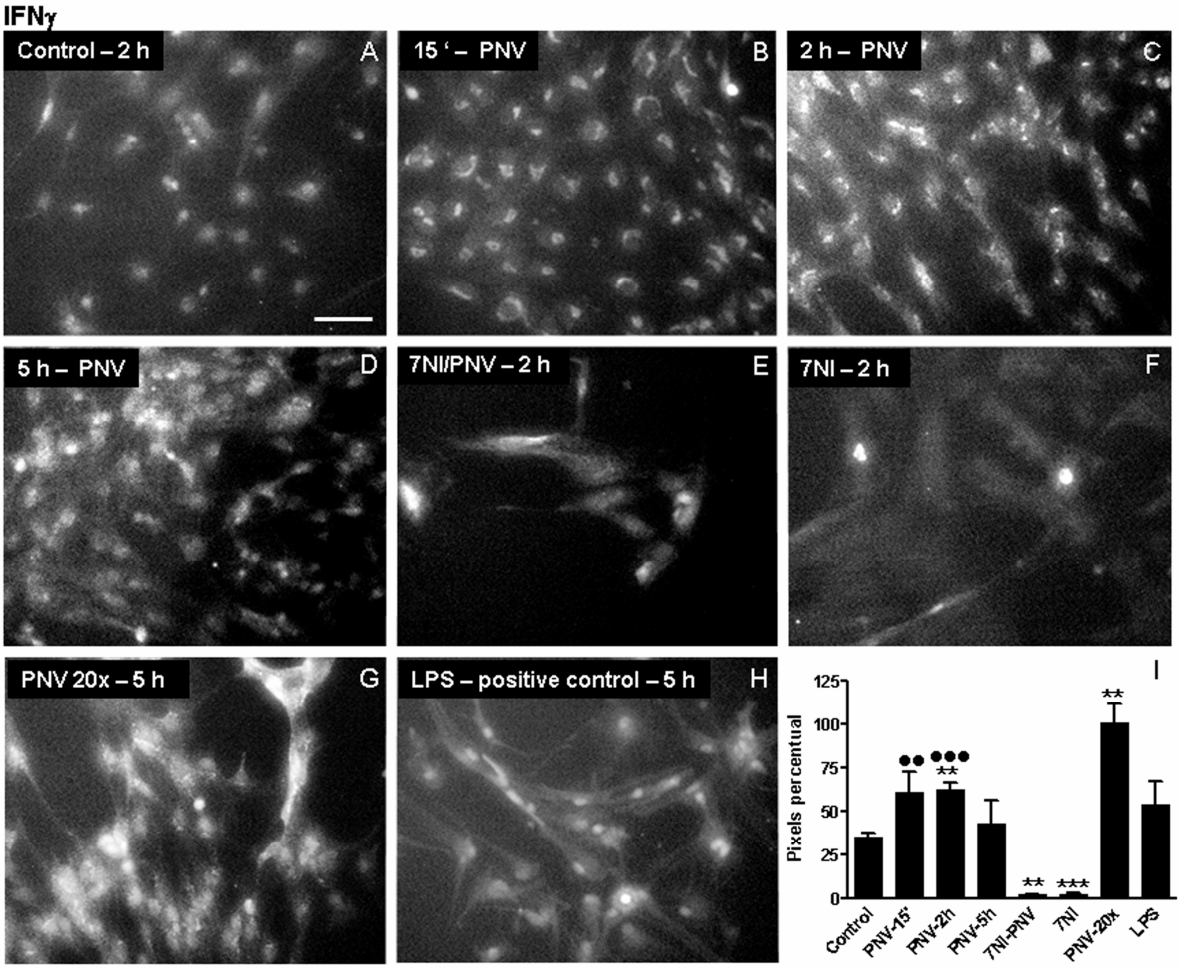
IFNγ
Control – 2 h
A
15 ' – PNV
B
2 h – PNV
C
5 h – PNV
D
7NI/PNV – 2 h
E
7NI – 2 h
F
PNV 20x – 5 h
G
LPS – positive control – 5 h
H
I
Pixels percentual
125
100
75
50
25
0
Control
PNV-15'
PNV-2h
PNV-5h
7NI-PNV
7NI
PNV-20x
LPS

Figure 3

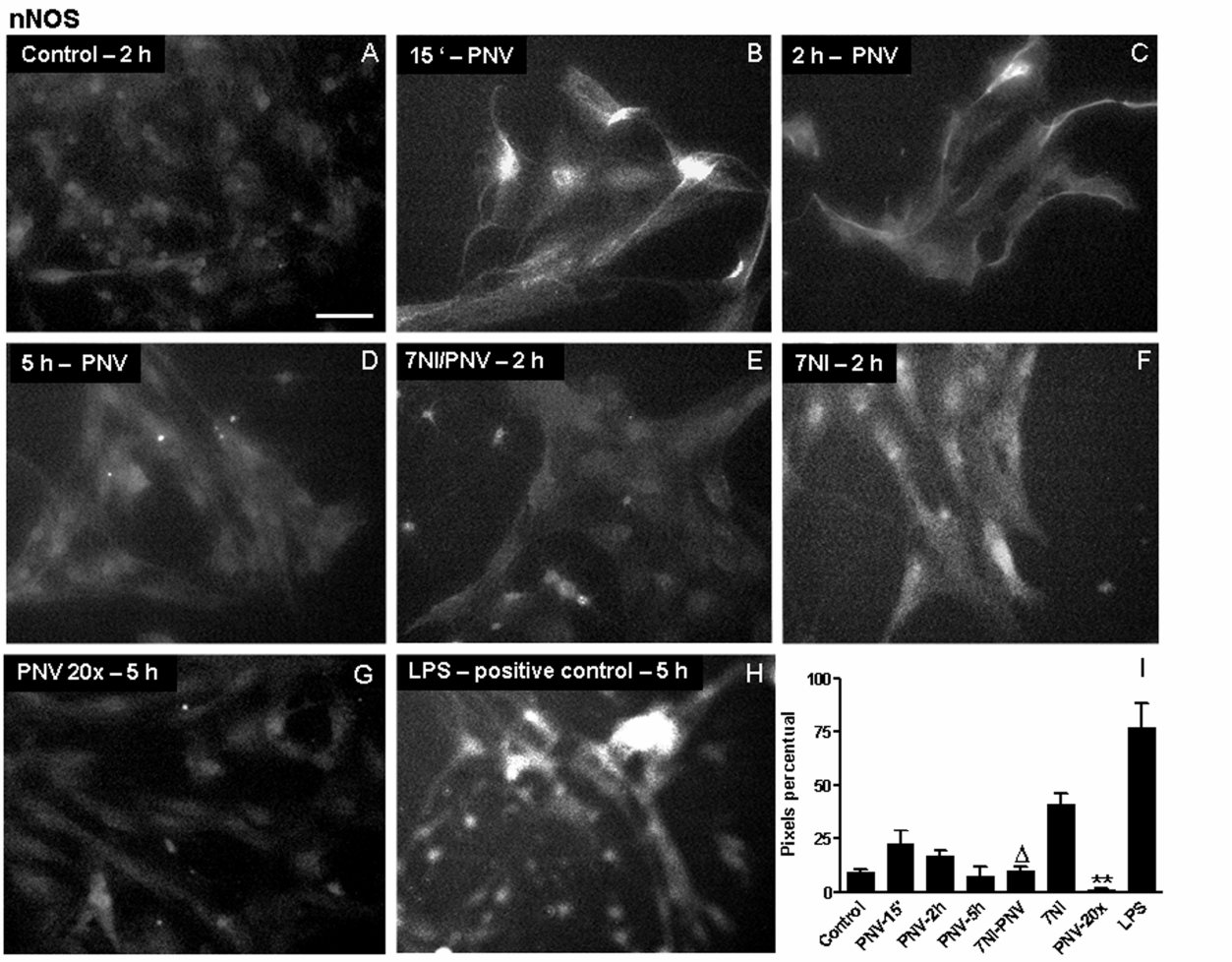
nNOS
Control – 2 h
A
15 ' – PNV
B
2 h – PNV
C
5 h – PNV
D
7NI/PNV – 2 h
E
7NI – 2 h
F
PNV 20x – 5 h
G
LPS – positive control – 5 h
H
I
Pixels percentual
100
75
50
25
0
Δ
**
Control
PNV-15'
PNV-2h
PNV-5h
7NI-PNV
7NI
PNV-20x
LPS

Figure 4

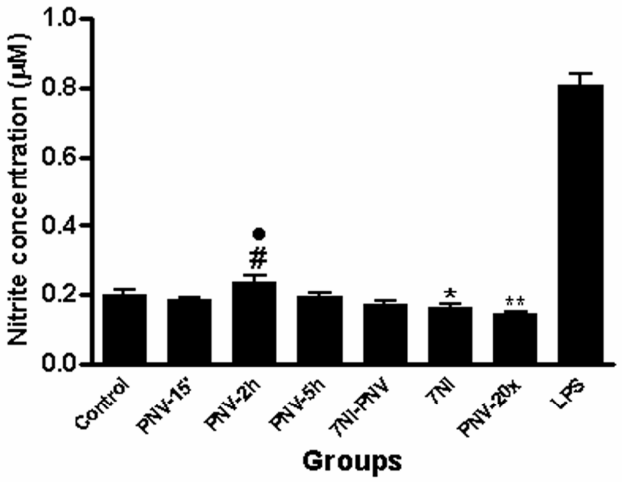
Nitrite concentration (µM)
1.0
0.8
0.6
0.4
0.2
0.0
●
#
*
**
Control
PNV-15'
PNV-2h
PNV-5h
7NI-PNV
7NI
PNV-20x
LPS
Groups

Figure 5

Purificação de toxinas do veneno de *P. nigriventer* e identificação de componentes responsáveis pela permeabilização da barreira hematoencefálica.

Rapôso C[1], Freddy I[2], Possani LD[2], Cruz-Höfling MA[1] *([1]Departamento de Histologia e Embriologia, Instituto de Biologia, Universidade Estadual de Campinas - UNICAMP, Campinas, SP, Brasil, [2]Institute of Biotechnology, National Autonomous University of México, Cuernavaca, México).*

Introdução

A aranha *Phoneutria nigriventer* (Ctenidae, Araneomorpha) é uma aranha brasileira, exptremamente agressiva, responsável pela maioria dos casos de envenenamento no Brasil. A observação dos sinais e sintomas (hiperemia, prostração, salivação, paralisia flácida e espástica dos membros posteriores, convulsão tônico-clônica, stress respiratório e morte) do envenenamento por *P. nigriventer* levaram a concluir que esse veneno é principalmente neurotóxico. Os efeitos neurotóxicos do veneno de *P. nigriventer* (PNV) atraíram a atenção de pesquisadores, uma vez que provavelmente o veneno teria alguma ação em alvos no sistema nervoso central (SNC). O PNV é um coquetel de toxinas (para revisão ver Gomez *et al*., 2002), portanto a purificação de toxinas e a identificação de seus efeitos podem ser úteis para aplicações médicas e em pesquisa.

Atualmente, vários peptídeos tóxicos têm sido isolados do PNV e seus efeitos biológicos têm sido testados. Diferentes peptídeos básicos agem em canais de Ca^{2+}, K^+ e Na^+, são capazes de provocar efeitos neurotóxicos excitatórios em mamíferos e insetos (Brazil & Vellard, 1925; Cruz-Höfling *et al*., 1985; Love & Cruz-Höfling, 1986), aumentam a permeabilidade vascular (Antunes et al. 1992) e a pressão arterial (Costa et al, 1996) e causam ereção peniana Nunes *et al*., 2008). Outros peptídeos modulam a liberação de neurotransmissores, tais como glutamato e acetilcolina (Oliveira *et al*., 2003, Gomez *et al*., 1995). Foi recentemente demonstrado que o PNV induz permeabilização da barreira hematoencefálica (BHE) (interface entre o sangue e o tecido neural, que restringe o acesso de moléculas ao tecido), quando administrado sistemicamente. A permeabilização da BHE ocorre em tempos precoces (1 e 2 horas) e tardios (24 h e 9 dias) após o envenenamento (Le Sueur *et al*., 2003; Rapôso *et al*., 2007).

A BHE é responsável pela manutenção do microambiente do SNC, protegendo-o contra toxinas e outros componentes presentes no sangue e transportando seletivamente os nutrientes. Portanto, um sistema altamente controlado de transportadores e receptores selecionam moléculas cuja passagem através do citoplasma das células endoteliais é permitida. Infelizmente, os mesmo mecanismos que protegem o tecido neural contra moléculas indesejadas, pode também frustrar

intervenções terapêuticas durante doenças do SNC, tais como tumores, epilepsia, doenças cerebrovasculares e desordens neurodegenerativas. O baixo sucesso terapêutico é principalmente devido à dificuldade no desenvolvimento de drogas que passem através da BHE e sejam disponibilizadas em quantidades suficientes ao tecido neural (para revisão, ver (Pathan *et al*., 2009).

Desde que o PNV é uma complexa mistura de peptídeos e outras classes de substâncias, e que o veneno bruto é capaz de permeabilizar temporariamente a BHE, houve o interesse em identificar toxinas purificadas, responsáveis por esse efeito nos microvasos cerebrais. A identificação de moléculas com ação conhecida na BHE pode determinar uma nova estratégia para disponibilizar drogas terapêuticas ao tecido neural. Portanto, a proposta deste estudo foi analizar toxinas isoladas do PNV, por HPLC, com o objetivo de identificar os componentes responsáveis pela permeabilização dos microvasos cerebrais. Um novo método de abertura temporária e controlada da BHE pode ser interessante para propostas terapêuticas e, além disso, moléculas ativas na BHE são potenciais ferramentas para uso em pesquisa.

Material e método

Animais e veneno

Ratos Wistar machos (*Rattus norvergicus*, 200–300 g, 8 a 10 semanas), obtidos do biotério central da UNICAMP, foram mantidos em temperatura controlada (25–28 °C), com ciclo de dia e noite de 12 horas e ração padrão (Purina), com livre acesso a água. O veneno bruto foi doado e purificado pelo professor Dr. Lourival Possani (Instituto de Biotecnologia, Universidade Nacional Autônoma do México, Cuernavaca, México), com a participação da Profa. Maria Alice da Cruz Höfling.

Procedimentos de purificação

O PNV liofilizado foi dissolvido em água e centrifugado a 10,000g por 10 min. A solução sobrenadante foi estocada à -20 ºC. As amostram foram separadas por Cromatografia Líquida de Alta Performance - HPLC (*high performance liquid chromatography* - Milford, MA, USA), em uma coluna analítica de fase reversa C18 (Vydac, Hisperia, CA), usando um gradiente linear de solvente A (0.12% ácido trifluoroacético, TFA, em água) a 60% de solvente B (0.10% TFA, em acetonitrila), com corrida por 60 min a velocidade de fluxo de 1 ml/min. Nessas condições, sete componentes foram obtidos na forma heterogênea (designados frações 1-7). Após, foram feitos ensaios para verificar quais dessas frações eram capazes de permeabilizar a BHE, fazendo-se injeção intra-vascular de corante vital Azul de Evans (ver abaixo detalhes do procedimento). A fração deteminada como capaz de romper a BHE foi submetida a uma segunda separação usando HPLC, e uma coluna analítica de fase reversa C18, correndo com gradientes ligeiramente

modificados, para melhorar a separação. O segundo procedimento de HPLC foi realizado usando a fração F1, a qual foi separada em 12 frações (chamadas F1-1 a F1-12). As frações F1-8 e F1-10 foram, então, submetidas novamente à purificação por HPLC, apenas para descartar os contaminantes e obter os picos principais.

Administração das toxinas purificadas do PNV

Para os estudos em microscopia de luz, com o corante vital Azul de Evans, um grupo de animais (n = 4 por fração) recebeu uma única injeção intravenosa (i.v.) das frações heterogêneas, purificadas no primeiro procedimento de HPLC (F1-F7) (12 μg/kg em 300 μl de salina estéril a 0.9%), na veia caudal, enquanto o grupo controle recebeu o mesmo volume do veículo. Após determinação da fração heterogênea ativa na BHE (F1), outro grupo de animais (n = 3 por fração) recebeu uma única injeção i.v. de cada componente de F1 (F1-1 a F1-12 – obtidos por purificação de F1) (12 μg/kg in 300 μl of 0.9% sterile saline), ou o mesmo volume de veículo. A dose escolhida foi baseada em estudo prévio (Nunes *et al*., 2008) com toxina purificada de *P. nigriventer*. Todos os grupos foram sacrificados 2 h após a injeção das frações ou do veículo. Após determinação das frações homogêneas ativas na BHE (F1-8 e F1-12), um grupo (n = 3 por fração) recebeu uma única injeção na veia caudal de uma ou outra fração (12 μg/kg em 300 μl de salina estéril a 0.9%), ou o mesmo volume do veículo, para análise de cortes semi-finos e ultrafinos, em microscópio de luz e eletrônico de transmissão, respectivamente. Para análise de cortes semi-finos e ultrafinos, os animais foram sacrificados 2 e 5 h após a injeção das frações ou do veículo. O protocolo experimental foi aprovado pelo Comitê de Ética em Experimentação Animal da UNICAMP (protocolo 1700-1).

Atividade das toxinas na BHE – Azul de Evans (AE)

Azul de Evans (0.2 ml; 2%) (Sigma) foi administrado através da veia caudal, 1,5 h após a injeção das toxinas (F1 a F7)do PNV ou de solução salina (veículo). Os animais anestesisados com combinação de xilasina e ketamina sofreram punção cardíaca e foram perfundidos através da artéria aorta, com paraformaldeído 4%, em tampão fosfato 0.1 M, 30 minutos após a administração do AE. Os cérebros foram removidos e pós-fixados por 2 h no mesmo fixador. Secções coronais (50 μm) foram cortadas em criostato. Regiões de extravasamento do AE nas secções foram observadas com microscópio de luz (Olympus, Nikon, Japan).

Estudo morfológico

Para confirmar se as frações (F1-8 e F1-10) induzem a quebra da BHE em estágios precoces, os ratos foram anestesiados 2 e 5 h após a injeção das frações ou salina e imediatamente sacrificados por perfusão através da artéria aorta, com 150 ml de solução pré-fixadora (100 mM de Tris, pH 7.2, 150 mM de NaCl, 5.6 mM de KCl, 1 mM de MgCl2, 2.5 mM de $CaCl_2$, 3.7 mM de glicose e 3.6 mM de procaina), seguida por 250 ml de fixador [2.5% de glutaraldeído e 0.5% paraformaldeído em 0.1 M de tampão cacodilato de sódio, pH 7.2, contendo 2% de nitrato de lantano (La_2NO_3)], com um marcador extracelular, usando bomba peristáltica. A pressão de perfusão foi monitorada com um manômetro de mercúrio e não excedeu 70 mmHg. Após a perfusão, os ratos foram mantidos à 4º C, *overnight* (18 h) antes da dissecação dos cérebros. Hipocampo e cerebelo foram removidos e amostras de 1 a 2 mm foram mantidas no mesmo fixador sem nitrato de lantano, *overnight*. As amostras do cerebelo incluíram tanto substância branca, quanto cinzenta e as do hipocampo incluíram todas as subregiões, escolhidas aleatoriamente. Após as amostras serem lavadas em solução de lavagem (0.15 M de NaCl, com 0.2 M de sacarose), foram pós-fixadas em 1% de OsO4, diluído em cacodilato de sódio 0.1 M, por 1 h, desidratadas em gradiente de acetona e embebidas em resina Epon 812. Para análise em microscópio de luz, secções semifinas (1 μm de espessura) foram cortadas em ultramicrótomo (Reichert S Ultra-Cut, Leica) e coradas com 1 % de azul de toluidina.

Obs.: *O material para análise de cortes semifinos (microscopia de luz) e ultrafinos (microscopia eletrônica de transmissão) foi coletado e processado. Os primeiros cortes semifinos foram obtidos (ver figura 3) e estão em análise. Estudos ao microscópio de luz e eletrônico de transmissão estão em andamento com o objetivo de quantificar e qualificar a ação dessas frações na permeabilidade da BHE.*

Resultados (apresentados na forma de legendas das figuras)

Figura 1: *Perfil cromatográfico* – (A) perfil cromatográfico obtido após a separação do veneno solúvel de *P. nigriventer*, por HPLC, com corrida em coluna analítica de fase reversa C18, do solvente A (0.12% de TFA em água), para 60% do solvente B (0.10 TFA em acetonitrila), durante 60 min com velocidade de fluxo de 1 ml/min. As marcações F1-F7, na base do gráfico, indicam os componentes eluídos e coletados. (*Tabela*) O componente ativo na BHE (F1) foi futuramente separado usando a mesma coluna, mas correndo de 10% para 45% de solvente B, por 20 min. Após o procedimento, foram obtidas as frações F1-1 a F1-12. (B) Os picos de eluição 2.99 (F1-8) e 3.91 (F1-10) foram submetidos a nova purificação, na mesma coluna, usando concentração constante de

20% do solvente B, com corrida por 20 min, para descartar contaminantes. RT ("retention time") - media do tempo de retenção do HPLC.

Figura 2: *Análise do extravasamento do corante Azul de Evans*: Os vasos com alterações na permeabilização foram avaliados pela injeção *in vivo* do corante vital azul de Evans e análise ao microscópio de luz. Nos animais do grupo controle (injetados com solução salina) não foram encontradas regiões com extravasamento do corante (A, B). Apenas a subfração F1 promoveu o extravasamento do corante (C-E). Também foi visto extravasamento nas frações F1-8 e F1-10, re-purificadas a partir de F1 (não demonstrado).

Figura 3: *Secções semifinas coradas com azul de toluidina*: (A e B) Hipocampo de animal controle, sacrificado 2 h após a injeção i.v. de solução salina. (C e D) Hipocampo de animal tratado com fração F1-10 e sacrificado 2 h após a injeção i.v. da fração. Note que os vasos sangüíneos de C e D (setas) apresentam espaço perivascular edemaciado, indicativo de edema vasogênco, enquanto o tecido perivascular de A e B (cabeça de seta) está íntegro, sem as áreas edemaciadas, vistas em C e D. Essa alteração indica passagem de moléculas, as quais são acompanhadas por líquido (plasma), através da BHE. A passagem de líquido para o tecido está ocorrendo devido a alterações na permeabilidade dos microvasos cerebrais, causadas pela toxina.

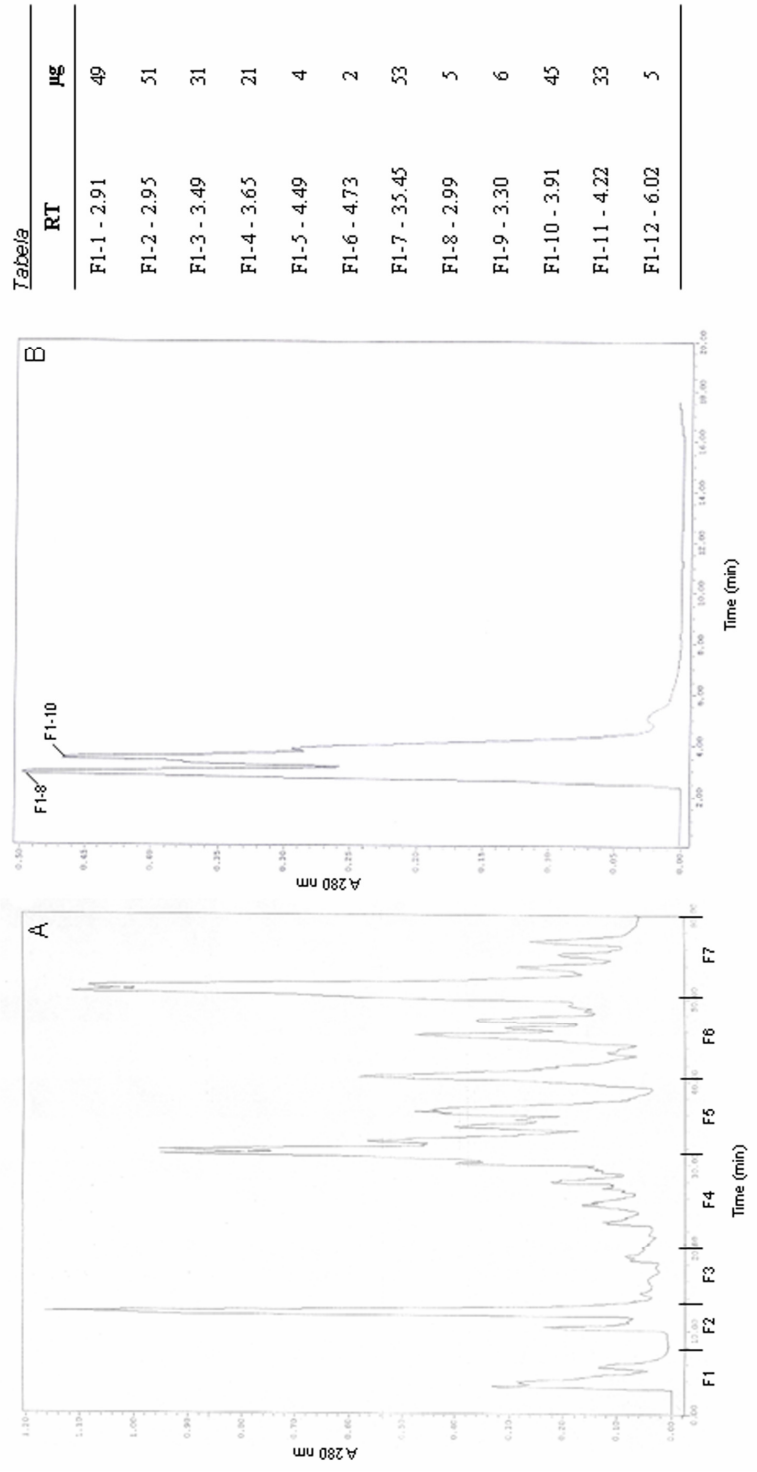

Tabela

RT	µg
F1-1 - 2.91	49
F1-2 - 2.95	51
F1-3 - 3.49	31
F1-4 - 3.65	21
F1-5 - 4.49	4
F1-6 - 4.73	2
F1-7 - 35.45	53
F1-8 - 2.99	5
F1-9 - 3.30	6
F1-10 - 3.91	45
F1-11 - 4.22	33
F1-12 - 6.02	5

Figura 1

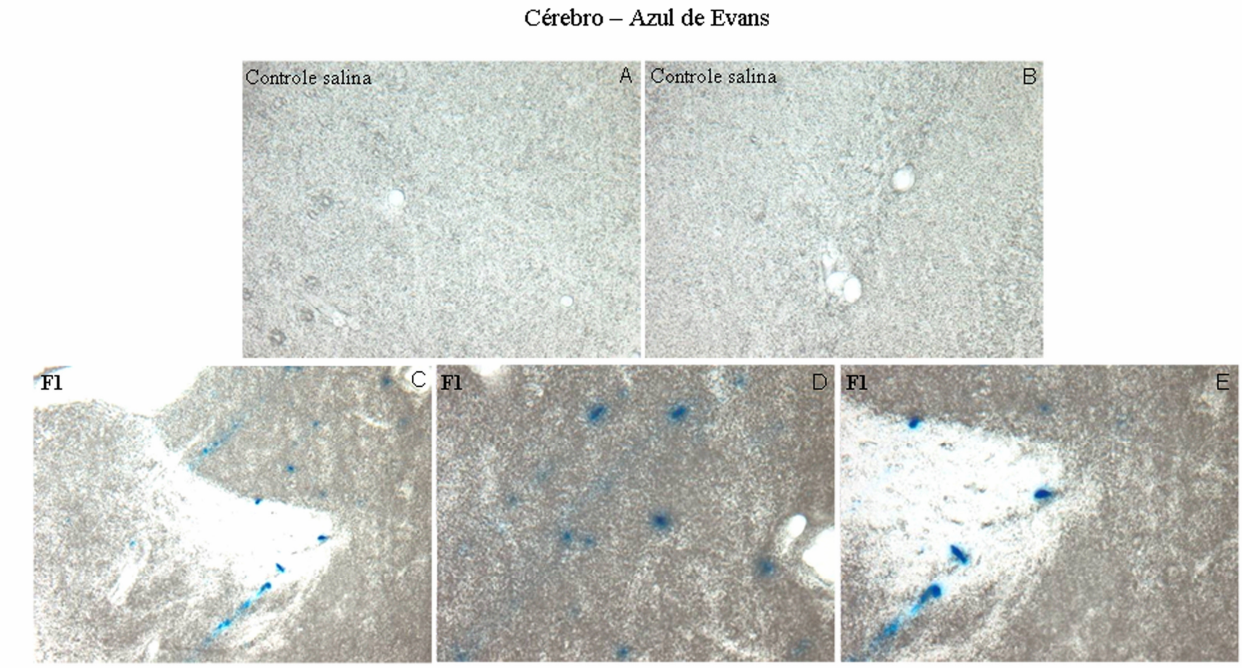
Cérebro – Azul de Evans
Controle salina
A
Controle salina
B
F1
C
F1
D
F1
E

Figura 2

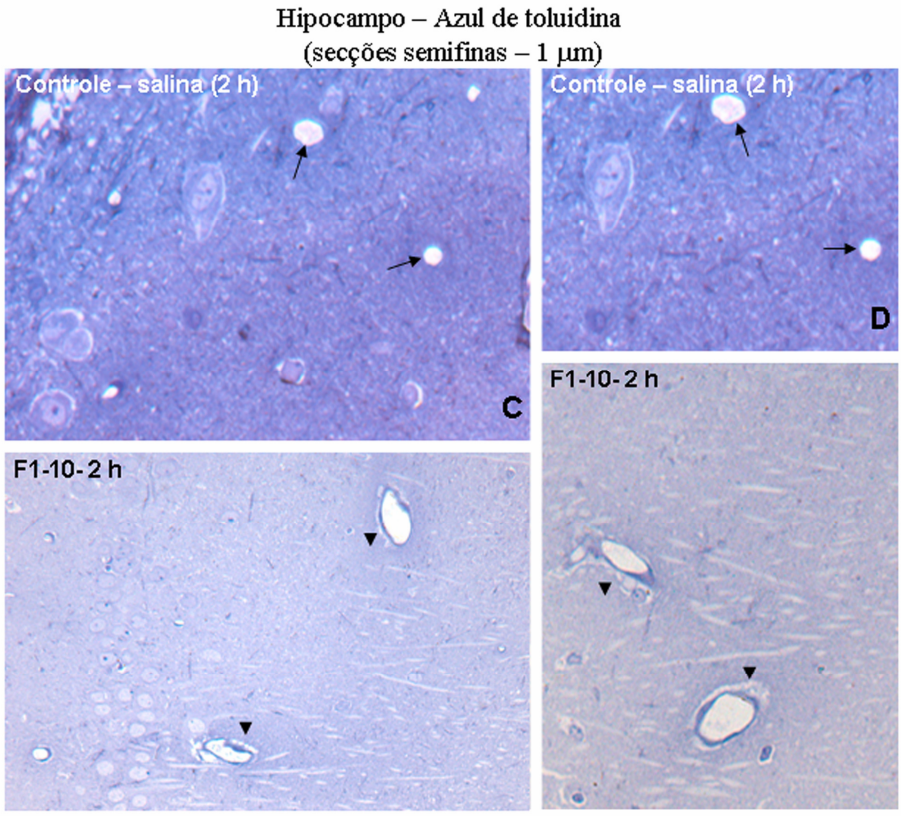
Hipocampo – Azul de toluidina
(secções semifinas – 1 μm)
Controle – salina (2 h)
C
Controle – salina (2 h)
D
F1-10-2 h
F1-10-2 h

Figura 3

Referências

Brazil V., Vellard J. Contribuição ao estudo do veneno das aranhas. *Mem Inst Butantan* (1925) **2**:5-77.

Costa S.K., Moreno H. Jr,, Brain S.D., De Nucci G., Antunes E. The effect of *Phoneutria nigriventer* (armed spider) venom on arterial blood pressure of anaesthetised rats. *Eur. J. Pharmacol*. (1996) **298:**113-120.

Cruz-Höfling M.A., Love S., Brook G., Duchen L.W. Effects of *Phoneutria nigriventer* spider venom on mouse peripheral nerve. *Q J Exp Physiol* (1985) **70**:623-640.

Gomez R.S., Casali T.A., Romano-Silva M.A., Cordeiro M.N., Diniz C.R., Moraes-Santos T., Prado M.A:, Gomez M.V. The effect of PhTx3 on the release of 3H-acetylcholine induced by tityustoxin and potassium in brain cortical slices and myenteric plexus. *Nuerosci Lett* (1995) **196**:131-133.

Gomez M.V., Kalapothakis E., Guatimosim C., Prado M.A. *Phoneutria nigriventer* venom: a cocktail of toxins that affect ion channels. *Cell Mol Neurobiol* (2002) **22**:579–588.

Le Sueur L., Kalapothakis E., Cruz-Höfling M.A. Breakdown of the blood-brain barrier and neuropathological changes induced by *Phoneutria nigriventer* spider venom. *ActaNeuropathol (Berl)* (2003) **105**:25-134.

Love S., Cruz-Hofling M.A. Acute swelling of nodes of Ranvier caused by venoms which slow inactivation of sodium channels. *Acta Neuropathol* (1986) **70**:1-9.

Nunes K.P., Costa-Gonçalves A., Lanza L.F., Cortes S.F., Cordeiro M.N., Richardson M., Pimenta A.M., Webb Rc., Leite R., De Lima M.E. Tx2-6 toxin of the *Phoneutria nigriventer* spider potentiates rat erectile function. *Toxicon* (2008) **51**:1197-1206.

Oliveira L.C., De Lima M.E., Pimenta A.M., Mansuelle P., Rochat H., Cordeiro M.N., Richardson M., Figueiredo S.G. PnTx4-3, a new insect toxin from Phoneutria nigriventer venom elicits the glutamate uptake inhibition exhibited by PhTx4 toxic fraction. *Toxicon* (2003) **42**:793-800.

Pathan S.A., Iqbal Z., Zaidi S.M., Talegaonkar S., Vohra D., Jain G.K., Azeem A., Jain N., Lalani J.R., Khar R.K., Ahmad F.J.CNS drug delivery systems: novel approaches. *Recent Pat Drug Deliv Formul* (2009) **3**:71-89.

Rapôso, C., Zago, G.M., Silva, G.H., Cruz-Höfling, M.A. Acute blood-brain barrier permeabilization in rats after systemic *Phoneutria nigriventer* venom. *Brain Res* (2007) **1149**:18-29.

DISCUSSÃO GERAL

A presente tese teve por objetivo avaliar a ação do veneno da aranha *Phoneturia nigriventer* (PNV), uma rica mistura de peptídeos neurotóxicos, na barreira hematoencefálica (BHE) e no tecido neural de ratos. O trabalho foi dividido em: **I) Estudo da ação do PNV na BHE – a)** análise da reatividade, através de imunofluorescência e/ou do conteúdo através de western blotting, de proteínas presentes nas junções de oclusão (ZO1, ocludina e claudina-5), de adesão (β-catenina), membrana basal (laminina), proteína de efluxo da BHE (Pgp) e proteína fosfatase 2A na sua forma fosforilada (pPP2A), no hipocampo e cerebelo, 15 min, 2 e 5 h após o envenenamento; **b)** análise, através de imunofluorescência e western blotting, da proteína de resistência multidrogas – MRP1, da proteína transportadora de glicose – GLUT1 e da proteína constituinte das junções *gap*, conexina-43 (Cx43), no hipocampo e cerebelo, 15 min, 2 e 5 h após o envenenamento. **II) Estudo da ação do PNV no tecido neural, observando a ativação de vias neuronais específicas, a reação de astrócitos em cultura e o envolvimento do óxido nítrico (NO) – a)** análise da ativação de regiões cerebrais específicas (córtex parietal motor - PMC, substância cinzenta periaquedutal partes ventral e dorso-lateral – vPAG e dlPAG, núcleo talâmico periventricular - PTN, núcleo supraóptico - SON e núcleo hipotalâmico paraventricular - PVN) pelo PNV, através da imunohistoquímica para proteína FOS. O envolvimento do NO na ativação dessas vias foi investigado tanto através do bloqueio da nNOS (enzima produtora do NO) pela injeção intraperitoneal de 7-nitroindazole antes da injeção sistêmica do PNV, como pela identificação de neurônios positivos para nNOS através de histoquímica para NADPH-d. Foi feita também dupla marcação FOS/NADPH-d, para identificar neurônios FOS e nNOS-positivos. As células com marcação simples para FOS ou NADPH-d ou co-marcadas para FOS/NADPHd foram contadas nas diferentes regiões cerebrais; **b)** análise da expressão da proteína presente nos filamentos intermediários do citoesqueleto de astrócitos, GFAP, cujo aumento indica gliose reativa, das citocinas mediadoras de processos inflamatórios, IFN-γ e TNF-α, e da isoforma neuronal da enzima produtora de NO, nNOS, em astrócitos cultivados, após exposição ao PNV, associado ou não ao 7-nitroindazol. **III) Estudo da permeabilização da BHE por frações purificadas do PNV** por HPLC, através da injeção do corante vital Azul de Evans e da análise de cortes semifinos (1 μm de espessura).

Os sinais clínicos observados nos acidentes provocados pela aranha *P. nigriventer*, bem como no envenenamento experimental (hipertensão, tremores, espasmos, sialorréia, paralisia flácida, paralisia espástica, convulsão, diminuição do volume urinário, edema pulmonar e, eventualmente, morte), apontavam os sistemas nervoso central e periférico como alvos das toxinas presentes no PNV. Esse fato motivou a investigação da ação tóxica do veneno no tecido neural e na

BHE. A necessidade de investigar as proteínas das JAs e JOs partiu dos resultados encontrados por Le Sueur *et al.* (2004), que sugeriam que o aumento da permeabilidade da BHE observado após 1 e 9 dias da administração i.v. do veneno não estava associado à diminuição na expressão e alteração da localização de proteínas das JAs e JOs, nem com o aumento na fosforilação de resíduos de tirosina. Entretanto, nós demonstramos recentemente que a injeção i.v. de PNV causa edema vasogênico, edema nos pés-astrocitários perivasculares e permeabilização da BHE em ratos adultos, particularmente no hipocampo, durante estágios agudos após a injeção do veneno (15 min, 1, 2 e 5 h) (Rapôso et al., 2007). Os mecanismos pelos quais a BHE é alterada em períodos precoces permaneciam obscuros. Com base nesses achados, nós hipotetizamos que, em períodos precoces após o envenenamento, as JAs e JOs, bem como a membrana basal poderiam ser afetadas. No presente trabalho, nossos dados mostraram que, de fato, ocorre significante diminuição na expressão das proteínas ZO1, ocludina, β-catenina e laminina e aumento na pPP2A, no hipocampo e cerebelo, nos períodos de 15 min e 2 h após a injeção de PNV, quando comparado com os controles sham. Além disso, embora as bandas do western blotting não tenham mostrado alteração significativa nos níveis teciduais da claudina-5, a imunofluorescência revelou uma diminuição sutil na sua reatividade no cerebelo, e alteração na sua localização, no hipocampo. Os dados mostraram recuperação total ou parcial das proteínas após 5 h, sendo mais significativa no cerebelo do que no hipocampo. Uma vez que a recuperação da expressão das proteínas das JOs e JAs e da laminina coincide com o início dos sinais de recuperação clínica dos animais envenenados (após 5 h os animais recuperam parcialmente a capacidade motora e exploratória, a função respiratória e ocorre normalização do fluxo salivar e hiperemia), nós sugerimos que os sinais clínicos de acometimento do SNC estariam relacionados à permeabilização da BHE em período agudos, provavelmente pela alteração da via paracelular. Concluímos que o veneno da aranha armadeira pode afetar tanto o transporte transcelular como o paracelular na interface sangue:cérebro.

Em relação à imunomarcação para Pgp, a imunofluorescência mostrou um declínio na expressão dessa proteína 15 min e 2 h após a injeção do PNV, com recuperação após 5 h, comparando com o controle. No hipocampo, a expressão após 5 h foi maior que a vista nos animais controle. A presença de transportadores de efluxo na membrana das células endoteliais e dos astrócitos adjacentes é uma das propriedades fisiológicas que fazem com que o endotélio dos microvasos cerebais seja diferente daqueles da periferia. Esses transportadores removem substratos (p.e. drogas e toxinas), antes que atinjam o microambiente neural. A expressão diminuída da Pgp 15 min e 2 h após a injeção do PNV apontam-na como alvo do veneno e pode ser um dos mecanismos que contribuem para a maior passagem de moléculas, inclusive citocinas exógenas, através da BHE nos animais envenenados. Por outro lado, o aumento da Pgp 5 h após a injeção do

PNV dá suporte à idéia de que o mecanismo direcionado para remover o agente tóxico do cérebro para a microcirculação foi desencadeado.

Nossos resultados mostraram, ainda, aumento no conteúdo da fosfatase 2A fosforilada (pPP2A), 15 min e 2 h após injeção do PNV, concomitantemente à diminuição da expressão das proteínas das JOs e JAs. Fosforilação da PP2A ocorre quando as proteínas de junção são hiperfosforiladas e, consequentemente, os contatos juncionais interendoteliais estão afetados. Portanto, a hipótese inicial de que o PNV altera a expressão das proteínas das JOs e JAs em períodos agudos após a injeção sistêmica do PNV foi confirmada. Isso explica, ao menos em parte, o início precoce dos sinais clínicos da intoxicação. Tais alterações ocorrem provavelmente por hiperfosforilação das proteínas juncionais. Essas alterações são muito rápidas e dinâmicas e caracterizam uma abertura juncional transitória.

Outro ponto abordado no sentido de avançar no conhecimento dos mecanismos moleculares de abertura da barreira pelo PNV foi a determinação da expressão de outras proteínas (MRP1, GLUT1 e Cx43) associadas com a função da BHE. A sugestão de que essas proteínas seriam alvos do PNV foi baseada no papel crítico que elas exercem no funcionamento da BHE. Nossos dados mostraram que a presença do PNV na circulação foi capaz de afetar as proteínas estudadas (MRP1, GLUT1 e Cx43). Houve maior conteúdo basal de MRP1 e GLUT1 no cerebelo do que no hipocampo; o cerebelo também mostrou menor variabilidade no nível das proteínas nos grupos tratados com PNV, durante os períodos examinados. Esses dados corroboram com estudos prévios mostrando que o hipocampo é mais suscetível ao PNV, com permeabilização mais evidente da BHE, enquanto o cerebelo ficou inalterado, pelo menos nos tempos mais tardios do envenenamento (Le Sueur et al., 2004), ou sua recuperação foi mais rápida (Rapôso *et al*., 2007). Em suporte à verificação de que o cerebelo é mais resistente à ação deletéria do PNV, estão os resultados mostrados também pelas proteínas das JOs e JAs, que no cerebelo mostraram recuperação mais significativa do que no hipocampo. O hipocampo apresentou, de fato, maior sensibilidade ao PNV, como visto pelo aumento mais significante nos níveis das proteínas estudadas (MRP1 e GLUT1). A alta expressão de MRP1 e GLUT1 entre 2 e 5 h após o envenenamento pode representar uma reação adaptativa do organismo dos animais para prevenir a entrada das toxinas do PNV no cérebro (MRP1), e para facilitar a entrada de glicose, permitindo o aumento no metabolismo, induzido pelo estresse do animal e/ou pela ação farmacológica do veneno (GLUT1). Os presentes resultados suportam estudos prévios que mostram que as alterações na função da BHE causadas pelo PNV resultam principalmente de alterações no transporte transcelular (Le Sueur *et al*., 2004), desde que foi demonstrado aqui que tanto o influxo transcelular (de glicose) quanto o efluxo (de toxinas do veneno) foram afetados na interface sangue-cérebro.

Os resultados mostraram, ainda, duas fases de reatividade da Cx43, caracterizadas por significante aumento visto após 15 minutos da exposição ao veneno, tanto no hipocampo quanto no cerebelo, seguida por significante diminuição no hipocampo, e uma tendência à diminuição no cerebelo. A Cx43 é a principal proteína presente nas junções gap (JG), e em particular nas JG do SNC. As JG são responsáveis por estabelecer uma rede de comunicação entre astrócitos, a célula glial em maior número e com a mais ampla gama de ações no SNC. As JG permitem comunicação entre astrócitos, os quais controlam o microambiente, bem como mantêm o fenótipo de barreira do endotélio cerebral. Os dados indicam que o PNV sistêmico afeta a estabilidade das junções comunicantes (*gap*) e, consequentemente, as interações entre astrócitos, provavelmente um dos mecanismos causadores do aumento da permeabilidade da BHE induzido pelo PNV.

Portanto, os resultados até o momento relatados mostram que o veneno da aranha *P. nigriventer* promove abertura transitória da BHE, cujas proteínas se recuperam total ou parcialmente 5 h após a injeção do veneno (Le Sueur *et al.*, 2003, Rapôso *et al*., 2007). A inibição da proteína de efluxo Pgp, o aumento da MRP1 nos períodos de 15 min e 2 h pelo veneno, associada à manutenção de transportadores de glicose, podem fornecer boas perspectivas para o uso de componente do veneno para a abertura temporária da BHE, com fins terapêuticos. A identificação de substâncias que regulam a permeabilidade do endotélio cerebral pode levar ao desenvolvimento de estratégias terapêuticas para superar o acesso restrito de drogas ao cérebro.

Uma vez que o PNV altera de maneira rápida as principais estruturas da BHE e, consequentemente, sua permeabilidade, e que causa sinais clínicos que indicam o acometimento do SNC, nós lançamos a hipótese de que o veneno teria ação no tecido neural, tanto na ativação de neurônios, quanto na indução de resposta astrocitária. Estudos recentes, com o mesmo desenho experimental utilizado para a investigação da BHE, mostraram que 2 h após a administração do PNV, neurônios de várias áreas relacionadas com motricidade/aversão/ansiedade/fuga (PCM, vPAG dlPAG e PTN), e estresse agudo (córtex rinal - RC e o núcleo septal lateral - LSN) exibiram ativação, como mostrado pelo aumento da expressão da proteína FOS (Cruz-Höfling *et al*., 2007). Além disso, neurônios positivos para a sintase neuronal do óxido nítrico (nNOS) predominaram no PTN, seguido por dlPAG e PCM, indicando que o NO é um mensageiro que pode estar envolvido no mecanismo da intoxicação pelo veneno (Cruz-Höfling *et al.,* 2007). Com o objetivo de aprofundar o entendimento sobre o possível papel do NO na intoxicação pelo PNV, estudos *in vivo* e *in vitro* foram realizados. A nNOS foi bloqueada seletivamente pelo 7-Nitroindazol (7NI), antes da injeção i.v. do PNV (estudo *in vivo*) ou antes da exposição de astrócitos em cultura primária (isolados do córtex de ratos Wistar neonatos) ao veneno (estudo *in vitro*). No estudo *in vivo*, foi investigada a ativação de neurônios, através de imunohistoquímica para proteína FOS, e a co-

localização da FOS com a NADPH diaforase (histoquímica). No estudo *in vitro*, GFAP, nNOS e as citocinas inflamatórias TNF-α e IFN-γ foram quantificadas por imunohistoquímica, para avaliar a gliose, a expressão da sintase do NO e a resposta inflamatória dos astrócitos. Além disso, a liberação de nitrito no meio de cultura foi quantificada como uma medida indireta da liberação de NO.

No estudo *in vivo*, os animais injetados com 7NI/PNV apresentaram alguns sinais, tais como prostração, hipersalivação e paralisia espástica dos membros posteriores, mais precoces e mais intensos do que nos animais injetados somente com PNV. Isso sugere que a ausência do NO agravou o quadro clínico de envenenamento e que, portanto, o NO apresenta um papel neuroprotetor, no caso. Comparado ao grupo controle injetado com solução salina, o grupo que recebeu PNV aumentou significantemente o número de neurônios FOS-positivos em todas as áreas investigadas, exceto no PTN; o número de neurônios positivos para NADPH-d aumentou na vPAG e no PVN. Comparado ao grupo injetado com veneno, o grupo que recebeu 7NI antes da injeção do mesmo teve menor número de neurônios positivos para FOS em todas as áreas examinadas, exceto no SON, onde esse número foi aumentado; neurônios NADHP-d positivos aumentaram em número somente na dlPAG. O número de neurônios duplamente marcados aumentou no PVN e no SON dos animais tratados com PNV, em relação aos animais controle salina e diminuiu nos animais tratados com 7NI mais PNV comparado com o PNV sozinho, somente no PVN. Esses dados indicam que ocorre ativação em áreas do cérebro relacionadas tanto com motricidade/aversão/ansiedade/fuga (PMC, vPAG, dlPAG), corroborando com os sinais clínicos vistos no envenenamento (paralisia flácida e espástica, tremores, espasmos, convulsão), quanto em áreas relacionadas com funções neurovegetativas (SON e PVN), o que também está de acordo com os sinais vistos no envenenamento (estresse respiratório, edema pulmonar, salivação intensa, hipertensão, diminuição do volume urinário). Outro dado importante do estudo *in vivo* é que, de fato, a inibição do NO interferiu na ativação de neurônios e na dupla marcação de neurônios FOS e NADPH-d positivos, indicando que esse gás tem papel na ação do veneno, tanto em áreas relacionadas a reações motoras, de ansiedade, aversão e fuga, quanto em áreas relacionadas às funções neurovegetativas. Os resultados demonstram também que a despeito da clara participação do NO na atenuação dos efeitos tóxicos do veneno (avaliados clinicamente), a diferença entre áreas do cérebro, ora mostrando ativação, ora diminuição da ativação neuronal, sugere a complexidade do processo e aponta um papel duplo ao NO, ora atenuando, ora potenciando a ativação neuronal.

O estudo *in vitro* com cultura de astrócitos demonstrou que ocorre aumento significativo da expressão de GFAP, TNF-α e IFN-γ após exposição ao PNV. Os estudos *in vitro* são interessantes quando se quer excluir interdependências nos mecanismos acionados no sistema vivo. O presente

estudo teve por objetivo comprovar a ação do PNV numa população isolada de astrócitos corticais e assim determinar se essa ação podia ser direta ou decorrente de segundos mensageiros desencadeados pelo envenenamento. Os resultados obtidos não excluem a existência dos segundos mensageiros, mas demonstra que o PNV pode ter ação direta concomitante. O tratamento com 7NI, antes do PNV, reduziu significativamente a expressão de GFAP, TNF-α e IFN-γ. Esses resultados apontam os astrócitos como mediadores da neuroinflamação desencadeada pelo PNV e o NO como um modulador da gliose e da resposta inflamatória induzidas pelo veneno. Esses dados complementam o estudo realizado paralelamente aos objetivos centrais da presente tese (Cruz-Höfling *et al.*, 2009), apresentado no *Apêndice*, o qual revelou que houve ativação de astrócitos e processo inflamatório *in vivo*, como mostrado pelas alterações na expressão da GFAP, S100, IFN-γ e TNF-α, após injeção i.v. do PNV. Porém, não estava claro se os astrócitos eram mediadores da inflamação e se o NO estava envolvido nesse processo. Ao considerarmos que o veneno aumentou significativamente o nível da proteína das junções comunicantes (Cx-43) rapidamente após a administração do PNV (15 min) (Odorissi et al., submetido) podemos inferir que a imediata gliose vista tanto *in vivo* quanto *in vitro* foi decorrência de rápido aumento de transferência de informações astrócito-astrócito. Por outro lado, a diminuição da expressãoda Cx-43 vista 5 h após o PNV, pode ser, a nosso entender, medida de proteção contra a liberação de neurotransmissores excitatórios pelos astrócitos ou contra peptídeos excitatórios do veneno.

Portanto, o PNV causa ativação de neurônios de áreas do cérebro relacionadas com motricidade/aversão/ansiedade/fuga e com funções neurovegetativas e o NO age modulando essa resposta. O NO também está envolvido na ativação e resposta inflamatória dos astrócitos. A riqueza de neurotoxinas presentes no PNV elege esse veneno como uma potente ferramenta para investigação de processos fisiopatológicos do SNC. Esses modelos, tanto *in vitro*, quanto *in vivo*, são úteis para o estudo da ativação de vias neuronais, reação inflamatória e gliose no cérebro. Além disso, o estudo do papel do NO pode contribuir para o entendimento dos mecanismos de envenenamento pelo PNV, bem como ser útil para o desenvolvimento de propostas terapêuticas.

Como último objetivo do presente trabalho, desde que o PNV é uma complexa mistura de peptídeos e outras classes de substâncias, e que o veneno bruto é capaz de permeabilizar temporariamente a BHE, o PNV foi purificado e as toxinas denominadas F1-8 e F1-10 apresentaram efeito em permeabilizar a BHE, 2 h após a injeção i.v.. Esta parte do trabalho ainda prosseguirá com estudos ao microscópio eletrônico de transmissão. A identificação de moléculas com ação conhecida na BHE pode determinar uma nova estratégia para disponibilizar drogas terapêuticas ao tecido neural.

RESUMO DOS RESULTADOS E CONCLUSÕES

1. A) A hipótese inicial de que o veneno de P. nigriventer altera a expressão de proteínas das junções de adesão e oclusão em períodos precoces após a injeção sistêmica foi confirmada. O mecanimo envolvido na alteração das proteínas juncionais decorreu aparentemente pela fosforilação de resíduos de treonina das proteínas. Essas alterações são muito rápidas e dinâmicas e caracterizam uma abertura juncional transitória e auto-limitante. É possível que esse mecanismo seja responsável pela abertura inicial e mais intensa da BHE, gerando alguns dos sinais clínicos que apontam envolvimento do SNC através de vias neuronais que ainda necessitam ser identificadas.

B) A Pgp é alvo do PNV em períodos precoces após o envenenamento, indicando que pode haver seletividade na ativação do tipo de transportador de efluxo em decorrência do tipo de agente tóxico. Nós sugerimos que o PNV pode promover uma permeabilização transitória da BHE e a identificação das toxinas purificadas, responsáveis por esse efeito, poderá contribuir para o desenvolvimento de novas estratégias para disponibilizar drogas terapêuticas ao tecido neural central.

2. A expressão aumentada da MRP1 e GLUT1 e a diminuição da Cx43 nos animais envenenados coincidem com o início da regressão dos sinais clínicos da intoxicação. Os resultados sugerem que ocorre a remoção (clearance) ao menos dos componentes mais leves do veneno do SNC e que pode estar ocorrendo a diminuição das interações entre astrócitos-astrócitos, astrócitos-neurônios e astrócitos-células endoteliais. Nossa hipótese é que a inibição das comunicações (diminuição do nível de expressão da Cx43) representa um mecanismo protetor desencadeado pelo organismo.
O conjunto dos dados reflete comprometimento da homeostase do SNC provocada pela permeabilização da BHE, devido à ação de neurotoxinas presentes no PNV. Os dados mostrando aumento nos níveis de expressão de GLUT-1 são um indicativo de reação do organismo, aumentando a disponibilidade desse combustível no cérebro em reação à presença do agente tóxico. Ao mesmo tempo demonstra a alta utilização local de glicose (metabolismo aumentado).

3. O PNV ativou áreas cerebrais relacionadas com motricidade e com funções neurovegetativas. Nossos achados apontam a diminuição da ativação das áreas relacionadas à motricidade/aversão/ansiedade/fuga e a hiperativação de áreas relacionadas ao controle de funções neurovegetativas, nos animais tratados com 7NI/PNV, comparados àqueles tratados apenas com o PNV. Portanto, durante o envenenamento, a presença do NO provavelmente ativa

neurônios das regiões relacionadas com controle da motricidade, aversão, ansiedade e fuga (desde que sua inibição diminuiu a ativação dessas áreas) e inibe a ativação de neurônios das áreas relacionadas com funções neurovegetativas (desde que sua inibição causou maior ativação dessas áreas). Isso aponta um papel duplo do NO no mecanismo de ação do veneno, dependendo da via neuronal que está sendo ativada. O balanço entre inibição/ativação das vias neuronais causado pelo NO pende para o papel protetor deste gás, uma vez que há o agravamento do quadro clínico nos animais tratados com 7NI/PNV. Nós concluímos que o NO está diretamente envolvido na geração de sinais neurotóxicos desencadeados nas vítimas de acidentes por P. nigriventer. O estudo do papel do NO pode contribuir para o entendimento dos mecanismos do envenenamento por Phoneutria, bem como pode ser útil para criar e aperfeiçoar propostas terapêuticas.

4. Os resultados mostraram que ocorreu gliose e reação inflamatória nos astrócitos in vitro, após a exposição ao PNV. O NO mostrou ser um eficiente mediador da inflamação e da gliose desencadeadas pelo veneno, desde que a inibição da nNOS pelo pré-tratamento com o 7NI reduziu a expressão da GFAP, TNF-a e IFN-γ e diminuiu a liberação de nitrito no meio de cultura, comparado com o tratamento com o PNV sozinho. É possível que o papel do NO na ativação das vias neuronais tenha como protagonista central os astrócitos através de interações homotípicas e heterotípicas. A riqueza de neurotoxinas no veneno de P. nigriventer aponta-o como uma ferramenta potencial para investigações de processos fisiopatológicos do SNC, incluindo processos inflamatórios. Esse modelo é útil para o estudo dos mecanismos da reação inflamatória e da gliose no cérebro.

5. As frações denominadas F1-8 e F1-10 apresentaram ação nos vasos sanguíneos cerebrais, aparentemente aumentando a permeabilidade da BHE. O presente trabalho contribuiu com dados iniciais na identificação de novas moléculas com capacidade de permeabilizar a BHE, que são de grande interesse farmacêutico para uso clínico e em pesquisa.

REFERÊNCIAS BIBLIOGRÁFICAS

Abbott N.J. Dynamics of CNS barriers: evolution, differentiation, and modulation. *Cell Mol Neurobiol* (2005) **1**:5-23.

Abbott N.J., Revest P.A. Control of brain endothelial permeability. *Cerebrovasc. Brain Metab Rev* (1991) **3**:39-72.

Allan S.M., Rothwell N.J. Cytokines and acute neurodegeneration. *Nat Rev Neurosci* (2001) **2**:734-744.

Andrade E., Villanova F., Borra P., Leite K., Troncone L., Cortez I., Messina L., Paranhos M., Claro J., Srougi M. Penile erection induced in vivo by a purified toxin from the Brazilian spider Phoneutria nigriventer. *BJU Int.* (2008) **102**:835-837.

Araujo D.A., Cordeiro M.N., Diniz C.R., Beirao P.S. Effects of a toxic fraction, PhTx2, from the spider *Phoneutria nigriventer* on the sodium current. *Naunyn Schmiedebergs Arch Pharmacol* (1993) **347**:205–208.

Aschner M. Immune and inflammatory responses in the CNS: modulation by astrocytes. *Toxicol Lett* (1998) **102-103**:283-287.

Barjavel M.J., Bhargava H.N. Nitric oxide synthase activity in brain regions and spinal cord of mice and rats: kinetic analysis. *Pharmacology* (1995) **50**:168-174.

Barone F.C., Feuerstein G.Z. Inflammatory mediators and stroke: new opportunities for novel therapeutics. *J Cereb Blood Flow Metab* (1999) **19**:819-834.

Barrett L.K., Singer M., Clapp L.H. Vasopressin: mechanisms of action on the vasculature in health and in septic shock. *Crit Care Med* (2007) **35**:33-40.

Bauer H.C., Bauer H. Neural induction of the blood-brain barrier: still an enigma. *Cell Mol Neurobiol* (2000) **20**:13-28.

Bazzoni G., Dejana E. Endothelial cell-to-cell junctions: molecular organization and role in vascular homeostasis. *Physiol Rev* (2004) **84**:869-901.

Begley D.J., Brightman M.W. Structural and functional aspects of the blood-brain barrier. *Prog Drug Res* (2003) **61**:39-78.

Benveniste H., Hedlund L.W., Johnson G.A. Mechanism of detection of acute cerebral ischemia in rats by diffusion-weighted magnetic resonance microscopy. *Stroke* (1992) **23**:746-754.

Bignami A., LeBlanc A., Perides G. A role for extracellular matrix degradation and matrix metalloproteinases in senile dementia? *Acta Neuropathol* (1994) **87**:308-312.

Braet K., Paemeleire K., D'Herde K., Sanderson M.J., Leybaert L. Astrocyte-endothelial cell calcium signals conveyed by two signalling pathways. *Eur J Neurosci* (2001) **13**:79-91.

Brazil V., Vellard J. Contribuição ao estudo do veneno das aranhas. *Mem Inst Butantan* (1925) **2**:5-77.

Brazil V., Vellard J. Contribuição ao estudo do veneno das aranhas. *Mem Inst Butantan* (1926) **3**:3-77.

Bredt D.S. Endogenous nitric oxide synthesis: biological functions and pathophysiology. *Free Radic Res* (1999) **31**:577-596.

Bredt D.S., Glatt C.E., Hwang P.M., Fotuhi M., Dawson T.M., Snyder S.H. Nitric oxide synthase protein and mRNA are discretely localized in neuronal populations of the mammalian CNS together with NADPH diaphorase. *Neuron* (1991) **7**:615-624.

Bredt D.S., Hwang P.M., Snyder S.H. Localization of nitric oxide synthase indicating a neural role for nitric oxide. *Nature* (1990) **347**:768-770.

Bredt D.S., Snyder S.H. Isolation of nitric oxide synthetase, a calmodulin-requiring enzyme. *Proc Natl Acad Sci U S A* (1990) **87**:682-685.

Brenman J.E., Bredt D.S. Nitric oxide signaling in the nervous system. *Meth Enzymol* (1996) **269:**119-129.

Brownstein M.J., Russell J.T., Gainer H. Synthesis, transport, and release of posterior pituitary hormones. *Science* (1980) 207:373-378.

Bruce T., Hope T., Gregory J., Michael S., Knigget K.M., Vincent S.R. Neuronal NADPH diaphorase in a nitric oxide synthase. Proc Nati Acad Sci USA (1991) 88:2811-2814.

Bucaretchi F., Deus Reinaldo C.R., Hyslop S., Madureira P.R., De Capitani E.M., Vieira R.J. A clinico-epidemiological study of bites by spiders of the genus *Phoneutria. Rev Inst Med Trop São Paulo* (2000) **42**:17-21.

Burke-Gaffney A., Keenan A.K. Does TNF-alpha directly increase endothelial cell monolayer permeability? *Agents Actions* (1993) **38**:83-85.

Calabrese V., Mancuso C., Calvani M., Rizzarelli E., Butterfield D.A., Stella A.M. Nitric oxide in the central nervous system: neuroprotection versus neurotoxicity. *Nat Rev Neurosci* (2007) **10**:766-775.

Castegna A., Thongboonkerd V., Klein J.B., Lynn B., Markesbery W.R., Butterfield D.A. Proteomic identification of nitrated proteins in Alzheimer's disease brain. *J Neurochem* (2003) **85**:1394-1401.

Chávez-Olortégui C., Bohorquez K., Alvarenga L.M., Kalapothakis E., Campolina D., Maria W.S., Diniz C.R. Sandwich-ELISA detection of venom antigens in envenoming by *Phoneutria nigriventer* spider. *Toxicon,* (2001) **39**:909-911.

Choi J., Koh S. Role of brain inflammation in epileptogenesis. *Yonsei Med J* (2008) **49**:1-18.

Cole S.P.C., Bhardwaj G., Gerlach J.H., Mackie J.E., Grant C.E., Almquist I.C.C., Stewart A.J., Kurz E. U., Duncan A.M.V, Deeley R.O. Overexpres sion of a transportergene in a multidrug-resistanhtumanlung cancercell line. *Scienee (WashingtonDC)* (1992) **258**:1650-1651.

Conrad K.P., Gellai M., North W.G., Valtin H. Influence of oxytocin on renal hemodynamics and electrolyte and water excretion. *American J Physiol* (1986) **251**:F290-F296.

Cordeiro M.N., Diniz C.R., Valentim A.C., Eickstedt V.R., Gilroy J., Richardson M. The purification and amino acid sequences of four Tx2 neurotoxins from the venom of the Brazilian 'armed' spider *Phoneutria nigriventer* (Keys). *FEBS Lett* (1992) **310**:153-156.

Cordeiro M.N., Figueiredo S.G., Valentim A.C., Diniz C.R., Eickstedt V.R., Gilroy J., Richardson M. Purification and amino acid sequences of six Tx3 type neurotoxins from the venom of the Brazilian 'armed' spider *Phoneutria nigrivente* (Keys). *Toxicon* (1993) **31**: 35-42.

Craner S.L., Hoffman G.E., Lund J.S., Humphrey A.L., Lund R.D. cFos labeling in rat superior colliculus: activation by normal retinal pathways and pathways from intracranial retinal transplants. *Exp Neurol* (1992) **117**:219-229.

Cruz-Höfling M.A., Love S., Brook G., Duchen L.W. Effects of *Phoneutria nigriventer* spider venom on mouse peripheral nerve. *Q J Exp Physiol* (1985) **70**:623-640.

Cruz-Höfling M.A., Zago G.M., Melo L.L., Rapôso C. c-FOS and n-NOS reactive neurons in response to circulating *Phoneutria nigriventer* spider venom. *Brain Res Bull* (2007) **73**:114-126.

Cruz-Höfling M.A., Rapôso C., Verinaud L., Zago G.M. Neuroinflammation and astrocytic reaction in the course of phoneutria nigriventer (armed-spider) blood-brain barrier (bbb) opening. Neurotoxicology (2009) **30**:636-646.

Dallas S., Miller D.S., Bendayan R. Multidrug resistance-associated proteins: expression and function in the central nervous system. *Pharmacol Rev* (2006) **58**:140-161.

Davson H., Oldendorf W.H. Transport in the central nervous system. *Proc Royal Soc Med* (1967) **60**:326-328.

Dehouck M.P., Meresse S., Delorme P., Fruchart J. C., Cecchelli R. An easier, reproducible, and mass-production method to study the blood–brain barrier *in vitro*. *J Neurochem* (1990) **54**:1798-1801.

Diniz C.R. Separação de proteínas e caracterização de substâncias ativas em venenos de aranhas do Brasil. *An. Acad Bras Ciênc* (1963) **35**:283-291.

Diniz C.R., Cordeiro M.N., Rezende Jr. L., Kelly P., Fischer S., Reimann F., Oliveira E.B., Richardson M. The purification and amino acid sequence of the lethal neurotoxin Tx1 from the venom of the Brazilian 'armed' spider *Phoneutria nigriventer*. *FEBS Lett* (1990) **263**: 251-253.

Dragunow M., Robertson H.A. Generalized seizures induce c-fos protein(s) in mammalian neurons. *Neurosci Lett* (1987) **82**:157-161.

Entwistle I.D., Johnstone R.A., Medzihradszky D., May T.E. Isolation of a pure toxic polypeptide from the venom of the spider *Phoneutria nigriventer* an its neurophysiological activity on an insect femur preparation. *Toxicon,*(1982) **20**:1059-1067.

Escoubas P., Diochot S., Corzo G. Structure and pharmacology of spider venom neurotoxins. *Biochimie* (2000) **82**:893-907.

Estrada G., Villegas E., Corzo G. Spider venoms: a rich source of acylpolyamines and peptides as new leads for CNS drugs. *Nat Prod Rep* (2007) **24**:145-161.

Farahani R., Pina-Benabou M.H., Kyrozis A., Siddiq A., Barradas P.C., Chiu F.C., Cavalcante L.A., Lai J.C., Stanton P.K., Rozental R. Alterations in metabolism and gap junction expression may determine the role of astrocytes as "good samaritans" or executioners. *Glia* (2005) **50**:351-361.

Farina C., Aloisi F., Meinl E. Astrocytes are active players in cerebral innate immunity. *Trends Immunol* (2007) **28**:138-145.

Farquhar M.G., Palade G.E. Junctional complexes in various epithelia. *J Cell Biol* (1963) **17**:375-412.

Feelisch M., te Poel M., Zamora R., Deussen A., Moncada S. Understanding the controversy over the identity of EDRF. *Nature* (1994) **368**:62-65.

Figueiredo G. de, Lima M.E. de, Cordeiro M.N., Diniz C.R., Patten D., Halliwell R.F., Gilroy J., Richardson M. Purification and amino acid sequence of a highly insecticidal toxin from the venom of the brazilian spider *Phoneutria nigriventer* which inhibits NMDA-evoked currents in rat hippocampal neuronas. *Toxicon* (2001) **39**:309-317.

Figueiredo S.G., Garcia M.E., Valentim A.C., Cordeiro M.N., Diniz C.R., Richardson M. Purification and amino acid sequence of the insecticidal neurotoxin Tx4(6-1) from the venom of the 'armed' spider *Phoneutria nigriventer. Toxicon* (1995) **33**:83-93.

Fontana M.D., Vital-Brazil O. Mode of action of *Phoneutria nigriventer* spider venom at the isolated phrenic nerve-diaphragm of the rat. *Braz J Med Biol Res* (1985) **18**:557-565.

Förstermann U., Schmidt H.H., Pollock J.S., Sheng H., Mitchell J.A., Warner T.D., Nakane M., Murad F. Isoforms of nitric oxide synthase. Characterization and purification from different cell types. *Biochem Pharmacol* (1991) **42**:1849-1857.

Garthwaite J., Boulton C. L. Nitric oxide signaling in the central nervous system. *Annu Rev Physiol* (1995) **57**:683–706.

Garthwaite J., Charles S. L., Chess-Williams R. Endothelium-derived relaxing factor release on activation of NMDA receptors suggests role as intercellular messenger in the brain. *Nature* (1988) **336**:385-388.

Gaudry C.A., Palka H.L., Dusek R.L., Huen A.C., Khandekar M.J., Hudson L.G., Green K.J. Tyrosine-phosphorylated plakoglobin is associated with desmogleins but not desmoplakin after epidermal growth factor receptor activation. *J Biol Chem* (2001) **276**:24871-24880.

Giepmans B.N. Gap junctions and connexin-interacting proteins. *Cardiovasc Res* (2004) **62**:233-245.

Giepmans B.N., Moolenaar W.H. The gap junction protein connexin43 interacts with the second PDZ domain of the zona occludens-1 protein. *Curr Biol* (1998) **8**:931-934.

Gomez M.V., Kalapothakis E., Guatimosim C., Prado M.A. *Phoneutria nigriventer* venom: a cocktail of toxins that affect ion channels. *Cell Mol Neurobiol* (2002) **22**:579-588.

González-Scarano F., Baltuch G. Microglia as mediators of inflammatory and degenerative diseases. *Annu Rev Neurosci* (1999) **22**:219-240.

Gutkowska J., Jankowski M., Mukaddam-Daher S., McCann S.M. Oxytocin is a cardiovascular hormone. *Brazilian Journal of Medical and Biological Research* (2000) **33**:625-633.

Haspel G., Rosenberg L.A., Libersat E. Direct injection of venom by a predatory wasp into cockroach brain. *J Neurobiol* (2003) **56**:287-292.

Hawkins B.T., Davis T.P. The blood-brain barrier/neurovascular unit in health and disease. *Pharmacol Rev* (2005) **57**:173-185.

Hayashi Y., Nomura M., Yamagishi S., Harada S., Yamashita J., Yamamoto H. Induction of various blood-brain barrier properties in non-neural cells by close apposition to co-cultured astrocytes. *Glia* (1997) **19**:13-26.

Herrera D.G., Robertson H.A. Activation of c-Fos in the brain. *Prog Neurobiol* (1996) **50**:83-107.

Herve´ J.C., Bourmeyster N., Sarrouilhe D. Diversity in protein–protein interactions of connexins: Emerging roles. *Biochim Biophys Acta* (2004) **1662**:22–41.

Hobbs A.J., Ignarro L.J. Nitric oxide-cyclic GMP signal transduction system. *Methods Enzymol* (1996) **269**:134-148.

Hoffman G.E., Lee W.S., Smith M.S., Abbud R., Roberts M.M., Robinson A.G., Verbalis J.G. c-Fos and Fos-related antigens as markers for neuronal activity: perspectives from neuroendocrine systems. *NIDA Res Monogr.* (1993) **125**:117-133.

Hughes P., Dragunow M. Induction of immediate-early genes and the control of neurotransmitter-regulated gene expression within the nervous system. *Pharmacol Rev* (1995) **47**:133-178.

Ignarro L.J., Buga G.M., Wood K.S., Byrns, R.E., Chaudhuri, G. Endothelium-derived relaxing factor produced and released from artery and vein is nitric oxide. *Proc Natl Acad Sci USA* (1987) **84**:9265-9269. **A milestone paper that reveals the identity of EDRF as NO.**

Imai H., Saio M., Nonaka K., Suwa T., Umemura N., Ouyang G.F., Nakagawa J., Tomita H., Osada S., Sugiyama Y., Adachi Y., Takami T. Depletion of CD4+CD25+ regulatory T cells enhances interleukin-2-induced antitumor immunity in a mouse model of colon adenocarcinoma. *Cancer Sci* (2007) **98**:416-423.

Jankowski M., Wang D., Haijar F., Mukaddam-Daher S., McCann S.M., Gutkowska J. Oxytocin and its receptors are synthesized in the rat vasculature. *Proc Natl Acad Sci USA* (2000) **97**:6207-6211.

Kacem K., Lacombe P., Seylaz J., Bonvento G. Structural organization of the perivascular astrocyte endfeet and their relationship with the endothelial glucose transporter: a confocal microscopy study. *Glia* (1998) 23:1-10.

Kadekaro M., Terrell M.L., Liu H., Gestl S., Bui V., Summy-Long J.Y. Effects of L-NAME on cerebral metabolic, vasopressin, oxytocin, and blood pressure responses in hemorrhaged rats. *Am J Physiol* (1998) **274**:R1070-R1077.

Kadowaki K., Kishimoto J., Leng G., Emson P.C. Up-regulation of nitric oxide synthase (NOS) gene expression together with NOS activity in the rat hypothalamo-hypophysial system after chronic salt loading: evidence of a neuromodulatory role of nitric oxide in arginine vasopressin and oxytocin secretion. *Endocrinology* (1994) **134**:1011-1017.

Klatt P., Heinzel B., John M., Kastner M., Böhme E., Mayer B. Ca2+/calmodulin-dependent cytochrome c reductase activity of brain nitric oxide synthase. *J Biol Chem* (1992) **267**:11374-11378.

Kniesel U., Wolburg H. Tight junctions of the blood-brain barrier. *Cell Mol Neurobiol* (2000) **20**:57-76.

Krukoff T.L. Expression of c-fos in studies of central autonomic and sensory systems. *Mol Neurobiol* (1993) **7**:247-263.

Le Sueur L., Kalapothakis E., Cruz-Höfling M.A. Breakdown of the blood-brain barrier and neuropathological changes induced by *Phoneutria nigriventer* spider venom. *ActaNeuropathol (Berl)* (2003) **105**:125-134.

Le Sueur L.P., Collares-Buzato C.B., Cruz-Höfling M.A. Mechanisms involved in the blood-brain barrier increased permeability induced by *Phoneutria nigriventer* spider venom in rats. *Brain Res* (2004) **1027**:38-47.

Li J., Shen H., Naus C.C., Zhang L., Carlen P.L. Upregulation of gap junction connexin 32 with epileptiform activity in the isolated mouse hippocampus. *Neuroscience* (2001) **105**:589-598.

Liang X.J., Aszalos A. Multidrug transporters as drug targets. *Curr Drug Targets* (2006) **7**:911-921.

Lima M.E. de, Stankiewicz M., Hamon A., Figueiredo S.G., Cordeiro M.N., Diniz C.R., Martin-Eauclaire M.F., Pelhate M. The toxin Tx4(6.1) from the spider *Phoneutria nigriventer* slows down Na+ current inactivation in insect CNS via binding to receptor site 3. *J Insect Physiol* (2002) **48**:53-61.

Liu F., Grundke-Iqbal I., Iqbal K., Gong, C.X. Contributions of protein phosphatases PP1, PP2A, PP2B and PP5 to the regulation of tau phosphorylation. Eur *J Neurosci* (2005) **22**:1942-1950.

Liu H., Terrell M.L., Bui V., Summy-Long J.Y., Kadekaro M. Nitric oxide control of drinking, vasopressin and oxytocin release and blood-pressure in dehydrated rats. *Physiol Behav* (1998) **63**:763-769.

Liu Q.S., Jia Y.S., Ju G. Nitric oxide inhibits neuronal activity in the supraoptic nucleus of the rat hypothalamic slices. *Brain Res Bull* (1997) **43**:121-125.

Lok J., Gupta P., Guo S., Kim W.J., Whalen M.J., van Leven K., Lo E.H. Cell-cell signaling in the neurovascular unit. *Neurochem Res* (2007) **32**:2032-2045.

Love S., Cruz-Hofling M.A. Acute swelling of nodes of Ranvier caused by venoms which slow inactivation of sodium channels. *Acta Neuropathol* (1986) **70**:1-9.

Love S., Cruz-Hofling M.A., Duchen L.W. Morphological abnormalities in myelinated nerve fibres caused by Leiurus, Centruroides and Phoneutria venoms and their prevention by tetrodotoxin. *Q J Exp Physiol* (1986) **71:**115-122.

Lucas S. Spiders in Brazil. *Toxicon,* (1988) **26**:759-772.

Luo Y., Kaur C., Ling E.A. Hypobaric hypoxia induces fos and neuronal nitric oxide synthase expression in the paraventricular and supraoptic nucleus in rats. *Neurosci Lett* (2000) **296**:145-148.

Mafra R.A., Figueiredo S.G., Diniz C.R., Cordeiro M.N., Cruz J.D., De Lima M.E. PhTx4, a new class of toxins from *Phoneutria nigriventer* spider venom, inhibits the glutamate uptake in rat brain synaptosomes. *Brain Res* (1999) **831**:297-300.

Marletta M.A. Nitric oxide synthase: function and mechanism. *Adv Exp Med Biol* (1993) **338**:281-284.

Martin P.E.M., Evans W.H. Incorporation of connexins into plasma membranes and gap junctions. *Cardiovasc Res* (2004) **62**:378-387.

Mayhan W.G. Regulation of blood-brain barrier permeability. *Microcirculation* (2001) **8**:89-104.

McAllister M.S., Krizanac-Bengez L., Macchia F., Naftalin R.J., Pedlev K.C., Mayberg M.R., Marroni M., Leaman S., Stanness K.A., Janigro D. Machanisms of glucose transport at the blood-brain barrier: an in vitro study. *Brain Res* (2001) **904**:20-30.

Miller G.Drug targeting. Breaking down barriers. **Science** (2002) **297**:1116-1118.

Minghetti L., Levi G. Microglia as effector cells in brain damage and repair: focus on prostanoids and nitric oxide. Prog *Neurobiol* (1998) **54**:99-125.

Ministério da Saúde, Araneísmo. Manual de diagnóstico e tratamento dos acidentes por animais peçonhentos. *Fundação Nacional da Saúde,* Brasília (1998) 49-53.

Moncada S., Palmer R.M., Higgs E.A. Nitric oxide: physiology, pathophysiology, and pharmacology. *Pharmacol Rev* (1991) **43**:109-142.

Mortari M.R., Cunha A.O., Ferreira L.B., dos Santos W.F. Neurotoxins from invertebrates as anticonvulsants: from basic research to therapeutic application. *Pharmacol Ther* (2007) **114**:171-183.

Neumann H. Control of glial immune function by neurons. *Glia* (2001) **36**:191-199.

Nicholson B.J. Gap junctions—From cell to molecule. *J Cell Sci* (2003) **116**:4479-4481.

Nunan E.A., Moraes M.F., Cardoso V.N., Moraes-Santos T. Effect of age on body distribution of Tityustoxin from *Tityus serrulatus* scorpion venom in rats. *Life Sci* (2003) **73**:319-325.

Ozaki H., Ishii K., Horiuchi H., Arai H., Kawamoto T., Okawa K., Iwamatsu A., Kita T. Cutting edge: combined treatment of TNF-alpha and IFN-gamma causes redistribution of junctional adhesion molecule in human endothelial cells. *J Immunol* (1999) **163**:553-557.

Palmer R.M., Ferrige A.G., Moncada S. Nitric oxide release accounts for the biological activity of endothelium-derived relaxing factor. *Nature* (1987) **327**:524-526.

Pathan S.A., Iqbal Z., Zaidi S.M., Talegaonkar S., Vohra D., Jain G.K., Azeem A., Jain N., Lalani J.R., Khar R.K., Ahmad F.J.CNS drug delivery systems: novel approaches. *Recent Pat Drug Deliv Formul* (2009) **3**:71-89.

Persidsky Y., Ramirez S.H., Haorah J., Kanmogne G.D. Blood-brain barrier: structural components and function under physiologic and pathologic conditions. *J Neuroimmune Pharmacol* (2006) **1**:223-236.

Prado M.A., Guatimosim C., Gomez M.V., Diniz C.R., Cordeiro M.N., Romano-Silva M.A. A novel tool for the investigation of glutamate release from rat cerebrocortical synaptosomes: the toxin Tx3-3 from the venom of the spider Phoneutria nigriventer. *Biochem J* (1996) **314**:145-150.

Ramsauer M., Krause D., Dermietzel R. Angiogenesis of the blood-brain barrier in vitro and the function of cerebral pericytes. *FASEB J* (2002) **16**:1274-1276.

Rapôso, C., Zago, G.M., Silva, G.H., Cruz-Höfling, M.A. Acute blood-brain barrier permeabilization in rats after systemic *Phoneutria nigriventer* venom. *Brain Res* (2007) **1149**:18-29.

Rash L.D., Hodgson W.C. Pharmacology and biochemistry of spider venoms. *Toxicon* (2002) **40**:225-254.

Rezende Jr. L., Cordeiro M.N., Oliveira E.B., Diniz C.R. Isolation of neurotoxic peptides from the venom of the 'armed' spider *Phoneutria nigriventer*. *Toxicon* (1991) **29**:1225-1233.

Richardson M., Pimenta A.M., Bemquerer M.P., Santoro M.M., Beirao P.S., Lima M.E., Figueiredo S.G., Bloch Jr. C., Vasconcelos E.A., Campos F.A., Gomes P.C., Cordeiro M.N. Comparison of the partial proteomes of the venoms of Brazilian spiders of the genus *Phoneutria*. *Comp Biochem Physiol C Toxicol Pharmacol* (2006) **142**:173-187.

Roura S., Miravet S., Piedra J., García de Herreros A., Duñach M. Regulation of E-cadherin/Catenin association by tyrosine phosphorylation. *J Biol Chem* (1999) **274**:36734-36740.

Rubin L.L., Hall D.E., Porter S., Barbu K., Cannon C., Horner H.C., Janatpour M., Liaw C.W., Manning K., Morales J., Tanner L., Tbmaselli K.J., Bard F. A cell culture model of the blood-brain barrier. *The Journal of Cell Biology* (1991) **115**:1725-1735.

Saad W.A., Gutierrez L.I., Guarda I.F., Camargo L.A., dos Santos T.A., Saad W.A., Simões S., Guarda R.S. Nitric oxide of the supraoptic nucleus influences the salivary secretion, sodium renal excretion, urinary volume and arterial blood pressure induced by pilocarpine. *Life Sci* (2004) **74**:1593-1603.

Sanders K.M., Ward S.M. Nitric oxide as a mediator of nonadrenergic noncholinergic neurotransmission. *Am J Physiol* (1992) **262**:G379-G392.

Santos R.G. dos, Van Renterghem C., Martin-Moutot N., Mansuelle P., Cordeiro M.N., Diniz C.R., Mori Y., de Lima M.E., Seagar M. *Phoneutria nigriventer* omega-phonetoxin IIA blocks the Cav2 family of calcium channels and interacts with omega-conotoxin-binding sites. *J Biol Chem* (2002) **277**:13856-13862.

Savettieri G., Di Liegro I., Catania C., Licata L., Pitarresi G.L., D'Agostino S., Schiera G., De Caro V., Giandalia G., Giannola L.I., Cestelli A. Neurons and ECM regulate occludin localization in brain endothelial cells. *Neuroreport* (2000) 11:1081-1084.

Schinkel A.H. P-Glycoprotein, a gatekeeper in the blood-brain barrier. *Adv Drug Deliv Rev* (1999) **36**:179-194.

Schulze C., Firth J.A. Immunohistochemical localization of adherens junction components in blood-brain barrier microvessels of the rat. *J Cell Sci* (1993) **104**:773-782.

da Silva G.H., Hyslop S., da Cruz-Höfling M.A. Lonomia obliqua caterpillar venom increases permeability of the blood-brain barrier in rats. *Toxicon* (2004) **44**:625-634.

Simard M., Arcuino G., Takano T., Liu Q.S., Nedergaard M. Signaling at the gliovascular interface. *J Neurosci* (2003) **23**:9254-9262.

Simionescu M., Simionescu N, Palade G.E. Segmental differentiations of cell junctions in the vascular endothelium. The microvasculature. *J Cell Biol* (1975) **67**:863-885.

Söhl G., Willecke K. Gap junctions and the connexin protein family. *Cardiovasc Res* (2004) **62**:228-232.

Srisawat R., Ludwig M., Bull P.M., Douglas A.J., Russell J.A., Leng G. Nitric oxide and the oxytocin system in pregnancy. *J Neurosci* (2000) **20**:6721-6727.

Stern J.E., Li Y., Zhang W. Nitric oxide: a local signalling molecule controlling the activity of pre-autonomic neurones in the paraventricular nucleus of the hypothalamus. *Acta Physiol Scand* (2003) **177**:37-42.

Streit W.J. Microglial response to brain injury: a brief synopsis. *Toxicol Pathol* (2000) **28**:28-30.

Sultana R., Poon H.F., Cai J., Pierce W.M., Merchant M., Klein J.B., Markesbery W.R., Butterfield D.A. Identification of nitrated proteins in Alzheimer's disease brain using a redox proteomics approach. *Neurobiol Dis* (2006) **22**:76-87.

Swanson L.W., Sawchenko P.E. Hypothalamic integration: organization of the paraventricular and supraoptic nuclei. *Annu Rev Neurosci* (1983) **6**:269-324.

Tanaka T., Tamada Y., Suwa F. Ifluence of age-related changes in nitric oxide synthase-expressing neurons in the rat supraoptic nucleus on inhibition of salivary secretion. *Okajimas Folia Anat Jpn* (2008) **84**:152-131.

Tao-Cheng J.H., Nagy Z., Brightman M.W. Tight junctions of brain endothelium in vitro are enhanced by astroglia.. J Neurosci (1987) **7**:3293-3299.

The Spider Myths Site. Myths about dangerous spiders, Available at: http://www.washington.edu/burkemuseum/spidermyth/myths/downunder.html

Tilling T., Korte D., Hoheisel D., Galla H.J. Basement membrane proteins influence brain capillary endothelial barrier function in vitro. *J Neurochem* (1998) **71**:1151-1157.

Toyofuku T., Yabuki M., Otsu K., Kuzuya T., Hori M., Tada M. Direct association of the gap junction protein connexin-43 with ZO-1 in cardiac myocytes. *J Biol Chem* (1998) **273**:12725-12731.

Troncone L.R., Georgiou J., Hua S.Y., Elrick D., Lebrun I., Magnoli F., Charlton M.P. Promiscuous and reversible blocker of presynaptic calcium channels in frog and crayfish neuromuscular junctions from *Phoneutria nigriventer* spider venos. *J Neurophysiol* (2003) **90**:3529-3537.

Troncone L.R., Lebrun I., Magnoli F., Yamane T. Biochemical and pharmacological studies on a lethal neurotoxic polypeptide from *Phoneutria nigriventer* spider venom. *Neurochem Res* (1995) **20**:879-883.

Ventura R.R., Giusti-Paiva A., Gomes D.A., Elias L.L., Antunes-Rodrigues J. Neuronal nitric oxide synthase inhibition differentially affects oxytocin and vasopressin secretion in salt loaded rats. *Neurosci Lett* (2005) **379**:75-80.

Ventura R.R., Gomes D.A., Reis W.L., Elias L.L., Castro M., Valença M.M., Carnio E.C., Rettori V., McCann S.M., Antunes-Rodrigues J. Nitrergic modulation of vasopressin, oxytocin and atrial natriuretic peptide secretion in response to sodium intake and hypertonic blood volume expansion. *Braz J Med Biol Res* (2002) **35**:1101-1109.

Vieira L.B., Kushmerick C., Hildebrand M.E., Garcia E., Stea A., Cordeiro M.N.,. Richardson M, Gomez M.V., Snutch T.P. Inhibition of high voltage-activated calcium channels by spider toxin PnTx3-6. *J Pharmacol Exp Ther* (2005) **314**:1370-1377.

Wagner R., Kachar B. Linear gap and tight junctional assemblies between capillary endothelial cells in the eel rete mirabile. *Anat Rec* (1995) **242**:545-552.

Walz W., Lang M.K. Immunocytochemical evidence for a distinct GFAP-negative subpopulation of astrocytes in the adult rat hippocampus. *Neurosci Lett* (1998) **257**:127-130.

Willoughby J.O., Mackenzie L., Medvedev A., Hiscock J.J. FOS induction following systemic kainic acid: early expression in hippocampus and later widespread expression correlated with seizure. *Neuroscience* (1997) **77**:379-392.

Wolburg H., Lippoldt A. Tight junctions of the blood-brain barrier: Development, composition and regulation. *Vascul Pharmacol* (2002) **38**:323-337.

Yamaguchi K., Hama H. A study on the mechanism by which sodium nitroprusside, a nitric oxide donor, applied to the anteroventral third ventricular region provokes facilitation of vasopressin secretion in conscious rats. *Brain Res* (2003) **968**:35-43.

Yasin S., Costa A., Trainer P., Windle R., Forsling M.L., Grossman A. Nitric oxide modulates the release of vasopressin from rat hypothalamic explants. *Endocrinology* (1993) **133**:1466-1469.

Yeh E.R., Erokwu B., LaManna J.C., Haxhiu M.A. The paraventricular nucleus of the hypothalamus influences respiratory timing and activity in the rat. *Nurosci Lett* (1997) **232**:63-66.

Yonamine C.M., Troncone L.R.P., Camilloa M.A.P. Blockade of neuronal nitric oxide synthase abolishes the toxic effects of Tx2-5, a lethal *Phoneutria nigriventer* spider toxin. *Toxicon* (2004) **44**:169-172.

Yuan F., Wang T., Luo L., Sun Y., Zhang L., Qu B. Development of cytotoxic cerebral edema in rats following intracaudatum injeciton of tACPD, an agonist of metabotropic glutamate receptors. *Chin Med J* (2000) **113**:728-732.

APÊNDICE – RESULTADOS OBTIDOS EM COLABORAÇÃO

NeuroToxicology 30 (2009) 636–646

Contents lists available at ScienceDirect

NeuroToxicology

Neuroinflammation and astrocytic reaction in the course of *Phoneutria nigriventer* (armed-spider) blood–brain barrier (BBB) opening

Maria Alice da Cruz-Höfling [a,*], Catarina Rapôso [a], Liana Verinaud [b], Gabriela Mariotoni Zago [a,c]

[a] Department of Histology and Embryology, Institute of Biology, P.O. Box 6109, University of Campinas - UNICAMP, Zip Code 13083-970 Campinas, SP, Brazil
[b] Department of Microbiology and Immunology, Institute of Biology, P.O. Box 6109, University of Campinas - UNICAMP, Zip Code 13083-970 Campinas, SP, Brazil
[c] Department of Farmacology, Faculty of Medical Sciences, University of Campinas - UNICAMP, Zip Code 13083-970 Campinas, SP, Brazil

ARTICLE INFO

Article history:
Received 15 December 2008
Accepted 12 April 2009
Available online 22 April 2009

Keywords:
Astrocytes
Neurons
GFAP
S100
Pro-inflammatory cytokines
Spider venom

ABSTRACT

Phoneutria nigriventer spider venom (PNV) causes uneven BBB permeability throughout different cerebral regions. Little is known about cellular and molecular responses which course with the PNV-induced BBB opening. We investigate by immunohistochemistry (IHC) and Western blotting (WB), the GFAP, S100, IFN-γ and TNF-α proteins expression in hippocampus and cerebellum after different time-points from venom or saline intravenous injection. All proteins variably altered its expression temporally and regionally. WB showed increased GFAP content at 15–45 min followed by a shift below the control level which was less pronounced in hippocampus. IHC showed reactive gliosis during all the trial period. In cerebellum, GFAP was mostly immunodetected in astrocytes of the molecular layer (Bergmann glia), as was S100 protein. The maximum S100 immunolabeling was achieved at 5 h. IFN-γ and TNF-α, expressed mostly by hippocampal neurons, increased along the trial period, suggesting a role in BBB permeability. In envenomed animals, closer contacts astrocyte–astrocyte, granule cells–granule cells and astrocytes-Purkinje cells were observed in cerebellum. Closer contacts between neurons–neurons–astrocytes–astrocytes were also seen in hippocampus. PNV contains serotonin, histamine, Ca^{2+} channels-blocking toxins, some of which affect glutamate release. The hypothesis that such substances plus the cytokines generated, could have a role in BBB permeability, and that calcium homeostasis loss and disturbance of glutamate release are associated with the marked GFAP/S100 reaction in Bergmann glia is discussed. The existence of a CNS mechanism of defense modulated differentially for fast synthesis and turnover of GFAP, S100, IFN-γ and TNF-α proteins was evident. A clear explanation for this differential modulation is unclear, but likely result from regional differences in astrocytic/neuronal populations, BBB tightness, and/or extent/distribution of microvasculature and/or ion channels density/distribution. Such differences would respond for transient characteristics of BBB disruption. This *in vivo* model is useful for studies on drug delivery throughout the CNS and experimental manipulation of the BBB.

1. Introduction

Astrocytes, the most abundant cell type in the CNS, are active players in normal brain physiology and CNS pathologies (Eng and Ghirnikar, 1994; Ransom et al., 2003). They play key role in the development and maintenance of the blood-brain barrier (BBB) (Abbott et al., 2006); vascular astrocytic end-feet processes form a sheath that strategically surrounds endothelium and basement membrane of brain vessels to form a complex which controls the bi-directional transit of substances across the blood–brain interface (Grieb et al., 1985; Hawkins et al., 2006; see Engelhardt, 2003 for review). Disturbances of BBB caused by toxic, traumatic or pathophysiological conditions can be evaluated by astrocytic markers such as glial fibrillary acidic protein (GFAP), glutamine synthase, and S100 protein (Walz and Lang, 1998; Savchenko et al., 2000). Astrocytes respond to CNS damage by hypertrophy and hyperplasia accompanied by upregulation of GFAP which is part of cytoskeletal intermediate filaments (Eng et al., 2000). S100, a family of proteins with calcium-binding ability, is expressed abundantly in astrocytes in the case of heart and brain injury (Rothermundt et al., 2003). Evidences show that astrocytes are also modulators of immune and inflammatory responses (Aschner, 1998) and hence coadjuvants in several neurological disturbances.

Impairment of BBB permeability can induce pro-inflammatory-mediated reaction creating a chain of interactions between blood-derived cells, neurons and glial cells (Wong et al., 2004). Neuroinflammation in the CNS comprises the activation of glial cells, recruitment of peripheral immune cells and production of

* Corresponding author. Tel.: +55 19 3521 6224; fax: +55 19 3289 3124.
E-mail address: hofling@unicamp.br (M.A. da Cruz-Höfling).

0161-813X/$ – see front matter © 2009 Elsevier Inc. All rights reserved.
doi:10.1016/j.neuro.2009.04.004

cytokines, such as Interferon-gamma (IFN-γ) and Tumor Necrosis Factor-alpha (TNF-α) (Lovell et al., 1998; Minghetti and Levi, 1998; Hirsch, 2000; Streit, 2000; Neumann, 2001; Liu et al., 2002). TNF-α mediates cytotoxic damage to glial cells and neurons, while IFN-γ seems to act by inducing cell surface molecules required for interactions between immune and brain cells (Imai et al., 2007).

Venoms produced by venomous animals are important source of pharmacologically active substances which may be useful tools for understanding CNS function in health and disease. *Phoneutria nigriventer* spider venom (PNV) is rich in voltage-gated sodium, calcium, and potassium channels-acting neurotoxins which affect peripheral and central neurotransmitter release (Cruz-Höfling et al., 1985; Fontana and Vital Brazil, 1985; Gomez et al., 2002). A bulk of information has been accumulated on the composition of PNV and some of the biological actions of their toxins were reported (Rezende et al., 1991; Prado et al., 1996; Gomez et al., 2002; Vieira et al., 2005; Lúcio et al., 2008), among which blockade of Ca^{2+} channel, inhibition of glutamate release and glutamate uptake in synaptosomes, and induction of hind limb flaccid paralysis when injected intracerebroventricularly. Clinically, *P. nigriventer* accidents graded as severe may cause convulsions particularly in children or debilitated victims (Bucaretchi et al., 2000).

Experimentally, we have shown that systemic PNV causes BBB permeability which though showed differential regional and temporal modulation. At acute stages, the venom causes differential downregulation of laminin expression and extravasation of extracellular tracer in cerebellum and hippocampus microvasculature (Raposo et al., 2007); also venom activates neurons at a number of motor- and stress-related areas of the CNS (Cruz-Höfling et al., 2007). At longer periods, only hippocampal BBB was disrupted whereas several areas of the CNS remained unaffected (Le Sueur et al., 2003). It was also shown that the hippocampal-enhanced permeability involved the transcellular pathway by a microtubule-dependent mechanism, whereas the paracellular route remained unaffected (Le Sueur et al., 2004). This BBB permeation was transient being thereafter gradually restored. Clinically, the signs of intoxication were vanished after 12 h and envenomed animals behavior becomes then indistinguishable from those injected with saline. The cellular events which course with the alterations of permeability of the blood–brain interface were not determined yet.

In this work, we investigate the expression of GFAP, S100, IFN-γ and TNF-α in the hippocampus and cerebellum of rats in the interval between 15 and 45 min, and 2 and 5 h after intravenous injection (i.v.) of PNV, corresponding to acute stages of envenoming. This study will contribute to shed light on the CNS response generated by circulating *P. nigriventer* spider venom, and which runs in parallel with the BBB breakdown. The fact that the effects are short-lived could give good prospect for future studies aiming to promote transient BBB opening viewing therapeutic purposes.

2. Materials and methods

2.1. Venom and animals

Lyophilized *P. nigriventer* crude venom was supplied by Instituto Butantan (São Paulo, SP, Brazil) and stored at −20 °C. The venom was dissolved in sterile physiological saline (0.9% (w/v) NaCl solution) at the moment of use and administered by i.v. route.

Male Wistar rats (3-week-old) were obtained from an established colony maintained by the Central Animal House Service at UNICAMP and kept under standard animal colony conditions including 12–12 h light–dark cycle, 22 ± 2 °C temperature with free access to food and water until reaching 8–10-week-old (250–300 g). At least 24 h before the experiment, the animals were transported in their home cages from the animal colony to the laboratory and allowed to habituate.

2.2. Envenoming procedure

Male rats were given a single i.v. injection of PNV (850 μg/kg in 0.5 ml saline) in the tail vein. The PNV concentration was selected based on previous studies in our laboratory (Le Sueur et al., 2003, 2004). To control group was given the same volume of 0.9% sterile saline solution (sham group). 15–45 min, 2 and 5 h after PNV or saline injection ($n = 5$/time interval), the animals were anesthetized with an i.p. injection (2 μg/mg body mass) of 3:1 mixture of ketamine chloride (Dopalen®, 100 mg kg^{-1} body weight) and xylazine chloride (Anasedan®, 10 mg kg^{-1} body weight) (Vetbrands, Jacarei, SP, Brazil). While 2 and 5 h were time-points after envenoming, 15–45 min was a time interval because animals were variably killed when clinical signs of envenoming predict that death seemed to be imminent. All procedures were carried out in accordance with the guidelines proposed by the "Principles of Laboratory Animal Care" (NIH publication no. 85-23, revised 1985) and approved by the Animal Care and Use Committee of the University of Campinas (UNICAMP).

2.3. Immunohistochemistry (IHC)

After anesthesia, the animals were transcardially perfused with physiological saline (150 ml) followed by 250 ml 4% paraformaldehyde in 0.1 M phosphate-buffered saline (PBS), pH 7.2. Then, the brain and cerebellum were immediately removed and post-fixed in the same fixative overnight. After, they were dehydrated in a graded ethanol series, cleared in xylol, and embedded in Histosec (Merck, Rio de Janeiro, RJ, Brazil). Sections of 5 μm thick were cut on an RM 2035 microtome (Reichert S, Leica), washed several times in 0.05 M PBS and then incubated in this buffer with 1% bovine serum albumin (BSA) for one hour for blocking nonspecific binding sites. Endogenous peroxidase was blocked by incubation in PBS containing 3% hydrogen peroxide for 30 min. Before incubation with primary antibodies, antigen retrieval was performed pre-treating the sections with 20 mM citrate buffer, pH 6.0 at 100 °C for 30 min. Four sections per animal in the three time-points considered for saline or PNV-injected animals were incubated with the following rabbit polyclonal primary antibodies: anti-GFAP and anti-S100 (DakoCytomation, CA,USA; Catalog numbers: ZO 334 and ZO 311, respectively), used at a dilution of 1:100 and 1:400, respectively; anti-IFN-γ and anti-TNF-α (Peprotech-Rocky Hills, NJ, USA; Catalog numbers: 500-P64 and 500-P119, respectively) both used at a dilution of 1:500, for 30 min at room temperature and then overnight at 4 °C. After washing, sections were overlaid for 1 h with a secondary antibody biotin-conjugated. The immunohistochemical reaction was amplified using the kit Rabbit Immunocruz Staining System (Santa Cruz, CA, USA), and visualized with 3′-3-diaminobenzidine (DAB) as chromogen. All incubations were carried out in a humidified chamber. The reactions were stopped by washing the slides in distilled water. The slides were then weakly counter-stained with Harris' hematoxylin, dehydrated in ethanol and mounted in Canada balsam. The stereotaxic coordinates of transversal planes and limits of regions analyzed were selected according to Palkovits and Brownstein's atlas of rat brain anatomy (1988). Preliminary observations were done at light microscope with 10× objective (Leica, Germany) to identify hippocampus and cerebellum regions. Then, using 20× and 40× objectives, an evaluation was done comparing the labeling intensity of control group at each period of envenoming. Fifteen images per group of saline- or venom-injected animals (three fields per animal or 15 fields per time-course) were captured using a Nikon Eclipse E800 light microscope (Japan) equipped with Image-Pro Plus image analyzer software (USA).

2.4. Western blot (WB)

15–45 min, 2 and 5 h after PNV or saline injection ($n = 5$ animals/time interval), the animals were anesthetized as described above, and killed by decapitation. Hippocampus and cerebellum from each time-point of PNV-injected animal were quickly dissected and each group homogenized in an extraction cocktail (10 mM EDTA, 2 mM PMSF, 100 mM NaF, 10 mM sodium pyrophosphate, 10 mM $NaVO_4$, 10 μg of aprotinin/ml and 100 mM Tris, pH 7.4). Hippocampus or cerebellum from animals killed 15–45 min, 2 h or 5 h after saline-injection was mixed and homogenized to form a control pool from each region ($n = 15$ total each region). This single control was used for evaluating WB of protein contents in hippocampus or cerebellum and comparison with the PNV-treated (15–45 min, 2 h or 5 h). Homogenates were centrifuged at 3000 × g for 10 min and the supernatant was collected and stored at −70 °C until use for immunoblotting. The proteins (50 μg) were separated on 6.5% (IFN-γ) or 8% (GFAP and TNF-α) sodium dodecyl sulfate–polyacrylamide by gel electrophoresis under reduced conditions and were electrophoretically transferred onto nitrocellulose membrane (Bio Rad, CA, USA, Ref. 162-0115). After blocking overnight at 4 °C with 5% or 2.5% non-fat milk in TBS-T (Tris-buffered saline 0.1% plus 0.05% Tween 20, pH 7.4), the membranes were incubated at room temperature, for 4 h, with rabbit polyclonal antibody against TNF-α, IFN-γ (both 1:200 dilution; Peprotech-Rocky Hills, NJ, USA) and GFAP (1:400 dilution, DakoCytomation, CA, USA), diluted in buffer solution TBS-T containing 3% non-fat milk. After washing (five times, 8 min each) in TBS-T, the membranes were further reacted with horseradish peroxidase-conjugated anti-rabbit secondary antibody (1:800 or 1:1600 dilution, Sigma, Ref. A6154), diluted in TBS-T with 1% non-fat milk, for 1 h, at room temperature. An enhanced chemiluminescence reagent (Super Signal, Pierce, Ref. 34080) was used to make the labeled protein bands visible and the blots were developed on X-ray film (Fuji Medical, Kodak, Ref. Z358487-50EA). For quantification, the density of pixels of each band was determined by the ImageJ 1.38 program (available at http://rsbweb.nih.gov/ij/download.html; developed by Wayne Rasband, NIH, Bethesda, MD). For each protein investigated the results were confirmed in three sets of experiments. Immunoblot for β-actin was done as a control for the above protein blots. After protein blots visualization with enhanced chemiluminescence, the protein antibodies were stripped from the membranes, which were reprobed with monoclonal anti-β-actin antibody (1:250 dilution, Sigma, USA) and subsequently protein densitometry was done. The ratio of GFAP/β-actin, TNF-α/β-actin and IFN-γ/β-actin was calculated and compared to saline-pooled (sham) control.

2.5. Statistic data analysis

The clinical signs of the envenoming presented by each animal were monitored by two observers and carefully registered.

The densitometric values of the immunoreactive bands (immunoblotting) were analyzed using the GraphPad Prism software package (San Diego, CA, USA). One-way analysis of variance (ANOVA) followed by the Dunnet test was used to compare groups. The results were expressed as means ± S.E. where appropriate. A value of $P < 0.05$ indicated statistical significance.

3. Results

3.1. Clinical observations

After venom administration the animals showed signals of intoxication which included variably hyperemia, piloerection, tremors, salivation, reduced locomotor's activity and some difficulty in breathing. Practically all animals presented flaccidity followed by spastic paralysis of posterior legs. At least two out of five rats used in each period showed tonic convulsion. Three animals died subsequently after venom injection, probably by respiratory arrest, since necropsy showed lung edema. After 3 h animals showed clear signal that recovery was underway; salivation, tremors and paralysis of members had vanished, but some prostration persisted. At 5 h post-PNV injection the clinical condition had improved, but it was only at 12 h that the complete recovery was achieved (Le Sueur et al., 2003). Rats injected with sterile saline (sham controls) appeared normal and showed none of the clinical signs described above whatever the survival period. Since clinically saline control from different time-points was indistinguishable from each other, hippocampus or cerebellum from all time-points were homogenized together to form a single control for WB assays.

3.2. Immunohistochemistry and Western blotting

3.2.1. Controls

GFAP and S100: In control group a basal expression of both proteins was seen by WB quantification. Despite some variability in the morphological pattern of astrocytes depending on its location, no difference in the intensity of IHC labeling was detected among the different survival periods post-saline injection.

TNF-α and IFN-γ: A physiological production of these proteins was seen by WB, however IHC labeling was similarly negative or was very faint for all survival periods (Figs. 1–4). Histopathological analysis showed no visible alteration in tissue morphology.

3.3. PNV-injected animals

3.3.1. GFAP

An immediate rise in GFAP immunolabeling (IHC) and content (WB) both in hippocampus and cerebellum of envenomed animals was seen at 15–45 min post-PNV injection (Figs. 1 and 2). At 2 and 5 h immunolabeling gradually decreased but remained stronger than the observed in control; in contrast WB data showed that after the increase seen at 15–45 min a progressive GFAP reduction led the protein content below the control level at 5 h post-injection. This discrepancy between IHC and WB can be more easily understandable for cerebellum, since GFAP labeling was enhanced in the molecular layer, and practically absent in granular and Purkinje layers. This region-specific gliosis was obscured after homogenization of cerebellum for WB assay. In the molecular layer of cerebellum, the long astrocytic processes were typically arranged in palisade perpendicular to the pia-mater (Bergmann glia). This spatial arrangement was more evident in PNV-treated animals (Fig. 2B–D) than in controls (Fig. 2A), given the higher GFAP reactivity, length and thickness of the cell processes, all of them indicative of astrocyte hypertrophy.

In hippocampus, reactive astrocytes of PNV-treated animals (mainly at 15–45 min) showed hypertrophy (Fig. 1B and C) in comparison to control (Fig. 1A). GFAP labeling in the astrocytes end-feet was heavier around vessels. Because the stained tiny astroglial ramifications were widespread all over the hippocampal parenchyma, the tissue background appeared shadowed in brown whereas in controls it appeared bluish (Fig. 1B and C *vs.* A). This feature was more evident at 15–45 min and 2 h post-PNV. In addition, vasogenic edema was observed in the PNV-treated animals (Fig. 1B and C).

The quantification of the protein content by immunoblotting showed no significant difference in relation to controls both in hippocampus and cerebellum; however, there was a significant difference between 15 and 45 min-PNV group (the peak of protein increase) and 5 h PNV-group (the peak of protein decrease).

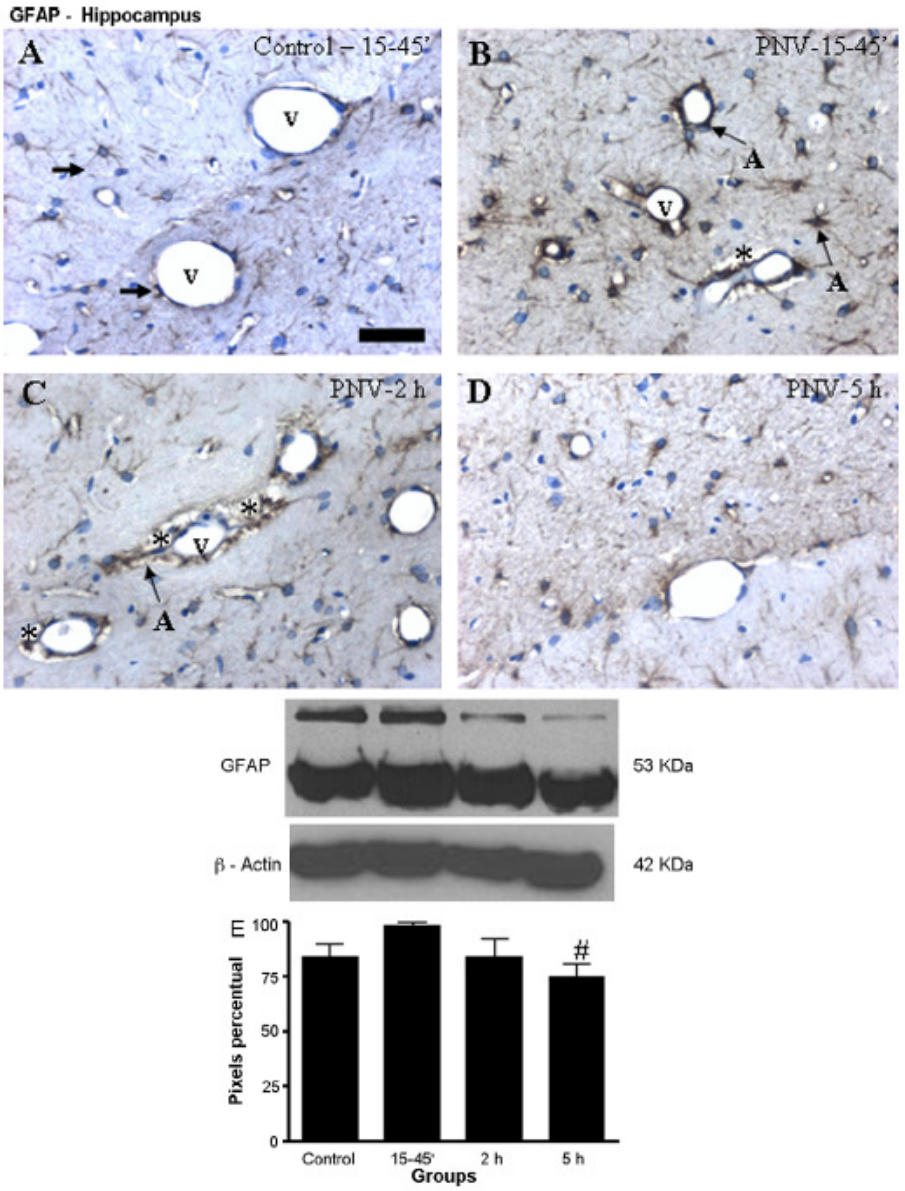

Fig. 1. Immunohistochemistry (IHC) and western blotting (WB) for glial fibrillary acidic protein (GFAP) in hippocampus. (A) Saline control (15–45 min after injection). (B–D) Hippocampus of PNV-injected rats after 15–45 min, 2 and 5 h, respectively. There was increase in the immunolabeling of GFAP at 15–45 min post-PNV, indicating astrocyte activation (A), after which it was gradually reduced. GFAP immunolabeling is seen both in cells body and cellular processes around blood vessels (v) and over the entire tissue ground (suggestive of reactive gliosis). Vasogenic edema (*) was seen around the affected vessels. Blots and corresponding columns representing pixels quantification are displayed in panel E. There was no significant difference between pooled-control and PNV-groups, but the GFAP content at 5 h was significantly reduced in relation to the GFAP content at 15–45 min ($^{\#}P < 0.05$). Data were analyzed by one-way ANOVA followed by the Dunnet test. The columns represent the mean ± S.E. of the protein investigated; the results were confirmed in three sets of experiments ($n = 5$ animals/time interval after PNV exposure compared to control pool, $n = 15$). Scale Bars: A–D = 40 μm; E–H = 80 μm.

3.4. S100

Intracellular S100 labeling increased progressively in the astrocytic cell bodies of cerebellum (Fig. 3E and G) and hippocampus (Fig. 3F and H) in all time-points after PNV injection in relation to matched control (Fig. 3A, B and C, D, respectively). In cerebellum, the strongest S100 labeling was seen in the nucleus and cytoplasm of astrocytes (Bergmann glia) located in the Purkinje layer around neurons. In the molecular layer, the labeling of the profuse delicate astrocytic processes gave the layer a brown shade. Purkinje cells were negative for S100 protein; astrocytes away from Purkinje layer were negative or much less reactive (Fig. 3E and G). Some S100 positive labeling was interspersed among granule neurons. It is of note that while in control group Purkinje cells were located in the limit between granular and molecular zone (Fig. 3B) and were surrounded only by a few

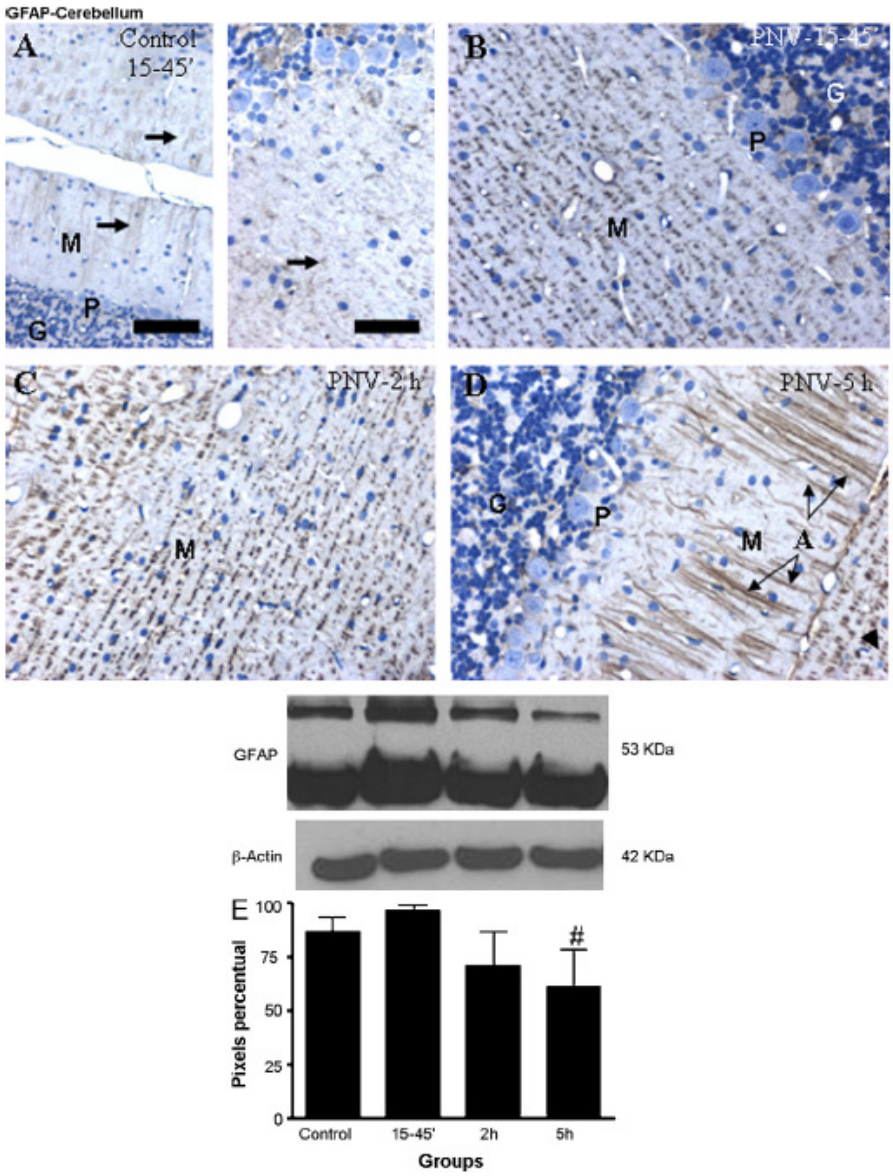

Fig. 2. Immunohistochemistry (IHC) and western blotting (WB) for glial fibrillary acidic protein (GFAP) in cerebellum. (A) Saline control (15–45 min after injection). (B–D) Cerebellum of PNV-injected rats after 15–45 min, 2 and 5 h, respectively, showed marked increase of GFAP immunolabeling in all time-points. Astrocytes from molecular layer (M) were more reactive (see A indicated by arrows); granular layer (G) showed negligible labeling. Observe the cross-sectional and regularly oriented profiles of the astrocytic processes (Bergmann glia) at the molecular layer (M); P: Purkinje cells layer. E-GFAP content measured by pixels quantification of WB bands showed no difference between envenomed groups and pooled control, but there was difference between 15 and 45 min-PNV- and 5 h-PNV-group ($^{\#}P < 0.05$). Data were analyzed by one-way ANOVA followed by the Dunnet test. The columns represent the mean ± S.E. of the protein investigated; the results were confirmed in three sets of experiments ($n = 5$ animals/time interval after PNV exposure compared to control pool, $n = 15$). Scale Bars: A = 40 μm; B–D = 80 μm.

astrocytes (Fig. 3A and B), in envenomed 5 h-group these cells were located deeper into the granular layer and astrocytes were more concentrated at the border between granular and molecular layers (Fig. 3E and G). As a result, closer contacts could be seen being established between Purkinje cells and S100 positive glia, and Purkinje cells and granular neurons.

In hippocampus, a tenuous S100 immunoreactivity was perceived in the perikaryon of astrocytes of saline-injected animals (Fig. 3C and D). However, a gradual increase in both the intensity and extent of labeling was seen in PNV-treated animals; highest labeling was noticed both in astrocytes nuclei and in the abundant branching of the tiny astrocytic processes at 5 h post-PNV injection (Fig. 3F and H).

Despite efforts we were unsuccessful to detect S100 by WB. Then, a semi-quantitative evaluation scored as strong (+++), moderate (++), weak (+) or negative (–) based on the relative amount/intensity of immunoreactivity of these cells in comparison to controls (Hess et al., 2008) was done by two observers for

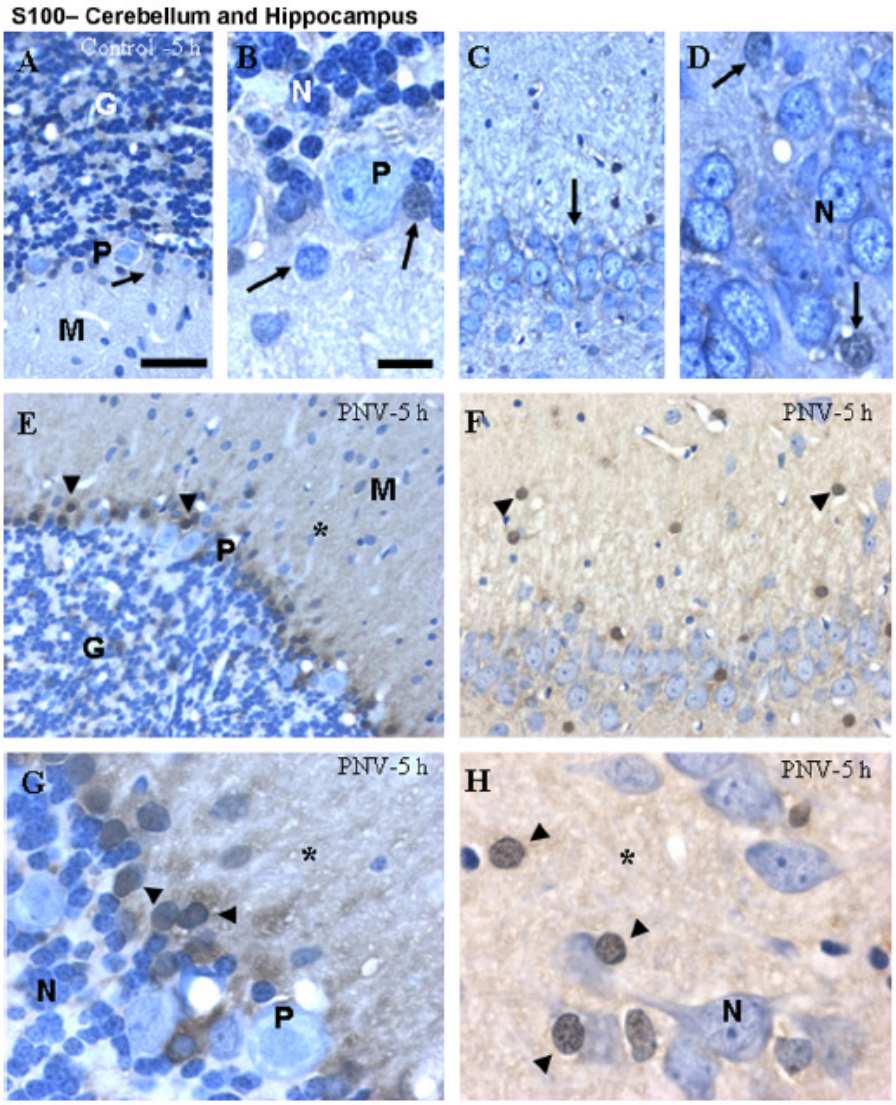

Fig. 3. S100 immunohistochemistry in cerebellar and hippocampal astrocytes. (A, B) Cerebellum. (C, D) Hippocampus. Note the very low expression of S100 in astrocytes of both regions from saline 5 h-control group (arrows). (E, G) Cerebellum of PNV-group (5 h p.i.): S100 expression increased strongly in astrocytes (arrowheads) localized mainly around neurons in Purkinje layer (PL), and in astrocytic processes throughout parenchyma of the molecular layer (asterisks, M), giving a brownish shadow to the tissue background. Glial and neuronal cells were more closely together. (F, H) Hippocampus of PNV-group (5 h p.i.). Both the astrocyte bodies (arrowheads) and processes (asterisk–brownish ground) exhibited S100 overexpression. G = Granular layer, M = Molecular layer. Bars: A, C = 40 μm; B, D, E, F = 12 μm.

cerebellum and hippocampus. The scores for cerebellum were (+) for control; (++) for PNV-15–45 min and 2 h and (+++) for PNV-5 h. The scores for hippocampus were (+) for control, (++) for PNV-15–45 min and (+++) for 2 and 5 h.

3.5. Cytokines: TNF-α and IFN-γ

IHC for TNF-α and IFN-γ in saline-injected animals showed imperceptible staining; however, WB quantification revealed a basal expression of both cytokines (Figs. 4 and 5). In envenomed animals, astrocytes and neurons were immunopositive for both pro-inflammatory cytokines, with neurons being more reactive than astrocytes, and hippocampus with stronger immunoreactivity than cerebellum. Interestingly, while in hippocampus and cerebellum of control groups, cytokine-negative-astrocytes and -neurons were separated apart from each other, in PNV-treated groups these cells were more closely contacting each other (compare Fig. 4B with E; D with F and compare Fig. 5B with E; D with F). In cerebellum, despite granular neurons were negative for both cytokines, they appeared more clustered; in addition, in 5 h-PNV-group astrocytes were more numerous around Purkinje cells. Both in hippocampus and cerebellum no neuronal death was noticed by histopathological analysis.

WB quantification showed that the increase of TNF-α level caused by venom was not statistically significant. However, IFN-γ in hippocampus showed significant increase in PNV-5 h compared

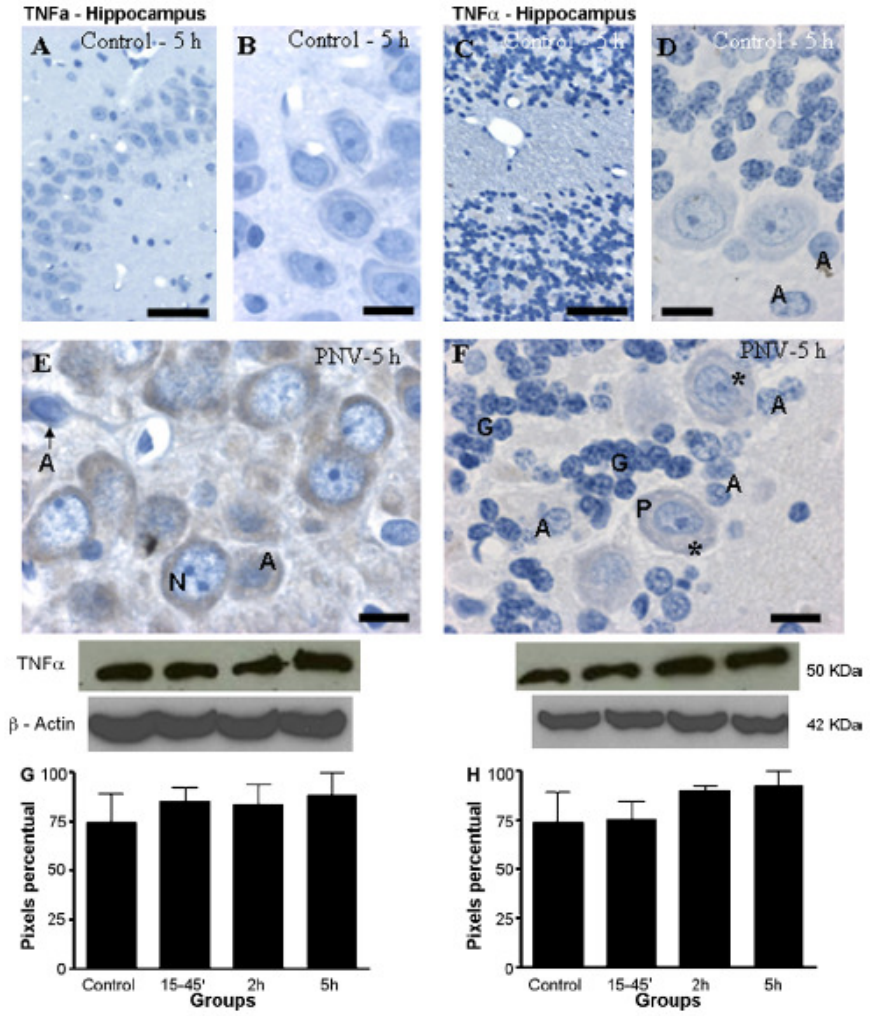

Fig. 4. Light micrographs of TNF-α immunohistochemistry in hippocampus (A, B, E) and cerebellum (C, D, F), and blots and quantification columns obtained from WB (G, H). No labeling was seen in control saline 5 h p.i. (A–D). Panel E shows hippocampus of PNV-treated animal (5 h p.i.) with strong labeling in neurons (N) and astrocytes (A): cells are closely apposed in envenomed animals in contrast to control where they are more dispersed (compare panels B and E). Panel F shows cerebellum of envenomed group (5 h p.i.): Purkinje cells (P) showed a relatively moderate cytoplasmic expression of this cytokine (*). Astrocytes (A) and granular neurons (G) are close to each other in envenomed animals (panels F) in comparison to control (panel D). Panels G and H show TNF-α blots and WB quantification represented by bars; no significant difference was seen regarding the cytokine both in hippocampus and in cerebellum. Data were analyzed by one-way ANOVA followed by the Dunnet test. The columns represent the mean ± S.E. of the protein blot investigated; the results were confirmed in three sets of experiments ($n = 5$ animals/time interval after PNV exposure compared to control pool, $n = 15$). Scale Bars: A, C, E, F = 40 μm; B, D, G–J = 12 μm.

to control ($P < 0.05$) and to PNV-15–45 min ($P < 0.01$). In cerebellum, there was a significant reduction of IFN-γ 15–45 min after PNV injection compared to control ($P < 0.05$). Afterwards, the level of cytokine rose and in PNV-5 h the increase of IFN-γ was significant compared to PNV-15–45 min ($P < 0.001$) and to PNV-2 h ($P < 0.01$) (Fig. 5G and H).

4. Discussion

P. nigriventer is an aggressive spider species responsible for the majority of accidents with venomous spiders in Brazil, however fatal cases are rare. The clinical manifestation seen following *P. nigriventer* bite indicates peripheral and central, including autonomic, nervous system involvement. This study aimed to characterize some cellular/molecular events which coursed with BBB permeability caused by the systemic presence of *Phoneutria* venom in the light of pharmacological actions of some of their neurotoxins. For clinical and immunohistochemical observations, matched controls for each time-point post-PNV exposure were used. For WB analysis each time-point post-PNV exposure was compared to a single control formed by mixing all the saline-injected at every time-point (i.e., $n = 15$ saline-injected animals). This was done because there is no visible difference in clinical signs or IHC results in the three time-points used.

The systemic presence of PNV promoted, soon at 15–45 min post-injection, a remarkable immunoreactivity of GFAP in astrocytes of hippocampus and in cerebellum mainly at the molecular layer. IHC data showed that GFAP labeling persisted stronger in the hippocampus and cerebellar molecular layer at 2 and 5 h compared to time-matched control. In contrast, the protein blots showed a transient astrogliosis, since the level of the protein in PNV-2 and PNV-5 h was inferior to pooled-control. Whether the shift in the

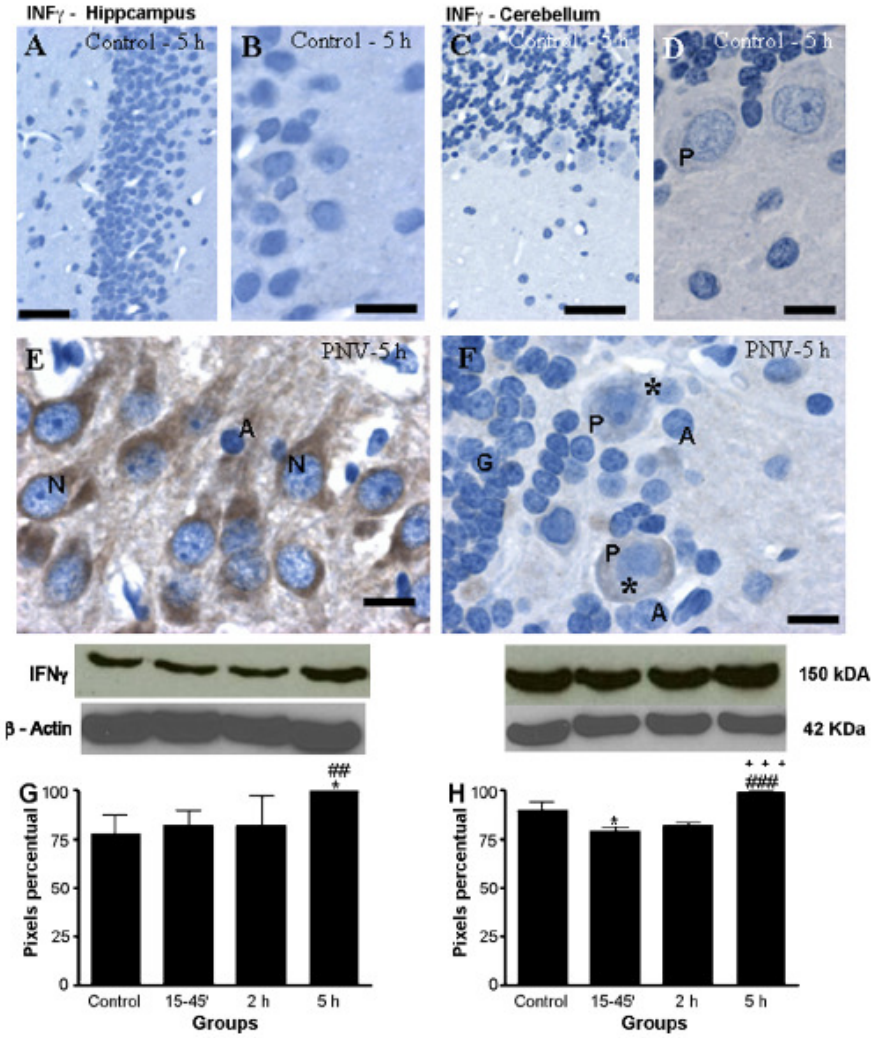

Fig. 5. Light micrographs of INF-γ immunolabeling in hippocampus A, B, E and cerebellum C, D, F. No expression of this pro-inflammatory cytokine was seen in saline controls (panels A, B and C, D display control after 5 h of saline injection). Panel E: Hippocampus of PNV-treated rats: observe that 5 h p.i. a very strong expression of INF-γ was seen both in Purkinje cells (P) and astrocytes (A). Panel F: Cerebellum of PNV-treated rats: after 5 h of systemic PNV injection, a moderate cytoplasmatic labeling was observed (asterisks). Both in hippocampus and in cerebellum closeness among cells was seen in envenomed animals. G: granular neurons, P: Purkinje cells; A: astrocytes. Panels G and H: in IFN-γ blots, the asterisk denotes significant difference in relation to control-pooled group ($P < 0.05$). ** and *** denotes significant difference to PNV-15–45 min group ($P < 0.01$ and $P < 0.001$, respectively) and *** means significant difference to PNV-2 h ($P < 0.001$). Data were analyzed by one-way ANOVA followed by the Dunnet test. The columns represent the mean ± S.E. of the protein investigated; the results were confirmed in three sets of experiments ($n = 5$ animals/time interval after PNV exposure compared to control pool, $n = 15$). Scale Bars: A, C, E, F = 40 μm; B, D, G, H = 12 μm.

GFAP expression seen at 5 h was followed by reactivation thereafter was not investigated here. The data indicated an uneven reactive astrogliosis in cerebellum and hippocampus, i.e., the reactive gliosis could be variably light in some regions and strong in others. A clear explanation for this was undetermined, but some hypothesis can be raised: the existence of intra- and/or inter-regional differences in the BBB permeability to the neurotoxins-containing venom; heterogeneity in the populations of astrocytes (receptors); differential density/distribution in microvasculature and/or ion channels. Ding et al. (2000) reported regional difference in GFAP and S100 expression in response to kainic acid administration, and attributed these differences to neuronal degeneration, astrocytic receptor set-up and/or on the blood–brain barrier.

S100 immunoreactivity seemed not to follow the GFAP time-course since its highest expression occurred 5 h post-envenoming. However, the evaluation of S100 expression was semi-quantitative based only on IHC assay, so unabling a clear quantification of the protein in the entire regions. However, when compared the IHC findings of GFAP and S100 showed a correspondence between the expression of both in cerebellum (compare Figs. 2B–D with 3E and G) and hippocampus (compare Figs. 1B–D with 3F and H). GFAP and S100 have been considered markers of CNS injury and a correlation of both proteins has been established. S100β, which is found only in astrocytes, inhibits the phosphorylation of different cytoskeletal proteins, including GFAP, resulting in cytoskeleton stabilization (Ziegler et al., 1998).

Particularly interesting was the marked positivity of both proteins in the molecular layer of cerebellum in PNV-treated group, and also the more concentration of granular neurons around Purkinje cells. Different from control, in envenomed animals a

higher number of strongly S100 positive astrocytic cell bodies appeared concentrated around, and in closer contact with the Purkinje cells. These astrocytes, named Bergmann glia were those, whose profuse and intense GFAP positive ramification, extended throughout the molecular layer. The cerebellar molecular layer is characterized by extensive synaptic contacts between granule neurons, parallel fibers and Purkinje cells (Matsui and Jahr, 2004). Bergmann glia expresses different types of glutamate receptors, and glutamate release from parallel fibers depolarizes glial cells, increases calcium ion influx and affects transcriptional and translational events (see Zepeda et al., 2008). S100, considered as a glial-derived cytokine, belongs to a calcium-binding family of proteins implicated in intracellular (regulation of enzyme activities, dynamics of cytoskeleton constituents, cell growth/differentiation and calcium homeostasis) and extracellular activities (regulation of inflammatory cells, neurons, astrocytes, microglia and endothelial cells) (see Donato, 2003). Intercellular interactions mediated by signaling pathways involving Ca^{2+} signals were reported between astrocytes, astrocytes-endothelial cells and astrocytes-neurons (Paemeleire, 2002; Simard et al., 2003), calcium being considered potent modulator of the strength of excitatory and inhibitory synapses. *P. nigriventer* venom consists of a rich mixture of pharmacologically active toxins, some excitotoxic and capable of altering voltage-gated Ca^{2+}, K^+ and Na^+ channels conductance in excitable tissues (Brazil and Veillard, 1925; Rezende et al., 1991; Gomez et al., 2002). In Bergmann glia, Ca^{2+} increases control the structural (including cytoskeleton) and functional interactions between these cells and Purkinje cell synapses (Metea and Newman, 2006). Some neurotoxic peptides of *P. nigriventer* venom block Ca^{2+} channels and inhibit glutamate release (Romano-Silva et al., 1993). We suggest that S100 protein could be involved in the disturbances of calcium homeostasis caused by PNV and interaction with reactive gliosis. We did not investigate if there were abnormal levels of glutamate in cerebellum, but if it does this can result in excessive calcium loading which could additionally become higher by the blockade of Ca^{2+} channels by toxins of the venom. Given Bergmann glia has glutamate transporters, is involved in calcium homeostasis and is known to enclose synaptic contacts in the molecular layer, the closer relationship glia:Purkinje cells, granular neurons:Purkinje cells, seen in this *in vivo* PNV/BBB model, could result from local unbalanced homeostasis involving calcium and glutamate disturbance caused by the venom toxic effect on Bergmann glia.

Another interesting point is the presence of serotonin and histamine in the composition of *P. nigriventer* venom (Schenberg and Pereira-Lima, 1978), and that PNV-induced vascular permeability in rat and rabbit skin has been associated with activation of histamine and serotonin receptors (Antunes et al., 1992). Also, PNV activates type 5-HT_4 receptors in vagus nerve preparations, probably a mechanism involved in pain and inflammation caused by venom (Costa et al., 2003). Interestingly, S100β release from astrocytes is mediated by serotonin, acting through 5-HT_{1A} receptors (Whitaker-Azmitia et al., 1990; Ramos et al., 2000). Since serotonin and histamine regulates blood vessels diameter, blood flow and transendothelial transport, and endothelial cells express membrane receptors for both (see Nitsch et al., 1985), the relationship of serotonin/histamine: S100/GFAP expression and their role in the BBB breakdown is an attractive matter to be investigated.

Our previous studies have shown that the systemic presence of PNV provoked end-feet astroglial swelling in hippocampus after longer periods of envenoming (Le Sueur et al., 2003, 2004) as well as vascular extracellular tracer leakage and perivascular edema formation in cerebellum and hippocampus at acute periods after envenoming (Rapôso et al., 2007). At longer periods (18 h and 9 days) the PNV-induced BBB leakage was shown to be due to increment in transcytosis mediated by microtubules (Le Sueur et al., 2004). In the present study, the histopathological analysis of cerebellum and hippocampus showed no evidence of neuronal death corroborating our previous observations. Nonetheless, the systemic presence of PNV promoted activation of neurons (as seen by FOS-early gene-expression) in several motor- and stress-related areas of the CNS, which, apparently, is modulated by nitric oxide (Cruz-Höfling et al., 2007). However, we did not find inflammatory cells infiltrated in any of the anatomical areas screened.

Nevertheless, we now demonstrated by immunoblotting that in hippocampus there was a trend for TNF-α increase, which though was not significant statistically, at least until 5 h after envenoming. However, immunohistochemistry showed that neurons were markedly labeled for this cytokine, suggesting that they were likely the major releasers of TNF-α in response to venom. Astrocytes showed only moderate labeling, but since they were higher in number than neurons the total amount of TNF-α released by astrocytes may match with that by neurons. The immunolabeling of neurons and astrocytes in cerebellum was less intense than that of hippocampus. The fact the content of TNF-α at 5 h post-PNV was similar both in cerebellum and in hippocampus (~90%, see Fig. 4G and H) can be attributed to the higher dimension of cerebellum than that of hippocampus.

In hippocampus, a significant increase in IFN-γ expression and a notable labeling of neurons was seen at PNV-5 h. In cerebellum, IFN-γ was significantly reduced by 15–45 min, and by 5 h it was significantly higher than at 15–45 min and 2 h. The data suggest a mediator role for both pro-inflammatory cytokines in BBB permeability and probably in the clinical signs of envenoming in this experimental model. It has been shown that TNF-α increases transcytosis by the activation of p42–44 mitogen-activated protein kinase (MAPK) and causes phosphorylation of the substrate through a mechanism mediated by plasma membrane receptor in an *in vitro* model of BBB (Cohen, 1996; Miller et al., 2005). Inflammatory mediators such as cytokines are, at least partly, responsible for the changes in vascular permeability. The time-course in the expression of TNF-α and IFN-γ seen here may suggest that the inflammatory mediators could have a proactive role in early periods after envenoming (at least in cerebellum) and a cytotoxic one later. However, the apparent region-selective and time-selective responses suggest that proinflammatory cytokines can be cytotoxic to some CNS regions and neurotrophic to others having the period of exposure to the toxicant a role in the modulatory action.

Diffuse cytoplasmic staining for TNF-α and IFN-γ was evident in neurons somata and this fact led us to suppose that that these neurons can express functional cytokine receptors. Biological activities of TNF-α are mediated by two different cell surface receptors (TNFR), the P75 TNFR and the P55 TNFR (Carlson et al., 1998; Haviv and Stein, 1998). Neumann et al. (1997) have demonstrated that functionally mature brain neurons derived from cultures of dissociated rat hippocampal tissue transcribe the α-chain of the interferon-type II receptor (binding IFN-γ) along with the p55 receptor for TNF-α. IFN-γ is required for interactions between immune and brain cells, increases microglia neuroprotective effect and induces neurotrophic factor receptors in ischemic pyramidal neurons (Imai et al., 2007). Interestingly, we found evidences of more close "physical contact" between TNF-α-positive or IFN-γ-positive neurons with TNF-α-positive or IFN-γ-positive astrocytes (respectively) in the PNV-group than in control (compare Figs. 4B with E; D with F, and 5B with E; D with F). Also, it was of note the dense packing of granular cells in cerebellum. Certainly, this assumption in this experimental model needs further investigations.

Immune responses protect the CNS against pathogens, but the fact that there is little dispensable tissue in the brain, a vigorous

regulation is necessary to avoid disastrous immune-mediated damage. So, neuroinflammation not only can be seen as a double-sided sword since it can cause neuronal damage but also has neuroprotective and neurotrophic effects at some stages. Our results suggest that the expression of pro-inflammatory cytokines in astrocytes and neurons is part of the immune response against the neurotoxic injury caused by *P. nigriventer* venom; at least partly, the expression of the cytokines could be involved in the transient characteristic of BBB permeability in the cerebellum and hippocampus. Besides, it was obvious the existence of a mechanism of defense in the CNS apt to promptly trigger machinery for the synthesis of proteins, GFAP, S100 and cytokines in response to circulating *P. nigriventer* venom. Whether the bulk of effects hitherto known result from a direct action of venom, and/or from secondary messengers (such as pro-inflammatory cytokines) elicited during envenoming is a matter to be investigated. The richness of neurotoxins in the *P. nigriventer* armed-spider venom elects it as a powerful tool for investigating physiopathological processes of the CNS, including inflammatory ones. This model is useful for studying CNS vascular permeability and for experimental manipulation of the BBB. It may have a potential application in experimental studies on drug delivery throughout the CNS. Relevant to this is the report that the PNV-induced BBB leakage was reversible with no detectable neurological sequel to the animal.

Conflict of interest statement

None.

Acknowledgments

The authors thank Instituto Butantan (São Paulo, SP, Brazil) for venom donation. The authors also thank Ms. Marta Beatriz Leonardo (BSc) for excellent technical assistance, and Mr. Miguel Silva and Mr. Silva for animal care. This work has been funded by grants from Fundação de Amparo à Pesquisa do Estado de São Paulo (FAPESP # 98/00341-0 and 07/50272-6), and FAEPEX-UNICAMP (Grant # 100207/07). G.M.Z. and C.R. were recipients of scholarships from Coordenação de Aperfeiçoamento de Pessoal de Nível Superior (CAPES) and FAPESP, respectively. M.A.C.H. is a IA Research fellow of Conselho Nacional de Desenvolvimento Científico e Tecnológico (CNPq # 522131/95-6).

References

Abbott NJ, Rönnbäck L, Hansson E. Astrocyte–endothelial interactions at the blood–brain barrier. Nat Rev Neurosci 2006;7:41–53.

Antunes E, Marangoni RA, Brain SD, De Nucci G. *Phoneutria nigriventer* (armed spider) venom induces increased vascular permeability in rat and rabbit skin *in vivo*. Toxicon 1992;30:1011–6.

Aschner M. Astrocytes as mediators of immune and inflammatory responses in the CNS. Neurotoxicology 1998;19:269–81.

Bucaretchi F, Deus Reinaldo CR, Hyslop S, Madureira PR, De Capitani EM. Vieira RJA clinico-epidemiological study of bites by spiders of the genus *Phoneutria*. Rev Inst Med Trop São Paulo 2000;42:17–21.

Brazil V, Veillard J. Contribuição ao estudo do veneno das aranhas. Mem Inst Butantan 1925;2:5–77.

Carlson NG, Bacchi A, Rogers SW, Gahring LC. Nicotine blocks TNF-alpha-mediated neuroprotection to NMDA by an alpha-bungarotoxin-sensitive pathway. J Neurobiol 1998;35:29–36.

Cohen P. Dissection of protein kinase cascades that mediate cellular response to cytokines and cellular stress. Adv Pharmacol 1996;36:15–27.

Costa SK, Brain SD, Antunes E, De Nucci G, Docherty RJ. *Phoneutria nigriventer* spider venom activates 5-HT_4 receptors in rat-isolated vagus nerve. Br J Pharmacol 2003;139:59–64.

Cruz-Höfling MA, Love S, Brook G, Duchen LW. Effects of *Phoneutria nigriventer* venom on mouse peripheral nerve. Q J Exp Physiol 1985;70:623–40.

Cruz-Höfling MA, Zago GM, Melo LL, Raposo C. c-FOS and n-NOS reactive neurons in response to circulating *Phoneutria nigriventer* spider venom. Brain Res Bull 2007;73:114–26.

Ding M, Haglid KG, Hamberger A. Quantitative immunochemistry on neuronal loss, reactive gliosis and BBB damage in cortex/striatum and hippocampus/amygdala after systemic kainic acid administration. Neurochem Int 2000;36:313–8.

Donato R. Intracellular and extracellular roles of S100 proteins. Microc Res Tech 2003;60:540–51.

Eng L, Ghirnikar F. GFAP and astrogliosis. Brain Pathol 1994;4:229–37.

Eng LF, Ghirnikar RS, Lee YL. Glial fibrillary acidic protein: GFAP-thirty-one years (1969–2000). Neurochem Res 2000;25:1439–51.

Engelhardt B. Development of the blood–brain barrier. Cell Tissue Res 2003;314:119–29.

Fontana MD, Vital Brazil O. Mode of action of *Phoneutria nigriventer* spider venom at the isolated nerve-diaphragm preparation of the rat. Braz J Med Biol Res 1985;18:557–65.

Gomez MV, Kalapothakis E, Guatimosim C, Prado MA. *Phoneutria nigriventer* venom: a cocktail of toxins that affect ion channels. Cell Mol Neurobiol 2002;22:579–88.

Grieb P, Forster RE, Strome D, Goodwin CW, Pape PC. O_2 exchange between blood and brain tissues studied with $18O_2$ indicatordilution technique. J Appl Physiol 1985;58:1929–41.

Haviv R, Stein R. The intracellular domain of P55 tumor necrosis factor receptor induces apoptosis which requires different caspases in naïve and neuronal PC12 cells. J Neurosci Res 1998;52:380–9.

Hawkins RA, Ó Kane RL, Simpson IA, Vina JR. Structure of the blood–brain barrier and its role in the transport of amino acids. J Nutr 2006;136:218–26.

Hess AP, Schanz A, Baston-Buest DM, Hirchenhain J, Stoff-Khalili MA, Bielfeld P, et al. Expression of the vascular endothelial growth factor receptor neuropilin-1 in the human endometrium. *J Reprod Immunol* November 7 2008 [Epub ahead of print]. doi:10.1016/j.jri.2008.09.001.

Hirsch EC. Glial cells and Parkinson's disease. J Neurol 2000;247:1158–62.

Imai F, Suzuki H, Oda J, Ninomiva T, Ono K, Ninomyia T, et al. Neuroprotective effect of exogenous microglia in global brain ischemia. J Cereb Blood Flow Metab 2007;27:488–500.

Le Sueur L, Collares-Buzato CB, Cruz-Höfling MA. Mechanisms involved in the blood–brain barrier increased permeability induced by *Phoneutria nigriventer* spider venom in rats. Brain Res 2004;1027:38–47.

Le Sueur L, Kalapothakis E, Cruz-Höfling MA. Breakdown of the blood–brain barrier and neuropathological changes induced by *Phoneutria nigriventer* spider venom. Acta Neuropathol (Berl) 2003;105:125–34.

Liu B, Gao HM, Wang JY, Jeohn GH, Cooper CL, Hong JS. Role of nitric oxide in inflammation-mediated neurodegeneration. Ann N Y Acad Sci 2002;962:318–31.

Lovell MA, Robertson JD, Teesdale WJ, Campbell JL, Markesbery WR. Copper, iron and zinc in Alzheimer's disease senile plaques. J Neurol Sci 1998;158:47–52.

Lúcio AD, Campos FV, Richardson M, Cordeiro MN, Mazzoni MS, de Lima ME, et al. A new family of small (4 kDa) neurotoxins from the venoms of spiders of the genus *Phoneutria*. Protein Pept Lett 2008;15:700–8.

Matsui K, Jahr CE. Differential control of synaptic and ectopic vesicular release of glutamate. J Neurosci 2004;24:8932–9.

Metea MR, Newman EA. Calcium signaling in specialized glial cells. Glia 2006;54:650–5.

Miller F, Fenart L, Landry V, Coisne C, Cecchelli R, Dehouck MP, et al. The MAP kinase pathway mediates transcytosis induced by TNF-alpha in an in vitro blood–brain barrier model. Eur J Neurosci 2005;22:835–44.

Minghetti L, Levi G. Microglia as effector cells in brain damage and repair: focus on prostanoids and nitric oxide. Prog Neurobiol 1998;54:99–125.

Neumann H, Schmidt H, Cavalié A, Jenne D, Wekerle H. Major histocompatibility complex (MHC) class I gene expression in single neurons of the central nervous system: differential regulation by interferon (IFN)-γ and tumor necrosis factor (TNF)-α. J Exp Med 1997;185:305–16.

Neumann H. Control of glial immune function by neurons. Glia 2001;36:191–9.

Nitsch C, Suzuki R, Fujiwara K, Klatzo I. Incongruence of regional cerebral blood flow increase and blood–brain barrier opening in rabbits at the onset of seizures induced by bicuculline, methoxypyridoxine, and kainic acid. J Neurol Sci 1985;67:67–79.

Paemeleire K. Calcium signaling in and between brain astrocytes and endothelial cells. Acta Neurol Belg 2002;102:137–40.

Palkovits M, Brownstein M. Atlas of rat brain anatomy. New York: Elsevier; 1988.

Prado MA, Guatimosin C, Gómez MV, Diniz CR, Cordeiro MN, Romano-Silva MA. A novel tool for the investigation of glutamate release from rat cerebrocortical synaptosomes: the toxin Tx3-3 from the venom of spider *Phoneutria nigriventer*. Biochemistry 1996;314:145–50.

Ramos AJ, Tagliaferro P, Lopez EM, Pecci Saavedra J, Brusco A. Neuroglial interactions in a model of para-chlorophenylalanine-induced serotonin depletion. Brain Res 2000;883:1–14.

Ransom B, Behar T, Nedergaard M. New roles for astrocytes (stars at last). Trends Neurosci 2003;26:520–2.

Rapôso C, Zago GM, Silva GH, Cruz-Höfling MA. Acute blood brain barrier permeabilization in rats after systemic *Phoneutria nigriventer* venom. Brain Res 2007;1149:18–29.

Rezende JL, Cordeiro MN, Oliveira EB, Diniz CR. Isolation of neurotoxic peptides from the venom of the "armed" spider *Phoneutria nigriventer*. Toxicon 1991;29:1225–33.

Romano-Silva MA, Ribeiro-Santos MA, Ribeiro AM, Gomez MV, Diniz CR, Cordeiro MN, Brammer MJRat cortical synaptosomes have more than one mechanism for Ca^{2+} entry linked to rapid glutamate release: studies using the *Phoneutria nigriventer* toxin $PhTX_2$ and potassium depolarization. Biochem J 1993;296:313–9.

Rothermundt M, Peters M, Prehn JH, Arolt V. S100B in brain damage and neurodegeneration. Microsc Res Tech 2003;60:614–32.

Savchenko VL, McKanna JA, Nikonenko IR, Skibo GG. Microglia and astrocytes in the adult rat brain: comparative immunocytochemical analysis demonstrates the efficacy of lipocortin 1 immunoreactivity. Neuroscience 2000;96:195–203.

Schenberg S, Pereira-Lima FA. Handbook of experimental pharmacology, vol. 48. New York, Berlin, Heilderberg: Springer; 1978 pp. 217–44.

Simard M, Arcuino G, Takano T, Liu QS, Nedergaard M. Signalling at the gliovascular interface. J Neurosci 2003;23:9254–62.

Streit WJ. Microglial response to brain injury: a brief synopsis. Toxicol Pathol 2000;28:28–30.

Vieira LB, Kushmerick C, Hildebrand ME, Garcia E, Stea A, Cordeiro MN, et al. Inhibition of high voltage-activated calcium channels by spider toxin PnTx3-6. J Pharmacol Exp Ther 2005;314:1370–7.

Walz W, Lang MK. Immunocytochemical evidence for a distint GFAP-negative subpopulation of astrocytes in the adult rat hippocampus. Neurosci Lett 1998;257:127–30.

Whitaker-Azmitia PM, Murphy R, Azmitia EC. Stimulation of astroglial 5-HT1A receptors releases the serotonergic growth factor, protein S-100, and alters astroglial morphology. Brain Res 1990;528:155–8.

Wong D, Dorovini-Zis K, Vincent SR. Cytokines, nitric oxide, and cGMP modulate the permeability of an in vitro model of the human blood–brain barrier. Exp Neurol 2004;190:446–55.

Zepeda RC, Barrera I, Castelán F, Soto-Cid A, Hernández-Kelly LC, López-Bayghen E, et al. Glutamate-dependent transcriptional regulation in bergmann glia cells: involvement of p38 MAP kinase. Neurochem Res 2008;33:1277–85.

Ziegler DR, Innocente CE, Leal RB, Rodnight R, Goncalves CA. The S100B protein inhibits phosphorylation of GFAP and vimentin in a cytoskeletal fraction from immature rat hippocampus. Neurochem Res 1998;23:1259–63.

DECLARAÇÃO

Declaro para os devidos fins que o conteúdo de minha **Tese de Doutorado** intitulada "Veneno e toxina da aranha *Phoneutria nigriventer*: Ação no sistema nervoso central".

( ) não se enquadra no Artigo 1°, § 3° da Informação CCPG 01/2008, referente a bioética e biossegurança.

( ) está inserido no Projeto CIBio (Protocolo nº _____), intitulado _____

(X) tem autorização da Comissão de Ética em Experimentação Animal (Protocolo nº 1700-1).

( ) tem autorização do Comitê de Ética para Pesquisa com Seres Humanos (?) (Protocolo nº _____).

Catarina Raposo D. Carneiro
Aluno(a): (Catarina Raposo Dias Carneiro)

Orientador(a): (Maria Alice da Cruz-Höfling)

Para uso da Comissão ou Comitê pertinente:

(X) Deferido ( ) Indeferido

Ana Maria Spanuda Guaraldo
Nome:
Função: Profa. Dra. ANA MARIA A. GUARALDO
Presidente
Comissão de Ètica na Experimentação Animal
CEEA/IB - UNICAMP